Holocene paleohydrology from Lake of the Woods and Shoal Lake cores using ostracodes, thecamoebians and sediment properties

by

Trevor Mellors

A Thesis submitted to the Faculty of Graduate Studies of

The University of Manitoba

in partial fulfilment of the requirements of the degree of

MASTER OF SCIENCE

Department of Geological Sciences

University of Manitoba

Winnipeg

ABSTRACT

Ten sediment cores (2.0-8.5 m long) from various locations in Lake of the Woods (LOTWs) and Shoal Lake (SL) were recovered in August 2006, using a Kullenberg piston corer. From the study of the macrofossils (primarily ostracodes and thecamoebians) and the sediments in six processed cores, variations in paleoconditions were observed both spatially and temporally, and the timing of these changes were identified in over 10,000 years of postglacial history. Ostracodes disappeared from the LOTWs record from about 9000 to 7600 calendar years before present (BP) (about 5800 in SL), after LOTWs became isolated from glacial Lake Agassiz. Thecamoebians appeared in many cores around 2000 calendar years BP, with the earliest appearance at 9200. Buried paleosols in three cores indicate portions of the lake dried on several occasions during the Hypsithermal, perhaps indicating the region's future climate response. One core contained a pink clay bed indicative of the Marquette readvance about 11,300 years (BP), and the subsequent input of water from the Superior basin.

ACKNOWLEDGEMENTS

I would like to thank my advisor, James T. Teller (University of Manitoba) for the opportunity to undertake this very interesting project enroute to a Master of Science degree in Geological Sciences. The project was very different from my Engineering background, and in light of my vintage I appreciate him accepting me as a student. I would also like to thank him for his patience as I asked a lot of sedimentological questions while I tried to come to grips with the intricacies of glacial Lake Agassiz and its deposits. Thank you for the financial support and all the fun. Thanks to Brandon Curry (Illinois Geological Survey) for giving his valuable time to help me to process the Lake of the Woods and Shoal Lake sediments and extract the ostracode record. I would also like to thank him for taking me into his home while I was in Champaign; I felt like I was one of the family during my brief but very enjoyable stay. Also thanks to Kristina Brady, Amy Mybro, Anders Noren and Mark Shapley of the Limnological Research Center at the University of Minnesota, for providing coring equipment and leading our effort to recover sediment cores from Lake of the Woods and Shoal Lake, their good company, and their patience and expertise in their lab as we sub-sampled the cores. Thanks to Jim McPhee for escorting us and loaning his equipment during our SL core recovery operations. I would also like to thank Alice Telka of Paleotec Services for her help in processing and picking macrofossils for radiocarbon dating. Thanks to my wife Joyce for putting up with me during my quest for a Master's degree in Geology, at this rather late stage in my continuing pursuit for knowledge.

LIST OF TABLES

LIST OF FIGURES

List of Copyrighted Material for which Permission was Obtained

The following is a list of figures for which copyright approvals were obtained from the copyright owners or the agencies tasked with granting approvals on their behalf. Each figure in the thesis including those used with permission of the copyright owner provides the reference source for the figure, and page number where the figure is located within the reference as appropriate. The specific reference source is provided in the References section of the thesis. Photos used in this thesis which were not taken by the author are used with permissions as noted. Copyright approvals for the macrofossil photos in the figures of Appendix B, Section 4, were provided by Alice Telka of Paleotec Services. The copyright approval for the modern counterpart photos as part of Figures B-2, B-3, and B-4 in Appendix B, Section 4, were provided separately as noted in the Figure listing below.

Figure 1. Early Holocene Configuration of Land, Ice and Water in North America, p.2, (Dean et al., 2002) approval obtained on July 04, 2010.

Figure 2. Configuration of the Land, Ice and Water in North America at Beginning of Mid-Holocene Warm Period, p. 3, (Dean et al., 2002) approval obtained on July 04, 2010.

Figure 3. Fluctuations in the Retreating Red River Des Moines Lobe of the LIS, p. 5, (Teller 1985) approval obtained on July 04, 2010.

Figure 4. Depiction of the Maximum Extent of Lake Agassiz, p. 6, (Leverington and Teller, 2003) approval obtained July, 2010.

Figure 5. Wind Directions Related to Glacial Limits and Proglacial Lakes, p. 10, (Wolfe et al., 2004) approval obtained on July 23, 2010.

Figure 6. Lake Agassiz Outbursts from the δ 18O Record in GISP2 Cores, p. 14, (Teller and Leveringon, 2004) approval obtained July, 2010.

Appendix B, Section 4:

Figure B-1. LOW 1A-1K-3, 99-101 cm; five curlytop knotweed (*Polygonum lapathifolium*) achenes, weighing 2.86 mg, (Telka, Paleotec Services) approval obtained on Aug.17, 2010.

Figure B-2. Left: image of curlytop knotweed, Polygonum lapathifolium; Right: LOW 1A-1K-3, 99-101 cm macrofossil achene of Polygonum lapathifolium, (Telka, Paleotec Services) approval obtained on Aug.17, 2010 and modern analogue (http://www.delawarewildflowers.org/plant.php?id=1534) approval obtained on Aug 18, 2010.

Figure B-3. LOW 1A-1K-3, 141-144 cm (inset); macrofossil achene of curlytop knotweed (*Polygonum lapathifolium*). Background photo: Curlytop knotweed, an annual herb of moist meadows and wet shorelines, approval obtained on Aug.17, 2010 and modern analogue (http://luirig.altervista.org:80/photos-int/polygonum-lapathifolium---persicaria-mayor.htm) approval obtained on Aug 18, 2010.

Figure B-4. LOW 4A-1K-1, 7-9 cm, (inset); macrofossil achene of bulrush (*Scirpus sp.*). Background: Photo of Scirpus validus, approval obtained on Aug.17, 2010, and modern analogue (http://plants.ifas.ufl.edu/images/scival/scival01.jpg) approval obtained on Aug 18, 2010.

Figure B-5. LOW 4A-1K-2, 22-23 cm; a wood fragment, weighing 28.2 mg, approval obtained on Aug.17, 2010.

Figure B-6. LOW 4A-1K-2, 42-43 cm; a wood fragment, weighing 33.7 mg. Bottom: opposite view of same wood fragment, approval obtained on Aug.17, 2010.

Figure B-7. LOW 4A-1K-2, 99-100 cm; three macrofossil bulrush (*Scirpus sp.*) achenes weighing 11.81 mg, approval obtained on Aug.17, 2010.

Figure B-8. LOW 5A-1K-4, 45-47 cm; two golden dock (*Rumex maritimus*) macrofossil calyx and achenes, approval obtained on Aug.17, 2010.

Figure B-9. LOW 5A-1K-4, 45-47 cm; left: golden dock (Rumex maritimus) macrofossil achene. right: goosefoot (Chenopodium sp.) macrofossil seed, approval obtained on Aug.17, 2010.

CHAPTER 1 INTRODUCTION

1.1 OBJECTIVES

The objective of this thesis is to reconstruct the Holocene paleohydrological history of Lake of the Woods and Shoal Lake (LOTWs and SL), and relate this to changes in regional paleoclimate. To achieve this objective, sediment cores were retrieved from key areas of LOTWs and in SL, and subsamples were obtained and processed to extract the ostracodes. Subsample processing was expanded to encompass other macrofossils such as insect and plant materials including charcoal, and rock and mineral lithic fragments. The physical nature and stratigraphy of the sediments were also studied to interpret the sedimentology of the processed cores. Interpreting the data also required consideration of the effects of differential isostatic rebound. Due to the limited numbers (and the disappearance) of ostracodes from the fossil record in upper portions of the cored sequence, the study was expanded to include the other paleoecological and paleoclimate proxies noted above, and thecamoebians. All of this was combined with 35 new radiocarbon dates to establish a history of hydrological change in LOTWs and SL during the past 9000 to 10,000 years BP (9-10 cal ka BP).

1.2 GENERAL PALEOHISTORY OF NORTH AMERICA SINCE THE LAST GLACIAL MAXIMUM

1.2.1 Introduction

The retreat of the Laurentide Ice sheet (LIS) started in the late Quaternary about 23 cal ka BP during the Late Wisconsinan (Dyke, 2005) following the last glacial maximum, and in due course led to the formation of large proglacial lakes along the ice margin, starting about 11.7 cal ka BP (Teller, 1985). Eventually amalgamation of some of these lakes led to the formation of very large proglacial lakes including Lake Agassiz and Lake Ojibway (Figure 1).

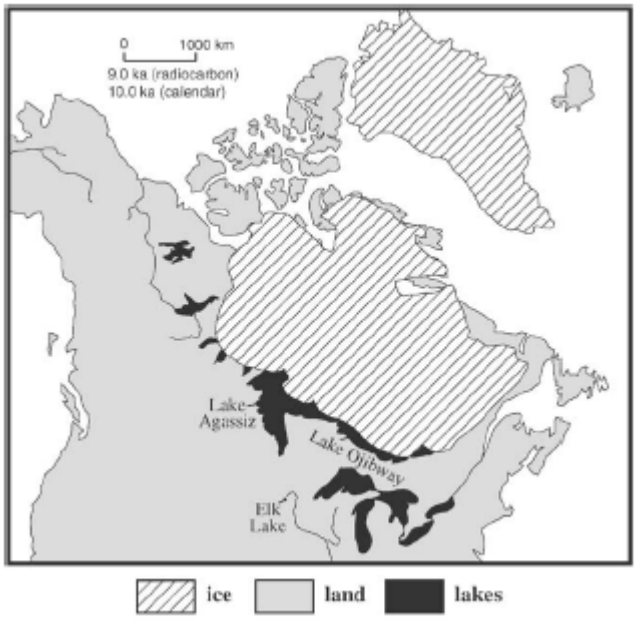

Figure 1. Early Holocene configuration of land, ice and water in North America showing the locations of Lake Agassiz and Lake Ojibway at about 10 cal ka BP (Dean, et al., 2002, p.1764).

The LIS and these very large proglacial lakes dominated the northern portions of North America for thousands of years until Lake Agassiz finally drained northward into Hudson

Bay at 8.2 cal ka BP or 7300 radiocarbon years before present (7.3 ^{14}C ka BP) at the start of the so-called 8.2 cal ka cold event, leaving isolated remnants of the LIS to slowly disintegrate (Figure 2) (Dean et al. 2002; Barber et al. 1999). The LIS had been decreasing in thickness and extent for thousands of years prior to this time as global climate moved into an interglacial period, although periods of readvance and surging occurred while the LIS margin retreated. Following Lake Agassiz's formation at the southern margin of the ice sheet, it varied in extent and volume, in concert with the margin of the melting glacier and the effects of isostatic rebound. These dramatic and complex events modified the climate of North America and elsewhere (Dean et al. 2002).

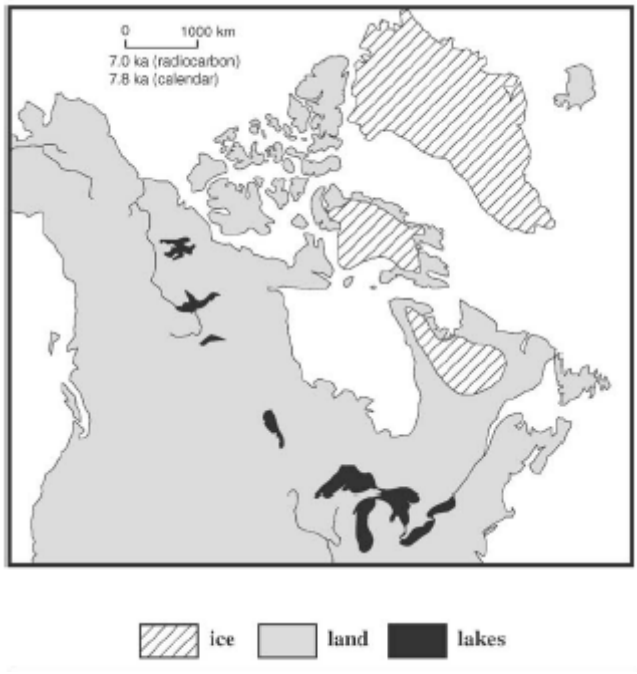

Figure 2. Configuration of the land, ice and water in North America at the beginning of the mid-Holocene warm period, subsequent to the 8.2 cal ka cold event (Dean, et al., 2002, p. 1764).

The final draining of Lake Agassiz initiated further dramatic climatic changes as the ice disappeared and land and water ratios changed, causing shifts in the climate of the

interior of North America (Haskell et al., 1996; Alley and Augustsdottir, 2005; Dean et al., 2002). Subsequently an unstable warm period established itself and dominated the region during the warm and unstable Hypsithermal interval of the mid-Holocene (Laird and Cumming, 2008; Clark et al., 2002). The polar air which had dominated the centre of North America shifted its location northward, and a region where the atmosphere flowed from the west began to interact with air from the Gulf of Mexico, and with the arctic air mass. This eventually established the more modern climatic conditions prevalent today (Dean et al. 2002; Laird et al., 2003; Dyke, 2005). As the transition to these more modern conditions took place, rapid variation in climate occurred creating periods of increased and reduced moisture, and temperature (Haskell et al., 1996). Following this transition period, the modern more stable climatic conditions were established, although climate variations continued to occur, including the Medieval Warm Period and the Little Ice Age intervals of the past millennium (Adam et al., 1999).

1.2.2 Glacial History of the Laurentide Ice Sheet

The retreat of the Laurentide Ice Sheet (LIS) began at about 23 cal ka BP (Dyke, 2005). Some of the proglacial lakes that formed along the south western side of the LIS amalgamated into Lake Agassiz (Teller, 1985; Leverington and Teller, 2003). As the ice margin slowly receded northward, glacial surges occurred at times, causing LIS lobes to readvance relatively rapidly (greater than 2 km/yr) (Figure 3) (Teller, 1985; Teller and Leverington, 2004). The surges and rapid calving off the glacier into Lake Agassiz

would have created very dynamic conditions in Lake Agassiz (Leverington and Teller, 2003).

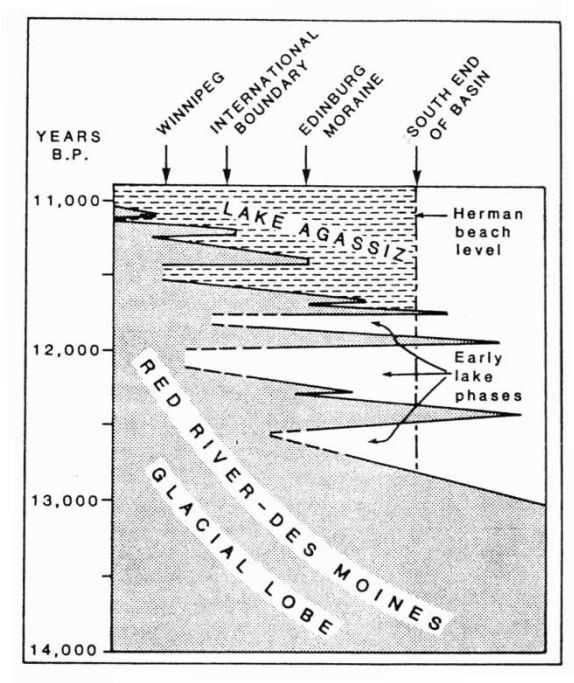

Figure 3. Fluctuations in the retreating Red River Des Moines Lobe of the LIS, indicating the growth of Lake Agassiz (Teller, 1985, p. 4).

The LIS ice margin also underwent a number of retreats and readvances responding to changes in climate, and large proglacial lakes next to the retreating ice margin correspondingly fluctuated in areal extent and depth as their outlets were covered or uncovered, and as differential isostatic rebound affected the elevation of their outlet channels (Teller and Thorleifson,1983; Teller, 1985). The geographic location of the outlets and the inputs from the LIS had major impacts on the extent and depth of Lake Agassiz (Teller and Leverington, 2003). Ice margin fluctuations and differential isostatic rebound opened and closed the overflow drainage pathways, resulting in variable routing of overflow, specifically down the Mississippi River to the south, the Saint Lawrence

River to the east, and to the northwest down the Mackenzie River drainage channel (Figure 4) (Leverington and Teller, 2003; Teller et al., 2005).

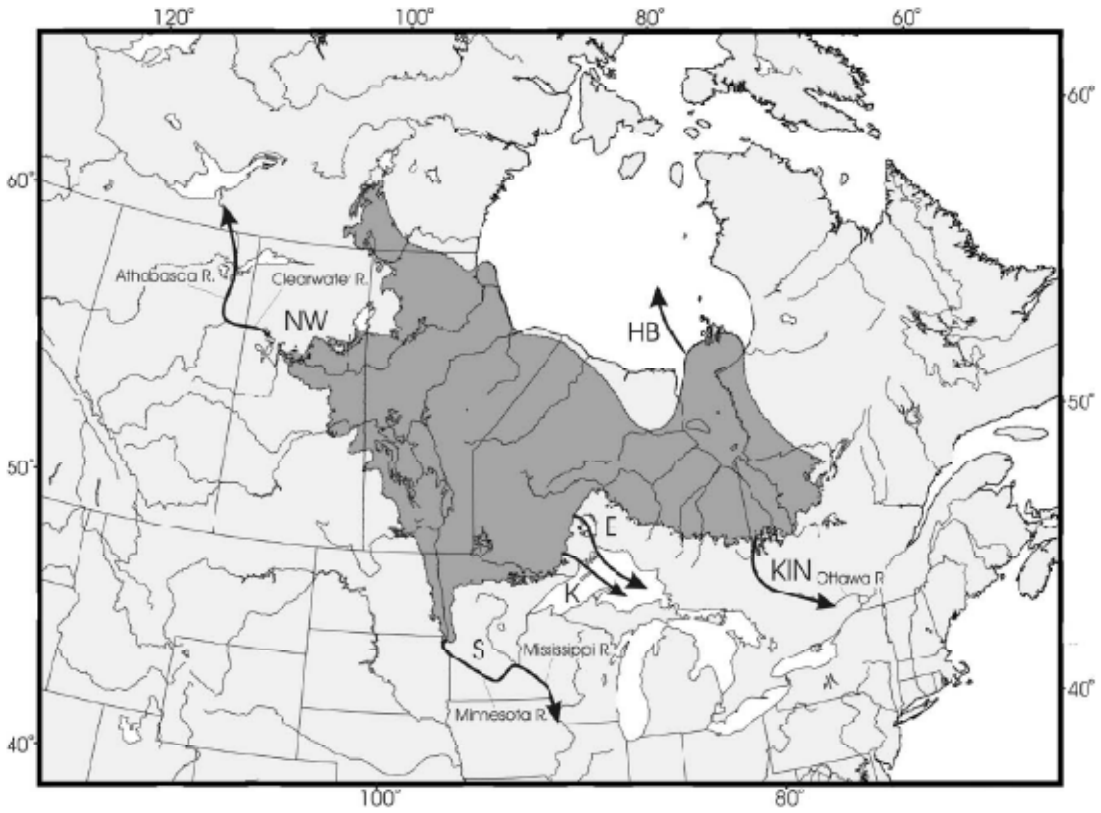

Figure 4. Depiction of the maximum extent of Lake Agassiz during its 5.0 ka cal yr history, indicating the three major outlets before the lake finally drained north into Hudson Bay. Main routes of overflow are indicated by arrows and letters; NW = northwestern outlet, S = southern outlet, K = eastern outlets through Thunder Bay area, E = eastern outlets through Nipigon basin, KIN = Kinojevis outlet, HB = Hudson Bay route of final drainage (Leverington and Teller, 2003, p. 1261).

The location of the discharge pathways not only affected the area and depth of Lake Agassiz (Teller and Leverington, 2003), it also affected the local and regional climate in the northern portions of North America, and more globally (Alley, 2000). Specifically, catastrophic Lake Agassiz discharges into the Arctic and/or North Atlantic oceans (Clark et al., 2001) affected ocean currents by interfering with ocean surface currents and deep ocean currents (Teller et al., 2005). This influenced the ocean conveyor belt circulation

which is associated with the Earth's heat distribution mechanism, and in turn affected global climate by reducing heat flow into the high (North Atlantic) latitudes (Teller et al., 2005).

As the ocean currents stalled or were dramatically reduced, climate cooled and in some areas, the ice margin readvanced southward (Teller et al., 2002). On one occasion, the rerouting of Lake Agassiz overflow prolonged the duration of the end of the last glacial period for about 1000 years around 11 ^{14}C ka BP (~ 12.9 cal ka BP) until about 10 ^{14}C ka BP (~ 11.5 cal ka BP) and initiated the Younger Dryas (Broecker et al., 1989). In the Superior basin this resulted in a lobe of the LIS moving south (the Marquette glacial readvance), covering the eastern Lake Agassiz outlets from about 10.1 to 9.4 ^{14}C ka BP (11.7 to 10.6 cal ka BP) (Teller and Leverington, 2004; Teller et al., 2005). After about 9.4 ^{14}C ka BP (10.6 cal ka BP) the ice margin withdrew far enough to once again permit flow out the eastern outlets (Teller and Thorleifson, 1983; Teller and Clayton, 1983; Teller and Leverington, 2004; Teller et al., 2005). The almost simultaneous changes in the local, regional, and broader paleoclimate indicators, which correspond with those in the Greenland ice cores, demonstrate that much of the Earth underwent abrupt nearly synchronous climate changes at this time (within a few decades) (Dyke, 2005).

The continued retreat of the ice margin down slope into Hudson Bay led to the merger of glacial Lake Agassiz and Ojibway (Figure 1) and eventually these lakes breached the ice margin and drained northward below the LIS ice sheet at about 8.2 cal ka BP (7.3 ^{14}C ka BP) (Barber et al., 1999; Dean et al., 2002). This event not only changed the routing of

overflow from Lake Agassiz and dramatically altered North American hydrology, it also had an impact on ocean circulation and climate, causing the so-called 8.2 ka cooling (Barber et al., 1999). The decay of the LIS continued for a short period after Lake Agassiz drained, and while portions of the ice sheet remained farther north (Figure 2), the major impact of the LIS and its dominating influence on the climate of North America was over (Dean et al., 2002).

1.2.3 Climatic Changes Since the Last Glacial Maximum

Until the end of the last glacial maximum about 23 cal ka BP (Dyke, 2005), the large anticyclone positioned over the ice sheet had dominated conditions south of the ice margin, as strong winds from the west developed from the Pacific to the Atlantic along the ice margin, in conjunction with katabatic winds blowing down slope off the ice sheet and across the thermal gradient between ice and terrestrial terrains (Dyke, 2005; Wolfe et al., 2004; Fisher, 1996). As the LIS margin slowly retreated northward the direct affects of the anticyclone would have moved northward, and would have shrunk in radius, likely dissipating over the region with the deglaciation of Hudson Bay about 7.6 cal ka BP (6.7 ^{14}C ka BP) (Dyke, 2005). The western portion of the continent was deglaciated earlier than the eastern portion, which affected the shape of the jet stream over the continent (Dyke, 2005).

Retreat of the LIS was interrupted during the Younger Dryas, as climate cooled as a result of a massive discharge of Lake Agassiz's fresh water about 12.9 cal ka BP (11.0

^{14}C ka BP) which altered ocean currents (Broecker et al., 1989). In places, the LIS readvanced as climate cooled for about 1300 calendar years (Teller and Leverington). After this, the LIS began its northward withdrawal and once again allowed the anticyclone to shift northward. The magnitude, extent and rapidity of the Younger Dryas climatic change has not been duplicated since this paleoclimatic change (Alley, 2000; Shuman et al., 2002), although several smaller cooling events did result from other influences of fresh water discharges into the oceans (Clark et al., 2001; Teller et al., 2002).

Factors beyond the direct influence of the proximity of the LIS and Lake Agassiz were also likely at play in shaping the atmospheric circulations in the northern portions of North America. The influence of the global climate changes, from glacial to interglacial, would have influenced the climate over central North America as the Pacific air mass became more influential, replacing the cold strong anticyclone winds to the south of the LIS margin, which retreated northwards with the ice sheet margin (Dyke, 2005). The west and northwest winds generated by the influence of Pacific air mass became more dominant (Dyke, 2005), however there were additional localized effects related to the location of the LIS. Katabatic winds across the margin of the ice sheet combined with the strong anticyclone winds circulating over the ice sheet and would have had strong influences over wind direction, frequently bringing winds out of the southeast (Wolfe, et al., 2004). These anticyclonic winds, which extended up to 200 km from the ice sheet, were prevalent up to about 9.0 cal ka BP in western North America and are reflected by the orientations of eolian dune fields (Figure 5) (Wolfe, et al., 2004). As the LIS

retreated to the northeast, the anticyclonic winds would have retreated with it. As the southeast wind reduced in frequency the prevalent direction of the winds of the central plains of North America became those of the more modern winds (i.e. from the west and northwest) (Wolfe, et al., 2004). This complex interrelationship between the changing climate, the retreating LIS, and changes in Lake Agassiz would have resulted in many changes in wind direction and climatic conditions in the region.

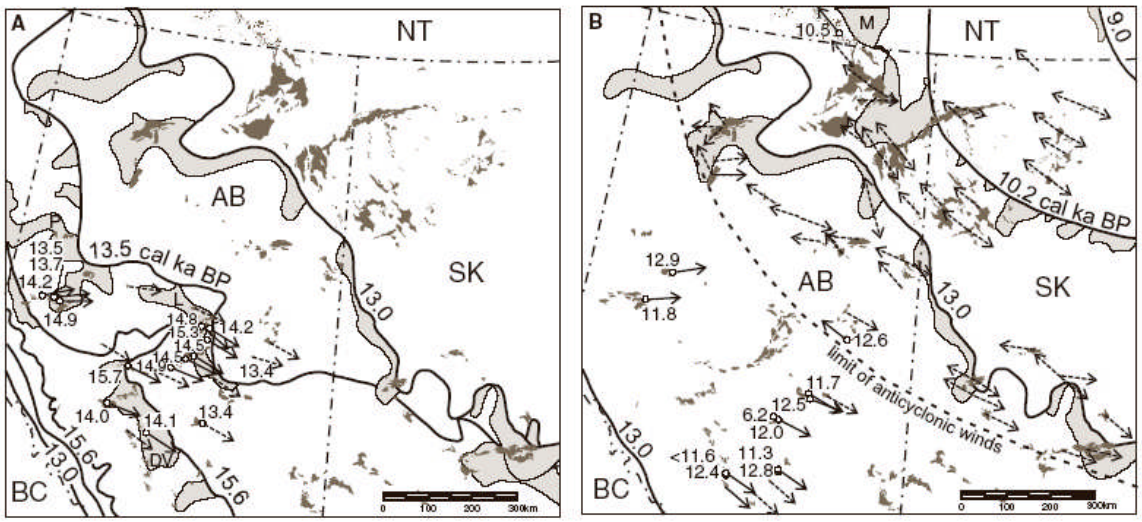

Figure 5. Wind directions, based on dune orientations, related to glacial limits and proglacial lakes for "A" 15.6 cal ka BP and "B" between 13.0 and 9.0 cal ka BP in Alberta and Saskatchewan, Canada. Wind direction is indicated by solid arrows with known timing, and dashed arrows with inferred timing. Glacial lakes are identified (P = Peace, L = Leduc, DV = Drayton Valley and M = McConnell). The limit of anticyclonic winds are identified in "B (Wolfe et al., 2004, p. 232).

The general early Holocene change in atmospheric circulation and its associated anticyclone continued until about 7 cal ka BP (~ 6.1 ^{14}C ka BP) and this climatic influence was reflected in the type and sequences in the biomes (i.e. vegetation and animal assemblages) (Dyke, 2005). These changes in ice margin position in conjunction with the development and fluctuations in margins of developing proglacial lakes, and the

fluctuating climate, resulted in limnological changes in the proglacial lakes (Dean et al. 2002). For example, lakes changed from well-stratified conditions surrounded by the developing boreal forests, to well-mixed open prairie lakes during the drier periods of the mid-Holocene (Dean et al. 2002). The lakes were subject to the more modern north westerly winds, and with the disappearance of forests in the region the exposed lakes were subject to increased mixing (Dean et al. 2002). Winds deposited eolian sediments from the west were recorded in the lacustrine sediments of the region (Dean et al. 2002; Fisher, 1996).

The 8.2 cal ka cold event was recorded in Greenland ice cores and other records on both sides of the Atlantic Ocean (Alley and Augustsdottir, 2005) when a fundamental change in atmospheric circulation occurred after Lake Agassiz drained into Hudson Bay. Following this was the mid-Holocene dry period (Hypsithermal), whose maximum was centred around 5.5 cal ka BP (4.8 ^{14}C ka BP) in central North America (Dean et al. 2002). The end of this unstable warm period marked the beginning of modern atmospheric circulation conditions (Dean et al. 2002).

1.2.4 General Overview of Glacial Lake Agassiz

The retreat of the LIS, discussed in Section 1.2.2, led to formation of a very large proglacial lake, Lake Agassiz, which during its maximum extent connected eastward through Lake Ojibway and discharged to the St. Lawrence River until about 8.5 cal ka BP (7.7 ^{14}C ka BP). Lake Agassiz stretched from the Northwest Territories into Ontario

(Figure 4) at various times in its 5000 year history along the melting glacial margin starting about 13.4 cal ka BP (11.7 ^{14}C ka BP) (Teller and Clayton, 1983; Teller 1985; Teller and Leverington, 2004). The lake was contained in a watershed of approximately 2 million km^2 with the lake's maximum extent (not occupied simultaneously) covering an area of 1 million km^2, primarily controlled by the location of the glacial ice margin and the location of its outlets (Teller and Thorleifson, 1983; Teller, 1985).

The changing climate discussed in Section 1.2.3, in conjunction with differential isostatic rebound and the location of changing outlets, brought about dramatic changes in extent and depth of Lake Agassiz. Five Lake Agassiz phases were identified based on changes in routing of overflow, which variably occurred to the south, northwest, east and north (Figure 4) (Fenton et al., 1983; Teller and Clayton, 1983; Teller, 1985). Many of these changes resulted in relatively rapid falls in lake level.

The fluctuations in this large lake resulted in a very challenging environment for the biota which were trying to establish themselves in these constantly changing conditions. Severe conditions were imposed on the biota such as icebergs, a short ice-free season, and large waves. High volume influxes of water from the west (Kehew and Teller, 1994) and rapid drawdowns of the lake resulting from breaches of the rebounding ice margin (Teller et al., 2002), further perturbed the environment of Lake Agassiz. The relatively rapidly changing extent and depth of the lake was repeated numerous times (Bajc et al., 2000; Teller and Leverington, 2004), adding further challenges to the biota's ability to adapt to the dramatically changing environment, especially at the margins of the lake.

Life did prevail however, and its signatures can be traced in sediments within modern lakes of the region.

Deglaciation of the Rainy River basin near LOTWs occurred during the Lockhart Phase, somewhere between about 11.7 and 10.8 ^{14}C ka BP (13.6 - 12.8 cal ka BP) when Lake Agassiz was at the Herman level (Bajc, 2000). Following deglaciation, water remained at the Herman level until the ice retreated north of the position of the Eagle-Finlayson Moraine to the east of LOTWs (Bajc, 2000). During the Lockhart Phase sediments were deposited in generally less than 100 m of water, while in the subsequent low water Moorehead phase of Lake Agassiz, much of the LOTWs basin was sub aerially exposed (Bajc, 2000; Yang and Teller, 2005). Deposition of Emerson Phase sediments began when the Marquette readvance occurred and the eastern outlets of the Superior Basin were dammed causing water levels to rise until at least 9.5 ^{14}C ka BP (10.7 cal ka BP) in the Rainy River watershed (Bajc, 2000). When the ice margin retreated to the north the eastern outlets again were exposed and the Lake Nipigon Phase of Lake Agassiz began (Figure 6) with the overflow directed eastward, first to Lake Superior, and then North of Lake Superior into Lake Ojibway and the Ottawa River (Teller and Leverington, 2005).

The final low-water phase of Lake Agassiz resulted in the isolation of the LOTWs basin, ending their common paleohydrology and subsequently initiated climatic changes in the LOTWs and SL watershed (Dean et al. 2002; Yang and Teller, 2005). The final drainage of Lake Agassiz was into Hudson Bay at 8.2 cal. ka B.P. (~ 7.3 ^{14}C ka BP) (Dean et al. 2002; Barber et al. 1999) which initiated the final phase of climatic change in the

Northern Great Plains and LOTWs region (Dean et al., 2002), which had separated from Lake Agassiz at about 9.0 cal ka BP (8.1 ^{14}C ka BP) (Yang and Teller, 2005).

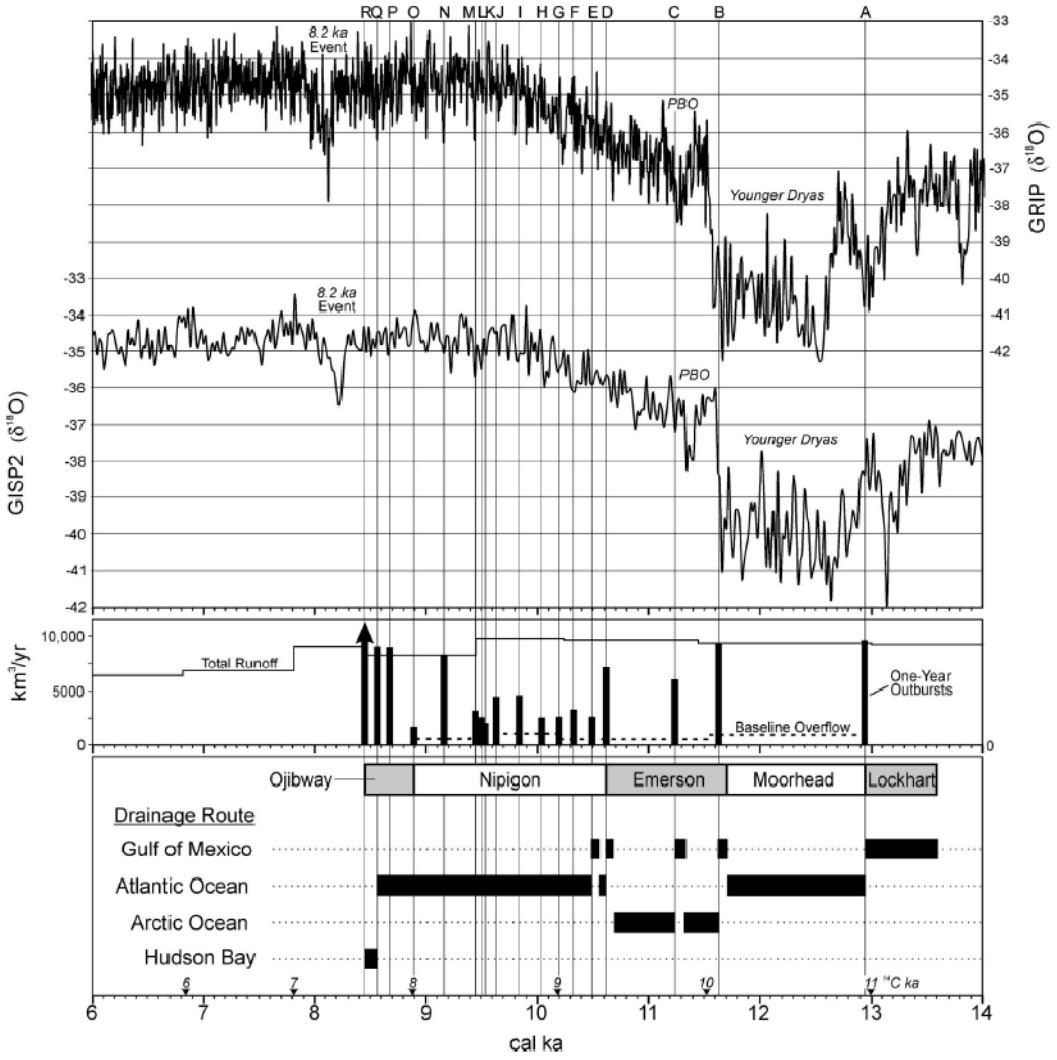

Figure 6. Lake Agassiz outbursts as indicated by the δ ^{18}O record in GISP2 cores plotted against cal ka dates. The five Lake Agassiz phases are indicated and catastrophic outbursts from Lake Agassiz are noted as A-R. Negative isotopic responses to the Younger Dryas, Preboreal Oscillation, and the 8.2 ka event are identified. Lake Agassiz outbursts were interpreted to occur over a 1 yr period and are depicted by a bar with its height related to total outburst volume, with the final outburst of 163,000 km^3 indicated by an arrow (Teller and Leverington, 2004, p. 739).

The final draining of Lake Agassiz initiated a dramatic change in climate of the north central portion of North America (Clarke et al., 2004; Dean et al. 2002), as the ice sheet

disintegrated and Lake Agassiz disappeared completely leaving only isolated remnants of the proglacial lake. A global climate perturbation once again rapidly occurred somewhat similar to the Younger Dryas event, as freshwater flooded into Hudson Bay and the North Atlantic, affecting thermohaline circulation (Figure 6) (Alley and Augustsdottir, 2005). This cooling event however was relatively short lived (Figure 6) as return to glacial conditions, in the absence of the large LIS, would no longer be likely with the ice sheet essentially gone. The cooling influences of the ice sheet and proglacial lake, and the associated influences of the large anticyclonic winds, were no longer at play. The cooling effect from the introduction of fresh water through Hudson Bay would likely be insufficient to allow the climate to cool significantly although other regions around North Atlantic do record a cooling for up to a century or two (Alley and Augustsdottir, 2005).

The final draining of Lake Agassiz occurred about 1000 years after Lake Agassiz and LOTWs were estimated to have separated at 9.0 cal ka BP (8.1 ^{14}C ka BP) (Yang and Teller, 2005). This ended the influence of both Lake Agassiz and the LIS on the climate of North America and the LOTWs region. The influence of the lake would have slowly declined in the LOTWs region as the remnants of Lake Agassiz slowly drained due to the influences of differential rebound, and the warming climate affected the hydrological budget of the remaining remnants of the lake such as LOTWs and SL. The climate continued to warm and moved through the unstable warm interval of the Hypisthermal, and finally reached the relatively stable modern climatic conditions.

1.3 GENERAL HOLOCENE HISTORY OF LAKE OF THE WOODS AND SHOAL LAKE

1.3.1 General

The LIS withdrew from LOTWs region before 11.0 cal ka BP (10 ^{14}C ka BP) (McMillan et al., 2003) and proglacial Lake Agassiz then dominated the region for the next thousand or so years. At about 11 cal ka BP (9.6 ^{14}C ka BP) Lake Agassiz was at its deepest (~ 132 m) in the LOTWs region (Yang and Teller, 2005). Lake Agassiz continued its complex hydrologic history and overflowed through the eastern outlets at times as significant outbursts above a baseline flow (Figure 6). As early as 10 cal ka BP LOTWs was barely linked to Lake Agassiz, and by about 9.0 cal ka BP (8.1 ^{14}C ka BP) LOTWs and SL became hydrologically independent from Lake Agassiz (Yang and Teller, 2005; Teller and Leverington, 2004).

The late Quaternary history of the LOTWs region slowly changed from being buried under the thick ice of the LIS to being part of the bathymetry of Lake Agassiz. When LOTWs became isolated from Lake Agassiz, it was already reacting to regional differential isostatic rebound from the withdrawal of the LIS to the northeast. This rebound, and the influences of the warming post glacial climate during the unstable warm climate of the Hypsithermal in the mid-Holocene, about 9.5 - 4.5 cal ka BP (8.4 - 4 ^{14}C ka BP) (Teller and Last, 1982; Laird and Cumming, 2008; Clark et al., 2002), affected the hydrology of LOTWs. The late Holocene environment progressively moved toward the slightly cooler modern environment of the past millennium (Teller et al., 2005). All of

these changes would have had a significant influence on the hydrologic budget of both LOTWs and SL.

Differential isostatic rebound would have resulted in a southward movement of the shoreline, as the LOTWs outlets into the Winnipeg River at the north end of the lake rose relative to the main body of the lake to the south. This generally increased the depth of LOTWs and SL south of the overflow outlet, and resulted in a southward transgression of the shoreline (Figure 10), assuming the hydraulic budget was positive (Yang and Teller, 2005). The relationship of SL with LOTWs would most likely be primarily driven by climate change influences alone, as the isostatic rebound between the Winnipeg River outlets and the shallow interconnecting channel sill to SL, at Ash rapids, would be minimal since it is at or near the same isobase on the northern portion of LOTWs (Figure 7).

From the spatial variation in the elevation of the beaches of Lake Agassiz and an empirical formula developed by Lewis and Thorleifson (2003), the isostatic rebound of both the Lake Agassiz period and later stages in the LOTWs region can be determined (Yang and Teller, 2005). Based on this information the reconstructions of the paleotopography of the region and the paleobathymetry of the LOTWs and a portion of SL were made showing their extent and depth (Figure 8, Figure 9 and Figure 10) (Yang, and Teller, 2005), and are presented below.

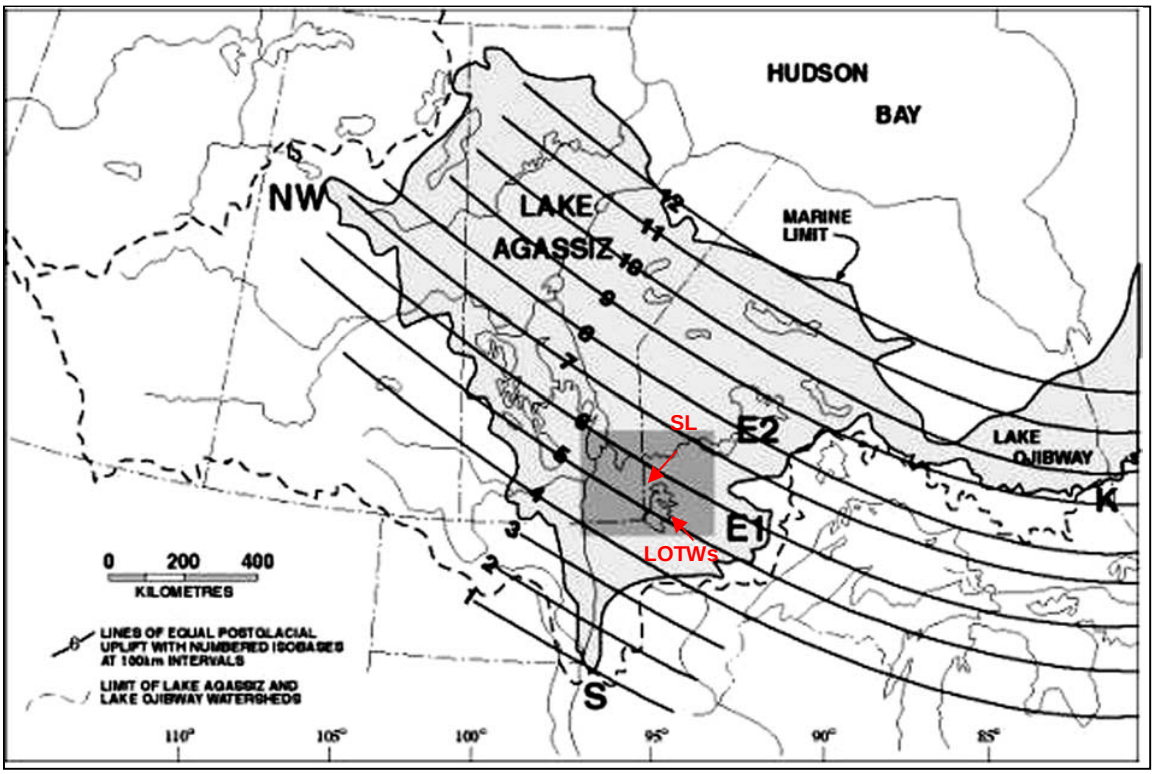

Figure 7. Map of glacial Lake Agassiz region with isobase lines (lines of equal uplift) indicated in bold and proglacial lakes Agassiz and Ojibway indicated in grey. Watershed limits are indicated by dashed lines and the location of the major outlets indicated (NW = northwest; K = eastern; and S = southern) (NW), the east (K) and the southern (S) outlets). The locations of SL and LOTWs are indicated in red. (After Yang and Teller, 2005, p. 485).

The isolation of LOTWs from Lake Agassiz was nearly complete by 10.0 cal ka BP (9.6 ^{14}C ka BP) resulting from the opening of the lower eastern outlets, which lowered the level of Lake Agassiz (Teller et al., 2008). This isolation allowed LOTWs and SL to operate within their own hydrologic systems (Yang and Teller, 2005).

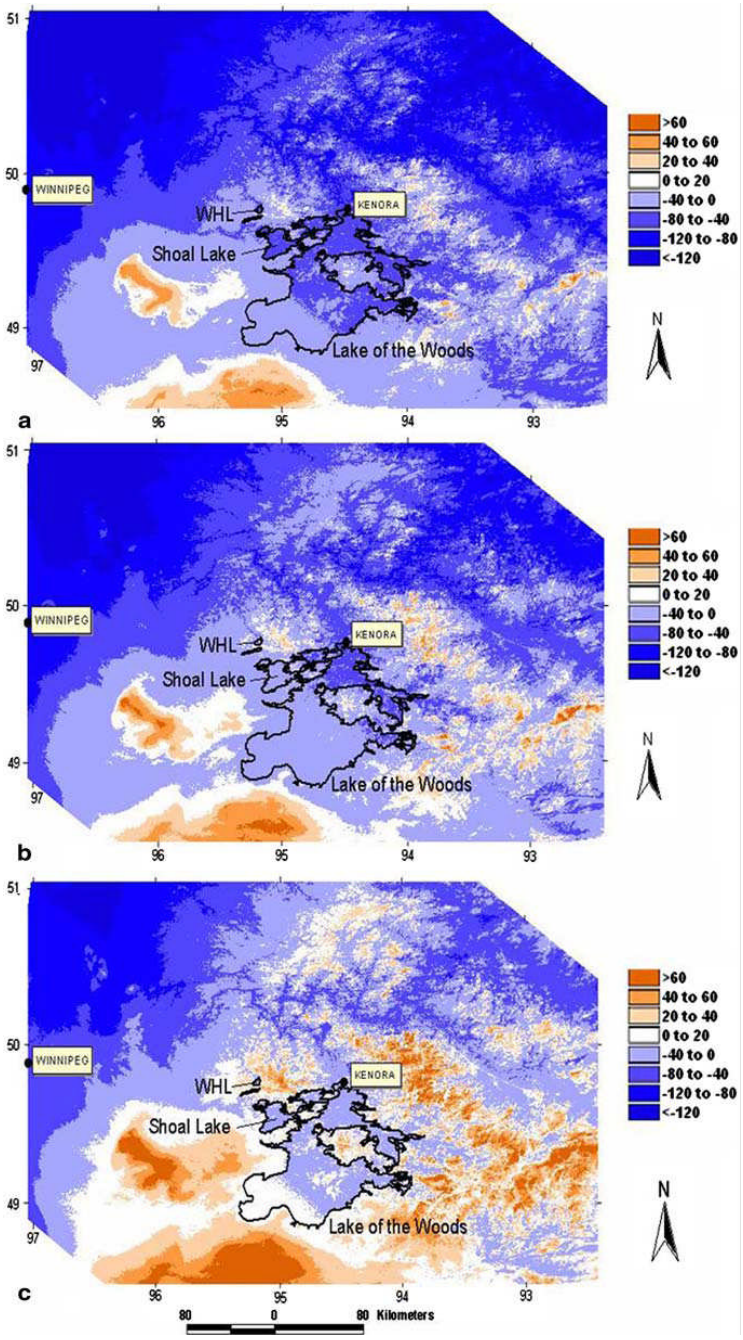

Figure 8. Paleomaps of the LOTWs region indicating the changes in topography and bathymetry as Lake Agassiz regressed from the region at (a) 11.0 cal ka BP, (b) 10.5 cal ka BP, and (c) 10.0 cal ka BP. Blue colours = water with depth in m, and white to dark brown = elevation at or above the water surface in m (Teller et al., 2008, p. 681).

1.3.2 Isolation of Lake of the Woods and Shoal Lake from Lake Agassiz

Following isolation of LOTWs and SL from Lake Agassiz, terrestrial inputs from the drying of former Lake Agassiz sediments surrounding LOTWs (Figure 9), would continue into the new hydrologically independent LOTWs and SL and their watershed, providing inputs of sediments containing $CaCO_3$ into the lakes. This persisting input of former Lake Agassiz sediments would likely continue prolonging the influence of Lake Agassiz over LOTWs and SL, until the newly exposed Lake Agassiz watershed was stabilized with the developing vegetative cover (Dean et al., 2002).

After the complete separation of Lake of the Woods from Lake Agassiz estimated at 9000 cal ka BP (8.1 ^{14}C ka BP) (Figure 9), LOTWs occupied the isostatically depressed northern part of the basin (Figure 10) (Yang and Teller, 2005).

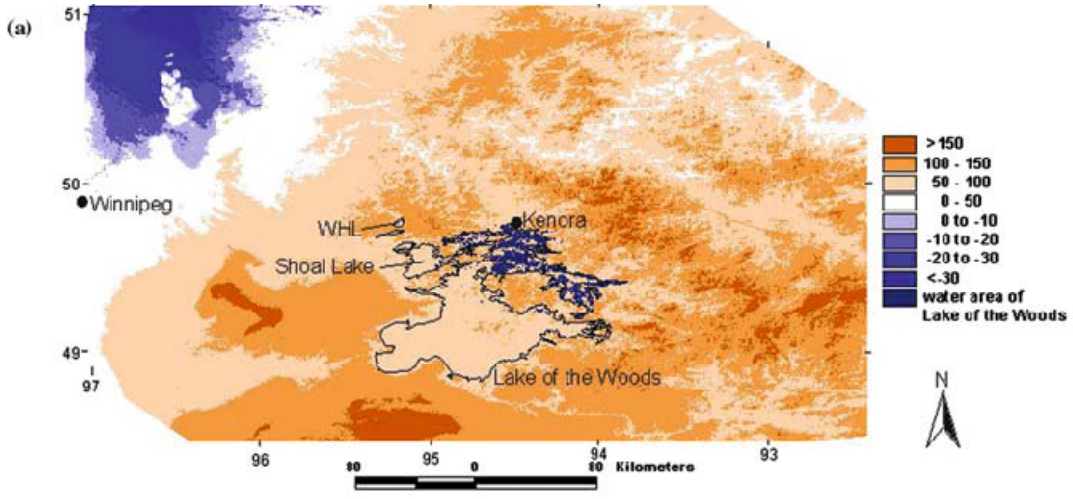

Figure 9. Paleomap of the LOTWs region indicating the topography and bathymetry of LOTWs after Lake Agassiz separated from LOTWs at about 9.0 cal ka BP. Blue colours = water with depth in m, and white to dark orange = elevation at or above the water surface in m (Yang and Teller, 2005, p. 493).

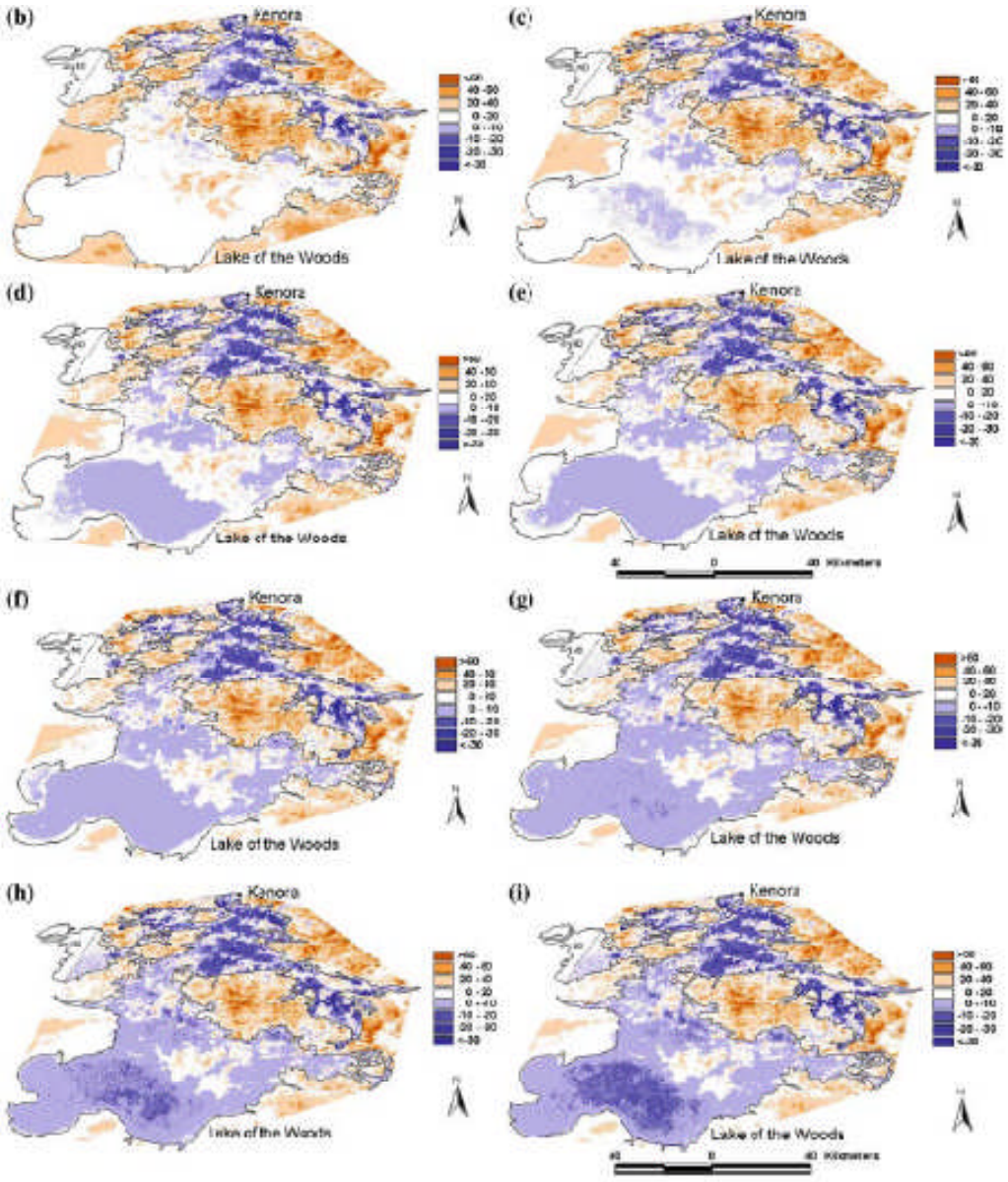

Figure 10. Paleomap of the LOTWs region indicating the topography and bathymetry of LOTWs after separation from Lake Agassiz and its transgression to the south; (b) 8.0 cal ka BP (c) 7.0 cal ka BP, (d) 6.0 cal ka BP, (e) 5.0 cal ka BP, (f) 4.0 cal ka BP, (g) 3.0 cal ka BP, (h) 2.0 cal ka BP, and (i)1.0 cal ka BP. Blue colours = water with depth in m, and white to dark orange = elevation at or above the water surface in m (Yang and Teller, 2005, p. 493).

The areal expansion of the lake shown in Figure 10 and Table 1, was controlled by the elevation of the northern outlets (overflow spilled into the Winnipeg River watershed and

subsequently into the Lake Winnipeg basin), and runoffs into LOTWs, with the main runoff into the modern lake from the Rainy River watershed.

Table 1: Evolution of Aerial Extent, Bathymetry and Volume of LOTWs

Periods	Cal yrs BP	Maximum Depth (m)	Mean Depth (m)	Area (km^2)	Volume (km^3)
LOTWs Period	Present	66.9	8.1	4524	37
	1000	67.0	7.6	4415	34
	2000	67.0	7.4	4292	32
	3000	66.0	6.9	4052	28
	4000	66.0	6.3	3676	23
	5000	65.0	5.8	3227	19
	6000	65.0	5.6	2857	16
	7000	64.0	6.1	1822	11
	8000	63.0	8.3	1061	9
	9000	61.0	8.5	858	7
Lake Agassiz Period	10,000	89.0	14.7	-	-
	10,500	116.0	31.4	-	-
	11,000	132.0	43.8	-	-

From Yang and Teller, 2005, p. 494.

Depending on the overall hydrologic budget, which would be strongly affected by the changing climate, the stabilizing effects of flora on the watershed's runoff, and the mechanics of the differential isostatic rebound, LOTWs either occupied the full extent of the new configuration of the lake basin, or a subset of the full extent of the basin based on the hydrologic budget (Figure 10) (Yang and Teller 2005).

The regional climate variability, in conjunction with the differential isostatic rebound, would have significant impacts on shallower portions of the LOTWs and on the interconnection into SL. Compartmentalization of portions of the shallow southern basin and disconnection of the northern and southern parts of the LOTWs basin would have been likely during lake lowstands. Deeper channels connecting the compartments and

the northern and southern basins would permit Rainy River input and overflow into the Winnipeg River. These flows would have decreased/ceased during negative water budget intervals. SL with its generally deeper basin would likely be less affected aerially, however would have become independent from LOTWs whenever the level of LOTWs fell below the shallow ledge in the interconnecting channel.

1.4 MODERN LAKE OF THE WOODS AND SHOAL LAKE WATERSHED

1.4.1 Introduction

The location of LOTWs along the international border between Canada and the U.S. makes it an international body of water. It is subject to a special treaty between the two countries, which was negotiated through the International Joint Commission's (IJC). Since 1925 this required the Canadian Lake of the Woods Control Board to regulate the outflows from the lake to maintain lake levels within specified limits. SL was also included in the IJC jurisdiction due to its interconnection with LOTWs and the city of Winnipeg's use of this body of water for its water supply.

LOTWs spans the border of the provinces of Manitoba and Ontario, as well as that of the state of Minnesota, and as such is subject to the laws of three state/provincial governments, and two federal jurisdictions. This multi-jurisdiction environment can make access to the lake complicated, especially due to the unusual border configuration

of the U.S./Canada border north of the 49th parallel and to the east of the Manitoba border with Ontario. This means this part of Minnesota (known as the Northwest Angle) cannot be reached by land directly from the rest of the state, requiring a border crossing between Minnesota and Manitoba, or alternately it can be reached directly by a water route from Minnesota, without a formal border crossing point.

1.4.2 Description of the LOTWs and SL and their Watersheds

LOTWs and SL are located at a latitude of about 49-50^{o} and a longitude of about 95^{o}, with LOTWs located at the conjunction of the Canadian provinces of Manitoba and Ontario, and the northern boundary of the U.S. state of Minnesota. LOTWs is a highly irregular body of water about 110 km long by 95 km wide, with a complex bathymetry ranging from a relatively shallow southern basin typically 10 m in depth, to much deeper bays in the north and northeast which range to over 70 m in depth. The lake covers approximately 386,000 ha (3860 km^2) and is composed of numerous and distinct basins, with more than 14,500 islands (Pla et al., 2005). The main inflow into LOTWs is from the Rainy River which supplies about 70-75% of the stream inflow (Pla et al., 2005; Yang and Teller, 2005). The inflow interconnects through the southern part of the basin to multiple deep and mostly narrow channels in the Northwest Angle area, into the deeper northern portions of the lake, discharging 13.59 km^3/yr (431 m^3/yr) into the Winnipeg River System (Yang and Teller, 2005). Overall watershed runoff is estimated to be 16.78 km^3/yr including 2.69 km^3/yr of precipitation directly onto the lake, with evaporation from the lake surface of 2.5 km^3/yr, just below the rate of precipitation (Yang

and Teller, 2005). Groundwater inflow and outflow is estimated to result in a net outflow of groundwater of 3.38 km^3/yr (Yang and Teller, 2005). Most of the lake lies on the granitic bedrock of the Precambrian Shield (Figure 15), however the Rainy River watershed and the southern part of LOTWs watershed (Figure 11) overlie the lake sediments of glacial Lake Agassiz (Figure 16) (Pla et al., 2005).

The LOTWs (including SL) watershed is part of a broader watershed which feeds the Winnipeg River joining other Winnipeg River watersheds (Figure 11) and ultimately feeds 45 % of Lake Winnipeg's total inflow into its southern basin (St. George, 2006). On average, about 50% of this total Winnipeg River inflow to Lake Winnipeg comes from LOTWs (LWCB, 2002).

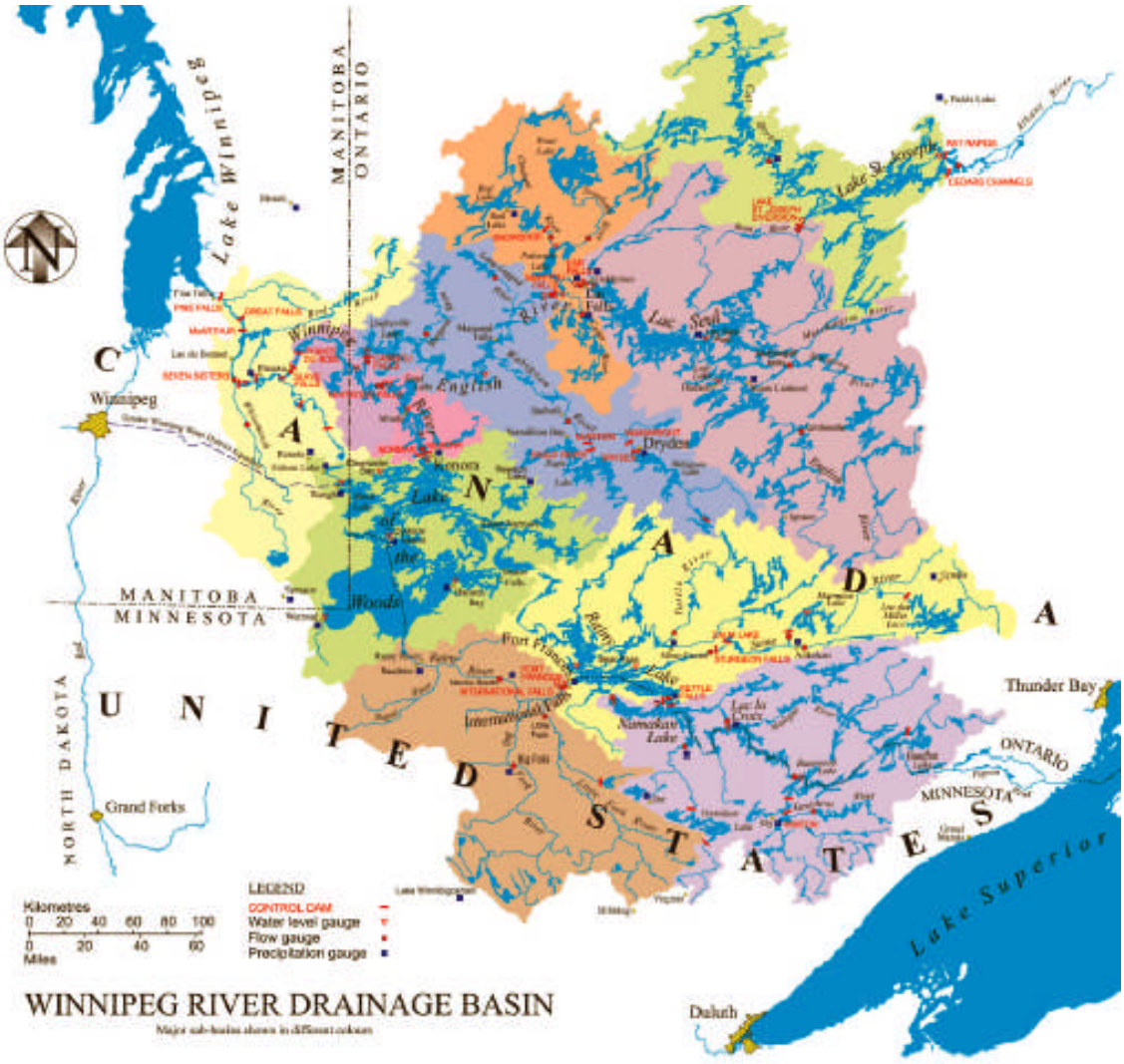

Figure 11. Winnipeg River watershed including the LOTWs and Rainy River watersheds (Lake of the Woods Control Board brochure, 2002, p. 10).

The lake is primarily separated into two zones by the Aulneau Peninsula which lies in an approximately east/west orientation and separates the shallow southern basin from the deeper basins in the north and northeast. The lake is a complex network of islands, channels, broad expanses of open water, and deep bays, many of which are almost independent of the main open portions of the lake (Figure 12).

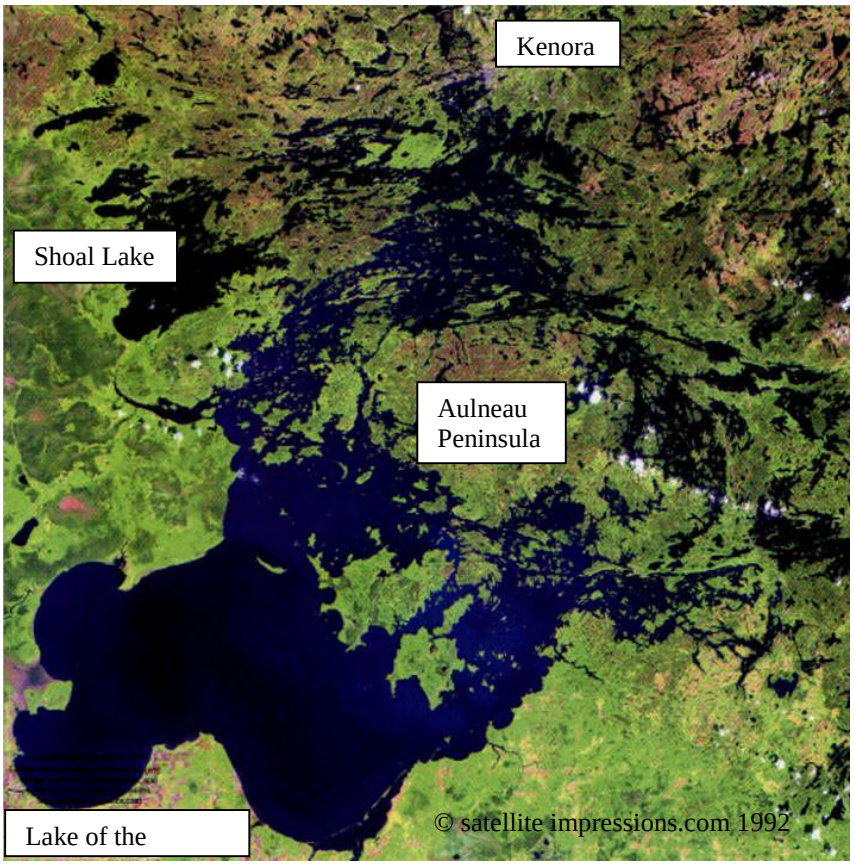

Figure 12. Aerial photo of LOTWs and SL indicating the location of Kenora and the nearby outlets to the Winnipeg River (after http://www.virtualnorth.net/satimp/).

There are three natural outlets in the northern portion of the lake into the Winnipeg River. Only two channels are currently operational as the third shallower intermittent channel was filled in (Figure 13) (LWCB, 2002). The third natural channel at Portage Bay operated during high water conditions (Figure 13) (LWCB, 2002). LOTWs outflow is now controlled through the jurisdiction of the Lake of the Woods Control Board, which regulates the flow through the enlarged eastern and western outlets (enlarged for power generation with the ability to permit compliance with international agreements for LOTWs level control) (LWCB, 2002). Lake levels typically fluctuate between 0.9 and 1.2 m (Pla et al., 2005).

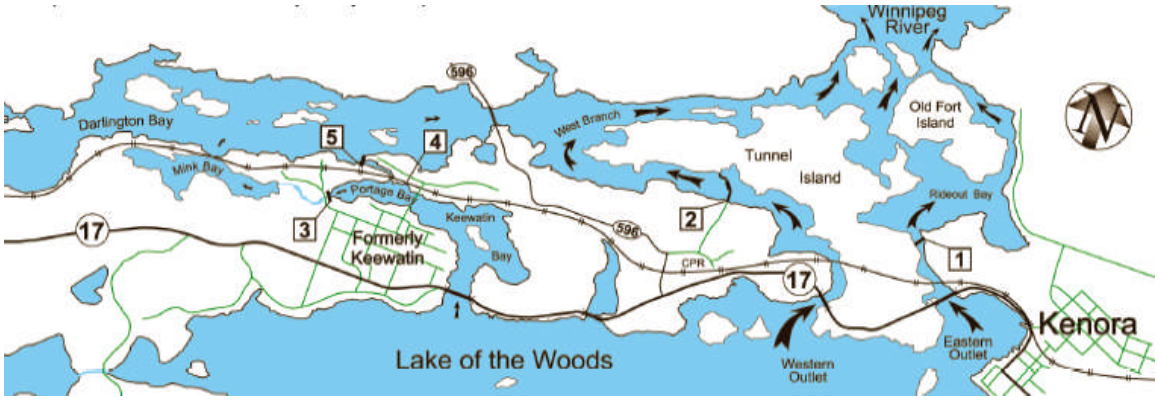

Figure 13. Winnipeg River outlets from LOTWs into the Winnipeg River near Kenora, Ontario. Site 1 (Kenora powerhouse) and Site 2 (Norman dam and powerhouse) are in the two main outlets into the Winnipeg River, with the Site 2 so-called Western channel taking about 75% of the flow. The third natural channel is through Portage Bay but only a small flow (3 m^3/s) can occur at Site 3 (gated culvert), with Site 5 (the old mill) no longer receiving any flow due to the filling of the channel to the mill at Site 4 (Lake of the Woods Control Board brochure, 2002, p. 7).

SL is located to the northwest of the main body of LOTWs straddling the Manitoba-Ontario Border at about 49.5 °N latitude and has a surface area of 260 km^2 which lies within a relatively small 960 km^2 watershed (Shoal Lake Watershed Management Plan, 2001). It receives inflow from the smaller Falcon Lake via High Lake watersheds through the Falcon River (Shoal Lake Watershed Management Plan, 2001). It generally has the same typically deep characteristics as the northern portions of LOTWs, with the exception of the interconnecting channel at Ash Rapids, which narrows and shallows. This interconnection was deepened around the turn of the 20th century, to its current 10 m width and 1.5 m depth (at the centre of the channel at the low level datum), subsequent to dams being constructed on the LOTWs Winnipeg River outlets (Shoal Lake Watershed Management Plan, 2001). The controls established in LOTWs in conjunction with the use of water from SL for the City of Winnipeg water supply, and variations in watershed runoff between the small SL watershed and much larger LOTWs watershed now causes

the natural inflow into LOTWs to reverse at times (Shoal Lake Watershed Management Plan, 2001).

The LOTWs and SL watershed, and the Rainy River watershed flowing into LOTWs from the south, are all currently near the western limit of the LOTWs Boreal Wetland Region (Figure 14) which is dominated by continental air masses (Bajc et al., 2000). The location of the air masses produce July mean air temperatures of 18 °C and January mean air temperatures of minus 15 °C, with ~ 710 mm of annual precipitation, two-thirds of which occurs as rain during summer (Bajc et al., 2000).

The high degree of complexity of LOTWs extends to its physical geography (Figure 12), bathymetry and ecological systems, and this produces highly variable biotic systems (Pla et al., 2005). LOTWs is an unusual Precambrian Shield lake influenced by glacial Lake Agassiz deposits, with relatively hard water and with a pH between 7-8 (Molot et al., 1987; Pla et al., 2005). LOTWs pH values vary from a low of 7.5 in Rainy River and 7.8 near Kenora with the south east portions of the lake lower, and the deeper northern bays such as Clearwater Bay ranging up to a pH of 7.9 (Molot, 1987; Pla et al., 2005). Big Traverse Bay in the south basin had a relatively uncharacteristic value of pH of 8.0 (Molot, 1987). Shoal Lake values are even higher at a pH of 8.2 (Molot, 1987). These variations across LOTWs including the Rainy River and SL are indicative of the complexity of LOTWs (Pla, et al., 2005) and its watershed. These variations in conditions are reflected in modern and historical ecology (Laird and Cumming, 2008).

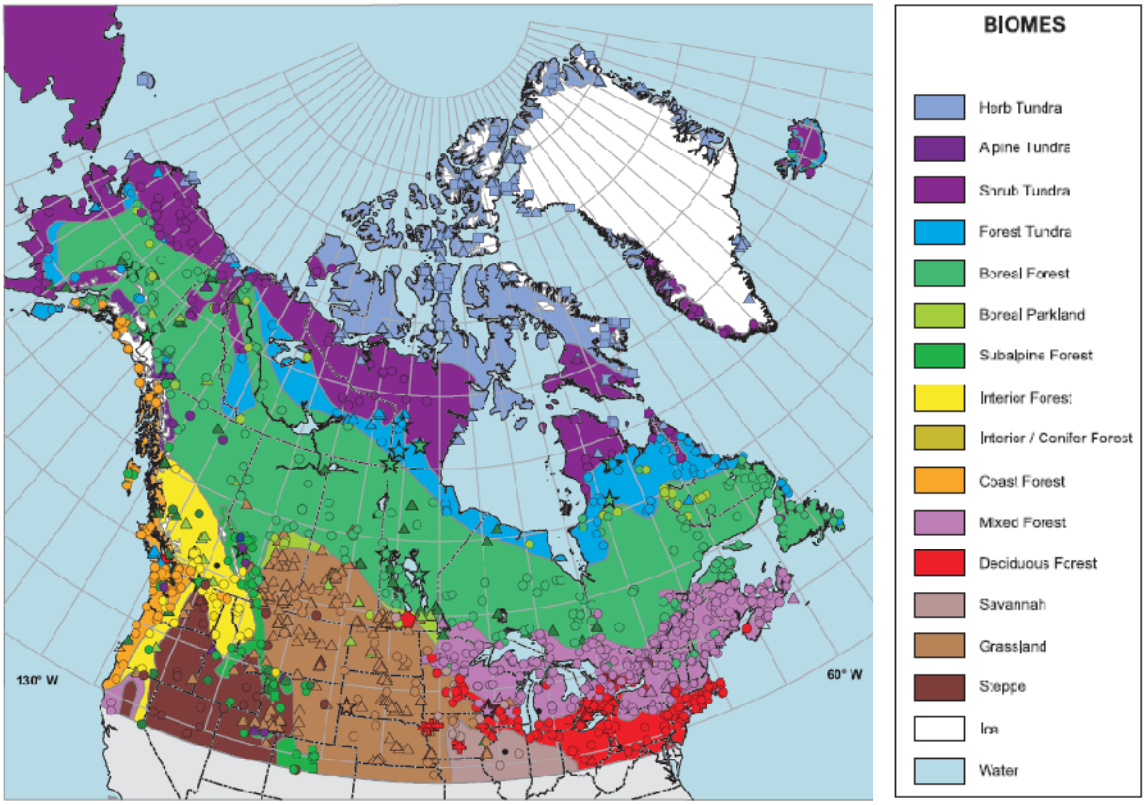

Figure 14. Biomes at 1000 yrs BP in the LOTWs region. This biome has remained relatively unchanged for the past millennium (after Dyke, 2005 p. 244).

1.4.3 Geology of the Modern Lake of the Woods and Shoal Lake Watershed/Region

LOTWs is underlain by Precambrian granite-greenstone of the Wabigoon Subprovince consisting of metavolcanic and metasedimentary rocks with granitoid intrusions (Minning et al., 1994) (Figure 15). The predominant underlying geology of the LOTWs watershed is a pink granodiorite, with overlying thin moss soils in places (Schindler et al., 1996). Quaternary deposits include glacial deposits consisting of tills, sands and gravels (with a few locations containing Paleozoic rocks), and include lacustrine silts and clays which occur in various locations within the LOTWs watershed and within the lake

basin (Figure 16), with generally thin and patchy Quaternary sediments with thicker glaciolacustrine deposits south of the Aulneau Peninsula and south of SL (Minning et al., 1994).

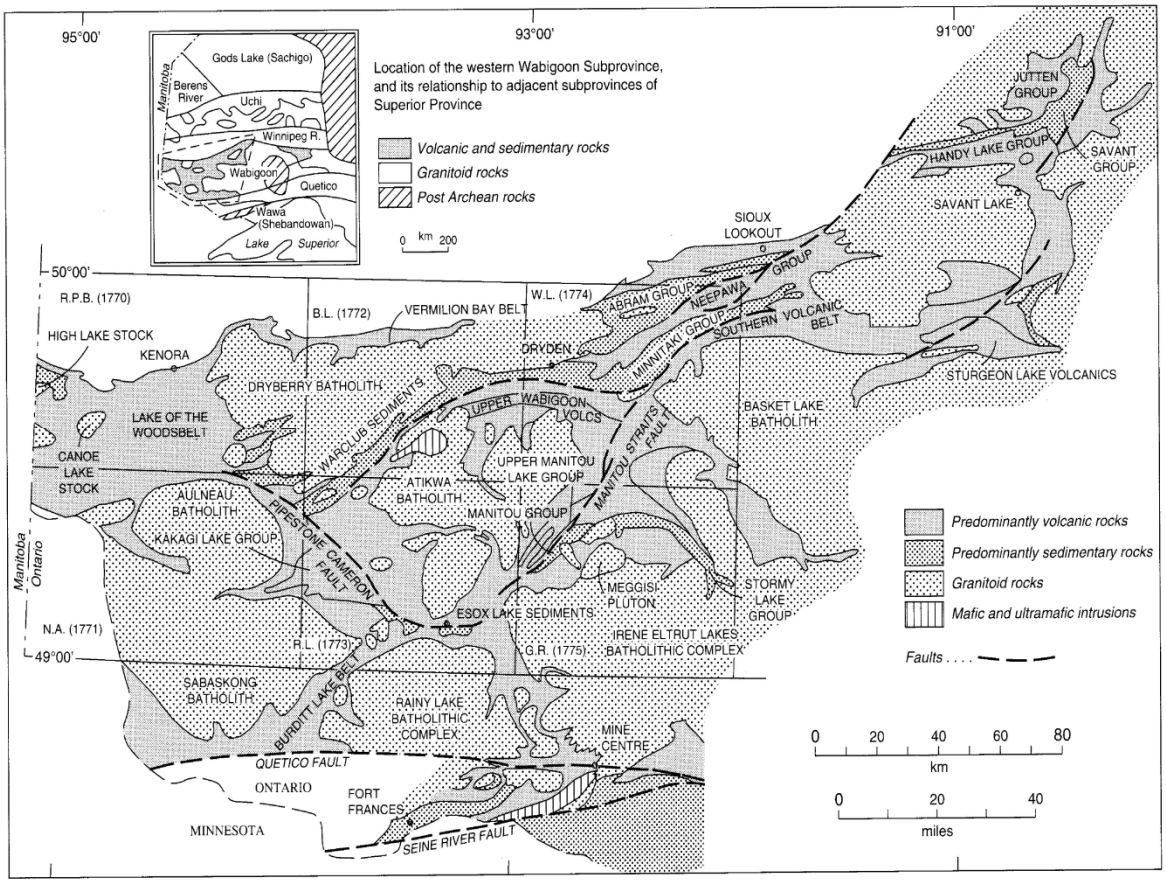

Figure 15. Western Wabigoon subprovince simplified bedrock geology including the LOTWs region (Minning et al., 1994, 2005 p. 11).

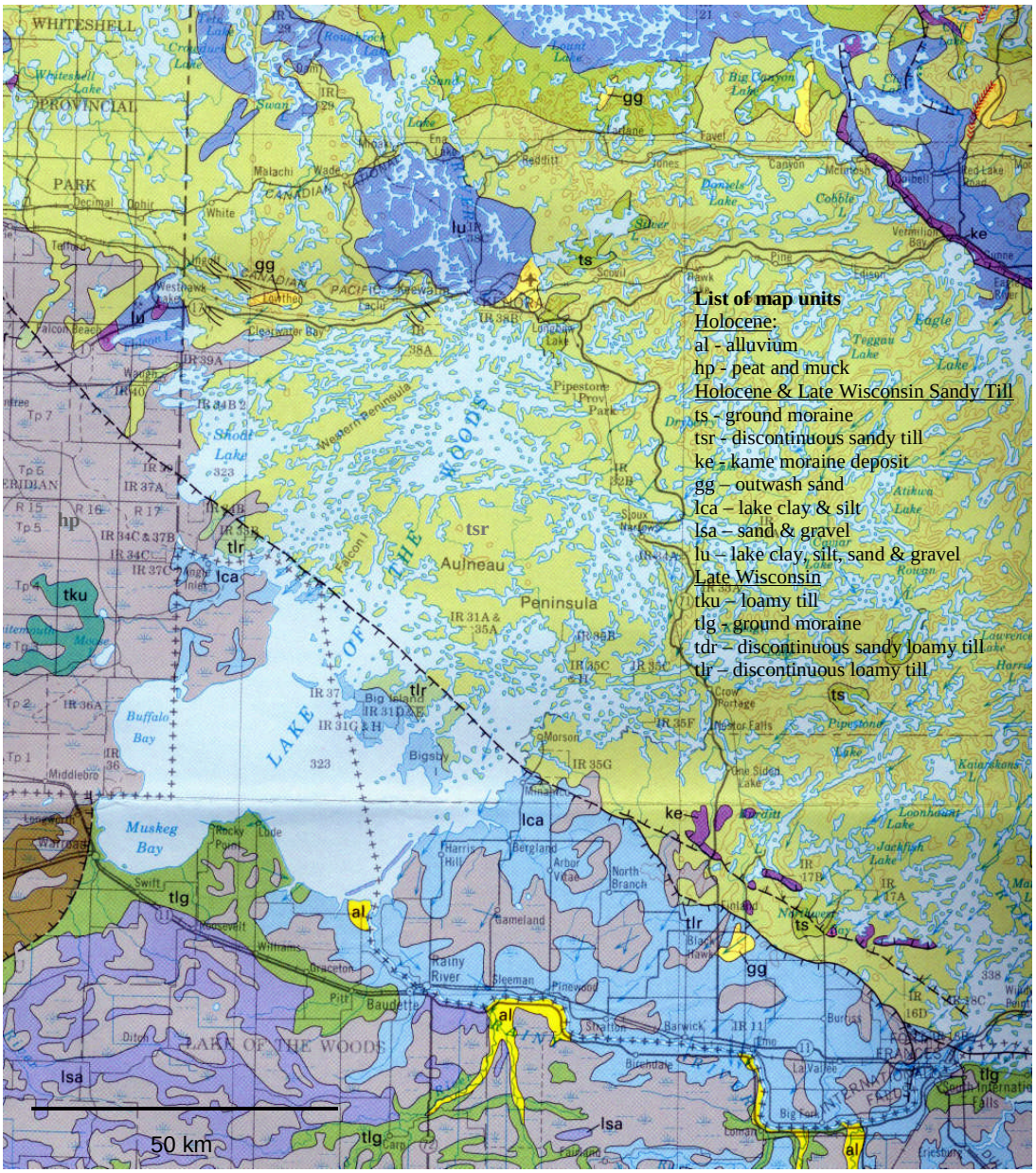

Figure 16. Quaternary geologic map of LOTWs. Note al unit not mapped in Ontario where a different alluvium is defined (after Sado et al., 1995, from map NM-15).

Thick deep water sediments (from 1-75 m) of laminated to varved clay, silt and fine sand, are found in depressions and are found throughout the watershed (Maps 1770A through 1175A; Minning et al., 1994). Calcareous components reportedly occur only rarely in

these thin widely spaced sediments based on Map 1771A (Surficial Geology Northwest Angle), although specifically sampled sediments and clasts in LOTWs reacted to dilute hydrochloric acid and are believed to be calcareous till and reworked till from Paleozoic bedrock carbonate debris, possibly from the Manitoba lowlands and Hudson Bay (Minning et al., 1994). A number of the units identified in Figure 16 include calcareous components (Sado et al., 1995). Unit "al" along the Rainy River is described as containing pebbles cobbles and boulders of limestone and dolomite while the Holocene and Wisconsin sandy till units (gg, lca, and lsa) contain non calcareous to weakly calcareous components, while the Late Wisconsin loamy till (tku) which likely underlies the peat and muck to the west of LOTWs and SL (unit hp) (Teller and Fenton, 1980) is described as having a very calcareous matrix with up to 50% carbonate (Sado et al., 1995). Additionally, Schindler et al., 1996, report Paleozoic carbonate rocks in the glacial drift are a source of carbonates to LOTWs and SL with further inputs from Lake Agassiz sediments. The availability of these calcareous components is important to any biota which develop $CaCO_3$ shells.

1.5 HOLOCENE PALEOCLIMATE HISTORY BASED ON OTHER STUDIES

1.5.1 General

Since the last glacial maximum, the climate of the LOTWs region has undergone dramatic changes. Proximity of the ice margin and extent of proglacial lakes, particularly Lake Agassiz, were major climate driving forces during the early post glacial period.

LOTWs region eventually emerged from the direct influence of the LIS and Lake Agassiz, however it remained closely linked to these influences as the local climate reacted to the katabatic winds, prevailing winds blowing off Lake Agassiz or the anticyclonic winds circulating above and beyond the margins of the glacier farther to the north. As the LIS continued its retreat, the influence of the ice to the northeast, and Lake Agassiz's large cold surface, diminished and the position of the jet stream slowly shifted to the north (Dyke, 2005). The large anticyclone over the ice sheet weakened and finally lost its influence as the position of the jet stream moved to its modern location sometime after the 8.2 ka cold event (Dyke, 2005; Dean et al. 2002).

Based on the electrical conductivity measurements in Greenland ice cores, rapid (decadal) changes in deposition of loess were identified at the glacial-interglacial transition, implying the relatively slow changes in solar insolation were also unlikely to have been the direct cause of the unstable climatic conditions in the Hypsithermal (Taylor et al., 1993). It is more likely changes in atmospheric circulation and temperature gradients between the high and mid-latitudes of North America increased, or decreased wind speeds, and affected the loess data in the Greenland cores (Taylor et al., 1993).

Mid to late Holocene paleoclimate proxies in the LOTWs region indicate significant variation in the location of climatic zones across the region (Dyke, 2005). These variations have been related to changes in the location of convergence zones of the air masses and the record of these changes has been identified in the study of the ecotones (Haskell et al., 1996; Dyke, 2005). The relatively dry westerlies driven by the Pacific air

mass, the outflow of the cold Arctic air mass, and the warm moist tropical Gulf air mass, all converge in the LOTWs region (Haskell et al., 1996; Dyke, 2005). Changes in the location of the convergence of these air masses can result in rapid changes in climate and can causing considerable variability in local climatic conditions (Haskell et al., 1996).

1.5.2 Early Holocene Climate

From about 18 to 7 cal ka BP (14.7 - 6.1 ^{14}C ka BP) the changing atmospheric circulation resulting from the changing geographical position of the convergence of the Pacific, Arctic and tropical air masses, were reflected in the sequencing of biome changes (Dyke, et al., 2005). Deglaciation of the Rainy River basin occurred between 11.7 and 10.8 cal ka BP (10.8 to 9.5 ^{14}C ka BP) (Bajc, 2000) with LOTWs becoming ice-free around 12.9 cal ka BP (11.0 ^{14}C ka BP) (Teller et al., 2000). Lake Agassiz followed the retreating ice and by about 10.2 cal ka BP (9 ^{14}C ka BP) the terrain around LOTWs slowly emerged from under the lake (Bajc, 2000). The emergent terrain was primarily covered by boreal forest (Bajc, 2000). As the climate continued to moderate, grasslands replaced the boreal forest in part of the LOTWs basin (Figure 17) by 8.9 cal ka BP (~8 ^{14}C ka BP) (Dyke et al., 2005).

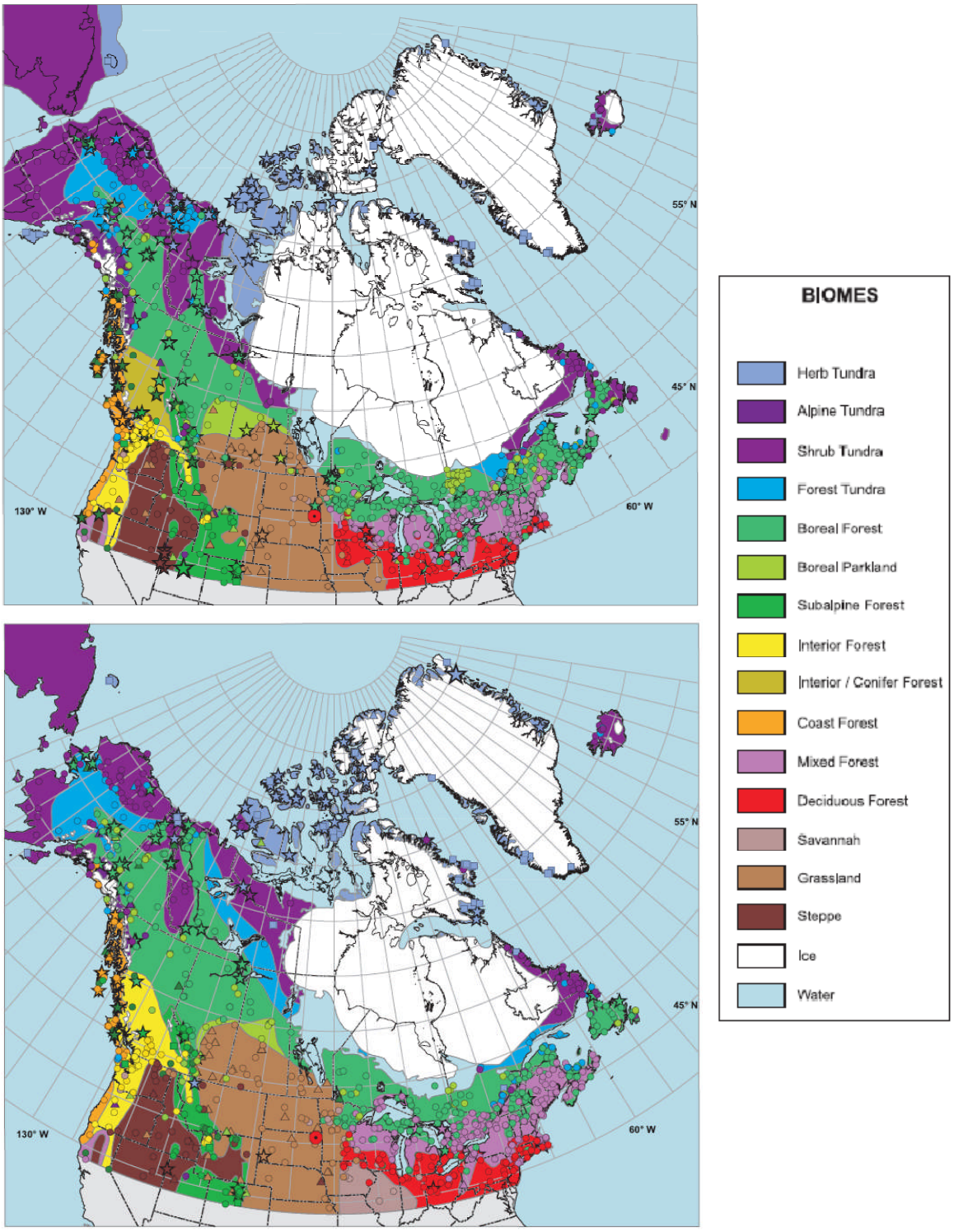

Figure 17. North American Biomes at 9 (upper) and 8 (lower) ^{14}C ka BP indicating locations of boreal forest and grassland biomes near LOTWs region and the position of the LIS and Lake Agassiz/Ojibway. The legend at the right provides the biome legend (stars = macrofossil, triangles = mammal, and circles = pollen sites) (after Dyke, 2005, p. 230 and p. 233).

Variations between boreal forest and grassland biomes followed the climate fluctuations in the early Holocene in the north central portions of North America (Dyke et al., 2005). Biome and climatic reconstructions in the Rainy River watershed, and nearby pollen profiles in northern Minnesota and northwestern Ontario, indicate that from about 11.5 cal ka BP (10.0 ^{14}C ka BP) until at least 10.7 cal ka BP (9.5 ^{14}C ka BP), biomes were similar to modern assemblages (Bajc, 2000). However, a distinct component from much farther north and west was present, making this assemblage similar to the mixed community sites in the mid-continent (Bajc, 2000).

Farther to the east in the Great Lakes it has been hypothesized these large lakes were hydrologically closed during the early to mid-Holocene, due to the drier climate (Lewis et al., 2001). This implies LOTWs and SL were also likely below their outlets at this time.

1.5.3 Mid-Holocene Climate

The mid-Holocene in central North America, about 8.0 - 4.0 cal ka BP (7.1 - 3.7 ^{14}C ka BP), was generally warmer and drier than today with rapid variations in temperature and precipitation occurring, similar to today (Forester et al., 1987). Ostracode studies in Elk Lake, Minnesota, about 300 km to the south of LOTWs, however, indicate portions of this period were colder and drier than today, notably in the interval from 7.8 - 6.7 cal ka BP (~ 6.9 - 5.9 ^{14}C ka BP) (Forester et al., 1987). Overall, the interval from 6.7 - 4.0 cal ka BP (5.9- 3.7 ^{14}C ka BP) had temperatures approaching the modern average mean (3.7 ^{o}C), with warm summers from 6.7 - 5.8 cal ka BP (~ 5.9 - 5.1 ^{14}C ka BP) and only

periodic warm summers in the interval from 5.8 - 4.0 cal ka BP (~ 5.1- 3.7 ^{14}C ka BP) (Figure 18) (Forester et al., 1987).

Sediments in lakes in the Experimental Lakes Area (ELA) near LOTWs, specifically Lake 239, indicate a drier climate with lake levels varying as much as 8 m from the early to the mid-Holocene from about 8.9 - 4.4 cal ka BP (8.0 - 4.0 ^{14}C ka BP) (Laird and Cumming, 2008). The sedimentary record in West Hawk Lake, a small deep lake 40 km to the northwest of LOTWs, indicates a drier interval between 7.1- 4.5 cal ka BP (~ 6.2 - 4.0 ^{14}C ka BP) (Teller at al., 2008). These low moisture conditions are also reflected farther west in Lake Winnipeg, and at the Wampum site just to the west of the south basin of LOTWs (Lewis et al., 2001; Teller et al., 2000). As the Wampum, Manitoba site became a lagoon with Lake Agassiz falling below the Upper Campbell beach level about 10.5 cal ka BP (9.3 ^{14}C ka BP), only minor hydrologic fluctuations (possibly due to groundwater inputs) were noted, except for a possible dry interval between 7.1 to 4.5 cal ka BP (6.2 - 4.0 ^{14}C ka BP); after this, peat accumulation began (Teller et al., 2000). The southern basin of Lake Winnipeg reflects this regional mid-Holocene aridity and Lewis et al., (2001) concluded the basin was desiccated for most of the mid-Holocene from about 8.2 - 4.3 cal ka BP (7.5 - 4.0 ^{14}C ka BP), as a result of this regional aridity and the effects of differential isostatic rebound. Yang and Teller, 2005 proposed that the mid-Holocene warming in the LOTWs region, in conjunction with the effects of differential isostatic rebound, caused the LOTWs to fall below its northern outlets.

Mid-Holocene aridity has been interpreted from lake level data in the northern prairies of the U.S. and Canada, from about 8.3 - 4.5 cal ka BP (~ 7.5 - 4 ^{14}C ka BP) (Laird and Cumming, 2008). Based on pollen, diatoms, and carbon and oxygen isotope data, low precipitation and higher temperatures were detected in nearby West Hawk Lake (Teller et al., 2008). Increasing pine versus spruce pollen between 9.5 and 5.0 cal ka BP (~ 8.4 - 4.4 ^{14}C ka BP) indicates drier conditions in the region, with cooler and wetter conditions evident after this, based on increased organic vs. mineral lithics in the lake sediments (Teller et al., 2008).

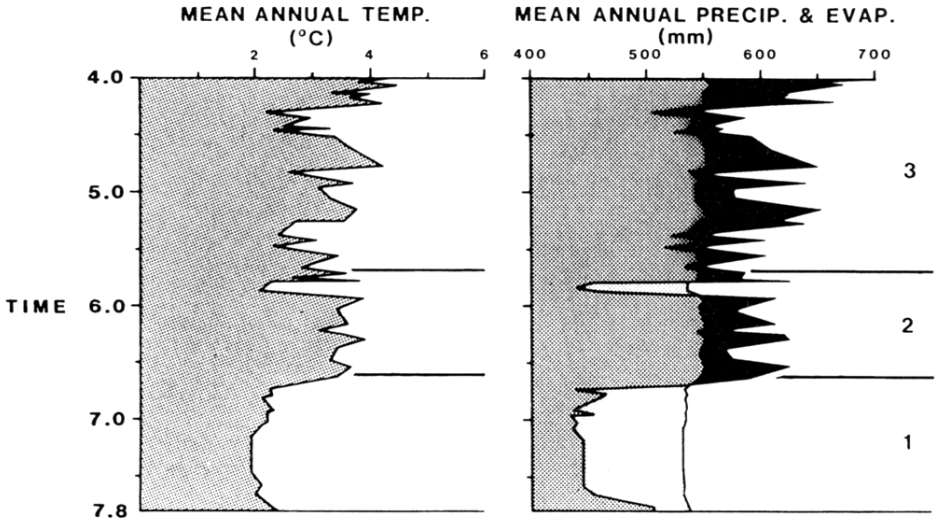

Figure 18. Mean annual temperature (left), and mean annual precipitation and evapotranspiration (right) versus time (cal ka BP), based on ostracode analogs (Forester et al., 1987, p. 266).

Conditions farther to the west in Devils Lake, indicated saline conditions between 10.5 and 8 cal ka BP (9.3 - 7.1 ^{14}C ka BP) with saline conditions reoccurring between 7.5 to 4.5 cal ka BP (~ 6.6 to 4 ^{14}C ka BP), but at a lesser frequency and duration (Haskell et al., 1996). The presence of struvite (hydrous Mg-ammonium-phosphate) in northern North

Dakota lakes during dry periods, deposited by high concentrations of migrating waterfowl, have been detected and related to the end of dry periods in the region (Donovan and Grimm, 2007). These arid periods range from 8.7 to 4.7 cal ka BP (~ 7.9 - 4.1 ^{14}C ka BP) and indicate frequent arid intervals in the early Holocene from about 8.7 to 8.1 cal ka BP (~ 7.9 - 7.2 ^{14}C ka BP) into the mid-Holocene, with the youngest identified in the late Holocene at 2.7 cal ka BP (~ 2.6 ^{14}C ka BP) (Donovan and Grimm, 2007).

The general location of major modern atmospheric circulation features, including the air masses and prevailing winds, are depicted in Figure 19 for the winter/summer atmospheric circulation patterns; these conditions may have been established in the late Holocene at about 3.0 cal ka BP (~ 2.9 ^{14}C ka BP) (Harrison and Metcalfe, 1985), or a little later (Forester et al., (1987). The location of these main atmospheric circulation features were much different in the past, and the mean westerly storm tracks associated with the late glacial period 18 cal ka BP (~ 14.7 ^{14}C ka BP) likely were centred much farther south than at present, at around 35° - 36° N latitude (Harrison and Metcalfe, 1985). Interestingly, the mid-Holocene location of these atmosphere features at about 6.0 ka BP (5.2 ^{14}C ka BP), reached their northernmost location at around 56° N latitude, which is much farther north of their modern location (Harrison and Metcalfe, 1985).

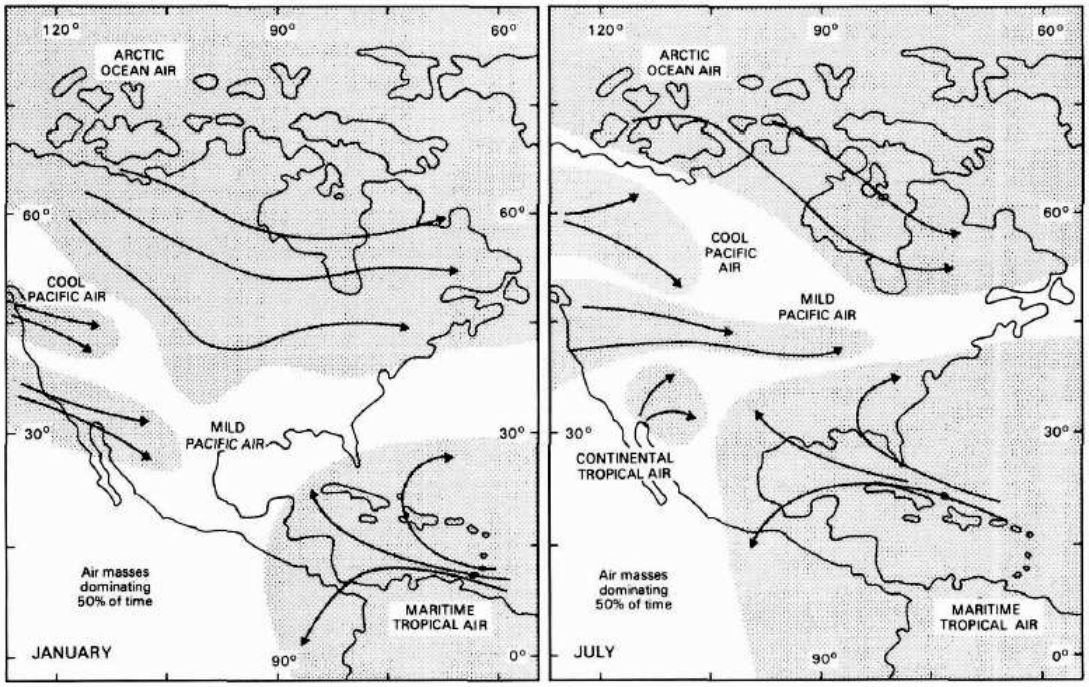

Figure 19. Location of the modern January and July air masses over North America (Harrison and Metcalf, 1985 p. 142).

The dominant pre 7.0 cal ka BP (6.1 ^{14}C ka BP) zonal pattern (long dry winters and cool dry summers) fluctuated and decreased in intensity, until the modern seasonal zonal and meridional patterns were established around 4.0 cal ka BP (3.7 ^{14}C ka BP) (Forester et al., 1987). The location of the air masses farther north in the Hypsithermal is likely the reason for the much warmer and drier conditions, and perhaps its variability resulted as the atmospheric conditions migrated north and south (Harrison and Metcalfe, 1985). Overall, the mid-Holocene climate was drier and warmer, with changes in climate occurring rapidly (in less than 50 years) between the main intervals of the mid-Holocene (Forester et al., 1987).

The variations in Holocene climate are reflected in the regional boreal forest during the

mid-Holocene as indicated by pollen data (Laird and Cumming, 2008). Vegetative cover changed to accommodate the drier and warmer climate as the prairie expanded farther eastward (Laird and Cumming, 2008). ELA lake pollen data imply an open grassy jack pine and poplar region, with junipers on the arid/windy hilltops during the mid-Holocene about 7-8 cal ka BP (7.1 - 6.1 ^{14}C ka BP). Interestingly there was little vegetative change during this period even though there were large lake level changes in Lake 239 associated with lower effective moisture (Laird and Cumming, 2008). These low moisture conditions are also reflected farther west in Lake Winnipeg (Lewis et al., 2001). The transition zone between the prairie and parkland boundaries of the northern plains including LOTWs and SL, is described as more humid than the prairie zone, with the Winnipeg River watershed flowing through a well forested region (Figure 20) (Lewis et al., 2001). Mid-Holocene conditions would likely have differed somewhat as the biome boundary responded to climate changes, however based on Lake 239 data, the prairie and parkland biome boundary does not appear to be dramatically different from that of today. Consistency in the location of biomes from the mid-Holocene to present has been noted by others (Williams et al., 2000), although within a biome, shifts in importance of functional plant types would have occurred due to climate changes. Nonetheless, the east/west boundary of the biomes of 6.8 cal ka BP (~ 6.0 ^{14}C ka BP) were approximately in the same position as they are today (Williams et al., 2000), although they extended farther north (Figure 20) (Laird and Cumming, 2008; St. Jacques et al., 2008).

Figure 20. Eastern portion of the Lake Winnipeg watershed including the Lake of the Woods region, indicating the location of the grassland border between 0 and 6.5 cal ka BP (solid green line) and the location of the parkland border farther east at 6.5 cal ka BP (dashed green line). The yellow area around LOTWs, Winnipeg River, Red River, and Lakes Winnipeg and Manitoba represents the extent of the Lake Winnipeg watershed (after Lewis et al., 2001, p. 744).

As can be seen in Figure 20, mid-Holocene data from U.S. sites locates the grassland border farther to the northeast of the modern boundary (Figure 21) (Laird and Cumming, 2008) than the modern boundary which brings the prairie region close to LOTWs. The parkland-boreal forest boundary during the mid-Holocene was interpreted to have moved to the east of LOTWs (Figure 17 and Figure **20**) (Lewis et al., 2001); this appears to be confirmed from studies of ELA Lake 239, which lies to the about 50 km to the northeast of LOTWs (Figure 22) (Laird and Cumming, 2008).

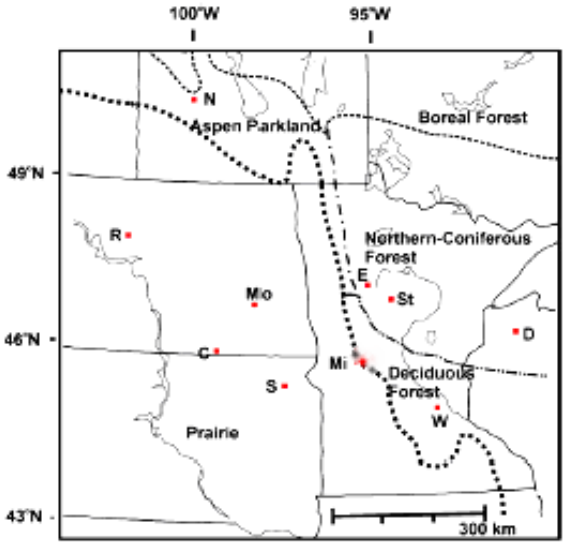

Figure 21. Map of Minnesota, Southern Manitoba and Lake of the Woods region of Northwest Ontario, indicating modern major modern vegetative biomes with the prairie forest border marked by a dotted line (after St. Jacques et al., 2009, p. 538).

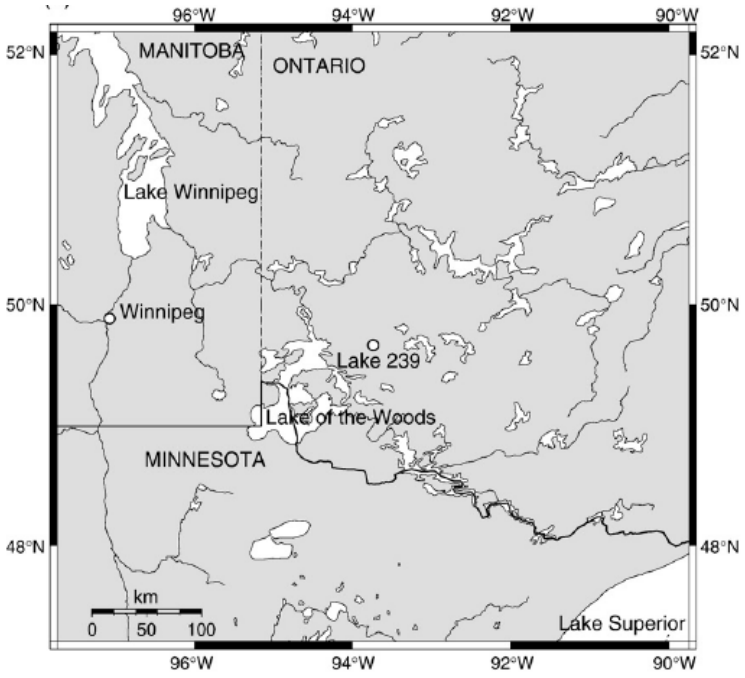

Figure 22. Location of ELA Lake 239 (Laird and Cumming, 2008, p. 294).

Although the changes in biomes in this region would have been slow to respond to variations in mid-Holocene climate, they do "average" the effects of the larger and longer changes in climate, and confirm the trends in the climate fluctuations of the mid-Holocene in this region. The biomes in the LOTWs region further confirm the location of the LOTWs near the contact zone of the Arctic, Pacific and maritime tropical air masses (Laird et al., 2003). This means the LOTWs region was likely subject to many climatic fluctuations in the mid-Holocene.

1.5.4 Late Holocene Climate

Overall, late Holocene climate in the northern plains regions of Canada and the U.S., in the past couple of thousands years, has been categorized as having periods of stability interspersed with large shifts between wet and dry (Laird et al., 2003; Clark et al., 2002). The timing of drought shifts is location specific, and is related to changes in the position of the jet stream and the associated storm tracks (Laird et al., 2003). Minor shifts in the position of the polar high pressure vortex have been hypothesised to be the driving force for spatial climate variations in the region and century-scale climatic variability have been tracked through climate proxies in small prairie lakes (Clark et al., 2002; Laird et al., 2003). Abrupt changes in the Northern Hemisphere climate condition have been detected through the late Holocene such as the transition from the Medieval Warm Period to the Little Ice Age, which corresponds to the beginning of a period of drought starting about 0.7 cal ka BP (Adam et al., 1999; Laird et al., 2003; Cook et al., 2007; St. Jacques et al., 2008). Looking backwards from this point in time, a 1200 yr cycle of drought has

been detected in British Columbia, with some sites correlating well with periods of increased fire frequency in the prairies (Laird et al., 2003). Other investigators associate increased fire frequency in grassland regions with increased charcoal in the sediments, which correspond with periods of increased precipitation which in turn produced an increase in vegetation, particularly grasses that provide fuel for fires (Clark et al., 2002; Brown et al., 2005). These opposing interpretations of high charcoal levels in sediments can complicate interpretations. Nonetheless, in both studies mid-Holocene century scale droughts and the late Holocene decadal scale droughts have been detected.

Cycles of extreme drought lasting about a century, in the northern U.S. plains and Canadian prairies have been linked to the proximity of this region to the polar vortex, and its associated ability to block or enable moist air from the Gulf of Mexico from reaching the region (Laird et al., 2003). The blocking of maritime tropical air masses from the south, by the drier and cooler Pacific air masses, has also been identified as a mechanism that may reduce precipitation (Lewis et al., 2001; St George, 2006). Late Holocene intervals of aridity, however, were not as pronounced as mid-Holocene droughts, and their durations were typically less than a century, unlike 600 year drought experienced around 8.0 cal ka BP (Clark et al., 2002).

Bog moisture variability studies using thecamoebians, peat humification, pollen, leaf stomata and plant macrofossils (Booth and Jackson, 2003) have found that over the past 2000 years in sites in southern Michigan and north-central Minnesota, there were intervals of extreme drought in both regions (Booth et al., 2006). These correlate with

large droughts identified much farther west in the Northern Great Plains and the Rockies (Booth et al., 2006).

Conditions in the late Holocene in the northern Great Plains region at Devils Lake, North Dakota, were wet from 4.5 to 3.5 cal ka BP with dry conditions (indicated by more saline lake conditions) returning at about 3 cal ka BP (Haskell et al., 1996). These conditions also occurred in lakes in the Canadian prairies where many basins were subject to drying conditions (Fritz et al., 2000). Farther east in Minnesota, nearly synchronous droughts are recorded (Haskell et al., 1996). At ELA Lake 239, the unstable and intermittent arid period of the mid-Holocene was reflected by large fluctuations in lake level, which stabilized in the last 3000 years (Laird and Cummings, 2008).

The droughts of the past few centuries including the more recent and well recorded 20th century climatic variabilities recorded in tree ring data (St. George and Nielson, 2002), are indicative of climatic variabilities. However, they are less intense and shorter in duration than those of the past several thousand years (Laird and Cumming, 2008; Cook et al., 2007). These shorter duration droughts occurred in relatively stable climatic conditions (Laird et al., 2003) and differ considerably from the intense century-scale mid-Holocene droughts during the instabilities of the Hypsithermal (Laird and Cumming, 2008; Clark et al., 2002).

Today's mixed forest, boreal parkland, boreal forest, and grasslands all converge in the LOTWs region. This is a change from the boreal forest and grasslands locations of the

early and mid-Holocene respectively (Figure 17 and Figure 20), and reflects the change in the climate (Dyke et al., 2005).

1.5.5 Mid-Holocene Climate: An Analogue to the Currently Warming Climate?

The unstable and warm mid-Holocene climate is frequently used as an analogue for future climate change, although modern warming appears to be driven by increasing CO_2 levels, whereas mid-Holocene warming is mainly related to earth-sun relationships (i.e. Milankovitch orbital relationships) (Ruddiman, 2002). This section briefly reviews the mid-Holocene in the LOTWs region and considers whether this analog can be used to predict the effects of current climate change.

There is agreement that prediction of climate changes through the development of climate models is indeed very complex, and using these models to predict regional climate is difficult (IPCC, 2007). However, the recent projections from the IPCC Report (IPCC, 2007) predicts a 1-2 ^{o}C increase in temperature for this region due to increases in CO_2, which is close to the increased temperatures inferred from the climate proxies used to establish the mid-Holocene climate (Laird and Cumming, 2008). The periodic century drought cycles of the mid-Holocene due to insolation driven climate variability implies that we may be faced with similar intense century scale droughts in the future (Clark et al., 2002).

Based on Clark's studies, mid-Holocene droughts were also more intense and longer in duration than those of the late Holocene, and the current climate warming may result in similar drought conditions to those of the mid-Holocene (Clark et al., 2002). However, the complexity of climatic change mechanisms will make it difficult to predict future climate changes, and there is considerable disagreement (Mitchell, 1990) as to whether the mid-Holocene climate variability can be used as a means to predict future climate changes, as past climate was likely driven by increased insolation and not increasing atmospheric CO_2 levels (Clark et al., 2002; Laird and Cumming, 2008).

In the case of the LOTWs region, the increasing temperatures in central North America due to climate change are likely to result in a drier climate (Clark et al., 2002) with reduced precipitation, ground water levels, stream flow and lake levels in the LOTWs region (Laird and Cumming, 2008). According to Clark, the future patterns of decadal-century climate fluctuations may actually be more intense that those predicted by General Circulation Models (GCMs), and much more intense than those droughts of the past century (Clark et al., 2002). It is suggested the mid-Holocene climate aridity and lower lake levels recorded in ELA Lake 239 in the mid-Holocene may be indicative of what may be in store for us as a result of future climate warming (Laird and Cumming, 2008). It appears the mid-Holocene conditions from Figure 23, and its periodic century intervals of drought and non drought intervals, may be an analogue of the greenhouse driven future climate changes currently underway.

Predicting where and when climate changes will occur, as well as the magnitude of the change, depends on the regions position with respect to the location of the contact zone of the Arctic, Pacific and maritime tropical air masses (Laird et al., 2003). The location of LOTWs near the edge of the interplay of these air masses likely means this region will be subjected to climate shifts in the future because slight movements in the boundary location can shift the region from one climate regime to another.

There is however a significant difference between the paleoclimate changes of the mid-Holocene and those that could occur due to future climate changes, which will further hinder the predictions based on these paleoclimate conditions (Dyke, 2005). In the past, climate warmings were associated with changing of the axial tilt of the Earth producing warmer summers and cooler winters, which were amplified in the mid to high latitudes (Dyke, 2005). The expectations for CO_2 forced climate warming are that summers and winters will both be warmer and once again amplified in the higher latitudes, this time by the more readily warmed land surfaces versus those of the LIS (Dyke, 2005). The reduced seasonality of a CO_2 induced climate change represents a major departure from the climate changes related to axial tilt (Dyke, 2005). Future climate change may not follow the same pattern as those in the past.

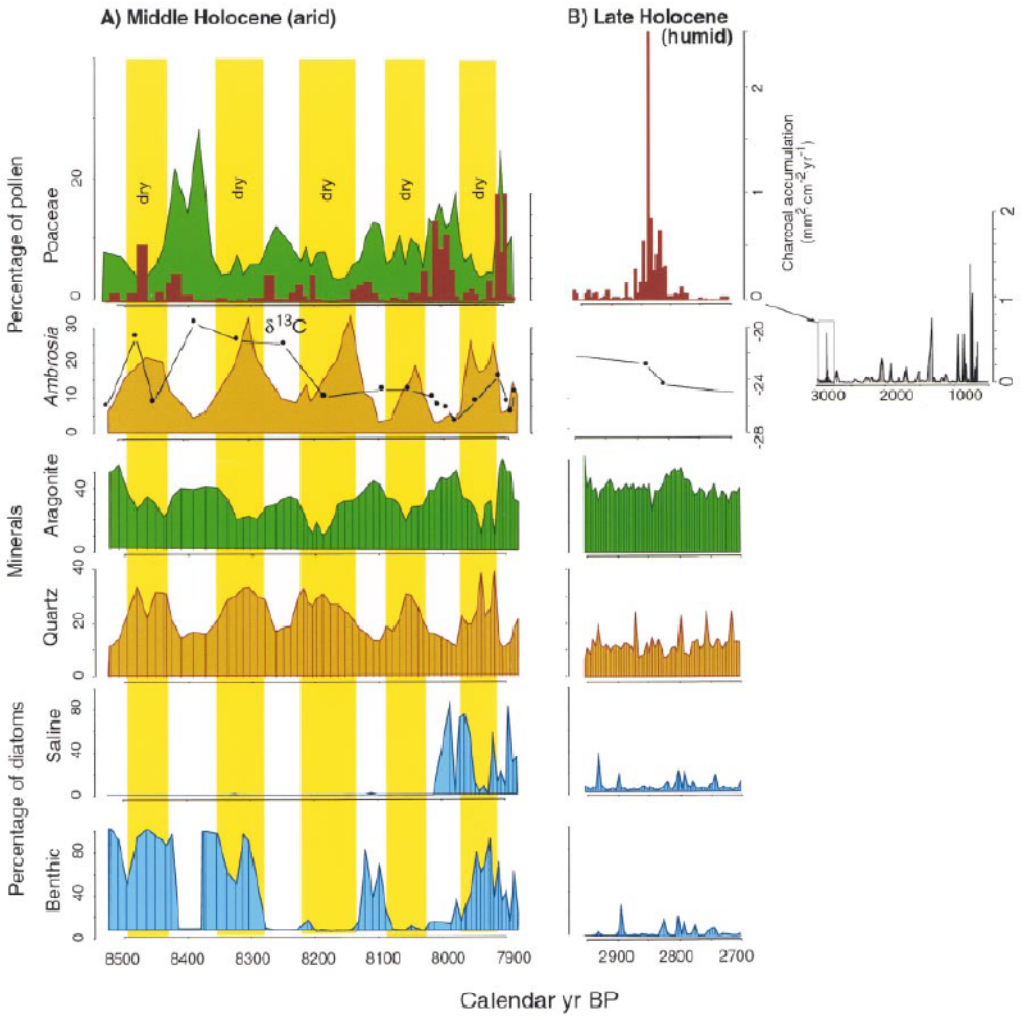

Figure 23. Periodic greater than century scale wet/dry climate cycles in central North America. "A" provides sedimentary evidence tracking a mid-Holocene periodic drought, characterized by dry intervals associated with accumulations of quartz and low levels of precipitated aragonite, low grass and high *Ambrosia* pollen levels. Wet and dry cycles are additionally tracked by benthic and saline diatoms. "B" indicates late Holocene humid conditions, tracked by mineralogy, with the high charcoal levels (inset) indicating intervals when the flora is sufficiently productive to support fires (Clark et al., 2002, p. 597).

CHAPTER 2 FIELD AND LAB METHODOLOGY, AND DESCRIPTION OF SAMPLING SITES

2.1 INTRODUCTION TO CORING

Personnel from the Limnological Research Center (LRC) at the University of Minnesota in Minneapolis, Minnesota, were contracted to perform lacustrine core recovery operations from LOTWs and SL in August 2006, using the LRC Kullenberg Rig. The LRC field team of 4 individuals, Kristina Brady, Amy Mybro, Anders Noren and Mark Shapley, was supplemented by personnel from the University of Manitoba, Trevor Mellors and James Teller.

The coring program was based on the need to provide paleohydrologic and paleoclimate data from LOTWs. Alternate sites were selected to ensure the resources of the LRC team were maximized and would not be unduly affected should adverse weather conditions be encountered. This preparation included an extensive review of available accommodations, including availability and flexibility during the busy tourist period, to ensure the field team could be accommodated should adverse weather require changes to the sequencing of the coring operations. Pre-scouting of the potential launching sites was carried out to ensure the Kullenberg Rig could access the sites and be assembled and launched. The suitability of accommodations and availability of food at the access sites, and access to a support/safety boat were also evaluated at each potential site. The availability of guiding services was also established for those portions of the lake where

shoals were of particular concern, or where remoteness of the coring site could increase the consequences of potential accidents during coring operations.

Border crossings to/from Minnesota to Manitoba and to/from Minnesota to Ontario for both Canadian and U.S. citizens, and the U.S.-owned LRC equipment required special attention to ensure delays were not encountered. Preapproved authorizations were obtained from U.S. and Canadian Customs for both Canadian and U.S. citizens, the LRC equipment and the retrieved cores. Complexities in these jurisdictional issues influenced site selections or affected the priority given to potential coring sites.

Taking the constraining conditions into account, the key criteria chosen for the core recovery program were related to deciding where to core on LOTWs and SL, and at what depths core retrieval should be conducted in order to obtain sufficient data for interpretation of past conditions in the lakes. A deep/shallow strategy was employed in order to help to track changes in bathymetry from climate fluctuations (described below).

2.2 CORING SITE SELECTION

2.2.1 Introduction

The basic requirements of the coring program were to sample in areas representative of the paleohydrological conditions in the various regions of LOTWs, the need to sample near the inlet and outlet of its major fluvial connections, and the decision to use a

companion core deep/shallow site coring strategy to try and track major hydrological changes due to changing paleohydrological conditions. The site selection process in LOTWs and SL were constrained by potential meteorological factors, factors related to the geographical/hydrological complexity of the lakes themselves (principally LOTWs), distance to sites from shore access points, and the numerous shoals which appeared as a consequence of the unusually low lake levels in 2006. Lake levels were approximately 1.7 m (5-6 feet) below the normal level of 322.7 m (1058.7 feet) (Yang and Teller, 2005). Due to the above considerations plans for alternate coring site selections were made and differing coring sequencing strategies were developed.

The selection of a lake for paleoclimate studies is very important. Small lakes are ideal, however they must be of sufficient depth to retain a minimum depth sufficient to ensure the biota for the selected climate proxy remains viable, and population and species signals remain. The Digerfeldt method which tracks shoreline positions and hence lake level, requires lakes be small (<50 ha) and relatively shallow (max depth 10 m), with a catchment to lake area of < 5:1 (Digerfeldt, 1986; Digerfeldt et al., 1992). Similarly, ideal plant macrofossil data sites are smaller bodies of water or bays (500 m in diameter and up to 10 m deep) since plant macrofossils do not easily reach beyond the littoral zone into the deeper portions of the lake basin (Birks, 2001). In temperate zones, steep sided small lakes with an overhanging forest or, in non forested regions small lakes with active inflow or slope washes, provide the preferred conditions (Birks, 2001). In addition groundwater inputs into lakes can interfere with climate signals, delaying or interfering with the signal, and therefore the ideal lake would have limited or constant groundwater

flows (Laird et al., 2003; Yansa et al., 2007). In addition, to the size of lakes, a thorough understanding of the ecology of modern species being used as proxies, is fundamental to most ecological studies.

Unfortunately LOTWs and SL do not meet these requirements due to the size and complexity of these lakes, and many proxies in the cores do not appear to be present and/or preserved over the core interval, increasing the complexity of interpretations. Specifically, thecamoebians are primarily found in about the top metre of most of the examined cores, and ostracodes, are absent in the top sediments of the cores. Although these shortcomings exist, LOTWs and SL still provide sufficient data to track hydrologic and climate signals through the use of multiproxies.

2.2.2 Site Access Requirements

Lake access for the Kullenberg Rig requires a large laydown area to facilitate rig assembly and disassembly. Additionally, the assembly/disassembly area must have either an available docking area, or a sandy beach area free of any rocks that could interfere with the assembly or launching of the rig. These minimum rig assembly and launch requirements also needed to be in relative close proximity to the coring site due to the relatively slow travel speed (~ 5 km/hr) of the rig platform. An accompanying motorized boat was employed as a safety boat to provide faster egress from the platform to shore in the event of medical emergencies and provided the ability to shuttle personnel in the case

of adverse weather. It additionally supported rig navigation in complex lake passages and/or shallow water locations essentially providing a pilotage service.

2.2.3 Kullenberg Rig Operational Restrictions

For the shallower of the deep/shallow companion coring sites, there were limitations on the length of core that could be retrieved, due to restrictions in the minimum depth in which the Kullenberg Rig can be operated. For safety reasons the core assembly length cannot exceed the depth of water below the Kullenberg Rig platform. This ensures the weight assembly at the top of the core barrel, remains below the rig decking, and avoids the hazards that could occur to the field personnel and equipment when the core barrel and weight assembly are released.

Kullenberg Rig operations are also somewhat affected by unknowns with respect to the lake bottom substrate. Ideally, the depth and nature of the bottom substrate are known through prior seismic profiling of the area, to help determine the stratigraphic characteristics sediments and to avoid possible damage to the core assembly and the rig itself should a hard substrate be encountered when the core barrel is released. Unfortunately, detailed knowledge of the substrate was not available.

2.2.4 Site Selections in LOTWs

Three primary areas were chosen in LOTWs based on availability of suitable lake access locations for the Kullenberg Rig while taking into account the potential weather related

risks and time required for the rig to traverse to the selected sites. These locations and the final coring sites are shown in Figure 24: (1) a southern basin location near the inlet from the Rainy River, (2) a northern location near the exit of the Winnipeg River from LOTWs and (3) two mid-lake locations in the northern part of the southern basin and nearby main channels connecting the shallow southern basin and the deep northern basin. Deep and shallow water cores were retrieved at each of the LOTWs locations and in SL, to ensure changes in lake depth could be tracked. The optimum deep site was designated as about 50 ft (~ 15 m) with the shallow companion site about 25 ft (~ 7.5 m). These nominal depths were adjusted as necessary at each site to suit local conditions, while taking into account the Kullenberg Rig restrictions.

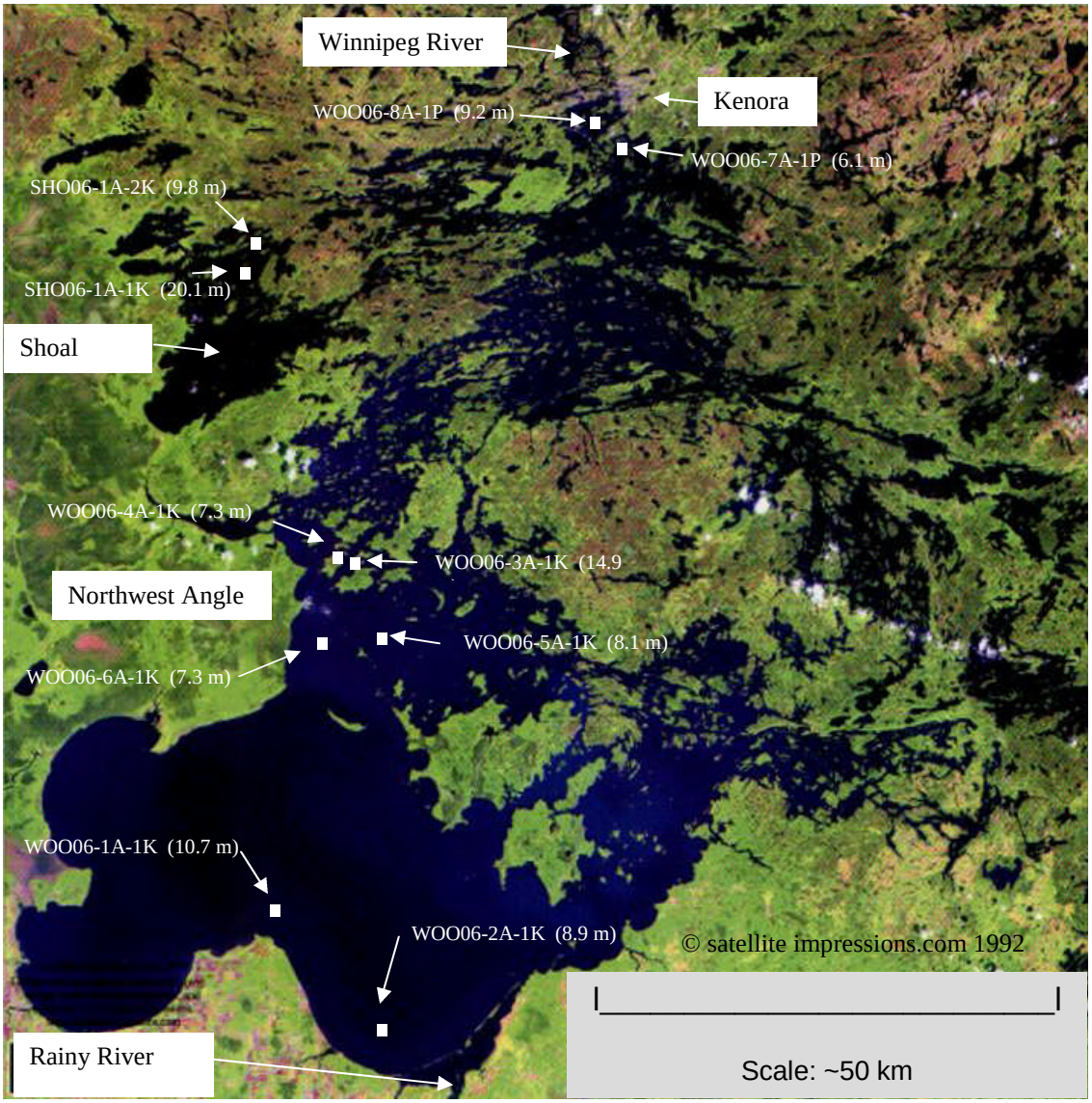

Figure 24. Regional aerial photo of LOTWs and SL indicating the approximate locations of coring sites in LOTWs and SL (indicated by white boxes), with the associated core labels and depths (after http://www.virtualnorth.net/satimp/).

The two cores near the Rainy River inlet,WOO06-1A-1K and 2A-1K, were chosen to provide data near this unique interface of the Rainy River/LOTWs environments and that of the nearby large open water southern basin. The location farther into the southern

basin (WOO06-1A-1K) should provide information more closely related to the timing of the southward lake transgression due to differential isostatic rebound. Although the WOO06-1A-1K site is located farther to the west, it should still be representative of both the southern basin paleoenvironment and the paleoenvironment associated with the inputs from the nearby Rainy River.

The four mid-lake sites in the Northwest Angle area, two in the open expanse at the top of the southern basin (WOO06-5A-1K and 6A-1K), and two additional sites in a deep but narrow channel leading to the deeper northern basin of the LOTWs (WOO06-3A-1K and 4A-1K) likely represent an intermediate time in the history of LOTWs when the southward LOTWs transgression entered the region (Yang and Teller, 2005). They should provide a differing set of data due to their likely distinct paleoenvironments from the southern basin.

The third LOTWs coring area near the northern outlets into the Winnipeg River drainage system is in the deep and oldest portion of the lake and the cores (WOO06-7A-1P and 8A-1P), should provide another unique set of paleoecological and paleohydrologic conditions. This location is near the outlets into the Winnipeg River and is in a deep portion of the LOTWs which formed in the deep basin at the edge of the receding ice sheet. This portion of the lake retained its relatively deep hydrology throughout the post isolation history of LOTWs (Figure 9 and Figure 10).

2.2.5 Site Selection in Shoal Lake

The deep/shallow coring strategy was also applied in SL with the restrictions/limitations related to rig operation and weather restrictions still applicable to the site selection process. The two coring sites were separated somewhat (Figure 24) due to the generally rocky shoreline and sharp offshore drop-offs in the lake in the selected coring area, and concerns related to encountering a rocky substrate should the shallower coring operation be conducted too close to shore. In addition a site too close to shore was undesirable due to the potential for subaqueous slumping of materials on the steep near shore slope of the lake bottom. This required some adjustments in final site selection. The SL coring locations (SHO06-1A-1K and 2A-1K) are located in the northern portion of a broad open expanse of the lake. SL provides data from a distinct paleoenvironment, and therefore should provide the means to compare changes with those in LOTWs. Based on its slightly higher elevation and location near the same differential isostatic rebound isobase, SL would have operated independently from LOTWs for most of its history.

The lack of bathymetric data for SL required some preliminary rough bathymetric data to be obtained prior to final site selection. Using a simple depth finder, several short transects were run near the chosen coring area.

2.2.6 Core Recovery Operations

The Kullenberg Rig from the LRC at the University of Minnesota (Figure 25) was used for sediment core recovery operations in LOTWs and SL. The Kullenberg Rig is composed of the masts of the superstructure, pulleys and hydraulic devices, weights, and the core barrel assembly, which is then assembled on a floating mobile platform consisting of two hulls with outboard motors bolted to the platform. The Kullenberg Rig is transported using a large SUV and trailer (Figure 26) to a shoreline location suitable for assembly and launching. A supply of core barrels of various lengths and associated polycarbonate liners, the necessary tools for field assembly and disassembly of the Kullenberg Rig platform, and the core barrel suspension superstructure and hoisting mechanisms are all transported with the SUV and trailer.

Figure 25. LRC Kullenberg Rig in the Southern basin of LOTWs, August 2006.

Figure 26. LRC Kullenberg Rig trailer and SUV, preparing for rig assembly in the southern basin of LOTWs August 2006.

The Kullenberg coring process is a gravity coring system which recovers a single long core within a polycarbonate (plastic) tube about 3 ½ inches (~ 9 cm) in diameter contained within the steel core barrel assembly. The core barrel assembly includes a cutter and core catcher assembly on the lead end of the core barrel, and a vacuum piston (Figure 27) which rises within the core barrel when it is released above the sediment water interface and is driven downward by the weight assembly attached to the top of the core barrel. The vacuum created by the entry of the sediments into the polycarbonate liner, in addition to the core catcher, ensures the sediments are retrieved when the core is

lifted to the rig platform using the hydraulic driven pulley assembly. The cross-shaped slot ("moon pool") in the platform allows the recovered core barrel to be manipulated onto the platform (Figure 28). A "muck core" is also positioned beside the core barrel on a trip lever, which is used to trigger the release of the core barrel assembly and to recover the sediments across the water-sediment interface where pore water content is very high (Figure 27) (Leroy and Colman, 2001). This short approximately 1 m core was concurrently collected with the longer core.

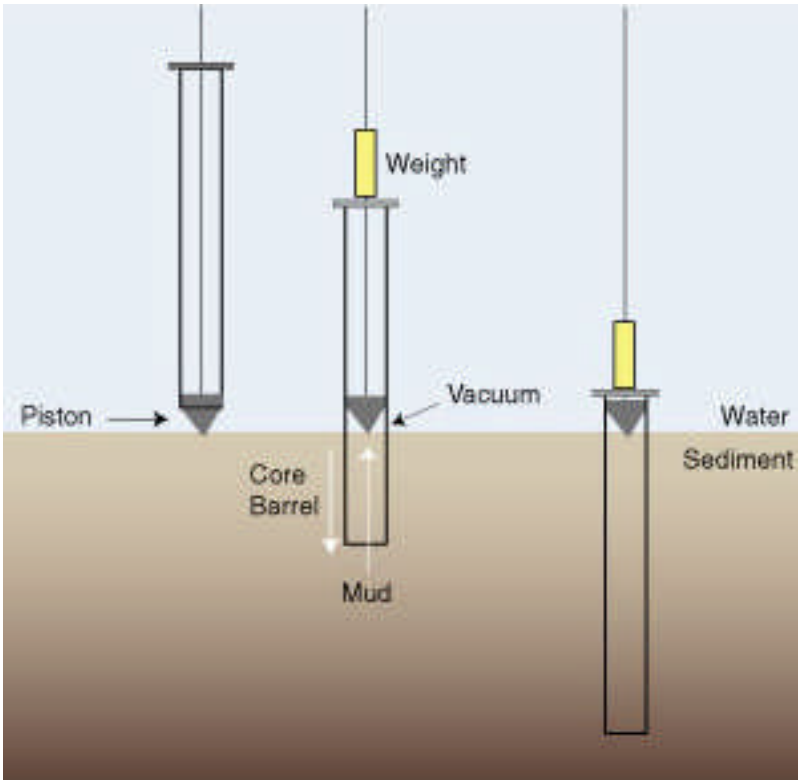

Figure 27. Kullenberg gravity piston corer schematic showing the major core barrel assembly components and the operation of the sliding vacuum piston used to help retain the sediments (from http://esp.cr.usgs.gov/info/lacs/piston.htm).

Figure 28. Core recovery operations using the LRC Kullenberg Rig. From top left clockwise: preparing to lower the core barrel and weight assemblies using the hydraulic winch system, recovering the core barrel and weight assemblies through the moon pool, and view of the sediment water interface through the polycarbonate tube of the muck core (photos by J. Teller).

The rig was used to recover ten cores and their associated muck cores) (Figure 28). Recovered cores were cut into manageable lengths (up to 1.5 m long) for ease of transport, and were capped, labelled (Figure 29), and transported on the LRC trailer for storage in walk-in coolers at the LRC facilities in Minneapolis, pending future examination and archival storage. Cores were transported in a horizontal position between coring sites and in final transport to the LRC facilities. During initial transport

cores were stored in ambient conditions, and were not placed into coolers until they arrived at the LRC.

Figure 29. Recovered cores in the polycarbonate liners cut and labeled in preparation for transport.

2.3 DETAILED DESCRIPTIONS OF CORING LOCATIONS

2.3.1 General

Coring location (Figure 24) details related to core recovery were recorded and are provided in the following sections. Longitudes and latitudes of the coring sites are also provided which are based on the readings from the LRC GPS unit on the Kullenberg Rig. Water depths at the coring site are also provided along with the length of the recovered core. It should be noted the normal water depths at the sites would be 5-6 feet (~2 m)

deeper than those recorded by the depth finder on the Kullenberg Rig, due to the unusually low water levels. UTM coordinates (unofficial reading taken near the Kullenberg Rig) were also taken using readings from a hand held GPS unit, or those provided from the guide boat for Northwest Angle sites, and have been included where available (for convenience). Similarly, unofficial water depth readings were taken, but have not been included.

Subsequent to the coring operations, seven LOTWs cores were split, examined, scanned, core logged and subsampled at the LRC Core Lab (WOO06-2A-1K and WOO06-8A-1P were not examined). In SL only the SHO06-2A-1K core was processed.

2.3.2 LOTWs Southern Basin

Two cores (WOO06-1A-1K and WOO06-2A-1K) were recovered from the southern basin (Figure 24) but only WOO06-1A-1K was processed at the LRC Core Lab. Access to the coring site was made from Long Point which had a sheltered docking facility and a wide sandy beach to facilitate Kullenberg Rig assembly/disassembly and had access to nearby accommodations.

WOO06-1A-1K: latitude 48.99229^{o}; longitude -94.92356^{o}

This site is the deeper of two companion coring sites located in the southern basin near the inlet from the Rainy River. It is directly off Long Point Resort, in the Minnesota portion of Big Traverse Bay of LOTWs, about 2.5 km offshore and 17 km to the northwest of the inlet of the Rainy River. Water depth at the site was ~ 10.7 m (35.1 feet), which was deemed suitable as the deep coring site, since the southern basin is relatively flat and the depth at this site was reasonably close to the common basin depth.

Adjacent UTM coordinates (taken from the support boat), for this site were Zone 15; E359287; N5428381. The recovered 3.3 m long core was cut into three core intervals (1A-1K-1, 1A-1K-2, and 1A-1K-3), and 80 cm of sediment in the muck core was also recovered.

WOO06-2A-1K: latitude 48.89121^{o} longitude -94.82602^{o}

This site is the shallower of two companion cores located in the southern basin near the inlet from the Rainy River, about 3.25 km directly off Zipple Bay. Water depth at the site was ~ 8.9 m (29.2 feet) which is only ~ 2 m shallower than the deeper companion core but is closer to the mouth of the Rainy River and is located about 12 km to the west northwest of the Rainy River inlet.

Adjacent UTM coordinates (taken from the support boat) were Zone 15; E366171; N5416751. The recovered 3.6 m long core was cut into three core intervals (2A-1K-1,

2A-1K-2, and 2A-1K-3), and 80 cm of sediment in the muck core was also recovered. This core was not processed and resides at the LRC core Lab.

2.3.3 LOTWs Northern Northwest Angle Channel Coring Sites

Two cores were recovered from Northwest Angle channel sites WOO06-3A-1K and WOO06-4A-1K (Figure 24), with both coring sites located about 10 km to the east of a sheltered docking facility at Young's Resort, which is located on the southern shore near the entrance to the Northwest Angle Inlet. Young's Resort provided a sheltered docking facility which accommodated the Kullenberg Rig assembly/disassembly and dockage, and provided access to nearby accommodations. It also provided official access to Canadian waters through a customs telephone service when access to the Ontario portion of the lake was necessary.

Site WOO06-3A-1K: latitude 49.34714^{o}; longitude -94.84379^{o}

This site is the deeper of two companion cores with both located in the northeast trending deep channel near Cyclone Island, to the east of the Northwest Angle Inlet. Water depth at the site was ~ 14.9 m (48.9 feet) which closely approximated the nominal 50 foot core depth for the deeper of the two companion LOTWs northern Northwest Angle channel cores.

The released core barrel hit a hard object in the substrate causing the coring platform to shake violently. The core was very difficult to retrieve but eventually was successfully

recovered to the deck of the Kullenberg Rig. The core barrel had been bent into a curve and the core cutter on the end of the core barrel sustained damage from the impact with a boulder or possibly bedrock. The weight stacker at the top of the core barrel assembly was also bent and required a return to the launch area to obtain a spare before the shallower companion core could be obtained. The polycarbonate liner was eventually recovered from the bent core barrel and processed at the LRC Core Lab.

Adjacent UTM coordinates (taken from the support boat) were Zone 15; E366107; N5467466. The 14.9 m long core was cut into six core intervals (3A-1K-1, 3A-1K-2, 3A-1K-3, 3A-1K-4, 3A-1K-5, and 3A-1K-6). Approximately 10 cm of core length were lost, with about 5 cm bagged when removing the polycarbonate liner between 3A-1K-2 and 1K-3. Similarly about 5.5 cm were lost between 3A-1K-4 and 1K-5. Overall about 7.5 m of core were recovered along with 57 cm of sediment in the muck core.

Site WOO06-4A-1K: latitude 49.33830^{o}; longitude -94.85979^{o}

This site is the shallower of two companion cores located in the channel near Cyclone Island. A slight current was noted in the channel. Water depth at the site was ~ 7.3 m (24 feet) which closely approximated the nominal 25 foot shallow site criteria.

Adjacent UTM coordinates (taken from the support boat) were Zone 15; E3664908; N5466509. The recovered 2 m long core was cut into two core intervals (4A-1K-1, and 4A-1K-2). The muck core material was lost during retrieval. A granular, possibly

pedogenic, greenish grey sediment was observed through the polycarbonate liner about 20 cm from the bottom of the core, overlain by 15 cm of dark grey sediment, with the interval above a grey clay like sediment.

2.3.4 LOTWs Northwest Angle Basin Coring Sites

Two cores (WOO06-5A-1K and WOO06-6A-1K) were recovered from the open basin to the south of the Northwest Angle (Figure 24) and processed at the LRC Core Lab. Shore access to these sites was the same as the two northern Northwest Angle channel coring sites.

Site WOO06-5A-1K: latitude 49.27928^{o}; longitude -94.82007^{o}

This site is the deeper of two companion cores located in a relatively open portion of the northern part of the southern basin, to the west of Massacre Island and about 13 km to the southeast of the entrance to the Northwest Angle Inlet. Water depth at the site was ~ 8.1 m (26.6 feet) which is much less than the proposed nominal depth for the deeper companion core site strategy (50 ft), but was the deepest water in this part of the lake.

Adjacent UTM coordinates (taken from the support boat) were Zone 15; E367641; N5459872. The recovered 5.5 m long core was cut into five core intervals (5A-1K-1, 5A-1K-2, 5A-1K-3, 5A-1K-4, and 5A-1K-5), with 60 cm of sediment in the muck core also recovered. Additionally, 6 cm within the core catcher were retrieved and 7 cm within the core bit. Bottom clays were noted half way up the weights at the top of the

core barrel, indicating that the top of the core may have penetrated a few tens of cms below the floor of the lake.

Site WOO06-6A-1K: latitude 49.28098^{o} longitude -94.89926^{o}

This site is the shallower of two companion cores located in a relatively open portion of the northern part of the southern basin, about 6 km farther to the west of the Massacre Island deeper coring site. Water depth at the site was ~ 5.9 m (19.4 feet) which although not close to the nominal depth for the shallow companion core site (25 ft), was as deep as possible in this part of the lake while remaining within the restrictions of the Kullenberg Rig.

Adjacent UTM coordinates (taken from the support boat) were Zone 15; E361907; N5460214. The recovered 3.8 m long core was cut into three core intervals (6A-1K-1, 6A-1K-2, and 6A-1K-3). The muck core failed to recover any sediment and manual actions were taken to recover about 45 cm of material from the sediment water interface.

2.3.5 LOTWs Northern Outlets - Kenora Coring Sites

Access to this portion of the lake was made using a docking facility at Anicinabe Park in the southern most portion of the town of Kenora, Ontario. Rig assembly was complicated somewhat by the relatively high volume of users at the docking facility. Two cores were recovered from the northern outlet Kenora region WOO06-7A-1P and WOO06-8A-1P (Figure 24), with only the WOO06-7A-1P core processed at the LRC Core Lab.

Site WOO06-7A-1P latitude 49.72984^{o} longitude -94.51310^{o}

This site is the deeper of the two companion cores located near the outlets to the Winnipeg River just south of the town of Kenora, Ontario, amidst a complex series of channels connecting to deeper portions of the deep northern basin. Water depth at the site was ~ 6.1 m (20 feet) which although not close to the targeted depth for the shallow core (25 ft) was reasonably close and as deep as possible in this part of the lake, under the low water conditions encountered during coring.

UTM coordinates (from the LRC GPS) for the site were Zone 15; E390931; N5509911. The recovered 4.6 m long core was cut into four core intervals (7A-1P-1, 7A-1P-2, 7A-1P-3 and 7A-1P-4) and about 80 cm of sediment in the muck core was also recovered.

Site WOO06-8A-1P: latitude 49.74471^{o} longitude -94.52096^{o}

This site is the deeper of two companion cores located in the northern basin near the outlets to the Winnipeg River and was located just to the south of Kenora on the south side of Coney Island, about 3 km to the south of the Winnipeg River outlets. Water depth at the site was ~ 9.2 m (30.2 feet) which is about 3 m deeper than the companion core. Adjacent UTM coordinates (taken from the support boat) were Zone 15; E390423; N5511358. The recovered ~ 4.25 m long core was cut into three core intervals (8A-1P-1, 8A-1P-2, and 8A-1P-3) with 60 cm of sediments in the muck core also recovered. A dark grey interval was noted at the top of the core down to about 77 cm before a distinct change to a lighter grey was noted; the dark colour may be due to anthropogenic inputs when the island was in heavy use as a cottage area. A rhythmically bedded sequence was noted in WOO06-8A-1P 2 and a distinct contact was noted about 0.5 m from the bottom of the core in between what appears to be clay, and a sandy silt. This core was not processed and resides at the LRC core Lab.

2.3.6 SL Coring Sites

Two cores were recovered from SL, SHO06-1A-1K and SHO06-2A-1K (Figure 24), with only SHO06-2A-1K processed at the LRC Core Lab. Access to the sites was made from a resort on the north shore about a 1 km to the west of Clytie Bay, which provided docking facilities.

Site SHO06-1A-1K: latitude 49.59605^{o} longitude -95.03322^{o}

This site is the deeper of two companion cores located in the northern part of an open basin of SL about 4 km from the north shore to the west of Clytie Bay. Water depth at the site was ~ 20.1 m (65.9 feet) which is considerably deeper than the nominal depth of 50 feet for the deep coring site.

Adjacent UTM coordinates (taken from the support boat) were Zone 15; E356323; N5497880 (using University of Manitoba GPS). The recovered 6.9 m long core was cut into six core intervals (SHO-1A-1K-1, SHO-1A-1K-2, SHO-1A-1K-3, SHO-1A-1K-4, SHO-1A-1K-5 and SHO-1A-1K-6) with 60 cm of sediments in the muck core also recovered. Difficulty was experienced in removing the polycarbonate liner from the core barrel as the liner had collapsed. Significant hammering was required to remove the core and as a result, this core was not processed but remains at the LRC core facility.

Site SHO06-2A-1K: latitude 49.59796^{o} longitude -95.03353^{o}

This site is the shallower of two companion cores located near the northern part of the open basin of SL, with this site about 1 km from the north shore near Clytie Bay in a narrowing part of the lake. Water depth at the site was ~ 9.8 m (32.2 feet) which is a little deeper than the targeted depth (25 ft) for the shallow core site.

Adjacent UTM coordinates (taken from the support boat) were Zone 15; E353057; N5495918. The recovered 6.8 m long core was cut into six core intervals (SHO-2A-1K-

1, SHO-2A-1K-2, SHO-2A-1K-3, SHO-2A-1K-4, SHO-2A-1K-5 and SHO-2A-1K-6) with about 50 cm of sediments in the muck core also recovered.

2.4 CORE PROCESSING AND SUBSAMPLING

2.4.1 Removal of Sediment from Core Barrel

Transported cores were recovered from the temporary storage coolers at the LRC and prepared for examination. The ~ 6.5 cm diameter polycarbonate liners of the cores were split using small vibrating cutters in a special core cutting machine at the LRC, which cut most of the way through the liner. A utility knife was then used to complete the cutting of the liner and care was taken to ensure that polycarbonate fragments were not introduced into the sediments within the liner. A long thin blade was placed along the cut length of the polycarbonate core liner and pressed through the sediments to separate the core into two halves. Alternately, when the consistency of the sediment within the liner was deemed sufficiently stiff, a fishing line was pulled along the length of the core to cut the core into two halves. The fishing line provides a cleaner cut but can only be used when the sediment is stiff enough to ensure the two halves remain apart.

One half of the split core was further processed, with the other half covered with a plastic wrap and scanned using a Geotek multi-sensor core logger. This core logger records density and magnetic susceptibility values along the core. Subsequently both core halves were carefully wrapped in a plastic wrap, inserted into a heavier plastic sleeve, sealed,

inserted into a hard plastic core storage box specially designed for core protection and efficient long term storage, and labelled. Half of the core was retained by the LRC in their long term archive facility.

The other half of the core was used for visual examination, core logging and subsampling. The split core was smoothed to enhance the visibility of stratigraphic features along the length of the core, using glass slides pulled carefully across the core until a smooth surface is obtained. The core was then scanned using a core scanning facility to obtain a permanent photographic image, which was subsequently used as part of a core logging and description process, and provides an undisturbed visual record of the core stratigraphy.

2.4.2 Subsampling Strategy

Core subsampling was conducted using the non-archive half of the split core, following core logging and description (Figure 30). Core subsample size was set at 15 mL, which corresponds with the plastic sampling containers available at the LRC, and seemed to be of a reasonable size to allow an ostracode population analysis. The objective was to obtain a minimum of 20 ostracode tests for species population studies in each sample. The 15 mL sample size spanned about 2 cm along the length of the half core and consumed about one half of that half (i.e. one quarter of the full core diameter) (Figure 30). Some sample sizes were based on the size of the targeted materials (e.g. wood fragments).

The initial core subsampling process was based on a number of factors, including the need to obtain a relatively consistent ostracode sample interval along the core, extraction of any observed biological carbon materials suitable for radiocarbon dating, and the time available for subsampling at the LRC facilities. These initial sampling intervals were later modified during subsequent resampling programs, based on the need for additional material for radiocarbon dating, the need to characterize or date additional stratigraphic intervals, and the need for additional biostratigraphic data (e.g. ostracodes and thecamoebians).

Figure 30. Core subsampling at the LRC of the non-archive half of the split core, using one quarter of the core diameter and the typical subsampling span along the core length of about 2 cm. The subsample plastic sampling containers are shown on the right (photos by J. Teller).

The initial sampling of the cores was based on a relatively wide sampling interval (typically every 20 cm) which tried to capture ostracode biostratigraphic information along the core length. Shorter sampling intervals and specific sample locations along the core were also selected based on the observations from the core logging and description process. These adjustments to the initial sampling interval or the decision to include specific sample locations were based on identification of specific stratigraphic features of interest, or the identification of locations which appeared to contain materials suitable for radiocarbon dating. The unexpected presence of paleosols in some cores required an immediate adjustment to the core sampling intervals in these regions.

When the subsample analysis of the initial set of sampled cores was completed, the sampling strategy was adjusted as required to obtain additional data. Specifically, the lack of ostracodes in the upper portions of the first cores studied (WOO06-5A-1K, WOO06-6A-1K, and SHOO06-2A-1K); indicated ostracodes were not present along the entire core length and hence could not provide a complete paleoenvironmental record of the entire core sequence as was initially anticipated. Subsequently, it was decided to add thecamoebians to the study as a means to add paleoenvironment information, particularly in the upper cores where ostracodes were not present. To obtain this additional thecamoebian data, sample intervals were adjusted in previously subsampled cores. In effect, the sampling program was iterative, and sampling was carried out in progressive steps as it became evident additional data was required.

Subsamples for radiocarbon dating were selected in order to establish the time frame of the stratigraphic sequences in each core. In some cases identifiable vegetative fragments and organic rich laminae were observed at the surface of the split core and were removed for dating. In other cases samples at specific intervals were taken and sent to Alice Telka of Paleotec Services in Ottawa, to pick suitable macrofossils that were likely to provide an unambiguous date (i.e. material that had not been reworked from older sediment). In addition, it was important to date the beginning and end of ostracode sequences, and beginning of the thecamoebian intervals. For certain cases, further subsamples were taken for radiocarbon dating to determining the beginning and end of paleosols identified in the WOO06-5A-1K, WOO06-6A-1K and WOO06-4A-1K cores. Samples were also taken to date pollen in those parts of the cores (primarily at the bottom of the cores), where there are very limited macrofossils with suitable organic materials available for radiocarbon analysis.

Further intensive sampling was undertaken in the Kenora and SL cores (WOO06-7A-1P and SHO06-2A-1K) to provide materials to permit a thecamoebian species analysis by a thecamoebian specialist. Unfortunately this analysis is not available at the time of the writing of this thesis. Similarly, samples were taken to permit a diatom study in the Kenora core (WOO06-7A-1P) by the Paleoecological Environmental Assessment and Research Laboratory (PEARL) at Queens University, Ontario Canada, but it is only partially complete at the time of the writing this thesis.

In addition, samples were taken to perform a moisture analysis on several cores, especially near the paleosol horizons in the deeper water of the southern Northwest Angle core (WOO06-5A-1K). Samples were also obtained from the Kenora core (WOO06-7A-1P) to perform a broad qualitative XRD analysis at the northern outlet, to see if there were any significant changes in the mineralogy at this location. Moisture Data is provided in Appendix D.

2.4.3 Macrofossil Processing Strategy and Methodology

2.4.3.1 **Ostracodes**

Sample processing was conducted using the techniques employed for studying ostracodes by Dr. Brandon Curry of the Illinois Geological Survey at the University of Illinois. This technique was subsequently used for all macrofossil sample processing, except those used by external contractors. Although this sample processing was developed for ostracode studies, the other macrofossils recovered using this methodology did not appear to have been adversely affected. As the core sampling program evolved to include thecamoebians, the same sample processing method for separating the clay and silt fractions was retained. Some sieving operations (discussed later) were modified somewhat, and examinations of the macrofossils broadened to identify the other macrofossils and record the data they provided.

Data was initially recorded on subsampling data sheets, primarily designed to facilitate the recovery of ostracode data, and relevant additional data such as those provided by

other macrofossils and sediment characteristics including mineralological lithics. These data sheets were revised following the processing and data extraction of the initial subsamples, to facilitate recording of observations including notes and sketches of observed macrofossils (Figure 31). This revised data sheet was used for most of the processed subsamples, with a similar though less structured sample form used to record the data of the initial processing campaign for the Northwest Angle open basin cores and the SL core (WOO06-5A-1K, WOO06-6A-1K, and SHO06-2A-1K).

The sampling intervals in the cores were initially selected to obtain a consistent sample interval along the core and hence the means to trend any changes in the ostracode populations. The core sampling intervals were modified in subsequent sampling campaigns for a number of reasons, with the sampling interval often supplemented in certain regions to obtain additional data to improve discrimination in regions deemed to be of particular interest (Figure 30). Additionally, the core sample interval was shortened to permit further discrimination near the point of disappearance of ostracodes and first appearance of thecamoebians. The data from the subsample data sheets are presented in Appendix A, Section 2 for each core.

Lake of the Woods Core Samples

#
MOMOS WOO06
Sample # _____
Depth in Core _____
Date _____

Sample Description
Colour _____ Consistency _____
Moisture Content _____

Petri Dish View:

Lithics
Type _____
Size _____
Roundness _____
Sample Proportion ____%

Organics
Plant Mat'l _____
_____
_____datable ?____
leaves ___ Stems ___ Wood Frgmts ___ Seeds___ Others _____
Sample Proportion ____%

sketches

Charcoal _____
_____datable ?____
Sample Proportion ____%

Insect Mat'l _____
_____
_____
exoskeleton ____ larvae cases ____
Sample Proportion ____%

Thecamoebans _____

Other organics _____

Datable Material Yes____ Description: _____

Ostracodes _____Type _____ Prelim. Count _____

Sieve # 35	
Sieve # 60	
Sieve # 80	
Pan	

Ostracode Totals

	Adults	A-1	Total
sub triangulata			
friabilis			
rawsoni			
sharpei			

Figure 31. Subsampling data sheet used to capture information related to ostracode populations and subsequently to gather the available data related to thecamoebians and other macrofossil data, including the abundance of lithics, plant material, charcoal, and insect material.

To reduce microbial growth in the sediment samples, the subsample containers were stored in a cooler whenever possible. Prior to processing of each sample, a rough estimate of the moisture content in each sample was made, and its general colour was noted. The amount of material in the sample container was also noted and recorded on the subsampling data sheets, since some containers were not completely full due to variabilities in sample consistency and difficulties in extracting samples. The consistency of each sample (i.e. how well the material held its shape) was also recorded.

The material was extracted from the sample containers and placed in a 500 mL beaker, and 1 g of baking soda and about 0.1 g of commercial Calgon (sodium carbonate, and sodium hexametaphosphate) were added to facilitate disaggregation of the clay to silt sized sediments (i.e. to deflocculate and disperse the material) and assist in the separation of the macrofossils from this material. About 150 mL of distilled water, heated to boiling in a microwave oven, was poured over the sediment, and the samples were allowed to disaggregate for several hours. The disaggregated sediment was then washed through a 12 inch # 100 mesh (150 micron) U.S. standard brass sieve (ASTM E-11 specification), using hot tap water sprayed onto the sample material using a flexible water spray hose. Care was taken during sieving to ensure material was not lost over the sieve edge. The sieve was tilted back and forth under the spray to separate sand-sized and coarser material, with the clay and silt fractions washing through the sieve and down the drain. In some cases, particularly in gyttja deposits, the sample had to be left overnight in the Calgon solution, or occasionally the process had to be repeated, before disaggregation occurred.

The disaggregated materials on the sieve were transferred to a petri dish using distilled water from a spray bottle, where a preliminary viewing of the recovered material was conducted using an optical (non-polarizing) microscope. Descriptions and sketches of the macrofossils were then recorded in the subsample data sheet. The petri dish was then placed in a fume hood, and allowed to dry at room temperature.

The > 150 micron dried materials were subsequently dry sieved. The dried materials in the petri dish were carefully transferred using a stiff brush into a nested set of three, 8 cm-diameter U.S. standard brass sieves [(ASTM E-11 specification) (#35, #60 and # 80 mesh; 500, 250 and 180 μ) and a catch pan]. The sieve set was then covered and tapped on a flat surface to complete the sieving process.

The materials from each sieve were transferred to a counting tray by tapping the contents of the sieve into a 9 x 5 cm black counting tray with 1 cm grids. The dark colour and grids facilitated identification and counting of the ostracode macrofossils using an optical binocular, non-polarizing microscope (Kyowa model FBO 99-001; 0.7 - 4.5 magnification). Sieve contents which were not released by tapping were brushed into the tray to ensure all the materials were transferred. This process was repeated for each of the three sieves, plus the catch pan. Ostracode species and their instars vary in size and are captured on the various sieves. The capture location of the ostracode shell on the various sieves assists in identification of the ostracode species and in identifying the adult and A-1 (last instar) shells. Both the adult and A-1 instars were counted and recorded.

All the ostracode macrofossils were then transferred to 3 x 1 inch (7.5 x 2.5 cm) microslides to permit storage of the materials and re-examination if necessary. The microslides have a 3.6 x 1.6 cm storage area with 4mm x 4mm grids and a glass cover which can be opened, permitting materials to be removed (e.g. for adding to radiocarbon samples).

Ostracode tests and other macrofossils, plus selected representative mineral rock fragments (lithics), charcoal and various organic materials, were transferred to the microslide with a picking brush (# 3/0). The picking brush was dipped in demineralized water to facilitate material transfer (the surface tension of the water causes any material the brush contacts to adhere to the brush). Additionally, most of the charcoal and datable organic materials collected on the sieves, and some of the larger pieces from the collection pan which captures materials which pass through the nested sieves, were also transferred to the microslide. Representative lithics, insect carapace fragments and larvae cases, and other materials including bones, teeth, fish scales and thecamoebians were transferred. In some cases where there were large amounts of organic materials (other than ostracodes) and only representative samples were transferred to the microslides. The remaining material from the counting tray and catch tray were then transferred back to the original 15 mL sample container and stored. The data from the observations made in the counting tray were transferred to the subsample data sheet and sketches were made of the biota. Ostracode species were identified using publications by Delorme (Delorme, 1970a; Delorme, 1970b; Delorme, 1970c; Delorme, 1970d; and Delorme, 1971a) and

through application of the training provided by Dr. Brandon Curry of the Illinois Geological Survey.

Following the sieving processes, the dry sieves were vigorously tapped to release all materials trapped in the sieves and the stiff brush was used to release and remove trapped materials to ensure cross contamination between various dry sieving operations were eliminated. Similarly the counting tray was tapped, brushed and cleaned with demineralised water and wiped with a lint free wipe (Kimwipe). The wet tray used to wash the sample was reverse flushed between sample processing operations to remove all visible materials. The picking brush and stiff brush were both visually inspected to ensure dried materials were not captured within the bristles.

2.4.3.2 **Thecamoebian Subsampling**

Thecamoebians were noted in the materials removed from the clay and silt fraction of the sediments during the initial sampling campaign for ostracodes. Although thecamoebian macrofossils are typically much more fragile than ostracodes, they did not appear to have been damaged by the processing, although transferring the thecamoebians after processing did result in some of them disintegrating, so special care was needed to transfer these tests intact. It is also likely some thecamoebians may have been damaged during the initial dry sieving operations to remove ostracode shells.

The subsampling process developed for ostracodes was used for extracting thecamoebians from the clay and silt sediment fractions. Once the subsample was processed and washed into the petri dish, preliminary observations were made and recorded. The objective of the thecamoebian sampling was only to identify their presence; hence there was no requirement to dry sieve the processed and dried subsample in non ostracode bearing intervals. After the initial sampling campaign if no ostracodes were observed in the petri dish, dry sieving was not conducted. In rare cases, a small number of ostracode tests were observed in the same sample as thecamoebians, and full processing was carried out including dry sieving to facilitate the capture of the ostracode data.

For the thecamoebian intervals the dried contents of the petri dish were transferred to the counting tray, and more thorough observations of macrofossils, were made to facilitate data recovery. Transfer of macrofossils to microslides was completed using the same process used for ostracodes.

2.4.3.3 **Macrofossil and Lithic Materials Subsampling**

Macrofossils were extracted when ostracode or thecamoebian samples were processed. Following wet sieving and drying of subsamples in a petri dish, and either dry sieving (ostracode samples), or direct transfer of dried materials (thecamoebian samples), the material was transferred to the counting tray. From here, all larger fragments of charcoal > 180 μ were transferred to the microslide including some of the charcoal fragments from the dry sieve catch tray (150-180 μ). Additionally, typical macrofossils and lithics were transferred to the microslide. These data were then recorded on subsample data sheets and sketches made. Observations related to the abundance of the macrofossils as well as the recording of the presence of other macrofossil materials such as bones, teeth, fish scales, seeds etc. were recorded on the data sheets. Additionally, the presence of potentially datable organic materials, based on the quantity of the material and whether fragile appendages were retained by the organic fragments, were recorded to assist in selecting materials and intervals suitable for future radiocarbon dating.

Initially, exposed organic materials were extracted from the split core for radiocarbon dating during the macrofossil subsampling process at the LRC. Subsequently, selected organic materials from processed subsamples which had been transferred to the microslides were sent to Paleotec Services along with additional core subsamples. Paleotec Services selected suitable materials from these sources for AMS dating and in some cases combined these materials if appropriate, to obtain sufficient material for radiocarbon dating. The selected organic materials were subsequently sent to the Keck

Carbon Cycle AMS Facility at University of California, Irvine. Through the iterative core sampling process, additional subsamples were also obtained, and sent directly to Paleotec Services. In addition, Paleotec Services identified selected flora and fauna, and used these data for ecological interpretations which are used to help assess paleoecological conditions in LOTWs.

The separated lithic materials were also observed. Their mineralogy and general physical attributes (size, roundness, and abundance) were recorded. Additionally, charcoal fragments were observed and noted when processing the subsamples, and their size and abundance in the sample were recorded.

2.4.4 XRD Analysis

Only a very qualtitative assessment from bulk sediment X-ray diffraction (XRD) samples was completed at several broadly spaced intervals in the Kenora core (WOO06-7A-1P). The objective was to see if any significant mineralogical changes through time could be identified in the LOTWs sediments near the outlet to the Winnipeg River. Five samples were taken in what appeared to be diverse sections of the core. Two samples were taken in the upper core, one near the top and the other mid-core. Additionally, one was taken near and above a pink clay unit; one in the pink clay unit; and one was taken below the pink clay unit near the bottom of the core. The bottom two samples were taken in what appeared to be Lake Agassiz sediment.

The XRD samples were obtained from freeze dried samples which had been used for moisture analysis. These were crushed to a fine powder, and then a paste was made and smeared onto slides. These slides were loaded into a Phillips PW1710 Powder Diffractometer using Cu radiation and scanned. The powder diffraction pattern produced was then read into MDI Jade 6.1 Pattern Processing Software to identify the major mineralogical components. The Jade XRD plots are located in Appendix C.

2.4.5 Moisture Analysis

To assess changes in sediment moisture content a series of subsamples were taken in several cores. Samples were prepared and processed by James Teller using the LRC freeze drying equipment and procedures. The wet subsamples were weighed in their original 15 mL sample containers and placed on a metal tray and frozen. They were then placed in the freeze drier and a vacuum was applied overnight or until the vacuum gauge read about 10^{-1} mbar. The dry subsamples were then weighed and the data was processed.

In the Northwest Angle core (WOO06-5A-1K), which contained a number of paleosols, extensive sampling was performed extracting 10 mL samples at 10 cm intervals, with shorter sample intervals near the buried soil horizons.

Other cores studied for moisture content include the southern basin core (WOO06-1A-1K), the deeper of the Northwest Angle channel area sites (WOO06-3A-1K), and the

Kenora core (WOO06-7A-1P). The latter was sampled along the entire core using a 10 cm sampling interval. A broad moisture profile was also taken in the SL core (SHO06-2A-1K); only the last two segments of this core were sampled with intervals 15-50 cm apart. All samples were processed at the LRC using LRC freeze drying equipment, and data is located in Appendix D.

CHAPTER 3 RELATIONSHIPS OF STUDIED PROXIES TO ENVIRONMENTAL CONDITIONS

3.1 GENERAL

Cores from LOTWs and SL provide evidence of changing paleohydrology and paleochemistry in the lake. For shell building biota the availability of $CaCO_3$ is essential. Carbonate is mainly derived from Paleozoic rocks, which are found in glacial erosional deposits and in subsequent aqueous transport and deposition in the LOTWs region, and in generally thicker glaciolacustrine deposits (Minning et al., 1994) (see Figure 16 and discussion in Section 1.4.3). This would have supplied bicarbonates and calcium ions to Lake Agassiz as well as LOTWs and SL. The shell building organisms within the LOTWs lacustrine cores, including those specifically adapted to the cold deep waters of Lake Agassiz, such as certain species of ostracodes, are markers and are useful in differentiating Lake Agassiz from the subsequent and more modern lake conditions.

Interpretations of the timing of the climatic responses and magnitude are however dependant on lake morphology, and the geological and hydrological settings (Laird et al., 2003). Influences from the groundwater inflows have been determined to be substantial in prairie lakes and affect the biota making it difficult to extract climate proxy data normally derived from evaporation and precipitation cycles (Laird et al., 2003). In larger complex lakes local inflows (surface and groundwater) can influence the chemistry in a region of the lake, or within a local bay (Laird et al., 2003). The groundwater inflows in the southern basin glacial and lacustine deposits of LOTWs may have had an influence

which differs from the groundwater inflows from other parts of LOTWs, which are located in Precambrian Shield topography (Figure 16). Groundwater influences on paleochemistry were noted in the Wampum site very near the western part of the southern basin of LOTWs.

Ostracode macrofossils and the nature of the sediment were studied in this thesis as the primary means to identify changes in paleohydrology and paleoenvironments. It is important however when attempting to extract climate signals from sediments that other means be used to confirm and enhance interpretations. Many proxies are available, and climatic interpretations are best made through the use of a multi-proxy approach (Booth and Jackson, 2003).

Thecamoebians were also used to gain insight into changing conditions. The presence of thecamoebians was noted and radiocarbon dates obtained to establish the timing of their appearance. A cursory thecamoebian species analysis was performed in some cores. Additionally, macrofossils of plant and insect biota, vertebrate bones, fish scales, and charcoal, were recovered as useful proxies for assessing changing paleoenvironmental conditions within the lakes (Birks, 2001; Booth and Jackson, 2003), as well as the means to obtain materials for radiocarbon dating.

The macrofossils within the sediments not only provide an indication of the ecological conditions within the lake, but also within the watershed of the lake, and in the case of many microfossils such as pollen, beyond the watershed (Birks, 2001). Macrofossil populations (including datable organic materials) are typically much lower than

microfossil populations, making sediment studies dependant on the availability of the macrofossil proxy (Birks, 2001), which forces a multiple proxy approach in order to understand paleoclimate conditions. This was encountered in LOTWs where the ostracode proxy populations were often limited, and in the upper portions of the cores unavailable in the record. Furthermore, in the case of larger lakes macrofossil dispersion can be limited, and their presence can indicate a more local lacustrine condition or nearby watershed terrestrial conditions (Birks, 2001), and hence can be better suited for establishing the local environmental.

Sediment data were also obtained from the study of core sediment structures and textures, including paleosols, moisture analysis, and a qualitative XRD analysis. The properties of the lithics in processed subsamples were also observed and recorded, including the physical and mineralogical properties of various large lithic grains, which provided further information on changes in the depositional environments.

In summary, a multiproxy approach was used, including available macrofossil, microfossil and sedimentological data from the cores, and was used to relate these data to the changing paleoclimate in the LOTWs region and the changing paleohydrology of LOTWs and SL.

3.2 USE OF OSTRACODES IN PALEOENVIRONMENT RECONSTRUCTIONS

3.2.1 General

Ostracodes are typically benthic or epi-benthic, and crawl or weakly swim to feed on the available detritus (which is a prime factor in their existence) (Cohen, 2003). Ostracodes undergo ecdysis (molting) and typically have up to eight instars in their juvenile stages before the adult stage (Horne et al., 2002). Ostracodes usually reproduce sexually but can reproduce by parthenogenesis when stressful environmental conditions are encountered (Curry and Yansa, 2004). Their eggs can remain viable for years up to decades, should they desiccate (Horne et al., 2002). Life spans range from a few months to up four years (Horne et al., 2002).

Ostracodes are aquatic crustaceans of the class Ostracoda with adults typically ranging from 0.5 to 3.0 mm. They mainly occupy marine and non-marine environments such as lakes, ponds and streams, although some species occupy moist terrestrial regimes such as those in mosses, soils and leaf litter (Holmes, 2001; Horne et al., 2002). Their bivalve carapaces are strongly calcified and preserve well, with their fossils ranging in age from the present to as far back as 500 million years (Horne et al., 2002). The ostracodes of interest for Holocene studies are Subclass Podocopa, Order Podocopida, which is well represented in Quaternary sediments (Horne et al., 2002), as long as the pH of the water is above 8.3, otherwise their calcite shells may not be produced because calcite saturation is inhibited, or their preservation made unlikely (Delorme, 1989; De Decker, 2002).

Ostracode bivalves enclose the body and 5-8 appendages which the organism uses for locomotion in crawling over the substrate or swimming (Horne et al., 2002; De Decker, 2002). Ostracodes are restricted to certain ecological conditions determined by available habitats and climate, and can be limited by the physical and chemical conditions of the habitat (Delorme and Zoltai, 1984; Curry, 1999).

Ostracodes can provide information about and trends in water chemistry, physical habitat, and paleoclimate from fossil records because they can be related to modern fauna ecological conditions (Delorme, 1989). The presence of certain ostracode species can also be used to try and identify paleoecological conditions, based simply on the presence and absence of the ostracode species (Curry and Yansa, 2004). Paleoecological analyses have been used to develop ecological models to indicate the environmental ranges of ostracodes (Smith and Horne, 2002).

The calcite ostracode shells preserve well and record the chemistry in the aquatic environments they occupied (Chivas et al., 1986). Ostracode shell geochemistry, including Sr/Ca and Mg/Ca ratios, have been used as a means to establish paleotemperatures and paleosalinity of lakes and this is then related to paleoclimate (Chivas et al., 1986). In some northern U.S. prairie lakes, paleoclimates have been reconstructed through salinity studies (Fritz et al., 2000; Haskell et al., 1996). Studies based on ostracode shell trace elements and sediment bulk-carbonates, compare well with the diatom-based salinity proxy (Fritz et al., 2000). These analyses have been

successfully used to identify and establish durations of drought sequences in regional climates although a multi-proxy approach is required (such as pollen) (Haskell et al., 1996; Ito, 2002). The best lakes for these studies are in simple closed-basins, with catchment areas that have not changed over the time interval of the study (Chivas et al., 1986).

3.2.2 Using Ostracodes as Paleoenvironmental Indicators

Ostracodes have been successfully used in many paleoenvironment reconstructions. An autecological method has been used to relate modern ostracode population data from specific bodies of water to fossil ostracode assemblages, by using a best match process to assess the paleo conditions (Delorme, 1969; Smith et al., 1992; Curry and Delorme, 2003). This, in conjunction with an understanding of the environmental tolerances of species, can provide a means to interpret the environments of the fossil ostracode assemblages (Delorme, 1969; Curry, 1999), although the farther back in time from the modern ostracode environments the greater the uncertainty (Smith, 1991). Environmental Tolerance Indices (ETIs) have been produced to assist in relating ostracodes species to specific environments (Curry, 1999; Smith and Horne, 2002; Davis et al., 2003).

Unlike terrestrial organisms, ostracodes do not rapidly respond to many climatic changes due to their isolation within the hydrosphere; they do however, respond to longer term climate variability, particularly precipitation/evaporation balance (Curry, 2003). This

balance affects the hydrochemistry of lakes and strongly influences ostracode populations (De Deckker and Forester, 1988) (see next section). Water temperatures also affect ostracodes but to a lesser degree (Curry, 2003).

Hydrochemical influences include basin overflows, groundwater inflows, and water residence times, as well as climate and the underlying geology of the lake and watershed (Curry, 2003). Even the surrounding overlying organic terrestrial materials can leach carbonates or other elements into the lake, due to the acidity of the organic litter (Delorme 1969).

Ostracode populations, both the species and their abundance, can be used to track changes in lake depth (Curry, 2003). Mobile ostracode species populations tend to increase in shallower conditions, due to the additional sunlight reaching the bottom which increases vegetation, and therefore the ostracodes (Curry, 2003). Shallow water environments are thermally variable and subject to wave action, and ostracode species living in this ecological zone need to be tolerant to a wide range of conditions including waves and wind induced currents (Curry, 1999). In deepening periods, benthic burrowing species increase in the dark and muddy water/sediment interface (Curry, 2003). The absence of ostracodes can also mean the shells were leached from the sediments due to diagenetic conditions, even if they originally lived in the lake; this is most likely to occur under low pH conditions (Delorme, 1969).

Variations in water energy regimes can be tracked by differing abundance of ostracode instars and adult shells (De Deckker, 2002). A complete spectrum from the relatively small instars to the larger adults implies a low energy regime where no sorting occurs. The presence of only adults indicates higher energy conditions (De Deckker, 2002). The presence of only adults can also be interpreted as a possible rapid change in oxic state, temperature or salinity, eliminating the juveniles before they progress to adults, leaving only adults for a short period of time (De Deckker, 2002). The shells of freshwater ostracodes do not have complex hinges (Holmes, 2001) and presence of articulated shells can be used as a measure of the degree of post mortem transport, or presence of high sedimentation rates (Holmes, 2001; Cohen, 2003).

In the case of LOTWs and SL, ostracodes were found in the bottom portions of all of the cores, but none were found in the uppermost portions of the cores. A spot check of modern LOTWs near shore environments did not produce any ostracodes and subsequent data from examined cores supported this as no ostracode shells were observed in uppermost core sediments. In addition, in a diatom study of LOTWs by PEARL in 2006, it was noted there were no ostracode shells present from short cores of the modern lake sediments (Ruhland, 2006).

The complexity of the bathymetry and topography of LOTWs during the Holocene would likely have resulted in considerable ostracode population variability due to the many different ecological niches, particularly as LOTWs evolved from its separation from Lake Agassiz, to its modern configuration. LOTWs would likely have had a very complex

response to climate changes, due to its large size and interconnections to other watersheds (Curry, 2006, personal communication). Of course the absence of ostracodes in the upper portions of the cores limits the use of this proxy in interpreting the entire environmental history of LOTWs. However, the ETIs do provide insight into the major paleohydrological and paleochemical conditions in those portions of the core which do contain ostracode populations, such as the presence and dominance of *Candona subtriangulata* ostracodes which are a prime indicator of deep, cold and low TDS levels (Burke, 1987), which are typical of Lake Agassiz waters, or near Lake Agassiz conditions (A. Breckinridge, 2007, personal communication).

LOTWs is not an ideal candidate for establishing and tracking of hydrological and hydrochemical changes. Normally, smaller bodies of water with limited or simple watersheds, and limited or well-understood groundwater inputs, are required to ensure climatic signals can be extracted from variations in ostracode populations (B. Curry, 2006, personal communication; Ito, 2002; Smith 1991). The added complexity of the regional differential isostatic rebound of LOTWs must also be taken into account when trying to extract a climate signal. Due to the size and complexity of LOTWs the discrimination available for identifying changes in climate based on variations in ostracode populations in is only qualitative. However, ostracodes do provide a broad indication of climatic variability and changes in lacustrine conditions.

3.2.3 Chemical Influences on the Presence of Ostracodes

The ecological niches preferred by different species of ostracodes may result in changes through time and space in the species present and the ostracode population mix. These variations provide a paleoclimatic/paleohydrologic signal. Even the absence of ostracodes in a core sequence can indicate changes in the paleochemistry of the lake. Additionally, specific species of ostracodes are favoured by hydrochemical (solute) conditions within the lacustrine environment. The ETIs which were developed for ostracode species provide the means to assess which paleoenvironmental conditions existed at the time the sediments were deposited (Davis et al., 2003).

Low pH conditions are unfavourable to the development the calcite shells of ostracodes, or their preservation (Benson et al., 2003). The thin shells of adult ostracodes produced by low pH levels are subject to post mortem bacterial destruction of their carapaces both on and within the sediment, as the thin protective organic sheath on the calcite shell is eaten by the bacteria exposing the calcite to chemical destruction (De Deckker, 2002). Ostracode shells can be eliminated by dissolution at the time of deposition, especially those with thin shells, including instar moults (Delorme and Zoltai, 1984; Holmes 2001; De Deckker, 2002). Alternately, fossil ostracode shells can be thinned by diagenetic processes.

Preservation of the ostracode tests is best in alkaline lakes, and their distribution is strongly tied to the balance of bicarbonates, calcium, and sulphates (Smith, 1991). This

solute balance is affected by climatic conditions (the precipitation and evaporation balance), the underlying mineralogy, watershed runoff, fluvial system throughput, and any inputs from groundwater (Smith, 1991).

The initial conditions of the lake, the underlying mineralogy of the lake and watershed, and the groundwater inputs, all interact with the climatic conditions in a very complex manner, to determine overall chemical composition of the lake and the levels of bicarbonate and calcite ions in the water. This chemical composition subsequently strongly affects the makeup of the ostracode population and the production of their shells (Ito, 2002; Smith, 1991), and their preservation (Benson et al., 2003). Inputs from river systems, and hence the chemistry of distant watersheds, can further influence the ionic balance (Smith, 1991).

Calcium and bicarbonate are the most common dissolved ions from the dissociation of carbonates and carbonic acid, and $CaCO_3$ typically precipitates either through the effects of algal photosynthesis within the water column, or as a result of reaching the calcite branch point (Figure 32) (Curry, 1999; Smith, 1991). If precipitation and runoff decrease and evaporation increases, mineralogical precipitation of $CaCO_3$ would continue until either Ca or CO_3 is depleted, enriching the lake in either Ca (if CO_3 depletes first) or CO_3 producing one of two types of saline lakes, which strongly influence ostracode populations (Smith, 1991).

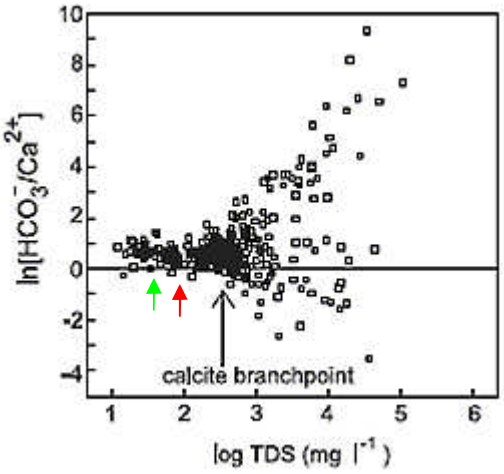

Figure 32. Modern ostracode data from 341 sampling locations in the continental U.S. database, plotted against the log of TDS of the water, indicating the calcite branch point at a TDS of 325 mg/L; bicarbonate enriched environments are locate above the dark line and more saline conditions to the right, with in filled boxes indicating where ostracodes were present at sample locations (Curry, 1999, p. 53). The red arrow indicates a TDS of 100, which is typical of Lake Agassiz (Curry, 1997), with the green arrow to the left indicating the estimated modern LOTWs TDS of about 50 mg/L (Pla et al., 2005).

Large changes in Ca or HCO_3 can occur depending on the source of the ionic inputs, with HCO_3 increasing with respect to Ca if evaporation exceeds precipitation (Curry, 1999; Mann, 1999). The diversity (number of species of ostracodes) is highest centred on the calcium branch point, which is often considered as the dividing line between fresh and saline waters (about a salinity of 0.3 g/L) (Figure 32) (Smith, 1991). The major ions in the water beyond the calcite branch point are key in determining which species are present however, not salinity (Figure 33) (Smith and Horne, 2002). Beyond this point the abundance of ostracodes continues to rise with increasing TDS until the non marine ostracode upper tolerance limit of about 100 g/L is reached (Holmes, 2001; Smith and Horne, 2002). The presence of ostracode species and their abundance is dependant on these complex relationships, with high bicarbonate conditions favouring ostracode presence (Curry, 1999). Establishing the specific reasons for the ostracode species and

population changes, and understanding the role of different hydrochemical conditions is difficult, and requires a good understanding of the modern system (Ito, 2002), which is not currently available for LOTWs.

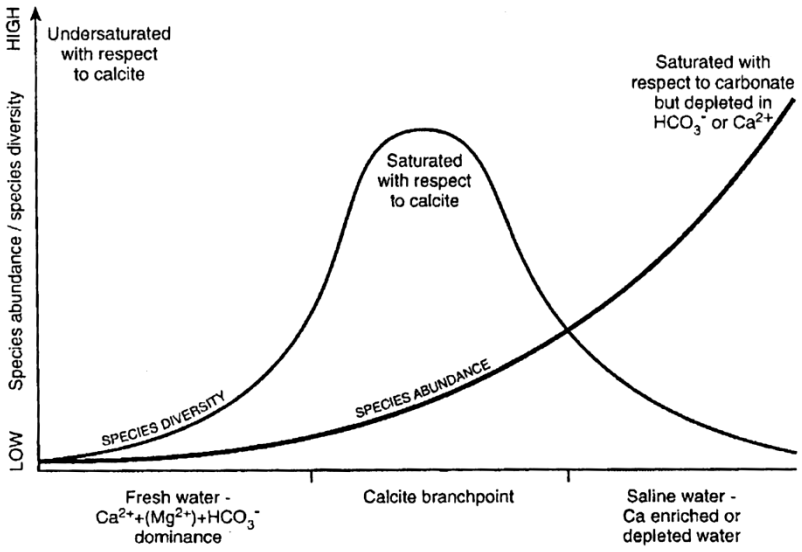

Figure 33. Plot of ostracode diversity and abundance, against salinity in lacustrine non marine environments (Holmes, 2001, p. 131).

3.2.4 The Influences of Environmental Conditions on LOTWs Ostracode Populations

Maps of modern ostracode populations have been prepared which indicate ostracode populations follow the climatic boundaries between the major air masses similar to the ecotones established for plant biomes in North America, and this relationship has been used to locate the paleo boundaries of air masses (Smith and Horne, 2002). Increases in diversity of ostracode species respond to increasing nutrient levels and their availability

during increases in erosion, and due to increases in salinity due to a warmer and drier climate (Burke, 1987).

A statistical analysis using a large database of sites in the U.S., the North American Non-Marine Ostracode Database (NANODe) has been completed which relates ostracodes to hydrochemical conditions and climate (Davis et al., 2003). It was consulted to help interpret paleoclimate conditions in LOTWs.

De Deckker and Forester (1988) hypothesized that ostracode diversity, as expressed by the number of species present, increases and then subsequently decreases as TDS increases (Figure 33). In the regional context, the initial low salinity hydrochemistry of Lake Agassiz estimated as having a TDS < 100 mg/L (Curry 1997), appears to have dropped to about half of this value over the period since isolation from Lake Agassiz (Pla et al., 2005), and is still well below the calcite branch point (Figure 32). The species richness of LOTWs and SL ostracode populations, in the ostracode interval of the examined cores of LOTWs and SL, were all relatively low, with only 4 ostracode species identified. This implies LOTWs and SL had mostly been quite fresh.

Four ostracode species were identified in LOTWs and SL; *Candona subtriangulata*, *Cyclocypris sharpei*, *Fabaeformiscandona rawsoni*, and *Limnocythere friabilis.* The following environmental relationships are associated with these species and are related to environmental conditions in LOTWs.

Candona subtriangulata ostracodes are benthic and prefer a low mean bottom temperature of about 5.5 ^{o}C within its broader tolerance range of 3-19 ^{o}C (Delorme 2001). This species is commonly found at depths of 45-305 m in modern Lakes Superior, Huron and Ontario, where bottom temperatures do not vary significantly (Delorme, 2001). This species is more restricted than most ostracodes to pristine, low salinity (including SO_4) conditions (Delorme, 2001) which restricts its modern geographic range (Delorme, 2001). The presence of *C. subtriangulata* alone, implies deep cold waters were always present (Dettman, 1995). This species is one of few benthic species which could have tolerated the cold and oligotrophic conditions of proglacial lake such as Lake Agassiz (Burke, 1987), including the comparatively low dissolved solute levels (Table 2) (Curry, 2003).

The presence of this species in the lower (older) portions of all LOTWs and SL cores indicates the waters were generally cold and deep like those that existed in Lake Agassiz (Curry, 2006 personal communication; A. Breckinridge, 2007, personal communication), or alternately the early stages of LOTWs and SL when the water was still cold and deep in certain regions of these lakes providing suitable conditions for *C. Subtriangulata*. After LOTWs separated from Lake Agassiz, terrestrial inputs and a rapidly eroding new shoreline and would continue to provide a source of $CaCO_3$ in LOTWs and SL suitable for the production of shells. The abundant and available chemical and organic nutrients washing into the basin would essentially retain similar hydrochemical conditions to those of Lake Agassiz and result in an increasing food supply. Overall the cold and deep portions of the lakes in conjunction with continuing favourable chemical conditions and

improved supplies of nutrients input from the watershed would continue to favour *C. Subtriangulata*. Ostracode diversity would have eventually increased as the nutrient levels remained high and salinity increased following the effects of drier climates, eventually giving preference to other ostracode species (Burke, 1987).

Table 2: Modern Environmental Ranges of Ostracodes which were Observed in LOTWs and SL Cores

Ostracode	TDS Range (mg/L) approximate	pH Range	Bottom Water Temp Tolerance Range ^{o}C	Habitat % Probability Lake (L), Pond (P), or Stream (S)
Candona subtriangulata	20-100	6-8	3-19	L-100
Cyclocypris sharpei	15-9000	5-11	3-24	L-20; P-60; S-20
Fabaeformiscandona rawsoni	50-11000	6.8 – 11.5	5-20	L-60; P-15; S-25
Limnocythere friabilis *				

* Modern data for *Limnocythere friabilis* is very limited and is not presented, however, this ostracode appears to prefer cold near tundra conditions similar to *Candona subtriangulata* and is an indicator of glacial conditions and has been associated with tundra like climatic conditions (Curry, 2003).

Modern environmental ranges of ostracodes observed in LOTWs and SL cores. Prepared from data in (Delorme, 2001, p. 821-825).

Cyclocypris sharpei are benthic ostracodes that occupy a broad range of TDS levels and a very broad pH range (Table 2). They have been recovered from lakes as well as very low dissolved oxygen level stream environments, and have the ability to survive broad temperature ranges forced by shallow water conditions, including flowing and standing water environments (Delorme, 2001).

Fabaeformiscandona rawsoni (formerly *Candona rawsoni* (Forester et al., 2005, www.kent.edu/NANODe) are benthic ostracodes (Xia et al., 1995) which prefer fresh to oligohaline water (0.5-5 0/00) with enriched bicarbonate levels. This species prefers lake and wetland habitats, with springs and streams and bicarbonate levels sufficient to allow this ostracode to become established (Davis et al., 2003). As noted in Table 2 this species can tolerate an extreme range of salinities, from 50-10,000 mg/L. Other authors note *F. rawsoni* is eurytrophic and can be found in both enriched and bicarbonate depleted environments in sulphate dominated regimes. However, it prefers and is most abundant in relatively low salinity oligohaline lakes (Smith, 1993; Smith 1991). *F. rawsoni* are often observed in cold environments in ephemeral lakes, as well as in permanent bodies of water (Table 2) including the Great Lakes and have been found in association with *C. subtriangulata* (Delorme 1969; Mann, 1999). They are noted to be highly tolerant of a variety of chemical conditions and salinities (Figure 34) (Table 2) (Curry, 1999). The change from an environment dominated by *C. subtriangulata* to one dominated by *F. rawsoni*, implies waters changed from fresh to the more saline waters tolerated by *F. rawsoni* (Dettman, 1995); because both species are tolerant of cold conditions (Table 2).

This ostracode was not abundant in LOTWs and SL. *F. rawsoni* has been correlated to the position and duration of the major air masses, and is currently restricted within the eastern boundary of the relatively dry Pacific air mass, and below the summer extent of the Arctic air mass (Pfaff, 2004). Its presence generally infers that precipitation is greater than evaporation as reflected in increasing but still relatively low salinity (Smith, 1991).

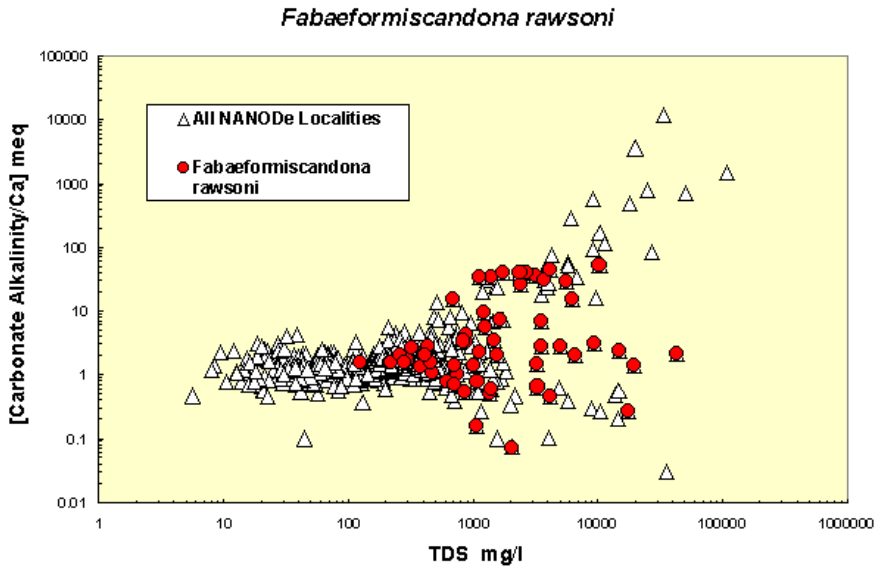

Figure 34. *Fabaeformiscandona rawsoni* ostracode species solute space distribution based on solutes; x axis TDS in mg/L, and y axis the ratio of bicarbonate and carbonate to calcium in mg/L (both shown on a log scale). Red circles are sites with living species, and white triangles are all NANODe sampled sites. sampled for ostracodes (NANODe Version 1, Species List, *Fabaeformiscandona rawsoni*) (Forester et al., 2005, www.kent.edu/NANODe).

Limnocythere friabilis is often present in ice marginal and supraglacial lake sediments (Curry and Yansa, 2004). Very few modern Canadian lakes still contain these ostracodes, but modern Lake Michigan and Lake Erie have populations at depths between 30 and 75 m, and below 15 m respectively, which are near or below the thermocline (Curry and Yansa, 2004). These relatively shallow depths imply that *Limnocythere friabilis* favoured paleoenvironments supplied with meltwaters or cold groundwater inputs (Curry and Yansa, 2004). Since major ions of water beyond the calcite branch point are critical in determining which species are present, not salinity (Figure 35), the

Limnocythere ostracode species exhibit a hydrochemical partitioning, and waters of the same salinity produce different ostracode populations, depending on the major ions available (Smith and Horne, 2002). This species is an indication of glacial conditions, cold water, low TDS, and near tundra conditions in surrounding terrain (Curry, 2003; Delorme 1971). A change from the deep cold species *C. subtriangulata* to *L. friabilis* implies the deep cold waters changed to shallower conditions, and slightly more saline conditions exceeding the abilities of *C. subtriangulata* to survive (Dettman, 1995).

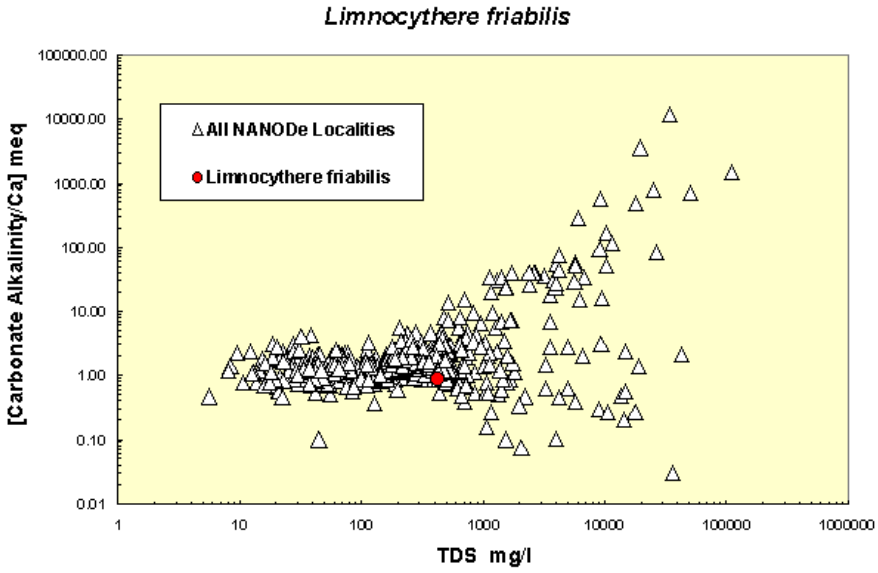

Figure 35. *Limnocythere friabilis* ostracode species solute space distribution based on solutes; x axis TDS in mg/L, and y axis the ratio of bicarbonate and carbonate to calcium in mg/L both shown on a log scale. Red circles are sites with living species, and white triangles are all NANODe sampled sites sampled for ostracodes (NANODe Version 1, Species List, *Limnocythere friabilis*) (Forester et al., 2005, www.kent.edu/NANODe).

3.3 USE OF THECAMOEBIANS IN PALEOENVIRONMENT RECONSTRUCTIONS

3.3.1 General

Thecamoebians are part of a group of testate rhizopods which include foraminifera, and are also known as testate amoebae (Scott et al., 2001). They are single celled protozoan organisms enclosed in a test which typically has a single aperture from which the organism extends its pseudopodium (extended foot); it primarily feeds on diatoms and bacteria (Scott et al., 2001). Thecamoebians are typically benthic detritus feeders which are sensitive to the quality and quantity of particulate organic matter, and hence can be related to the trophic state of their environment, with modern thecamoebians correlating with pH, specifically higher acidity environments typically have lower thecamoebian concentrations, especially in those taxa that are less acid tolerant (Cohen, 2003; Wall et al., 2008).

Their tests are made by the secretions from the organism (autogenous) or are constructed by the agglutination of foreign particles (xenogenous), or both, and are typically < 0.5 mm (Scott et al., 2001; Medioli and Scott, 1988). The size of the test is primarily related to the availability of food prior to reproduction which affects the size of the cytoplasm, with some influence from accessible suitable xenosomes for production of the test (Medioli and Scott, 1988). Thecamoebian morphology can be broadly categorized into three groups; beret-shaped, sack-shaped and others (Scott et al., 2001). These general

morphologies can be somewhat affected in the xenogenous thecamoebians, by the nature of the particles they incorporate into their tests, and by environmental conditions (Medioli and Scott, 1988).

Thecamoebians reproduce asexually by binary fission but can reproduce sexually, and can form cysts when stressful environmental conditions are encountered, allowing them to withstand desiccation, freezing, extreme pH, etc. (Scott et al., 2001). These cysts can be transported by the wind, and either on migratory birds or within their guts (Scott et al., 2001). Thecamoebians do not grow after initial fission and their tests are essentially made to cover and protect the amoeba at the time of fission (Scott et al., 2001).

The taxonomy of thecamoebians is very confused and has caused the development of a highly disorganized terminology and nomenclature, with multiple synonyms being used in the literature such as rhizopods, testate amoebae, and arcellaceans (Medioli et al., 2003). The confusion occurred as a result of studies from a global spectrum of researchers with differing perspectives and regional interests (Medioli et al., 2003). Over-splitting of thecamoebian taxa at the species level in European studies and others, has led to many of these studies becoming almost impossible to use by other researchers (Medioli et al., 2003).

Classifications at the higher taxonomic levels are based on the nature of their pseudopodia (lobose, recticulose, or filose) with a species level classification now developed based on test morphology (Medioli et al., 2003; Scott et al., 2001). Variations

in the species morphology can occur as a result of environmental conditions, creating a high morphological variability (Medioli and Scott, 1988). Despite this variability, a system of classification has been applied successfully to freshwater taxa (Sarcodina) (Medioli et al., 2003; Scott et al., 2001; Patterson and Kumar, 2002).

Modern thecamoebians have been associated with specific pH levels, preferring low acidity conditions (Cohen, 2003; Wall et al., 2008). The tests are preserved in most freshwater sediments including those with low pH (Scott et al., 2001; Limaye et al., 2007).

3.3.2 Thecamoebians as Paleoenvironmental Indicators

In LOTWs and SL thecamoebians have been identified in sediments in the upper portions of all examined cores. In some cores the thecamoebian interval, as sampled, is continuous, whereas in others there are gaps where they are not present. It is not surprising to find gaps in observed thecamoebians within the sediments, as they rapidly respond to changing paleoclimate or paleohydrology due to their high reproduction rates (Scott et al., 2001). Changes in thecamoebian populations can be associated with changes in climatic conditions, or to increases in nutrient levels (Patterson and Kumar, 2000; Wall et al., 2008). Thecamoebians are also sensitive to the presence of suspended organic matter and they respond when organic materials are transported from watersheds into the lake (Wall et al., 2008). Increased runoff, or as runoff containing organic materials increases in the surrounding watershed as the quantities of surrounding

vegetation increases, causes an associated increase in lake and thecamoebian productivity (Wall et al., 2008).

Species such as *Centropyxis aculeate, Difflugia oblonga, Difflugia proteiformis, Difflugia (Nebela) numata, Difflugia urceolata, and Difflugia globulus,* were identified in LOTWs (Figure 36). *Difflugia* have been related to eutrophic conditions while *Centropyxis* are associated with oligotophic and eutrophic conditions (Tolonen, 1986; Scott et al., 2001). *D. oblonga* in one study have been associated with pH levels as low as 6.2 (Scott et al., 2001). In another study, *D. oblonga* is associated with warm periods, and *C. aculeate* with cooler intervals (Patterson and Kumar, 2002).

A detailed thecamoebian analysis to the species level was not undertaken in the examined cores of LOTWs and SL. Species were identified however, and the number of different species were recorded.

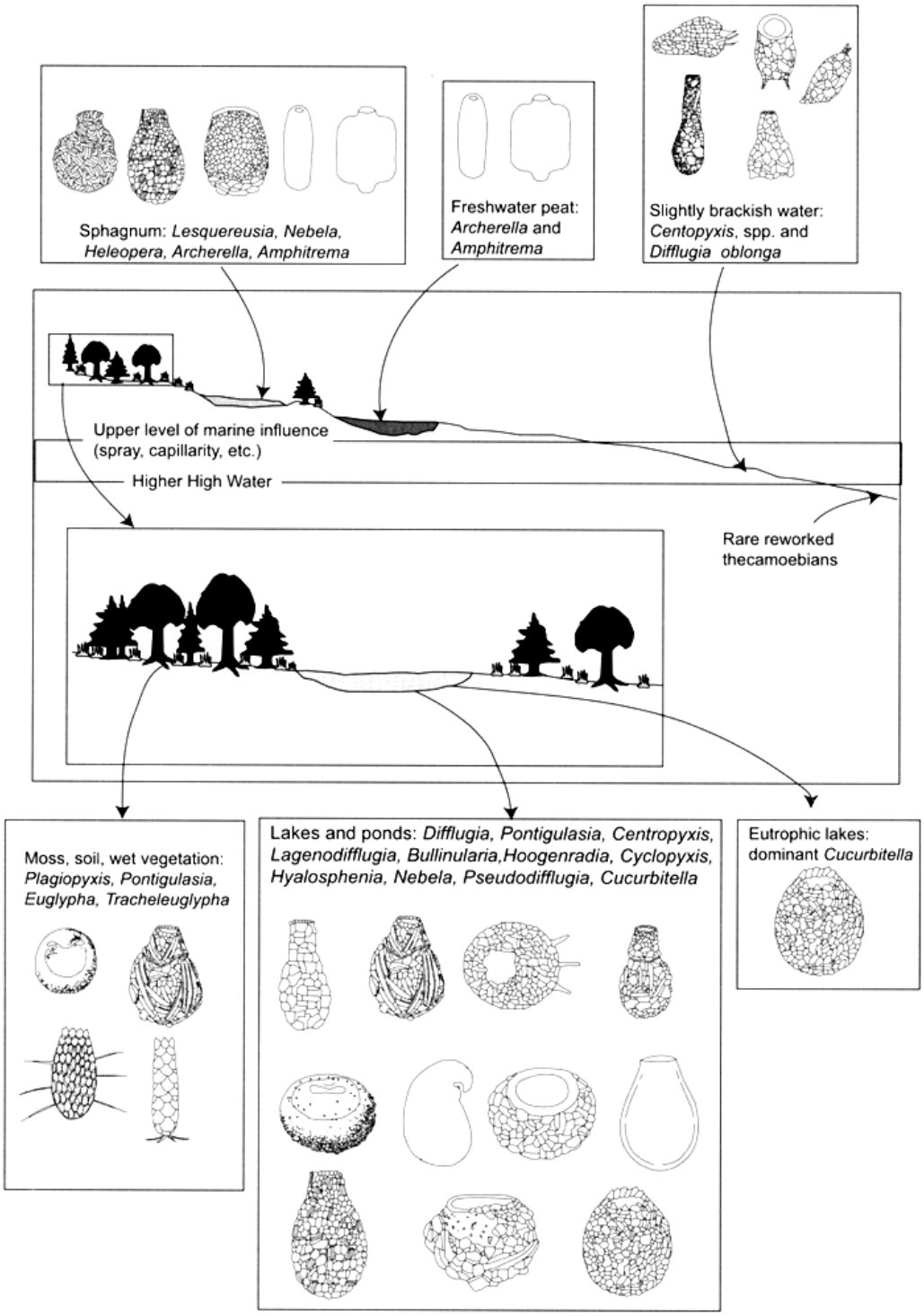

Figure 36. Diagnostic thecamoebian species for typical forest-lake-wetland environments. (Scott et al., 2001, p. 98).

3.4 USE OF OTHER PROXIES IN LOTWs AND SL PALEOENVIRONMENT RECONSTRUCTION

3.4.1 General

Detailed studies of other macrofossils were not undertaken. However during examination of the subsamples for ostracodes, notes were taken when other macrofossils were observed including plant, insect, and charcoal fragments. Additionally, observations were made and recorded related to the lithics encountered in the subsamples. Although detailed studies of lithics and macrofossils other than ostracodes were not undertaken, these potential paleoclimate proxies were roughly quantified to see if a hydrologic or climatic signal could be extracted.

3.4.2 Plant Materials

Detailed paleoenvironmental information can be obtained form plant macrofossils and they have been used in numerous paleoenvironmental studies (Birks, 2001; Warner, 1990). They can also be used to assess whether the microfossil plant materials are from local plant ecosystems (Birks, 2001). When pollen microfossil studies are undertaken, larger organic macrofossils can be used to assess whether the pollen is from local sources or, as is often in the case in post glacial studies, from long distance refugia sources (Birks, 2001). The aquatic plants in a lacustrine environment and the surrounding terrestrial plants operate on different time scales, with changes in aquatic plants somewhat tempered by their environments (Cohen, 2003). Terrestrial plants respond

much more slowly due to their relatively long lifetimes, providing a time averaged climatic response (Cohen, 2003). Variations in the abundance of aquatic and terrestrial plants in lacustrine sediments, and the type of terrestrial plant materials and seeds washing into lacustrine basins, can provide a rough indication of the magnitude and duration of changing conditions in the lake, as well as in the surrounding watersheds.

The organic materials directly deposited into the basin are ideal materials for radiocarbon analysis and dating of the sediments (Birks, 2001). However, some aquatic plants incorporate non atmospheric carbon ("old" carbon) from the geological substrates, skewing the radiocarbon dates away from the date the plants lived (Birks, 2001). Terrestrial plant materials are not subject to the hardwater effect that some aquatic organisms are subject to (Birks, 2001). Plant materials are also subject to reworking from older deposits, and care must be taken to select the "right" macrofossils for dating to ensure organic materials from older terrestrial deposits are not selected. Reworking and incorporation in contemporary sediments can result in dates that do not reflect the age of deposition of the bed in which they are found, leading to difficulties in interpretation (Nambudiri et al., 1980; Warner, 1990).

LOTWs and SL are not ideal locations for the study of plant macrofossils, the littoral zone of small round lakes with limited throughputs are deemed ideal (Birks, 2001; Curry 2003). LOTWs in particular with its large open expanses, complex and highly variable bathymetry and shape (with numerous islands), and the input from the Rainy River watershed make it particularly challenging to interpret. However, plant macrofossils

were observed in all cores and are useful in association with other proxies in interpreting the paleoenvironment. Fossil seeds were recovered from many cores providing materials for radiocarbon dating and the means to identify the specific plants growing in the watershed (Wasylikowa, 1986) and, in turn the means to interpret paleoclimatic conditions. Plant macrofossils, especially seeds that retain their ornate and fragile structures, are good indicators of a low degree of transport, and therefore reflect nearby environmental conditions. These data are presented in the subsample data tables in Appendix A, Subsection 2 for each core.

3.4.3 Paleosol or Buried Soil Indicators

Paleosols in a lacustrine sequence are a clear indicator of major paleohydraulic changes that may be linked to climatic variations (Teller and Last, 1982). Low water lake conditions or dry lake floors may be identified in lake sediments, and have been linked to drier conditions experienced in the northern Great Plains, notably to those during the Hypsithermal between 9.5 to 4.5 cal ka BP (~ 8.4 to 4 ^{14}C ka BP) in Lake Manitoba (Teller and Last, 1982). Buried soils may be recognized by pedogenic features such as soil structures, low moisture zones produced by desiccation of exposed lake muds, secondary mineral occurrences, increased organic content related to roots, and various aspects related to weathering such as progressive upward changes in mineralogy. Pellets derived from the soil structural peds may be present at the top of a soil, and are also good indicators of subaerial exposure (Teller and Last, 1982).

3.4.4 Charcoal

The presence of charcoal in sediments can be related to the proximity and frequency of occurrence of fires, which in turn can be related to regional climate aridity (McMillan et al., 2003). Other factors can influence the quantity and size of the charcoal such as fire intensity and duration, the type of vegetative cover, and hydrologic processes which may wash charcoal into the basin (McMillan et al., 2003). The relative sizes of the charcoal fragments can be related to the intensity of the fires (burning more material and dispersing larger fragments) and their proximity to the site, however interpretations can be difficult (McMillan et al., 2003).

In grasslands, the presence of charcoal can be related to the abundance of the grass itself, with more precipitation producing more grass and hence fuel, which shorter term dry weather conditions can then ignite and burn (Clark et al., 2002; Camill et al., 2003). In very dry conditions the grass biota may not be present and although the fire frequency may increase, the lack of fuel would limit the amount of charcoal transported (Clark et al., 2002). The use of charcoal abundance and size to interpret climatic changes is a useful proxy but other proxies are needed to extract the climatic signal (Camill et al., 2003).

Grassland fires are low intensity fires and dispersal of the charcoal fragments are typically charred herbaceous fragments, and usually indicate relatively wetter conditions which tend to result in the growth of prairie grasses (Whitlock and Larsen, 2001; Clark et

al., 2002). The quantities of non eolian charcoal, referred to as secondary charcoal, are related to the subsequent time delayed deposition of the charcoal from the watershed. These overland deposits of charcoal can often be associated with increases in magnetic susceptibility in the sediment which are related to the increased clastic inputs washed into the lake from the geological substrate (Whitlock and Larsen, 2001).

Charcoal fragments smaller than 150 μ would have been washed through the sieve during subsample processing leaving only larger fragments for subsequent viewing, so fine grains are not part of the sample population evaluated in LOTWs. The 2 cm subsample interval along the core length typically represents at least several decades, within the interval between samples (nominally 10 cm) representing at least 100 years, both depending on the sedimentation rate at the time the sediments accumulated, and the amount of subsequent compaction the sediments underwent. Subsamples with high quantities of charcoal in consecutive samples, could indicate long term trends in fire incidence, providing a climate signal. The presence of larger fragments should provide a qualitative assessment of long term trends in regional fire frequency within the LOTWs and SL watersheds. The relative amount of charcoal fragments, including notes related to their size, and if possible its source biota, were noted on the subsample data sheet and are presented in the subsample data tables in Appendix A, Subsection 2 for each core.

3.4.5 Lithic Grains

The relative quantity and type of lithic fragments within the sediments may provide information related to paleoenvironmental conditions within the watershed or reflect changes in shoreline erosion. These lithics (all > 150 μ due to lab methodology) could reflect unstable (possibly low vegetation) conditions in the watershed associated with a nearby recent fire, or a dry climate, unstable conditions along the shoreline leading to subaqueous gravity flows, wave action, or rafting by winter ice. In some cases these lithics are concentrated in laminae and consist of pedogenic fragments derived from soils and clay balls, so may correlate with erosional events associated with increasing lake levels and flooding of previously dry former lake floors.

Lithic particles were observed and noted on the subsample data sheets. The presence of carbonate lithics in some subsamples were also noted and recorded providing evidence of paleochemical conditions. Sediment lithics from LOTWs and SL cores were obtained using the same process as was used for sieving ostracodes from the sediments and are presented in the subsample data tables in Appendix A, Subsection 2 for each core. Observing and recording the characteristics of the lithics in the subsamples provides additional evidence of changing conditions within the lakes.

3.4.6 Other Organic Macrofossils

Other organic macrofossils can provide valuable information related to environmental conditions which can complement the data provided by other available macrofossils, such

as ostracodes and thecamoebians. In LOTWs and SL sediment macrofossils contained aquatic invertebrate fossils including the shells of calcareous organisms (*periostracum*), and vertebrate fossils including vertebrae and fish scales, all of which can provide useful data (Birks, 2001; Booth and Jackson, 2003). Terrestrial vertebrate remains were also noted including small mammalian teeth. Due to limited macrofossil dispersion in larger lakes, such as LOTWs, the presence of these macrofossils tend to indicate a more local condition (Birks, 2001). These data are presented in the subsample data tables in Appendix A, Subsection 2 for each core.

In addition insect macrofossils were also observed in the recovered sediments. Paleoentomology studies have been used by others to establish paleoclimatic effects (Morgan and Morgan, 1990). Insects have chitinous exoskeletons that preserve well and provide a direct indication of the ecological conditions in lake sediments (Morgan and Morgan, 1990). For LOTWs and SL variations in the deposits of aquatic insect macrofossils were recorded which in conjunction with plant macrofossils, provides a means to identify oligotrophic/eutrophic trends within the LOTWs and SL. Additionally, terrestrial insects were identified which provide indications of the nearby terrestrial environment.

CHAPTER 4 CORE DESCRIPTIONS, DATA AND OBSERVATIONS

4.1 GENERAL

The following sections provide the descriptions of the core, and the data and observations from each of the examined cores. The data recovered from the cores is quite variable due to the complex paleoecology within the LOTWs. Appendix A contains additional data retrieved from the examined cores including the subsample data and observations, and scanned core images. Additionally, a number of specific vegetation and insect macrofossils were identified by Paleotec Services and are included Appendix B, Table B-1 with selected photos in Appendix B, Section 4.

4.2.1 South Basin Site - WOO06-1A

4.2.1.1 General

The WOO06-1A-1K coring location, latitude 48.89121^{o}**;** longitude -94.82602^{o}**,** in the south basin of LOTWs (Figure 24) is described in Section 2.3.2. The retrieved data is presented in Appendix A, Subsections 1.1 and 1.2, with detailed photographic images in Appendix A, Subsection 1.3. The WOO06-1A-1K core is located in the southern portion of the broad flat basin of the southern LOTWs about 2.5 km offshore, in 10.7 m (35.1 ft) of water. The retrieved length is about 3.3 m.

4.2.1.2 **General Stratigraphic Description**

The stratigraphy for the WOO06-1A core is described for the three sections of the core WOO06-1A-1K1, 1K2 and 1K3 in

Figure 37, Figure 38, and Figure 39. In this core there are two primary stratigraphic units.

Unit 1 is a relatively low moisture unit, primarily a slightly sandy silty clay, with distinct laminations and occasional black organics near the top of the unit at about 2.65 m (at about 83 cm in Figure 39) , including a thin (~ 0.3 cm) organic bearing interval at the top. Unit 2 from about 2.65 m to the top of the core, trends from a low moisture content to a relatively high moisture content upwards. It also trends from distinctly laminated silty clay to a very silty clay with faint laminations becoming less distinct upwards and disappearing near the top.

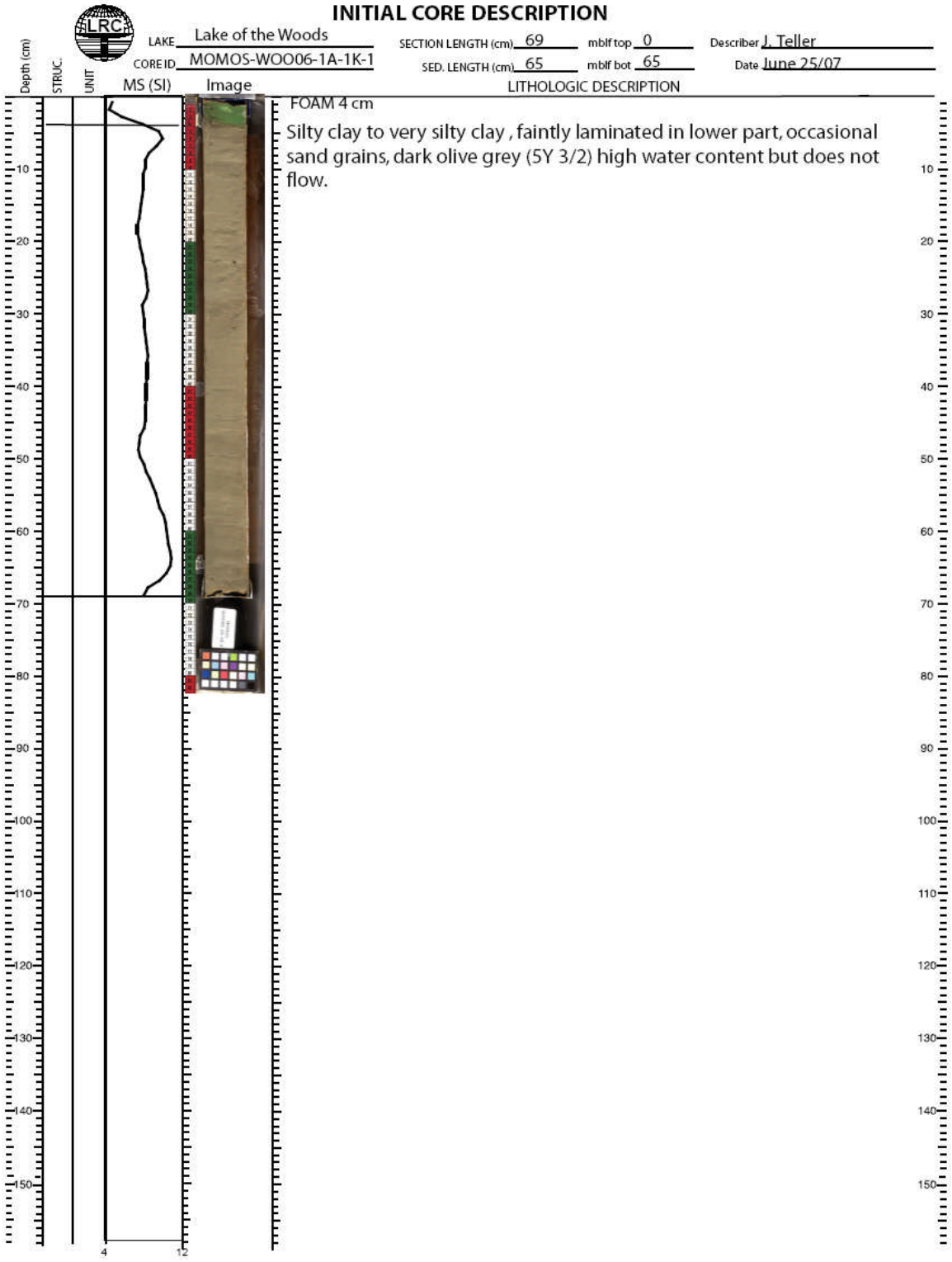

Figure 37. Photographic Record and description of WOO06-1A-1K1.

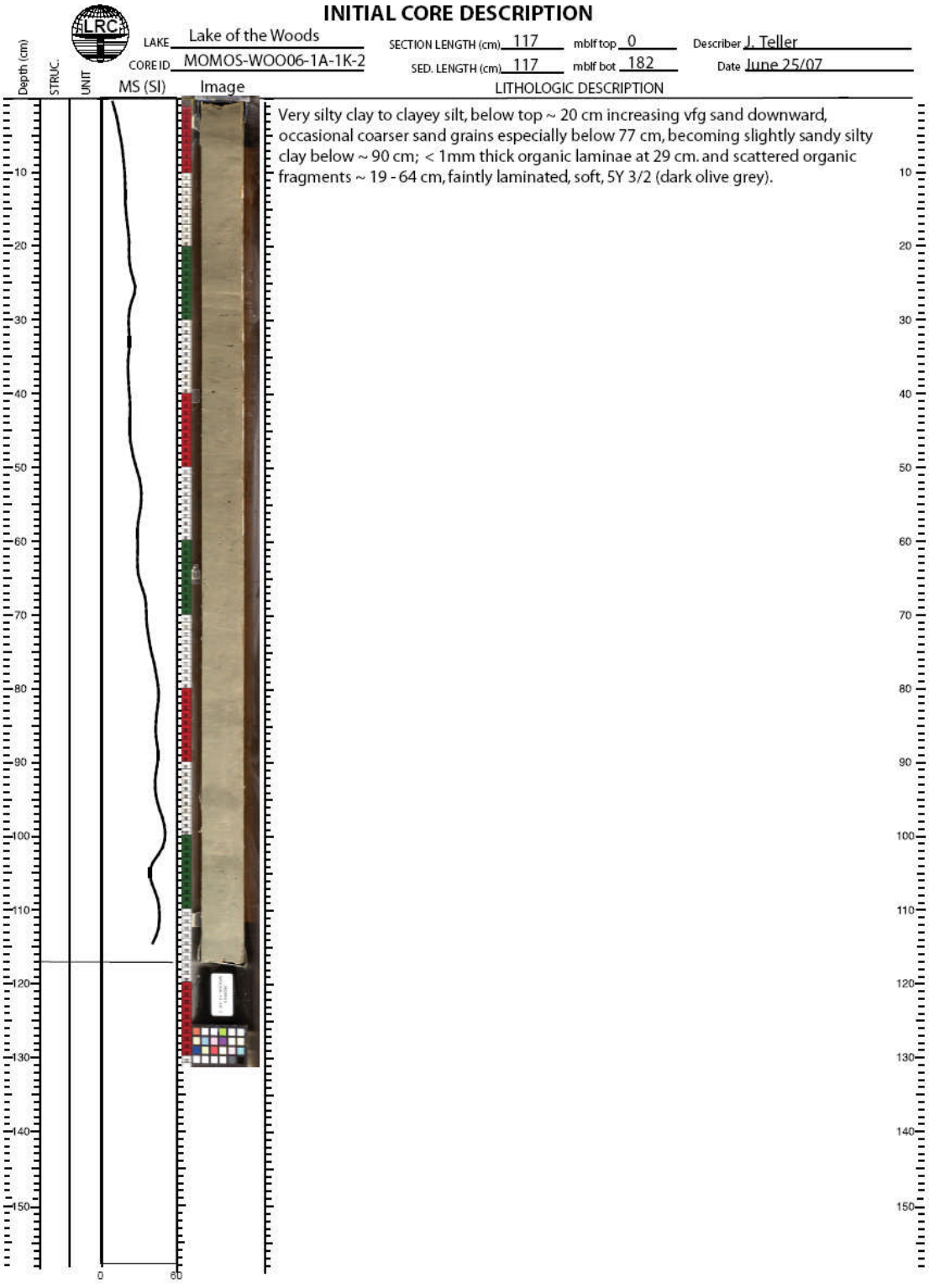

Figure 38. Photographic record and description of WOO06-1A-1K2.

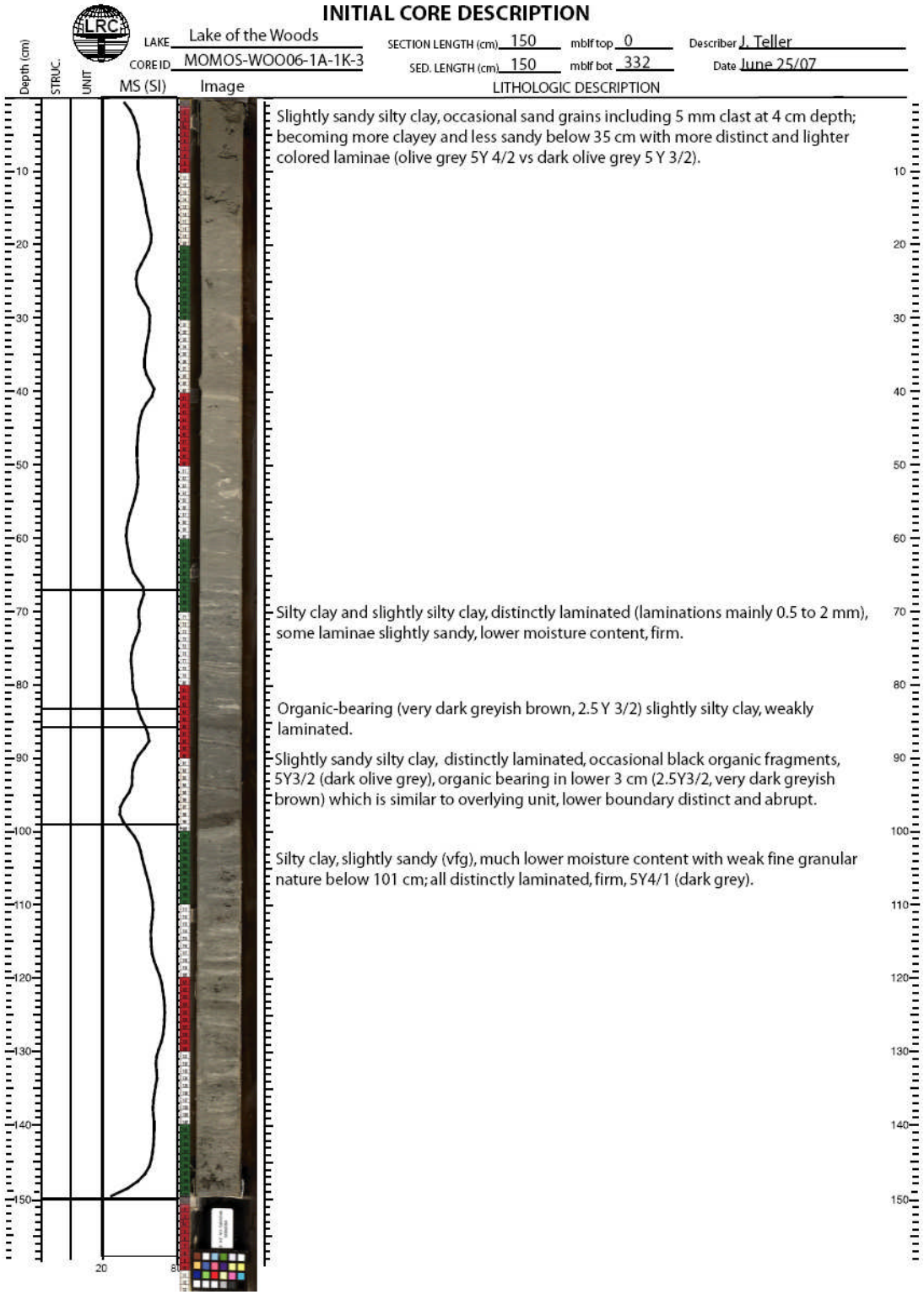

Figure 39. Photographic record and description of WOO06-1A-1K3.

4.2.1.3 **Ostracodes**

An Ostracode population graph for this core is shown in (Figure 40), with the associated data located in Appendix A, Subsection 1.1, with additional ostracode observations included in Subsection 1.2. There is an exclusively *C. Subtriangulata* interval at the bottom of the core, with a later co-occurrence of *L. friabilis*, overlain by a thin zone near 2.8 m depth containing both *L. friabilis* with *F. rawsoni* near 2.8 m. The shells of all species were noted to be coated (Appendix A, Subsection 1.2) with thin shells in other nearby intervals. There is a rapid upward decrease in ostracode numbers at ~ 2.7 m without a preceding trend in shell thinning. Subsequently ostracodes disappear from the record in this core above 2.7 m.

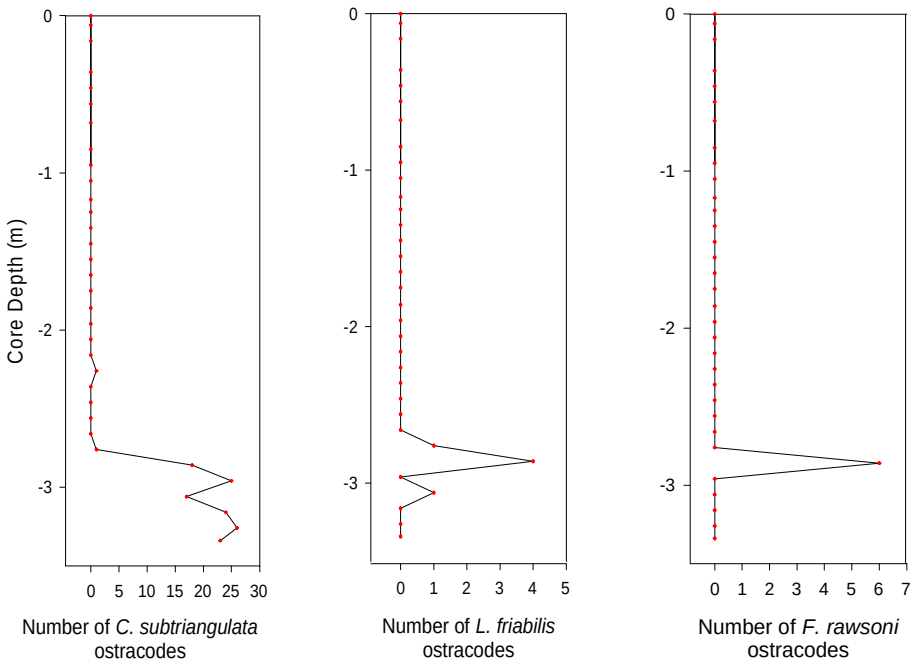

Figure 40. Ostracode population variation for WOO06-1A-1K; from the top of the core to the bottom at 3.4 m. The small crosses indicate sample locations. Note the scale for the number of ostracodes varies, with the *C. subtriangulata* ostracode population much higher than the others.

4.2.1.4 **Thecamoebians**

The locations where thecamoebians are present in the core are identified in (Figure 41) with detailed thecamoebian observations included in Appendix A, Subsection 1.2. Thecamoebians first appear above 1.4 m, corresponding with an increase in plant material and generally high abundance of insect macrofossils (Figure 41), possibly indicating an increase in productivity towards more eutrophic conditions in the lake at this time.

Up to five species of thecamoebians were observed in some intervals including *Difflugia oblonga* and *Centropyxis aculeate* which have been associated with warmer and cooler conditions respectively (Section 3.3.2).

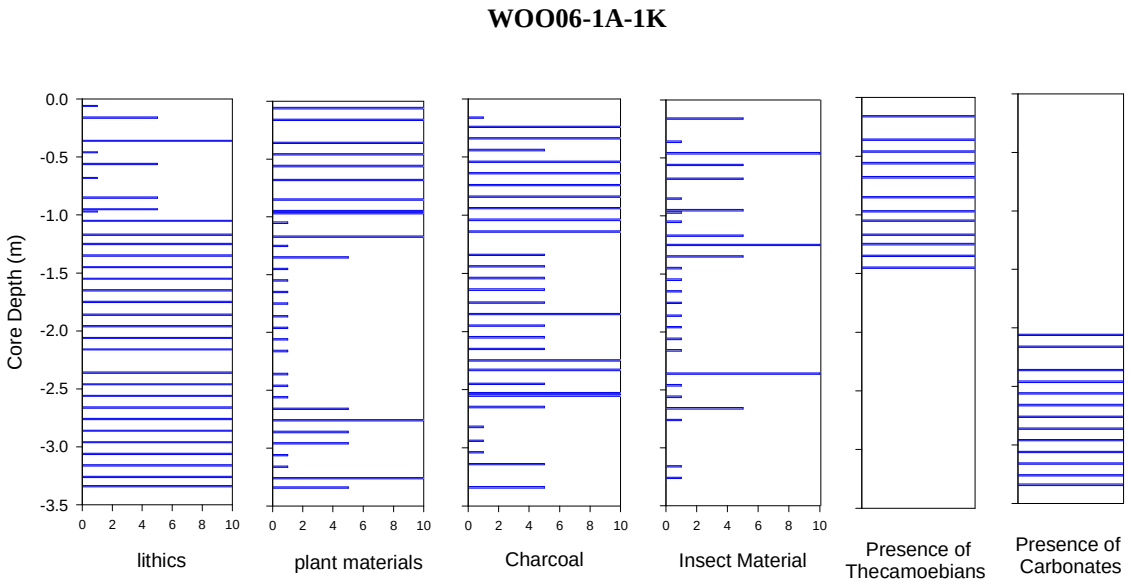

Figure 41. Plots of thecamoebians lithic materials and various macrofossils for WOO06-1A-1K. Sampled locations are the same as those in Figure 40. Lithics, plant, charcoal, and insect material are indicated by a bar reflecting their abundance in the sample on a scale of 0 (absent) to 10 (abundant) and were recovered from the subsamples after wet sieving. Presence of thecamoebians and carbonates in a sample are shown only by a bar, and do not imply any quantity.

4.2.1.5 **Other Macrofossils**

Figure 41 includes macrofossil data plots generated from the subsample data. Detailed data and observations are located in Appendix A, Subsection 1.2.

There is a relatively high abundance of charcoal and a similar relatively high abundance of plant materials in the lower portion of the core which falls to generally lower levels in the mid-core regions before becoming abundant near the top of the core. The charcoal

fragments include fine/intricate internal structures and attachments and therefore do not appear to have been transported. Numerous mammal molars, an incisor, a claw attached to a bone, and vertebrae were found in the interval from 2.3 to 1.8 m. This interval is below the thecamoebian interval and where plant and insect biota increase, and about 0.5 m above the end of the ostracode interval. The articulated claw and bone imply relatively low energy conditions and limited (if any) reworking. Macrofossil identification was conducted for some samples and is included in Appendix A, Subsection 1.2 and Appendix B, Table B-1. For this core achenes of curlytop knotweed (*Polygonum lapathifolium*) were identified with photos provided in Appendix B, Figures B-1, B-2 and B-3.

4.2.1.6 **Lithic Grains**

Figure 41 indicates the changing abundance of lithics in the subsamples, and identifies those locations where carbonate lithics, including clay balls, were detected. Detailed observations of lithics and clay balls are included in Appendix A, Subsection 1.2. A low overall volume of lithic materials (but high relative abundance when compared to other components) occurs in subsamples near the bottom of the core from 3.3 to 2.2 m. Upward in the core, the volume of the lithic component increases in the subsamples, and the relative abundance of lithics remains high up to about 1.1 m. Most organic macrofossils in these intervals do not appear to have been transported.

Above 2.0 m, well above the main sequence of ostracodes and about 20 cm above the interval where a single ostracode shell was noted, carbonate lithics and clay balls were no

longer identified. The presence of carbonates corresponds with the intervals where ostracode shells were noted to have been coated, and includes the 70 cm above the ostracode interval.

Typically maximum lithic size is around 4 mm throughout the core decreasing in size somewhat to 2-3 mm in the uppermost metre of the core. Lithics were consistently abundant and represented a high relative proportion of the sample volume until a depth of about 1.4 m, when plant and insect macrofossils increased upward in abundance and the number of thecamoebians increased, indicating more productive conditions in the lake (Figure 41).

4.2.1.7 **Moisture Analysis**

Moisture data is plotted below in Figure 42. The increase in moisture levels around 2.8 m corresponds with the end of the interval where ostracodes were abundant (Figure 40). It is unclear why there is a sharp increase sediment moisture at 1.7 m.

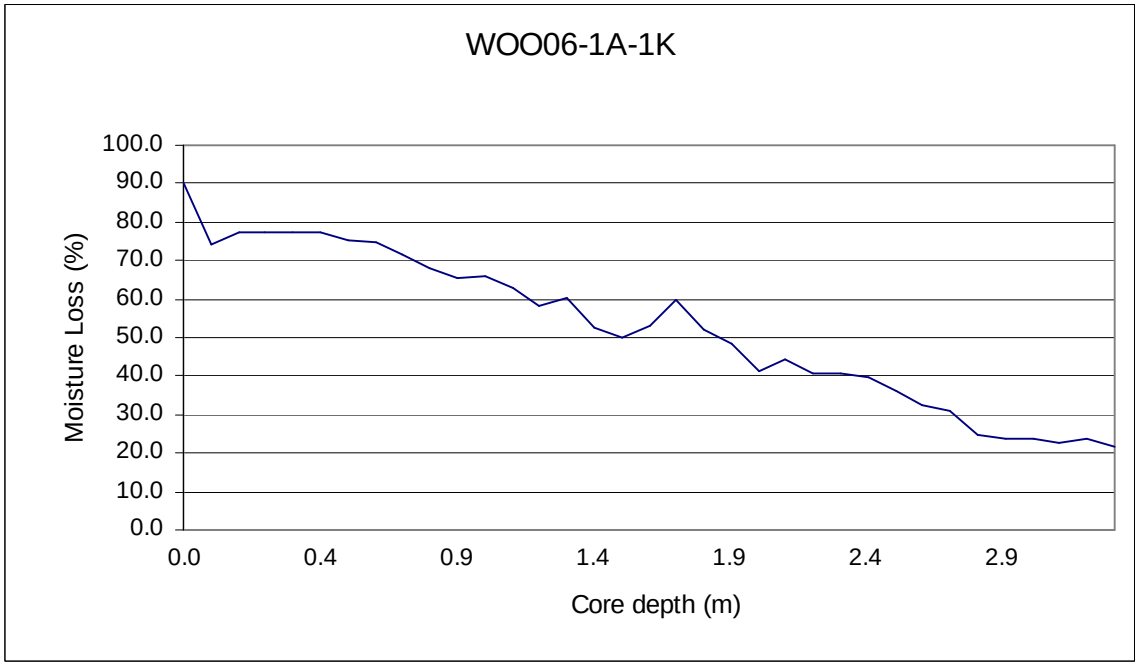

Figure 42. Plot of % moisture loss based on freeze drying of samples, against depth in the WOO06-1A-1K core, with the bottom of the core to the right.

4.2.1.8 **Radiocarbon Dates**

Two radiocarbon dates near the bottom of the core (Figure 43) were primarily obtained from seed materials, refer to Appendix B, Section 2, Table B-1 and Section 3, and Appendix B, Section 4, Figures B-1, B-2 and B-3. The lowermost and younger date of 7.140 ^{14}C ka BP (7.973 cal ka BP) at 3.2 m is about 0.4 m below the older date of 7.375 ^{14}C ka BP (8.228 cal ka BP). An articulated ostracode shell was identified between these intervals possibly implying little reworking occurred. Pollen was dated at 12.260 ^{14}C ka BP (14.365 cal ka BP) 0.4 m above the 7.375 ^{14}C ka BP (8.228 cal ka BP) date at a core depth of 2.4 m. This pollen date is rejected, because the region is known to have been covered by the LIS at this time; almost certainly the pollen has been reworked from older materials.

The two upper core radiocarbon dates are in sequence, with the lower of these dated at 1.675 ^{14}C ka BP (1.579 cal ka BP) defining the beginning of the thecamoebian sequence at about 1.4 m.

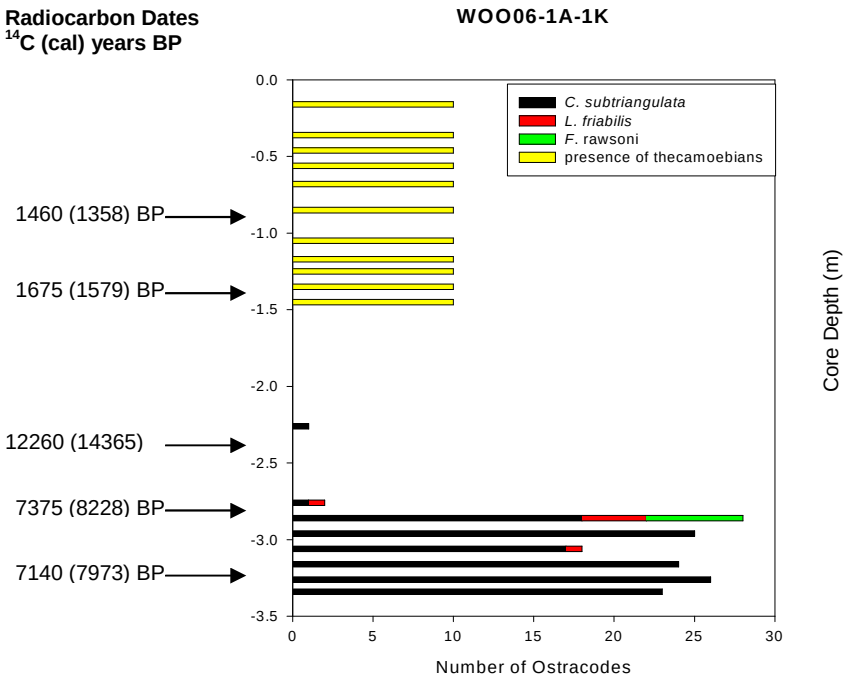

Figure 43. Radiocarbon dates for WOO06-1A-1K showing the ostracode and thecamoebian intervals. Sampled locations are the same as those in Figure 40. The yellow bars represent the presence of thecamoebians. All dates are from the radiocarbon analysis reports in Appendix B. The total number of ostracodes includes all species as are reported in the details of Figure 40

4.2.2 Northwest Angle Site - WOO06-3A

4.2.2.1 General

The WOO06-3A-1K coring location, latitude 49.34714^{o}; longitude -94.84379^{o} in a narrow deep channel (Figure 24) is described in Section 2.3.3. WOO06-3A-1K is located in the northeast trending channel near Cyclone Island about 10 km to the east of the Northwest Angle Inlet and is in about 14.9 m (48.9 feet) of water. The retrieved length is about 7.5 m.

During the coring operation the WOO06-3A-1K core deflected and the core barrel was permanently bent. The liner containing the sediment was recovered after considerable force was applied to extract the liner from the bent core barrel, and the core was subsampled and processed similar to the other cores. It was noted the split core was essentially devoid of the sedimentary structures observed in the other cores, possibly as a result of the core deflection or hammering forces applied to remove the liner. Initially, the core data appeared relatively normal. Due to the deviation of the core from the vertical when dropped into the sediments, data in this core is suspect and have not been included, although general observations have been provided where deemed appropriate.

4.2.2.2 **General Stratigraphic Description**

The stratigraphic data in this core were not suitable for assessment due to the core deflection from the vertical.

4.2.2.3 **Ostracodes**

No ostracodes were observed in this core.

4.2.2.4 **Thecamoebians**

Thecamoebians were observed throughout most of the top portion of the core and were found near the core bottom with an apparent hiatus in between. The thecamoebian hiatus appeared to be quite extensive (i.e. from about 7 m to 1.4 m) although the deflection of the core sideways is possibly responsible for the long hiatus. These uncertainties make interpretation of the data from this core very difficult and there is little confidence in the thecamoebian data from this core.

4.2.2.5 **Other Macrofossils**

Macrofossils including fish scales and typical plant, insect and charcoal components were observed throughout the cored sequence. Due to the uncertainties in these data due to the core deflection, a detailed assessment of processed macrofossils was not completed.

4.2.2.6 **Lithic Grains**

Intervals of abundant granitic and quartz lithics were observed throughout the core.

4.2.2.7 **Radiocarbon Dates**

Only one radiocarbon sample was sent for analysis. The analysed sample at about 7.3 m in this very long core (7.47 m) indicated an unusually young radiocarbon date for this length of core. A sample of organic materials at 7.34 m including a birch and *Verbena* (flowering plant) seed, and an ant mandible, and a small weevil elytron was dated at 2.915 ^{14}C ka BP (3.070 cal ka BP).

4.2.3 Northwest Angle Site - WOO06-4A

4.2.3.1 **General**

The WOO06-4A-1K coring location, latitude 49.33830^{o}; longitude -94.85979^{o}**,** in a narrow deep northeast trending channel near Cyclone Island in the North West Angle area of LOTWs (Figure 24) is described in Section 2.3.3. The retrieved data is presented in Appendix A, Subsections 2.1 and 2.2, with detailed photographic images in Appendix A, Subsection 2.3. The WOO06-4A-1K core is located in the interconnecting channels between the large southern basin and the deep portion of LOTWs to the north (Figure 24), in 7.3 m (24 feet) of water. The retrieved length is about 2 m.

It was anticipated the sediments in the channel sites might be somewhat different from the open Northwest Angle basin sites to the south and that a different paleoenvironment may be present. This shallower of the two companion channel site cores does have considerable organic accumulation and the development of pedogenic blocky structures in an indistinct possible paleosol just below 70 cm from the top of the core (Figure 45).

4.2.3.2 **General Stratigraphic Description**

The stratigraphy of the WOO06-4A core is described for the two sections of the core WOO06-4A-1K1 and 1K2, in Figure 44 and Figure 45. In this core there are four primary stratigraphic units.

Unit 1 below about 1.55 m (about 100 cm in Figure 45) is a silty clay grading downward to a slightly sandy clayey silt, with a low moisture content. It is dramatically different from those units directly above (Figure 45). Near the bottom of the core there are "root-like" structures.

Unit 2 starts at a depth of 1.55 m and ends at a depth of about 0.7 m (about 23 cm in Figure 45). The lower boundary is indistinct with a dark 5 cm thick organic rich bed of silty clay overlying the unit below. Organic laminations appear above the bed upwards from a depth of about 1.3 m, to a depth of about 0.9 m. Above a depth of 1.55 m the unit changes upwards from a primarily well laminated to poorly laminated silty clay, including occasional zones of organic laminae. The top portion of Unit 2 contains a

crumbly fine angular blocky pedogenic zone, decreasing downward to a depth of 1.3 m. Two distinct black beds and other black laminae occur in this unit. Abundant plant and charcoal fragments are prevalent throughout the unit, with clay balls and ball fragments near the top at about 0.9 m. The microscope observations of the processed subsamples generally confirm the visual core descriptions in this unit.

Unit 3 is a silty clay grading downward to a clayey silt, with no visible laminae from 0.1 m to the gradual lower boundary at a depth of about 0.7 m (about 10 cm in Figure 44 and 2.3 cm Figure 45). From observations of the subsamples prior to processing, Unit 3 is a relatively high moisture content unit when compared to the units below.

Unit 4, the uppermost unit above a core depth 0.1 m, is a non-laminated interval of high moisture sandy gyttja, with a distinct lower boundary (Figure 44).

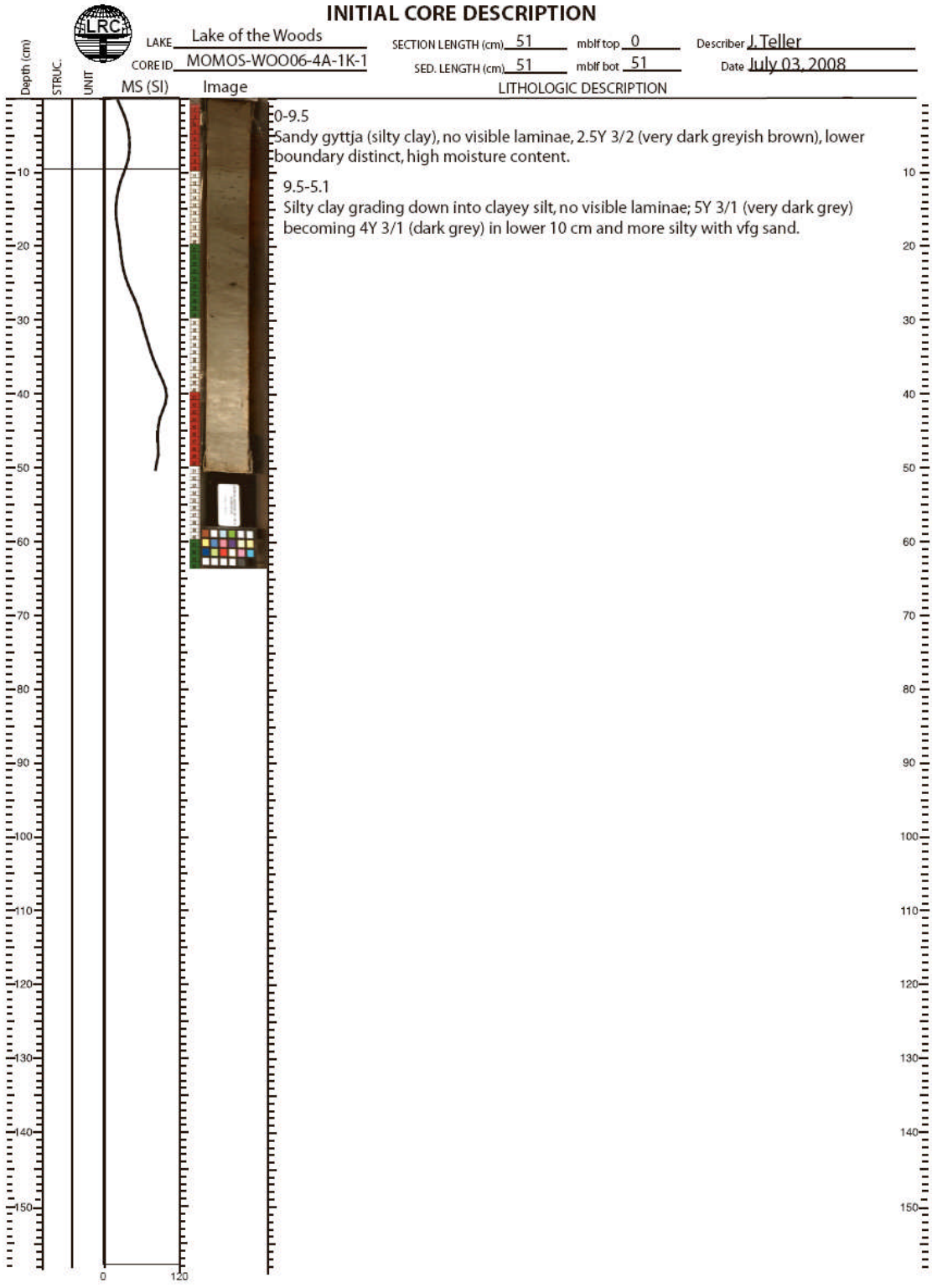

Figure 44. Photographic record and description of WOO06-4A-1K1.

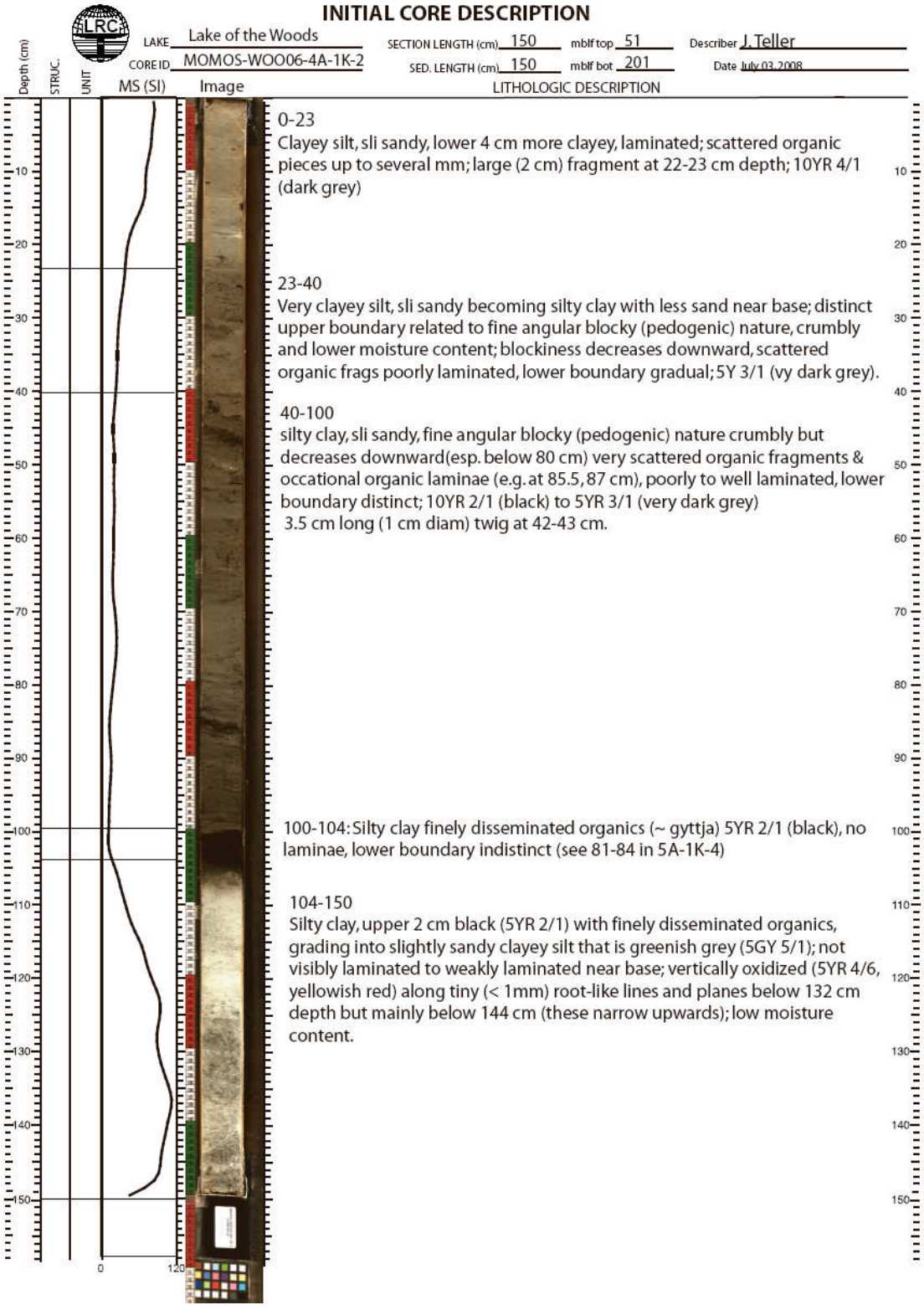

Figure 45. Photographic record and description of WOO06-4A-1K2.

4.2.3.3 **Ostracodes**

An ostracode population graph is shown in (Figure 46), with the data located in Appendix A, Subsection 2.1 with additional ostracode observations in Section 2.2. The *C. subtriangulata* ostracode species is the only ostracode identified in the core. The ostracode interval ends about 0.2 m above the bottom of the core at ~ 1.8 m. In addition to the presence of *C. subtriangulata* at the bottom of the core, a high quartz lithics component and a low plant, insect and charcoal macrofossil abundances were noted.

There are a limited number of ostracode shells within the ostracode interval, with the most abundant concentration at the bottommost sampled interval. The ostracode shells are thin and mostly broken with light deposits on the shells, but do not have a corroded appearance.

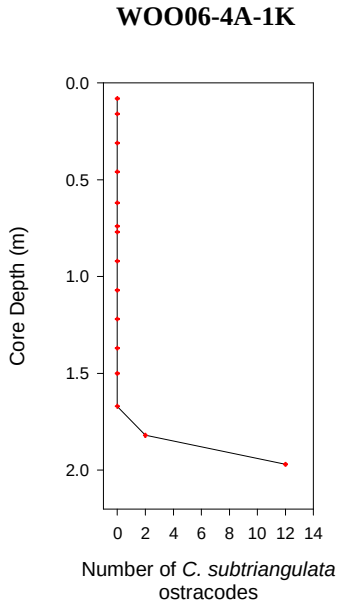

Figure 46. Ostracode population variation for the WOO06-4A-1K core from the top of the core to the bottom at about 2 m. The small crosses indicate sample locations.

4.2.3.4 **Thecamoebians**

The locations where thecamoebians are present are identified in (Figure 47) with detailed thecamoebian observations included in Appendix A, Subsection 2.2. The first thecamoebian interval which includes two species is located at about 0.77 m, between intervals that have abundant large plant and charcoal fragments. A hiatus appears above this point with the next interval continuing upwards of 0.31 m, which contains relatively abundant thecamoebians with four species identified.

The uppermost appearance of thecamoebians occurs within a zone of high relative abundance of plant and charcoal fragments, and insect macrofossils. The plant material includes abundant seeds, including terrestrial and near shore plants, and abundant large charcoal fragments, all indicating a near shore paleoenvironment, which corresponds with the modern configuration of this narrow channel. Observed thecamoebian species include both *Difflugia oblonga* and *Centropyxis aculeate*.

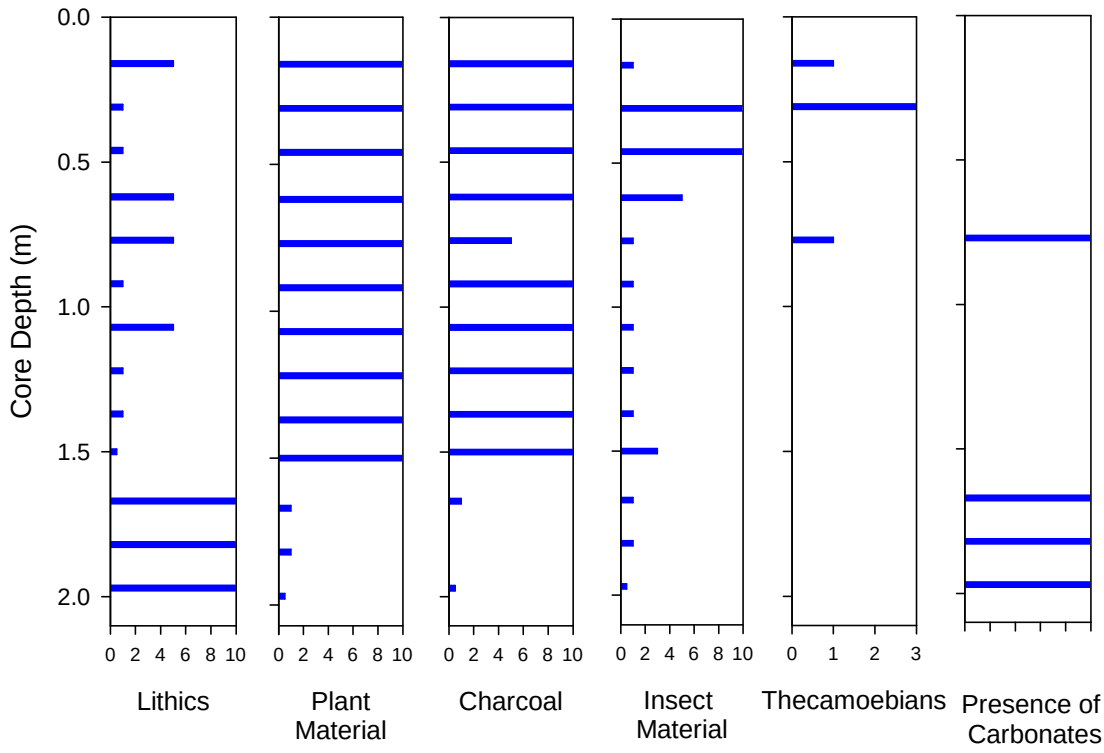

Figure 47. Plots of lithic materials and macrofossils for WOO06-4A-1K. Sampled locations are the same as those in Figure 46. Lithics, plant, charcoal, and insect material are indicated by a bar reflecting their abundance in the sample on a scale of 0 (absent) to 10 (abundant) and were recovered from the subsamples after wet sieving. Presence of thecamoebians and carbonates in a sample are shown only by a bar, and do not imply any quantity.

4.2.3.5 **Other Macrofossils**

Figure 47 includes macrofossil data plots generated from the subsample data. Data and observations are located in Appendix A, Subsection 2.2.

Fish vertebrae and scales occur between 0.6 to 0.3 m in an interval where thecamoebians underwent a hiatus. High abundance of plant and charcoal macrofossils, and increased insects material, all begin above a black organic rich interval at about 1.5 m, indicating a

change in conditions at this site. The proportion of lithics also decreases above the same interval. The scanned split core (Figure 45) clearly shows these dramatic changes across this contact.

A gradational lower boundary at the base of the 5 cm thick black interval and a sharp boundary at the top, marks the beginning of a transition from a low organic material interval below this the black interval, to a zone of abundant plant and seed macrofossils with large charcoal fragments within and above. This black organic interval includes terrestrial and near shore plants, such as curlytop knotweed (*Polygonum lapathifolium*) and bulrush (*Scirpus validus*) (Appendix B, Section 4, Figures B-1, B-2, B-3, and B-4), with the insect materials also increasing somewhat in the interval.

The insect component remains low throughout most of the middle portion of the core (except in the black organic layer), and starts rising to a maximum after the first thecamoebian interval. The relative proportion of insects then continues at a high level through the highest thecamoebian population interval (Figure 47), and then falls to low levels as the thecamoebian population also starts to drop to a low level near the top of the core. A reduction was noted in overall volume (but high relative abundance when compared to other components) of organic and large charcoal components in the processed samples above 0.74 m.

4.2.3.6 **Lithic Grains**

Abundant quartz, mica, and carbonate lithics, are present in the bottom ~ 0.4 m of the core below the distinct black boundary located at about 1.5 m. This boundary lies below an interval of non-laminated to weakly laminated sediments at about 0.9 to 1.5 m (Figure 45).

The abundance of lithics changes dramatically upward at about 1.5 m over a short interval at the black organic interval. The bottom two subsample intervals in the core include non disaggregated clay balls which tested positive for carbonates (using dilute HCl), with the interval above including a carbonate grain. Interestingly, the lithics in the portion of the core containing ostracodes (Figure 46) are dominated by quartz. Other intervals above this point at about 1.3 m (Figure 47) had some carbonate rich clay balls (Appendix A, Subsection 2.2). Some of these clay balls may have been eliminated if the subsamples were processed father, but hard carbonate rich pellets were also observed in one interval near the bottom of the core, indicating carbonate pellets/balls were relatively common in this lower portion of the core.

Although there are variations in the observed lithology in the core above 1.5 m, the processed samples have a limited variability in the type of lithics except at the second pedogenic-like interval at about 0.74 m. At this point carbonate grains reappear, and then disappear above.

4.2.3.7 **Radiocarbon Dates**

The four radiocarbon dates (Figure 48) were obtained from large macrofossils (Appendix B, Section 2, Table B-1 and Section 3), the top and bottom dated samples come from multiple *Scirpus validus* (bulrush) achenes ad are shown in Appendix B, Section 4, Figures B-5 and B-6. These achenes did not have attached bristles and some of the achenes were split open. The uppermost date of 2.495 ^{14}C ka BP (2.604 cal ka BP) was obtained from a sample very near the top of the recovered core at 0.08 m. The lower dated samples at 0.74 and 0.92 m, 6.370 ^{14}C ka BP (7.319 cal ka BP) and 6.955 ^{14}C ka BP (7.787 cal ka BP) are from twigs up to one cm long (Appendix B, Section 4, Figures B-7). Both of these dated intervals also have high abundances of plant and charcoal macrofossils above and below. The interval between a depth of about 0.9 and 1.3 m (Figure 45) contained an angular blocky crumbly textured slightly sandy silty clay, which appears to be near pedogenically altered.

The distinct black interval at 1.5 m, was radiocarbon dated at 7.655 ^{14}C ka BP (8.443 cal ka BP) using a *Scirpus validus* (bulrush) seed. The processing of this subsample revealed a heavily matted organic residue composed of terrestrial plant components such as leaves, stems and seeds.

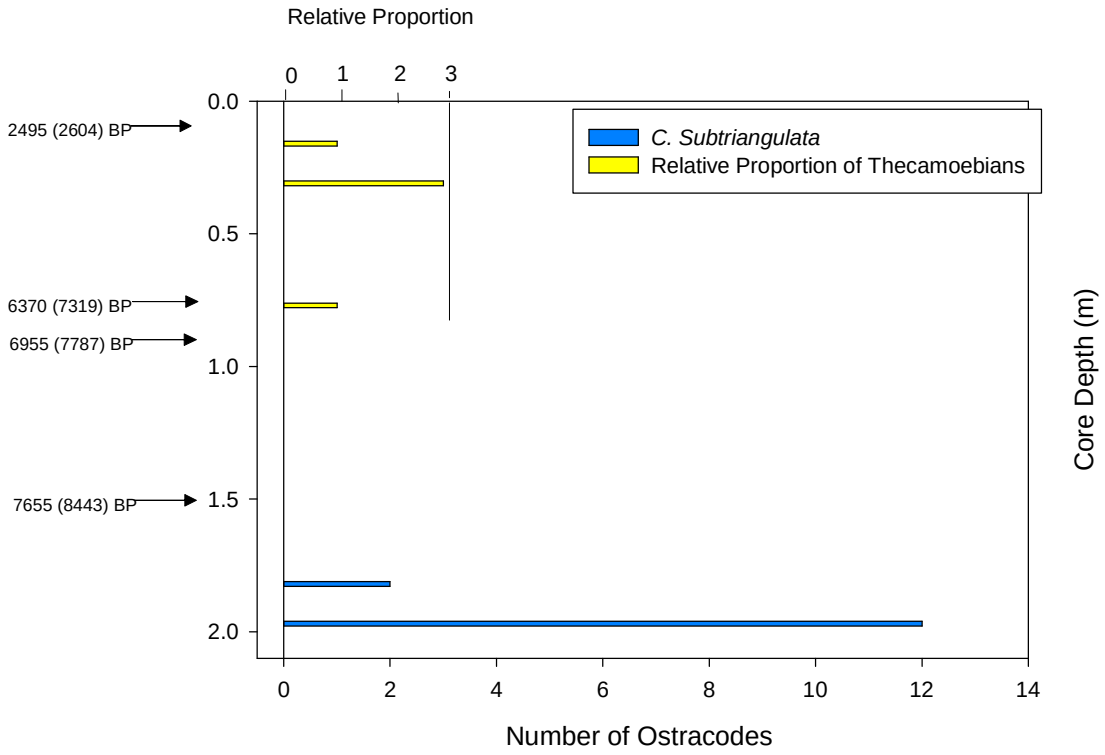

Figure 48. Radiocarbon dates for WOO06-4A-1K showing the ostracode and thecamoebian intervals. Sampled locations are the same as those in Figure 46. The yellow bars represent the presence of thecamoebians. All dates are from the radiocarbon analysis reports in Appendix B.

4.2.4 Northwest Angle Site - WOO06-5A

4.2.4.1 General

The WOO06-5A-1K coring location, latitude 49.27928°; longitude -94.82007°, in the northern portion of the southern basin (Figure 24) is described in Section 2.3.4. The retrieved data is presented in Appendix A, Subsections 3.1 and 3.2, with detailed photographic images in Appendix A, Subsection 3.3. The WOO06-5A-1K core is located at the north/south mid-point of the modern extent of LOTWs, beyond the broad open southern basin in a large partially sheltered broad bay just to the south of the

Northwest Angle Inlet. This core is located about 7 km from the western shore near Massacre Island, adjacent to the U.S./Canada border, in 8.1 m (26.6 feet) of water. The retrieved length is about 5.48 m.

4.2.4.2 **General Sratigraphic Description**

The stratigraphy for the WOO06-5A core is described for the five sections of the core WOO06-5A-1K1, 1K2, 1K3, 1K4 and 1K5, in Figure 49, Figure 50, Figure 51, Figure 52, and Figure 53. In this core there are eight primary stratigraphic units, including three paleosols.

Unit 1 is the lowermost unit from the bottom of the core at about 5.47 m to about 4.0 m (about 150 to 0 cm Figure 53). It is a very silty clay with a relatively low moisture content in the upper 50 cm. Below this it becomes a silty clay with more distinct laminations and organic streaks downward with a lower moisture content. It becomes softer below 4.6 m, with more distinct laminations and a higher moisture content. The results of a moisture analysis are presented in Section 5.2.4.7 with the trends in moisture also observed in the subsamples (Appendix A, Subsection 3.2). A fault was noted at about 4.9 m.

Unit 2 is the first paleosol which extends from about 3.9 to 3.33 m (about 150 to 85 cm Figure 52) and contains a crumbly very dry fine texture with all peds < 2 mm. The top 9 cm includes fine organics between granular peds, and includes shell fragments including

bivalves and gastropods, which were also observed during subsampling and noted in Appendix A, Subsection 3.2. The subsample observations also reflect paleosol conditions and closely correlate with the top surface of the unit, with the lower surface extending farther downward about 20 cm to 3.9 m. Unit 3 is located above the first paleosol surface at about 3.33 m, extends upwards to about 3.1 m (about 85 to 54 cm Figure 52), and is a poorly laminated silty clay with decreasing moisture upward. Unit 4 is the 2nd paleosol which is weakly granular and about 5 cm thick, with an upper boundary at about 2.97 m (about 54 to 48 cm Figure 52). The location of the top boundary of the 2nd paleosol, based on the core description, is also confirmed by observations from the subsamples. The lower boundary as identified in the core description, appears to extend downward a further 15 cm to about 3.2 m from the observations of the subsample (this observation is similar to those observed in other paleosols), although the lowermost boundary appears to be most distinct around 3.1 m.

Unit 5 extends from the bottom of the top paleosol at about 2.8 m, down to about 2.97 m (30 to 48 cm Figure 52) where the 2nd paleosol is located. Unit 5 is a poorly laminated silty clay with an abrupt increase in organics about 10 cm below the top of the unit. The lower boundary is variable between the non-granular components of this unit and granular components of the paleosol of Unit 4 at about 3 m. Unit 6 from 2.4 to 2.67 m (about 140 cm Figure 51 to about 20 cm Figure 52) is a paleosol. The top 10 cm have about 80% hard (some round) granules, some > 5mm in diameter, in a dark grey silty clay matrix, which appears infiltrated from above. The granules appear to be detrital and some appear bluish, possibly containing vivianite. The blocky structures above decrease

and disappear downward about 18 cm below the top of the unit. A moisture minimum occurs about this point (refer to Section 5.2.4.7). Subsample data (Appendix A, Subsection 3.2), closely corresponds with this paleosol interval, although extends the apparent boundary downward slightly (10 cm) to about 2.8 m.

Unit 7 starts at about 2.4 m (about 140 cm Figure 51) and is a very silty clay with occasional faint laminae, with a 10 cm darker interval (more organic rich) starting about 0.5 m from the top of the unit at about 0.7 m (about 55 cm Figure 50). Moisture gradually decreases downward, and in the lower 10 cm, abundant angular granules increase to abundant and the unit changes from a very silty clay to a matrix increasing in silt and very fine grained sand content. The lower boundary is defined by an abrupt increase to very abundant dry granules, which help define the end of the last soil horizon. The lower 10 cm includes hard and dry granules increasing to abundant at the base of the unit. Unit 8 is the uppermost unit, and is 0.7 m (starting about 55 cm Figure 50) of a high moisture silty clay with occasional light laminae, and an irregular lower boundary.

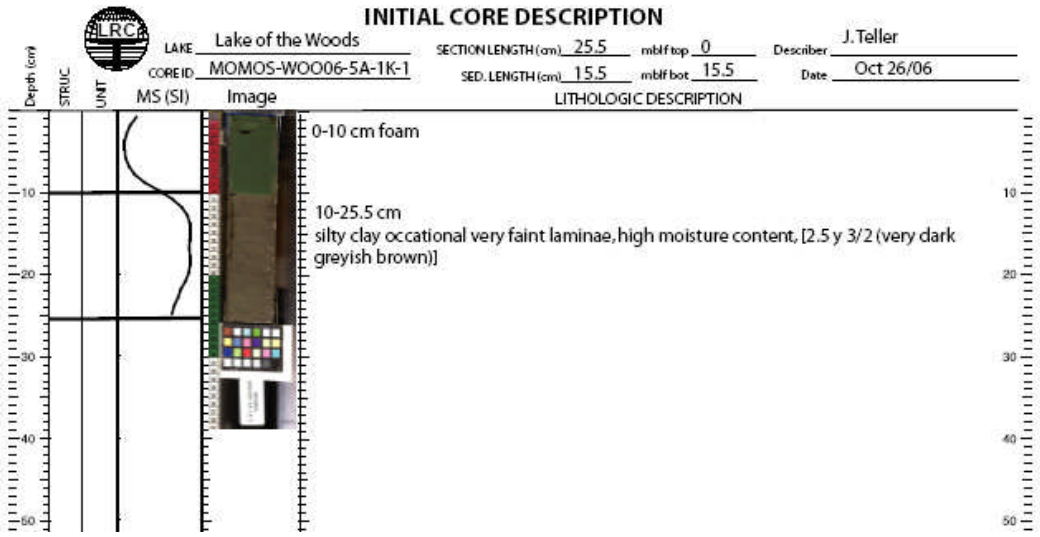

Figure 49. Photographic record and description of WOO06-5A-1K1.

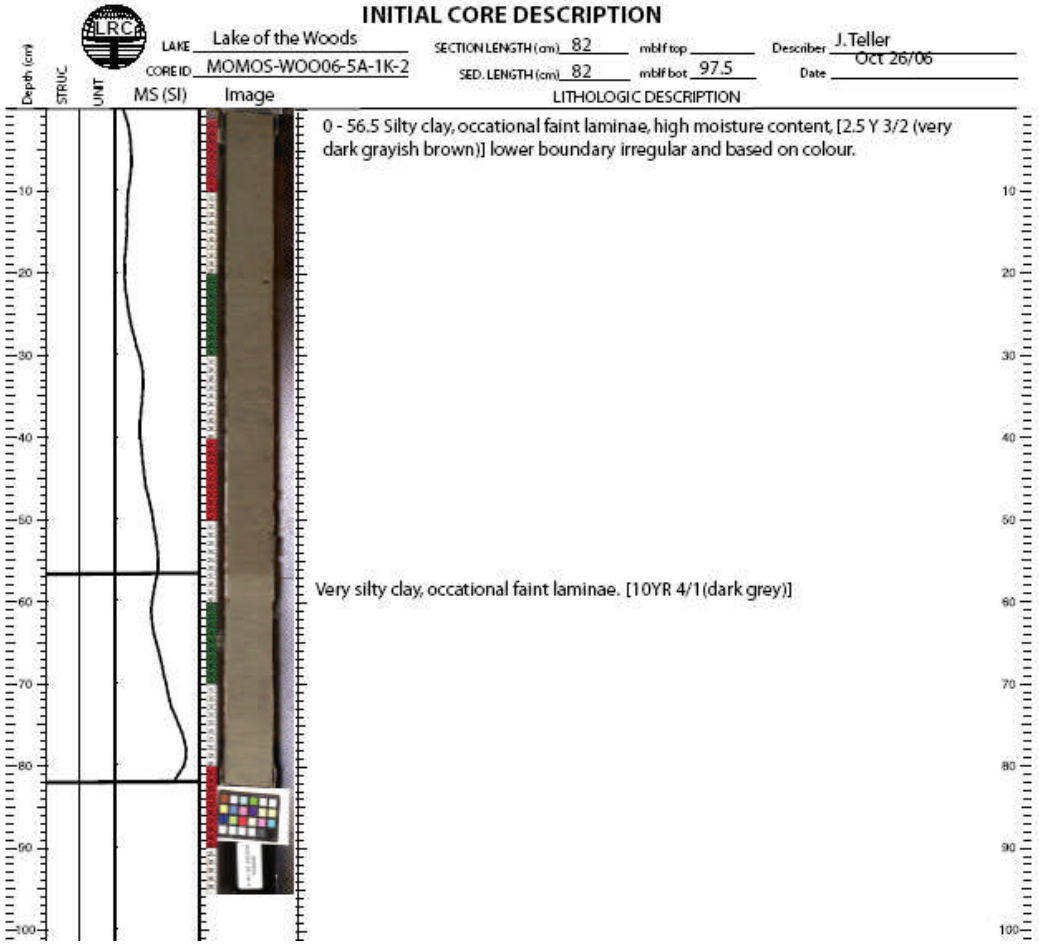

Figure 50. Photographic record and description of WOO06-5A-1K2.

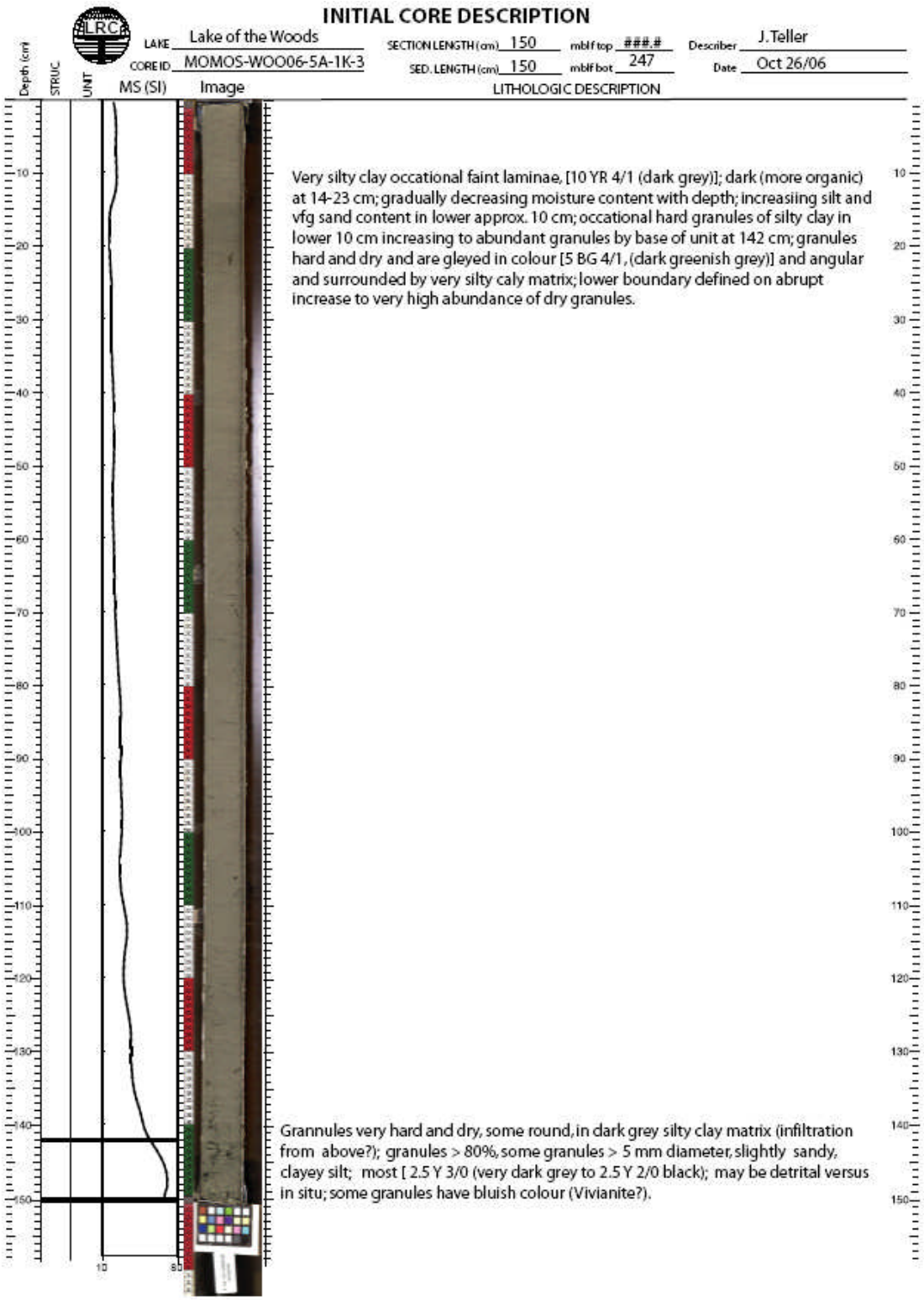

Figure 51. Photographic record and description of WOO06-5A-1K3.

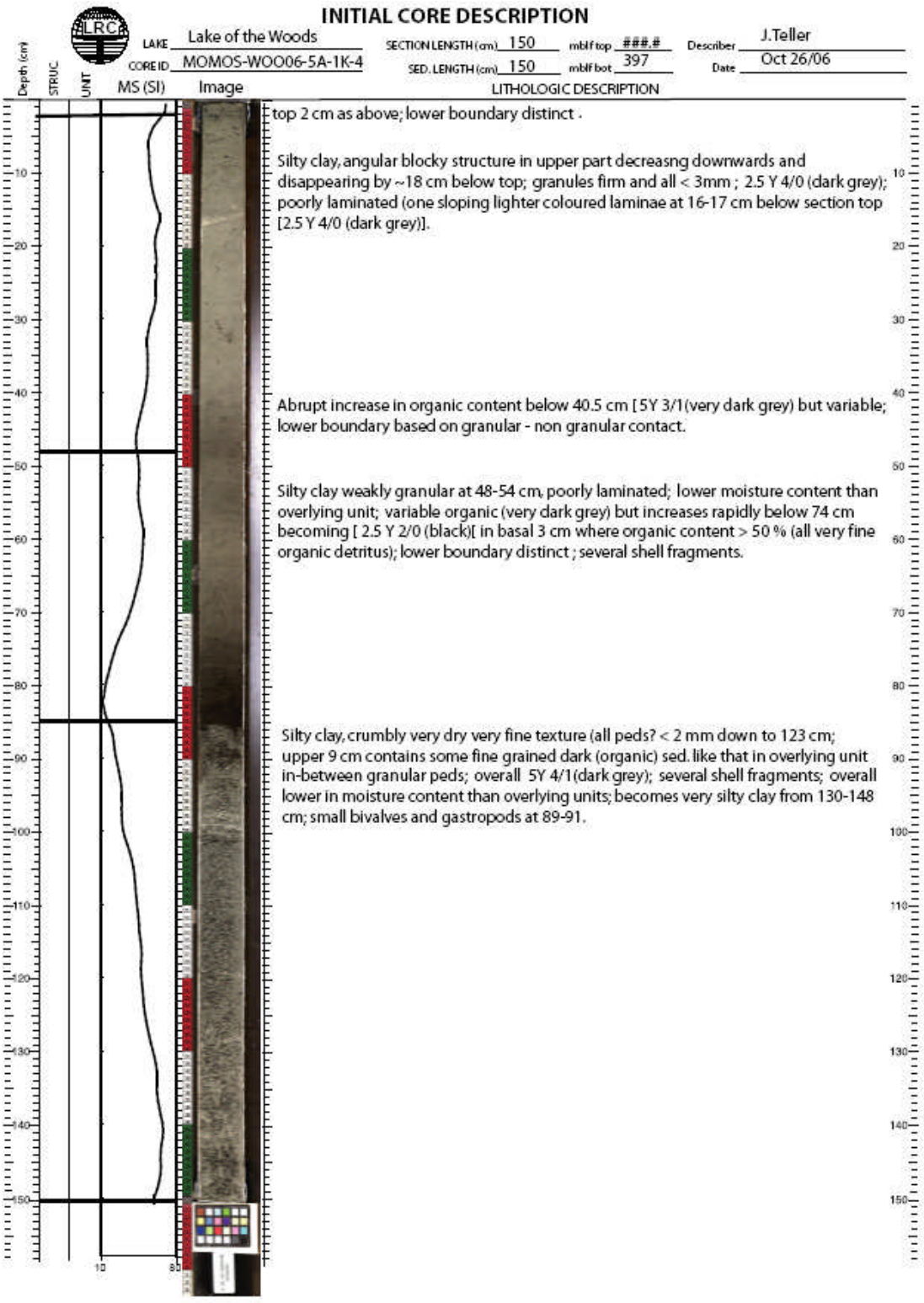

Figure 52. Photographic record and description of WOO06-5A-1K4.

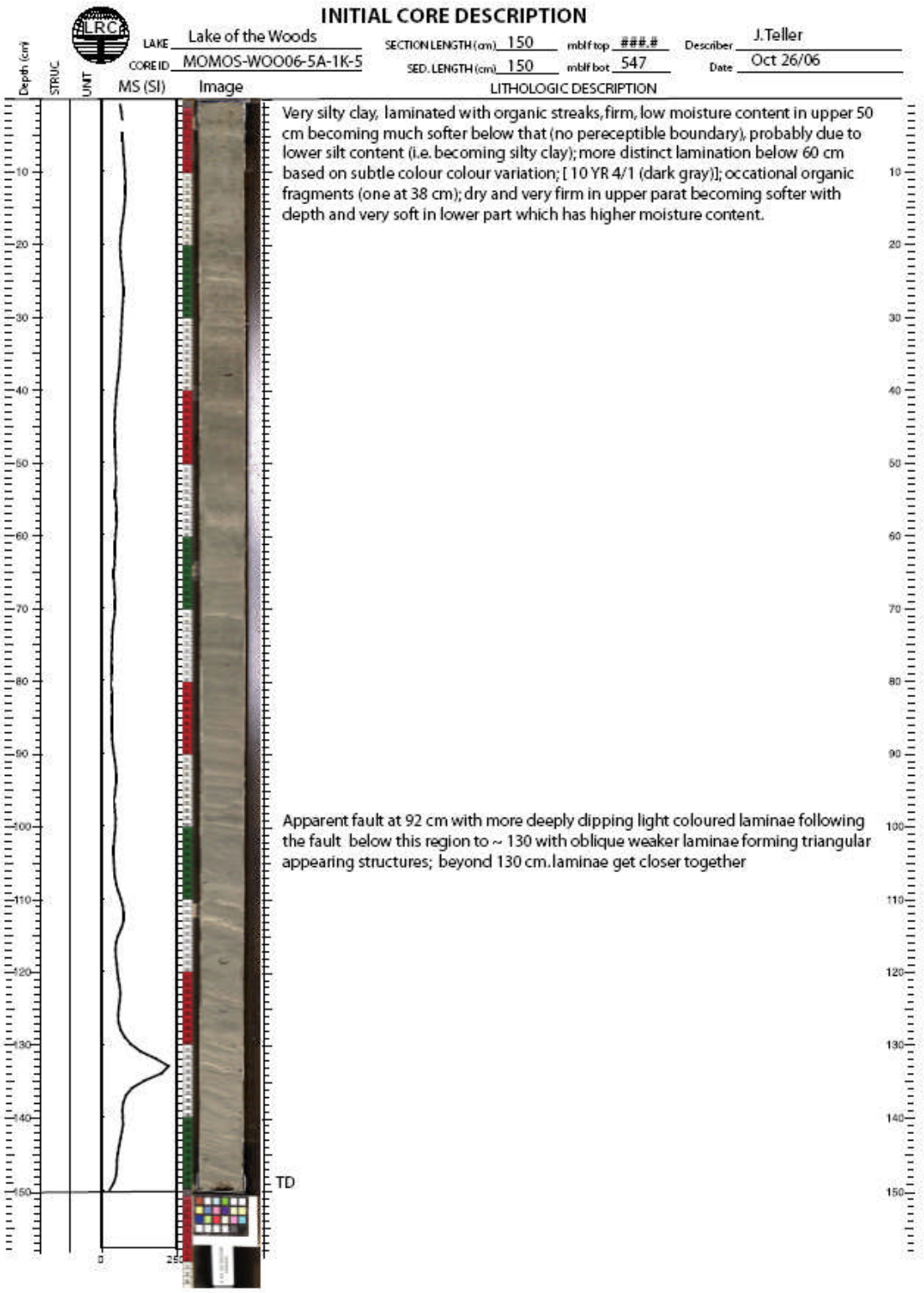

Figure 53. Photographic record and description of WOO06-5A-1K5.

4.2.4.3 **Ostracodes**

The ostracode sequence identified from the bottom of the core at 5.47 m to about 4.6 m is composed of an exclusive *C. subtriangulata* interval, changing to a more mixed sequence including *L. friabilis* from 4.5 to 4.1 m. *C. subtriangulata* disappear at 3.7 m with *L. friabilis* dominant in an interval from 3.8-3.4 m, which also contains *C. sharpei* and *F. rawsoni* (Figure 54). Above 3.4 m ostracodes again disappear completely for a period of time until they reappear at about 3.0 m, and finally disappear above 2.7 m. Above the mid-point of the first paleosol *C. subtriangulata* disappear, except for one interval within the last paleosol which includes rare appearances of other ostracodes. The absence of ostracodes in the upper portions of the core repeats a similar pattern in other cores.

Ostracode shells near observed paleosol horizons appear crushed. Deeper ostracode shells are mostly broken and thin and have a corroded appearance (particularly below the first soil horizon). Articulated ostracode shells were observed within the first paleosol horizon. The lowermost (3.7 - 3.3 m) and uppermost (2.7 - 2.4 m) paleosol horizons include intervals with ostracodes present. The 2nd thin paleosol around 3.1 m does not have any ostracode shells within it.

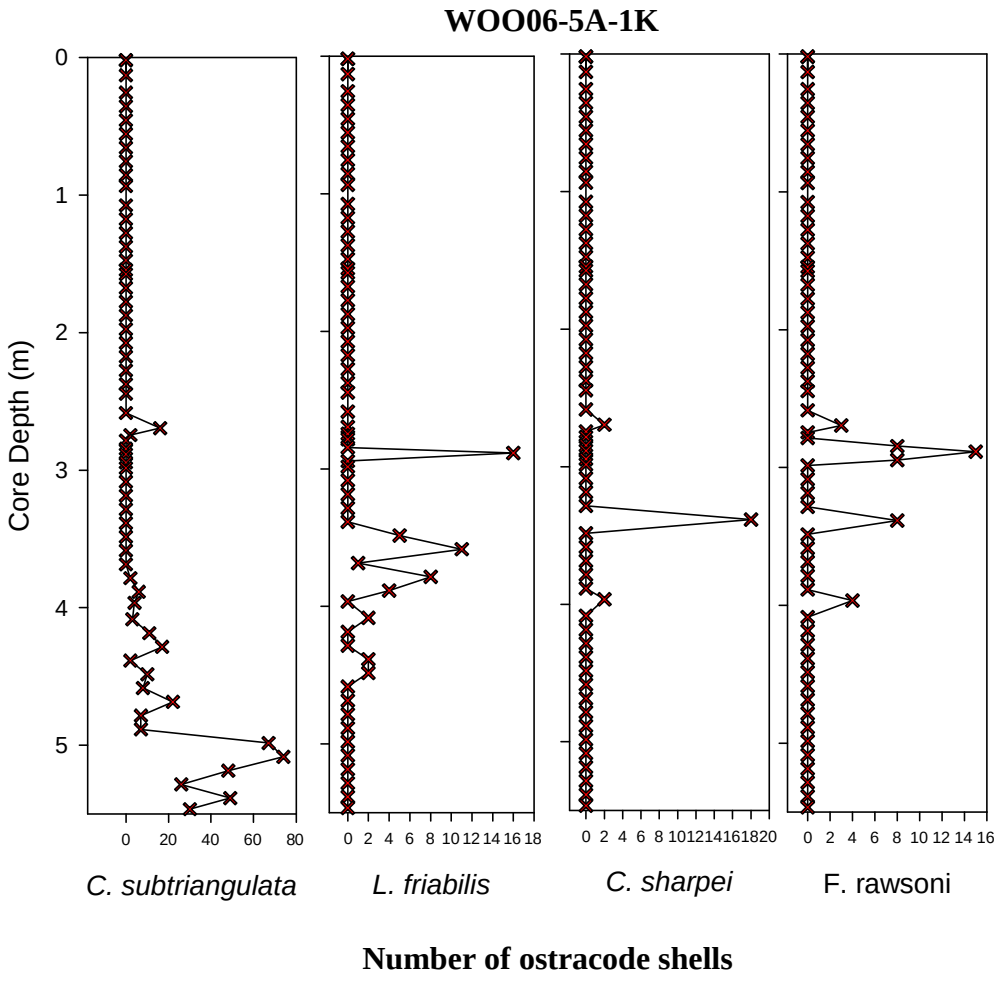

Figure 54. Ostracode population variation for WOO06-5A-1K from the top of the core to the bottom at 5.47 m. The crosses indicate sample locations. Note the number of ostracodes scale varies, with the *C. subtriangulata* ostracode population much higher than the others.

4.2.4.4 **Thecamoebians**

Thecamoebians appear at about 0.8 m (Figure 55) in an interval which was already relatively abundant in plant and insect materials. A detailed thecamoebian species analysis was not conducted for this core, however up to four species were noted when subsamples were re-examined subsequent to the initial ostracode examinations (Appendix A, Subsection 3.2).

4.2.4.5 **Other Macrofossils**

Figure 55 includes macrofossil data plots generated from the subsample data. Data and observations are included in Appendix A, Subsection 3.2.

Relatively large volumes of plant and charcoal were observed in the lower portion of the core (Figure 55). Higher concentrations of plant material, particularly seeds and charcoal materials, were also noted near paleosol horizons with high volumes of organic material observed within the paleosols (Appendix A, Subsection 3.2). Within and near the second paleosol horizon, seeds of shallow water plants including S*cirpus sp* (bulrush), and other terrestrial seeds such as *Rumex maritimus* (golden dock) and *Chenopodium sp* (goosefoot) (Appendix B, Section 4, Figures B-8, B-9, and B-10), are found in abundance. The uppermost soil horizon includes birch nutlets. The zones between the paleosol horizons include seeds and twigs, rare ostracode shells, abundant gastropod and pelecypod shells, indicating an overall shallow water environment. The middle soil horizon contains abundant matted plant material and charcoal.

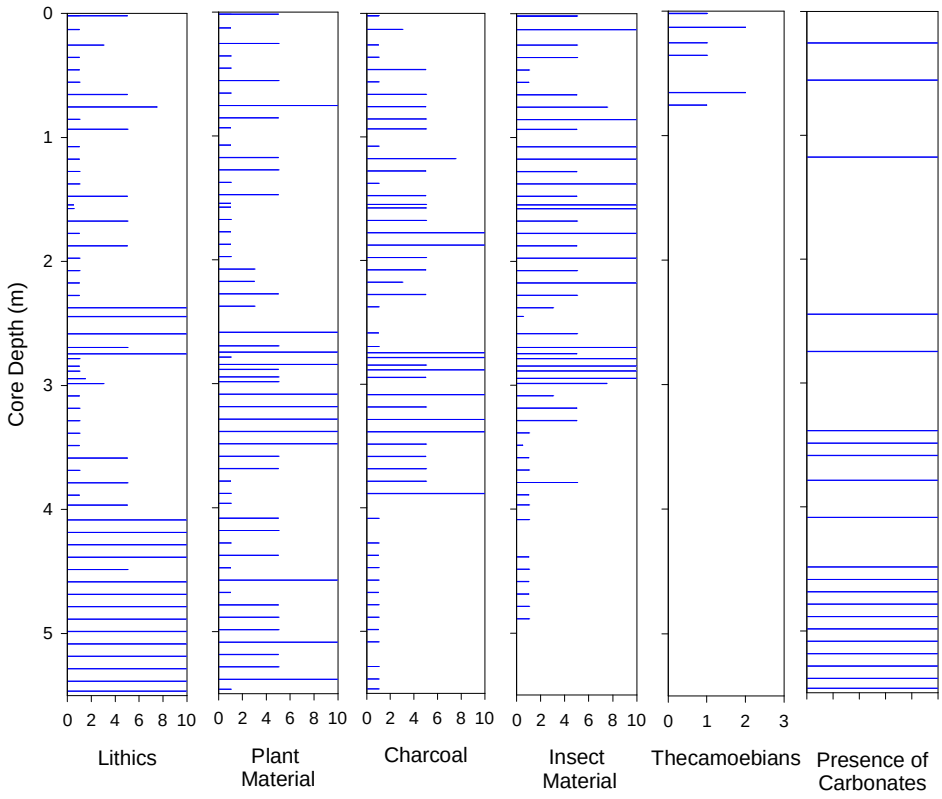

Figure 55. Plots of thecamoebians lithic materials and various macrofossils for WOO06-5A-1K. Sampled locations are the same as those in Figure 54. Lithics, plant, charcoal, and insect material are indicated by a bar reflecting their abundance in the sample on a scale of 0 (absent) to 10 (abundant) and were recovered from the subsamples after wet sieving. Presence of thecamoebians and carbonates in a sample are shown only by a bar, and do not imply any quantity.

4.2.4.6 **Lithic Grains**

Quartz lithics are abundant from the bottom of the core upwards to the beginning of the first soil horizon (Figure 55). Included in the bottommost 0.5 m of this core are iron stained lithic grains ranging from brown to black carbonate pellets (i.e. react to dilute HCl), and carbonate clay pellets and balls (Appendix A, Subsection 3.2). Above this, quartz lithics become the dominant lithic up to the first paleosol horizon. Within the

paleosol horizons quartz becomes rare, with clay balls and pellets becoming the predominant lithics. Above the last paleosols horizon lithics are predominantly quartz, but overall are primarily in low relative concentrations.

4.2.4.7 **Moisture analysis**

Moisture data is plotted below in Figure 56. Moisture levels start to drop above about 4.4 m and then start to rise again above 2.4 m, with two distinct low moisture zones between about 4.4 and 3.4 m and about 3.2 and 2.6 m with an intervening high moisture zone between them. These changes in moisture levels are also reflected in the moisture estimates performed during the subsample processing (Appendix A, Subsection 3.2). The lowermost soil horizon between about 3.9 to 3.3 m, ocurrs near the top of the lower low moisture zone. The two upper observed paleosol horizons at about 2.8 to 2.4 m, and around 3.2 to 3.0 m occur within the upper low moisture zone between about 3.2 and 2.6 m. This further supports the classification of these intervals in the core as paleosols.

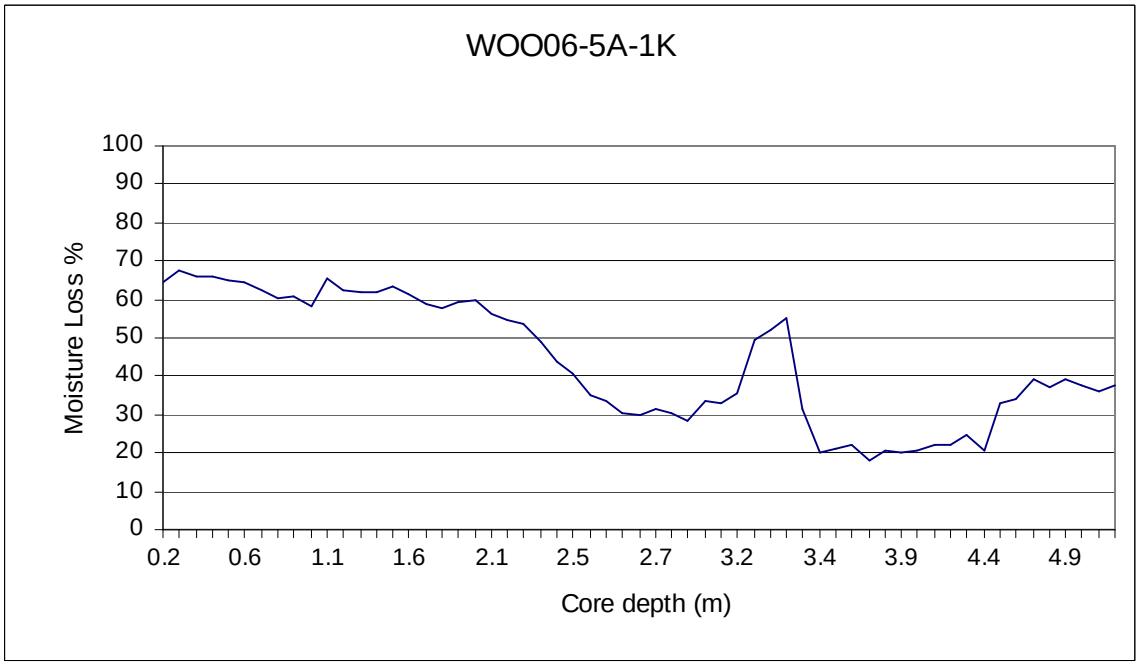

Figure 56. Plot of % moisture loss based on freeze dried samples, against depth in the WOO06-5A-1K core, with the bottom of the core to the right.

4.2.4.8 **Radiocarbon Dates**

Six of the nine radiocarbon dates for this core were obtained from dating of macrofossils including seeds and terrestrial plant materials (Appendix B, Section 2, Table B-1). These six dates all fell in a normal chronological sequence. A well rounded twig at about 4.3 m was dated at 15.62 ^{14}C ka BP (18.8 cal ka BP). This twig was within the *C. subtriangulata* ostracode sequence. There are also two pollen dates bounding this interval, 17.56 ^{14}C ka BP (20.97 cal ka BP) and 17.04 ^{14}C ka BP (20.36 cal ka BP).

One of the key objectives in the dating strategy for this core was to obtain radiocarbon dates for the paleosol intervals in the core. Six samples were taken within the paleosol horizons. Two of these samples, 8.245 and 8.405 ^{14}C ka BP, were from the same interval

at 3.3 m; when averaged the age of that interval is 8.345 ^{14}C ka BP (9.377 cal ka BP). Figure 57 presents the radiocarbon dates for the core but does not include two old pollen dates [(1.7040 ^{14}C ka BP (20.236 cal ka BP) and 1.7560 ^{14}C ka BP (20.970 cal ka BP)] which were rejected. The radiocarbon dated twig of 15.62 ^{14}C ka BP (18.8 cal ka BP) was also rejected.

The end of the lower paleosol closely corresponds with a radiocarbon date of 8.345 ^{14}C ka BP (9.377 cal ka BP), with a nearby (0.6 cm higher) sequential date of 8.065 ^{14}C ka BP. The 7.630 ^{14}C ka BP (8.419 cal ka BP) radiocarbon date corresponds with the top of the 2nd paleosol, with a nearby (0.5 cm higher) sequential date of 7.510 ^{14}C ka BP. The uppermost date of 7.510 ^{14}C ka BP (8.308 cal ka BP) at 2.9 m is close to what appears to be the bottom of the top paleosol (at about 2.8 m).

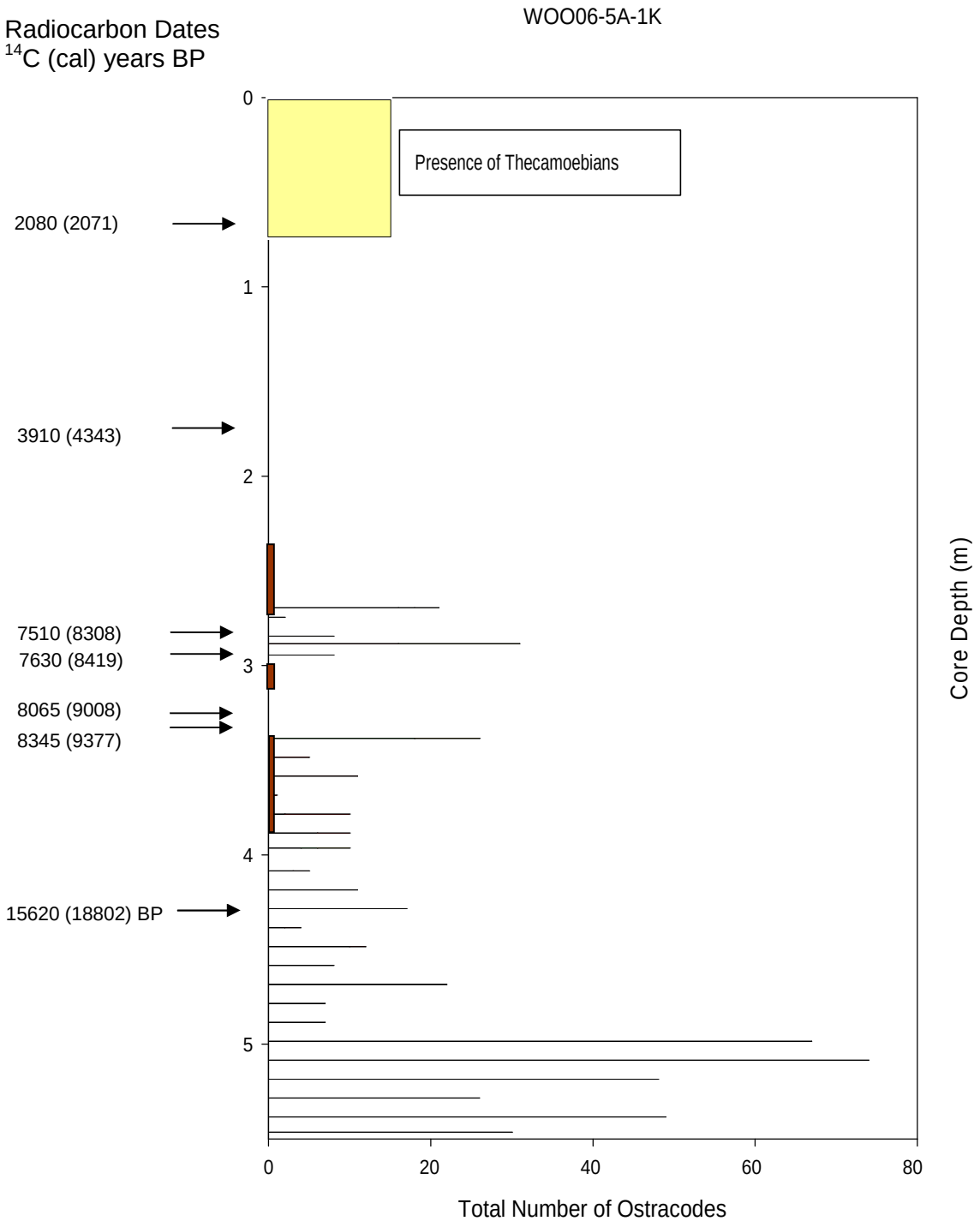

Figure 57. Radiocarbon dates for WOO06-5A-1K showing the ostracode and thecamoebian intervals. Sampled locations are the same as those in Figure 54. The light yellow area is the interval where thecamoebian are present. The positions of the three paleosol intervals are shown as brown bars on the left scale. The total number of ostracodes includes all species as are reported in the details of Figure 54. All dates are from the radiocarbon analysis reports in Appendix B.

4.2.5 Northwest Angle Site - WOO06-6A

4.2.5.1 General

The WOO06-6A-1K coring location, latitude 49.28098^{o} longitude -94.89926^{o}**,** in the northern portion of the southern basin (Figure 24) is described in Section 2.3.4. The retrieved data are presented in Appendix A, Subsections 4.1 and 4.2, with detailed photographic images in Appendix A, Subsection 4.3. The WOO06-6A-1K core is located at the approximate north/south mid-point of the modern extent of LOTWs, beyond the broad open southern basin in a large partially sheltered broad bay just to the south of the Northwest Angle Inlet. This coring site is located about 1.5 km from the western shore about 6 km to the west of the companion core (WOO06-5A-1K), in 5.9 m (19.4 feet) of water. The retrieved length is about 3.8 m.

4.2.5.2 General Stratigraphic Description

The stratigraphy for the WOO06-6A core is described for WOO06-6A-1K1, 1K2, and 1K3, in Figure 58, Figure 59 and Figure 60. In this core there are three primary stratigraphic units, including one paleosol.

Unit 1 extends upwards from the bottom of the core at about 3.8 m (Figure 58) and ends at the paleosol at about 2.0 m (about110 cm in Figure 59). It is a well laminated silty clay to clayey silt, with the lighter coloured silty laminae typically a 1-5 mm thick and 1-3 mm darker silty laminae, with some laminae about 8 mm thick. These structures are

repetitive within this unit from the bottom of the core upwards. Unit 2 is a paleosol with a distinct top boundary at about 1.8 m (about 90 cm in Figure 59), and appears to be about 20 cm thick based on the core description and from the subsample observations (Appendix A, Subsection 4.2). The top very silty clay portion has an 8 cm interval of hard and abundant 1-3 mm granules in a clayey matrix. The lower boundary appears to extend downward to about 2.0 m based on the 3mm clay pellets observed in the subsamples. A 3.2 cm rounded piece of mafic bedrock was noted in upper part of the unit (possibly ice rafted). Near the bottom of the interval containing granules, a decomposed bivalve was observed and the bivalve and nearby shell debris, were radiocarbon dated at 6.760 ^{14}C ka BP (7.616 cal ka BP). Unit 3 (starting at about 90 cm in Figure 59) is the uppermost unit and is a poorly laminated, very clayey and very fined grained silt, grading downward to slightly more clayey around 0.9 m. Darker banding occurs below 0.62 m which becomes lighter downward. Near the bottom of the unit at 1.8 m, about 4 cm above the obvious colour difference, hard granules were noted and increase in number downward indicating the presence of a paleosol below.

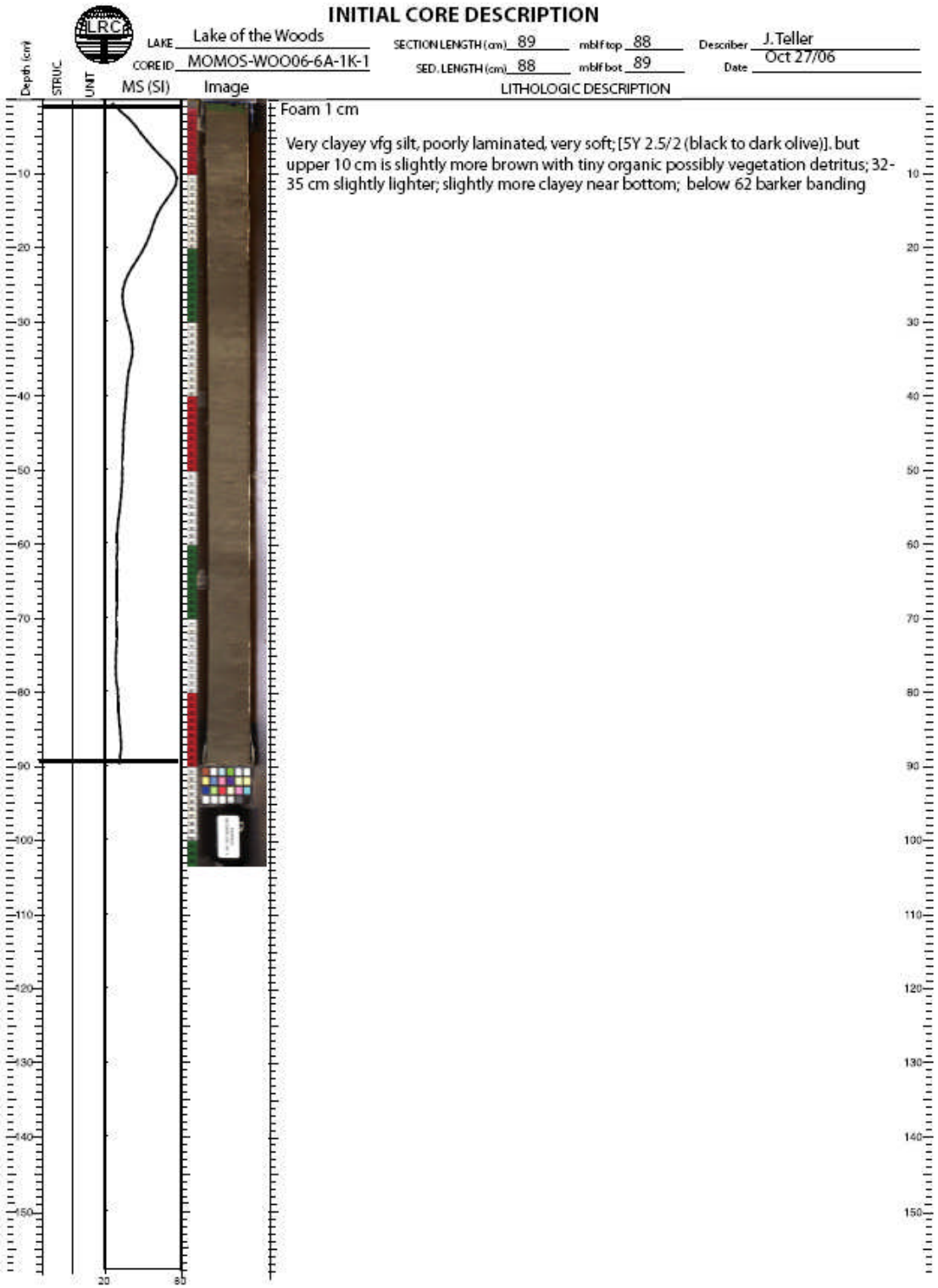

Figure 58. Photographic record and description of WOO06-6A-1K1.

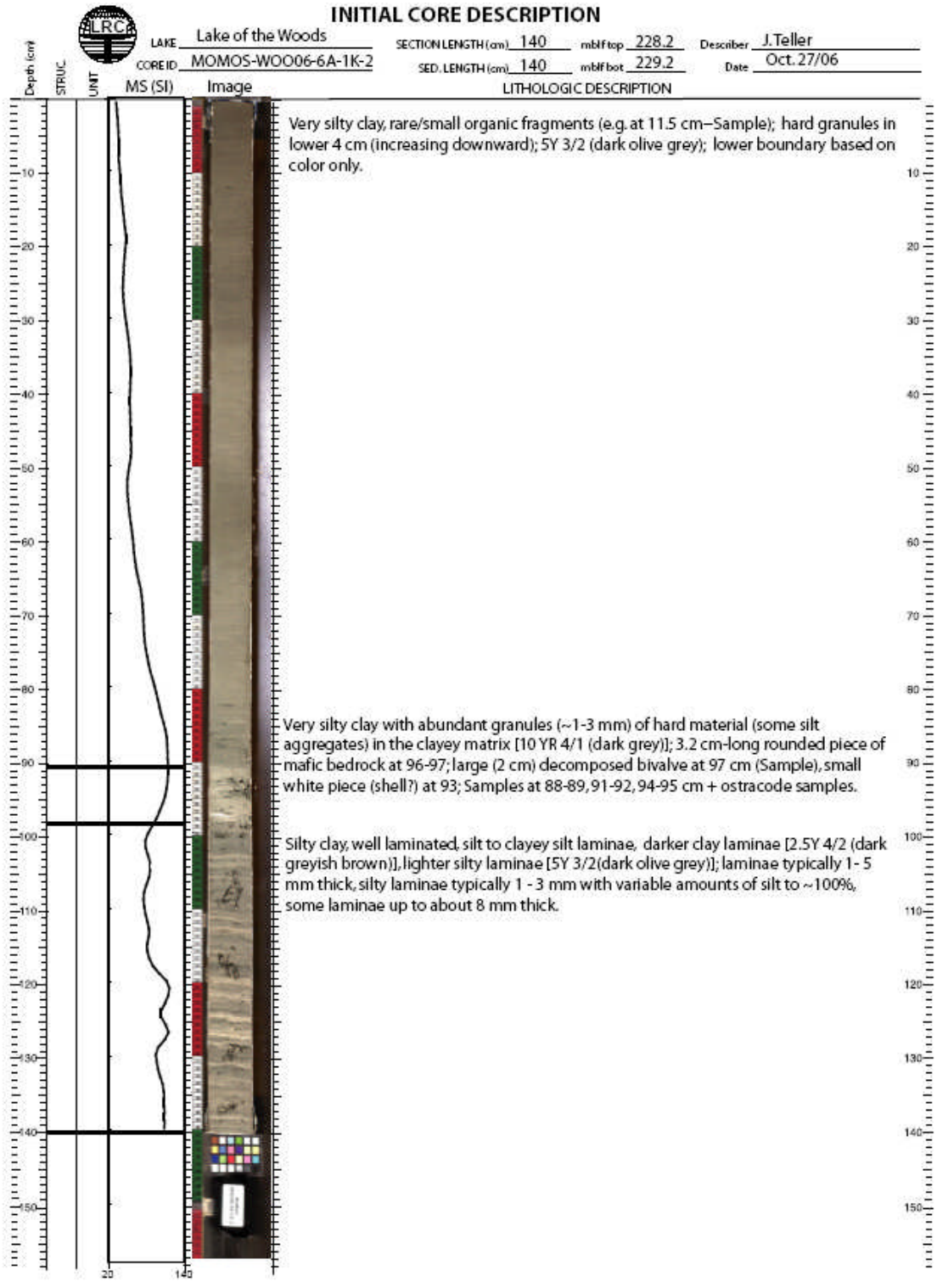

Figure 59. Photographic record and description of WOO06-6A-1K2.

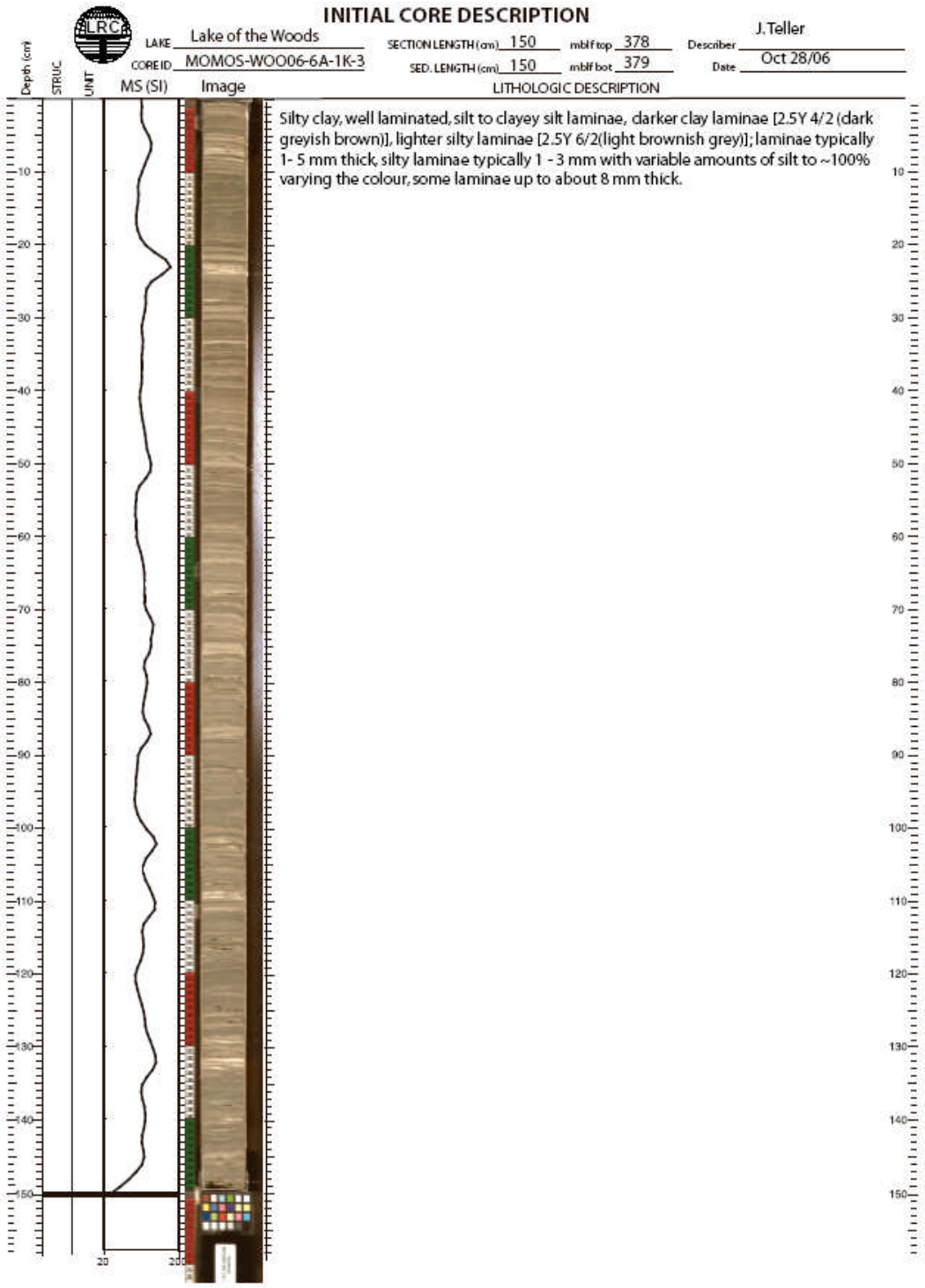

Figure 60. Photographic record and description of WOO06-6A-1K3.

4.2.5.3 **Ostracodes**

The ostracode sequence identified in the bottom of the core at 3.8 m to about 2.8 m (Figure 61) is composed of two ostracode species *C. subtriangulata* and *L. friabilis*. *C. subtriangulata* is the dominant species in the core and they extend from the bottom to about 1.8 m. One rare interval of *C. sharpei* occurs at about 3.1 m when both *C. subtriangulata* and *L. Friabilis* populations disappear.

The end of the ostracode interval in this core at about 1.9 m, is very close (8 cm below) the radiocarbon dated interval 6.760 ^{14}C ka BP (7.616 cal ka BP) near the end of the paleosol. The absence of ostracodes in the upper portions of the core repeats a similar pattern present in other cores.

C. s*ubtriangulata* shells are typically broken and thin and have a corroded appearance. Two intervals with articulated ostracode shells were observed and some *L. friabilis* shells appeared to be crushed. The ostracode shells at the bottom of the core (~ 0.4 m from the bottom) do not have the same mechanical damage or corroded appearance as those above.

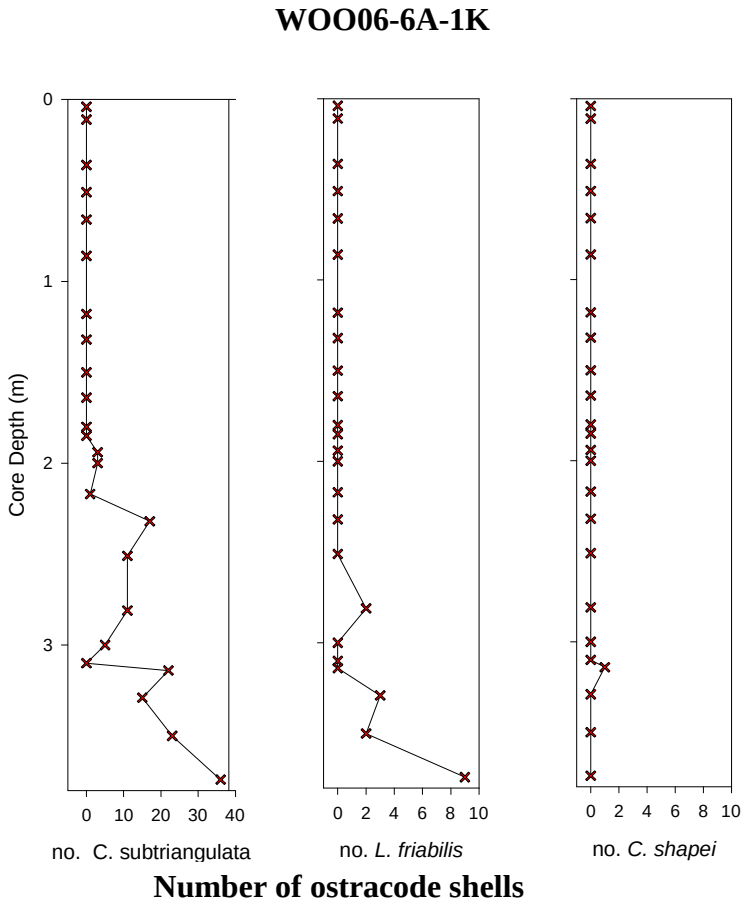

Figure 61. Ostracode population variation for WOO06-6A-1K from the top of the core to the bottom at 3.8 m. The crosses indicate sample locations. Note the number of ostracodes scale varies, with the *C. subtriangulata* ostracode population much higher than the others.

4.2.5.4 **Thecamoebians**

Thecamoebians appear at about 1.3 m in an interval below which there was already a relatively abundant zone of lithics, plant, insect and charcoal materials (Figure 62). A detailed thecamoebian species analysis was not conducted for this core, however up to four species of thecamoebians were noted. This thecamoebian interval is about 0.5 m above the end of the paleosol zone (Appendix A, Subsection 4.2).

4.2.5.5 **Other Macrofossils**

Relatively large volumes of plant and charcoal in the lower portion of the core in conjunction with *C. subtriangulata* ostracodes are observed in a zone below the observed paleosol interval, at about 1.9 m (Figure 62). This interval contains high volumes of plant materials, including large fragments of charcoal, and gastropod shells (Appendix A, Subsection 4.2). Above the paleosol, plant materials, charcoal and insect materials increase dramatically.

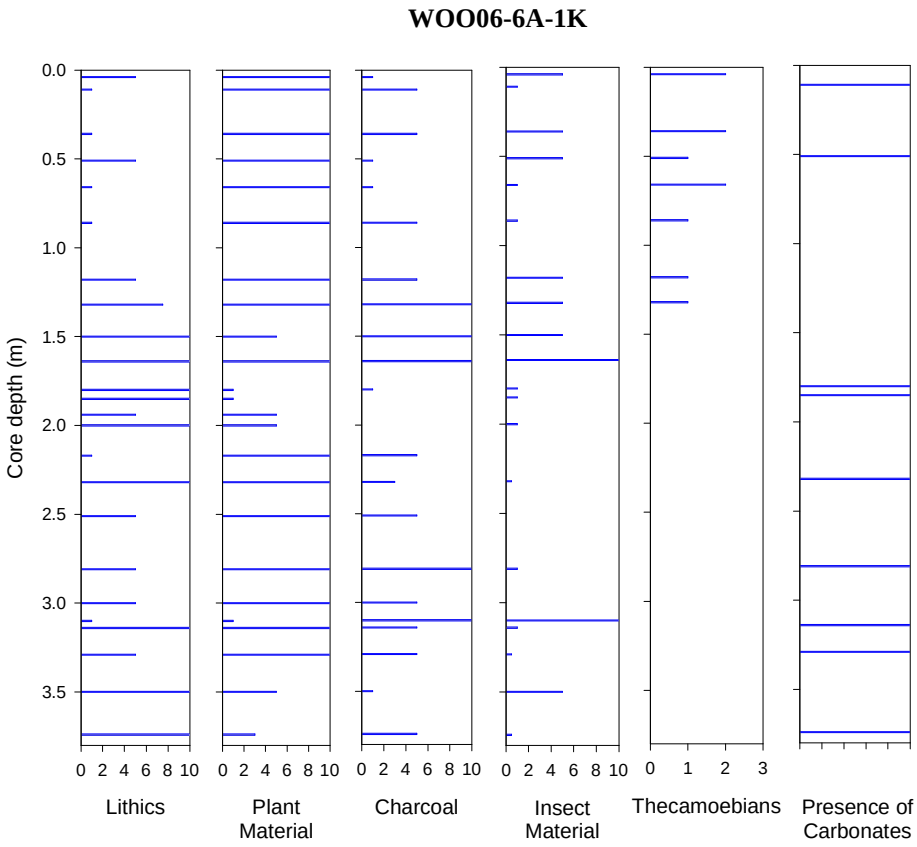

Figure 62. Plots of lithic materials and macrofossils for WOO06-6A-1K from the top to the bottom of the core at 3.8 m. Sampled locations are the same as those in Figure 61. Lithics, plant, charcoal, and insect material are indicated by a bar reflecting their abundance in the sample on a scale of 0 (absent) to 10 (abundant) and were recovered from the subsamples after wet sieving. Presence of thecamoebians and carbonates in a sample are shown only by a bar, and do not imply any quantity.

4.2.5.6 **Lithic Grains**

Quartz lithics are present in conjunction with clay pellets from near the bottom of the core upwards to the end of paleosol horizon (Figure 62), where quartz becomes the dominant lithic (Appendix A, Subsection 4.2). Quartz lithics decrease in relative quantity to the top of the core, while clay pellets disappear completely. Quartz lithics dominate in the bottommost ~ 0.3 m. Iron stained carbonate rich pellets are present from near the bottom of the core to the top of the paleosol, and they are often in conjunction with coated ostracode shells.

4.2.5.7 **Radiocarbon Dates**

Three radiocarbon dates were obtained for this core (Figure 62) from available macrofossils (Appendix B, Section 2, Table B-1). Near the top of the paleosol at a depth of about 1.9 m a mollusc shell was dated at 6.760 ^{14}C ka BP (7.616 cal ka BP). This date is very near to the top of the interval where ostracodes disappeared. A date of 2.11 ^{14}C ka BP (2.091 cal ka BP) was obtained above the paleosol from blackened organic material at 1.0 m and is located above the beginning of the thecamoebians at 1.3 m. A date of 3.245 ^{14}C ka BP (3.481 cal ka BP) was obtained from beetle parts at 1.5 m. This date is below the beginning of the thecamoebian interval.

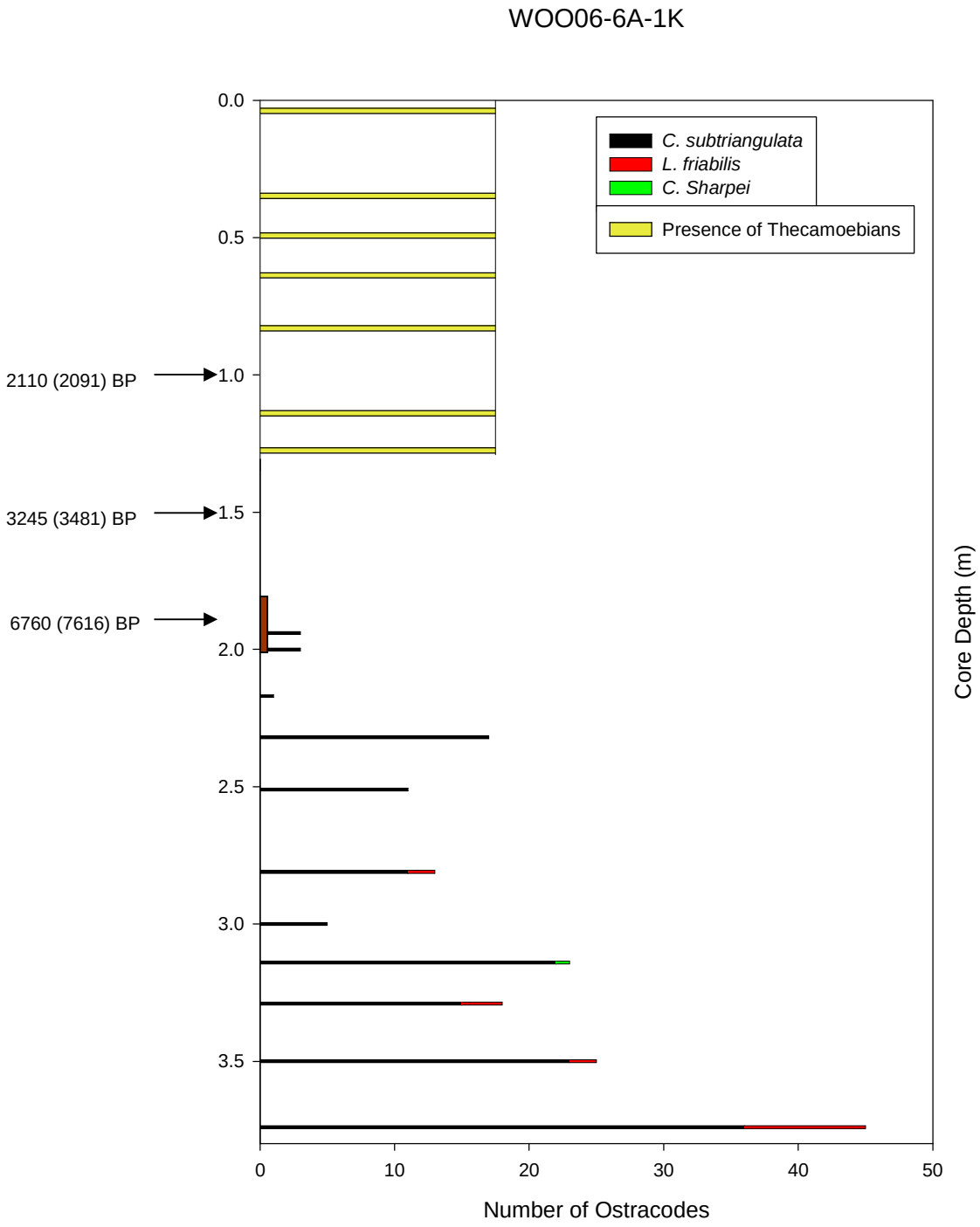

Figure 63. Radiocarbon dates for WOO06-6A-1K showing the ostracode and thecamoebian intervals. Sampled locations are the same as those in Figure 61. The yellow bars represent the presence of thecamoebians. The brown bar on the left scale indicates the location of a paleosol. The total number of ostracodes includes all species as are reported in the details of Figure 61. All dates are from the radiocarbon analysis reports in Appendix B.

4.2.6 Kenora Site - WOO06-7A

4.2.6.1 General

The WOO06-7A-1P coring location, latitude 49.72984^{o} longitude -94.51310^{o}, in a complex channel system south of the outlets to the Winnipeg River and the town of Kenora, Ontario (Figure 24), is described in Section 2.3.5. The retrieved data is presented in Appendix A, Subsections 5.1 and 5.2, with detailed photographic images in Appendix A, Subsection 5.3. The WOO06-7A-1P core is located in a complex channel system connecting to more open waters to the south, in about 6.1 m (20 feet) of water. The retrieved length is about 4.65 m.

4.2.6.2 General Stratigraphic Description

The stratigraphy for the WOO06-7A core is described for the four sections of the core WOO06-7A-1P1, 1P2, 1P3, and 1P4, in
Figure 64, Figure 65, Figure 66, and Figure 67. In this core there are three primary units.

Unit 1 ends at about 3.85 m (about 75 cm in Figure 67) at a distinct colour boundary. It is a laminated sandy silty clay becoming a weakly laminated silty clay upward from the bottom of the core at 4.65 m, to a pink clay bed occurring at about 4.0 m. Above this it becomes a weakly laminated slightly sandy silty clay. The lowermost portion of Unit 1 has common 2-10 mm sand laminae with the laminae thinning to < 2mm upwards. The

pink clay has an underlying silty clay 0.5 cm interval of tan coloured clay. These clay intervals are smoother and contain less silt, and no sand.

Unit 2 is a sandy silty clay with weakly to distinct sandy clayey silt laminae, which are increasingly sandy downward. A distinct colour change occurs at the lower boundary at 3.85 m, and the upper boundary at about 2.9 m (at about 130 cm in Figure 66) is distinguished by the transition to the non-laminated unit above.

Unit 3 is the uppermost unit (Figure 64 and Figure 65) and is a non-laminated, high moisture, gelatinous and slightly sandy silty clay, trending to more sandy below, down to about 2.9 m.

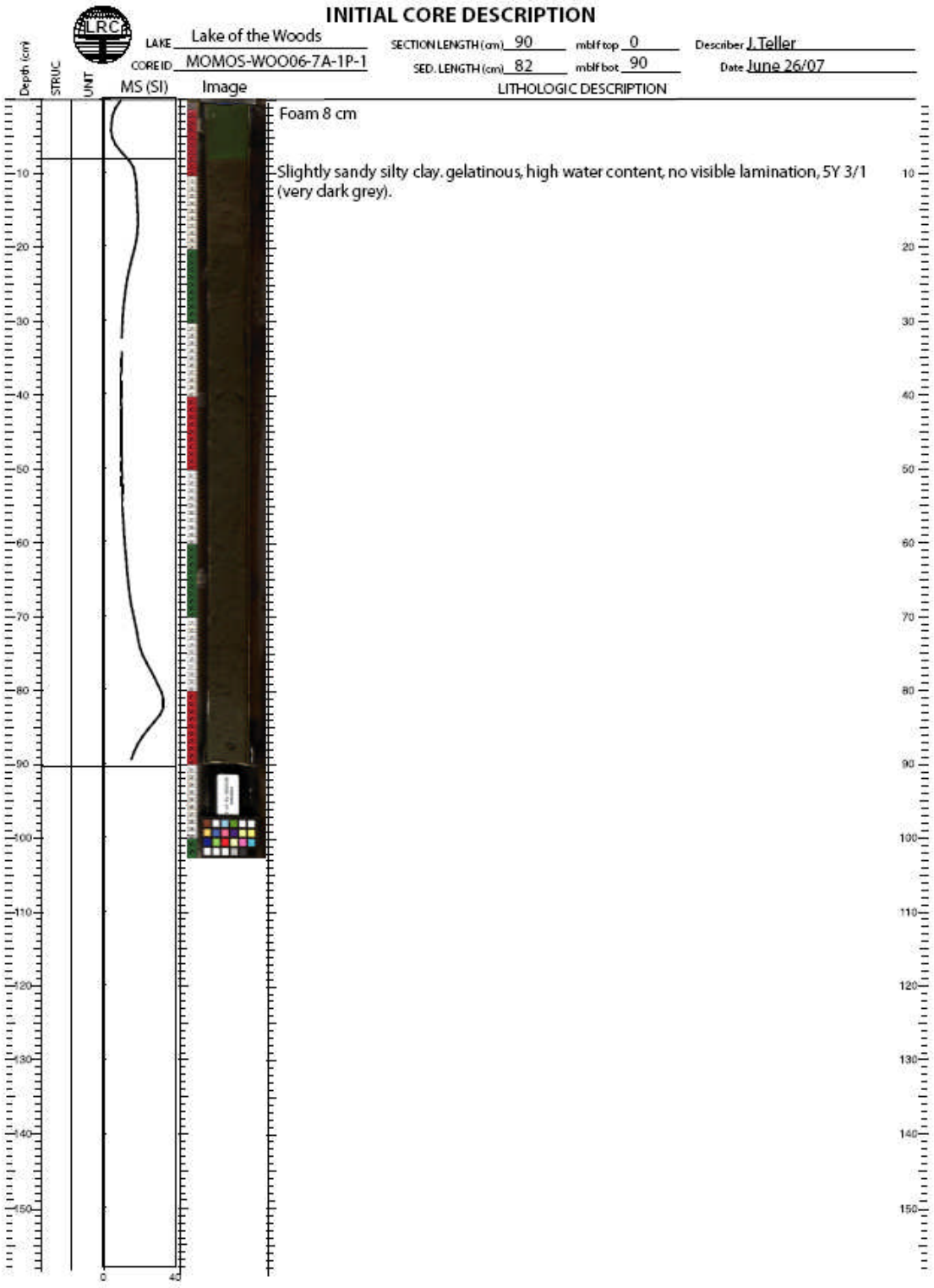

Figure 64. Photographic record and description of WOO06-7A-1P1

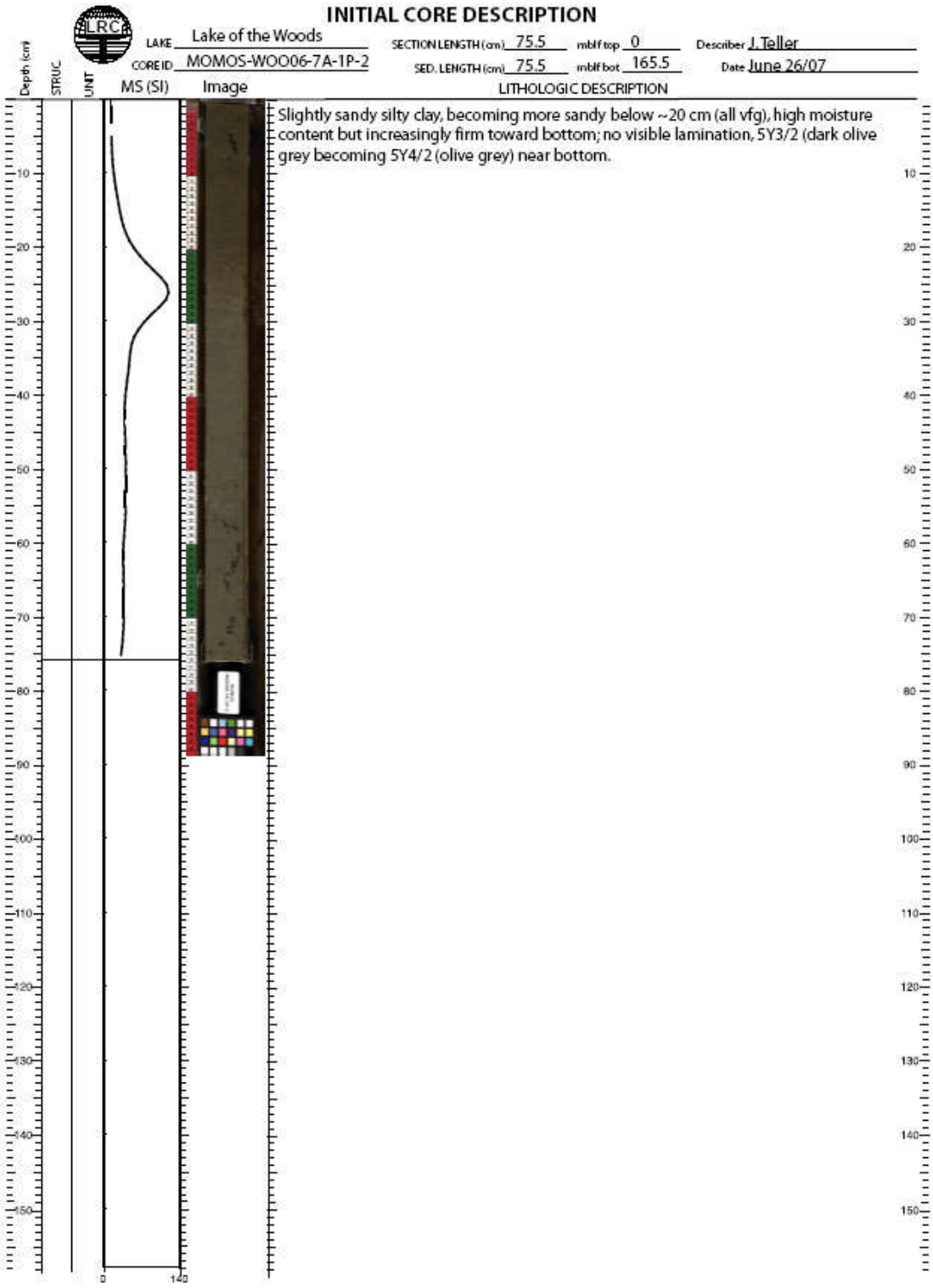

Figure 65. Photographic record and description of WOO06-7A-1P2

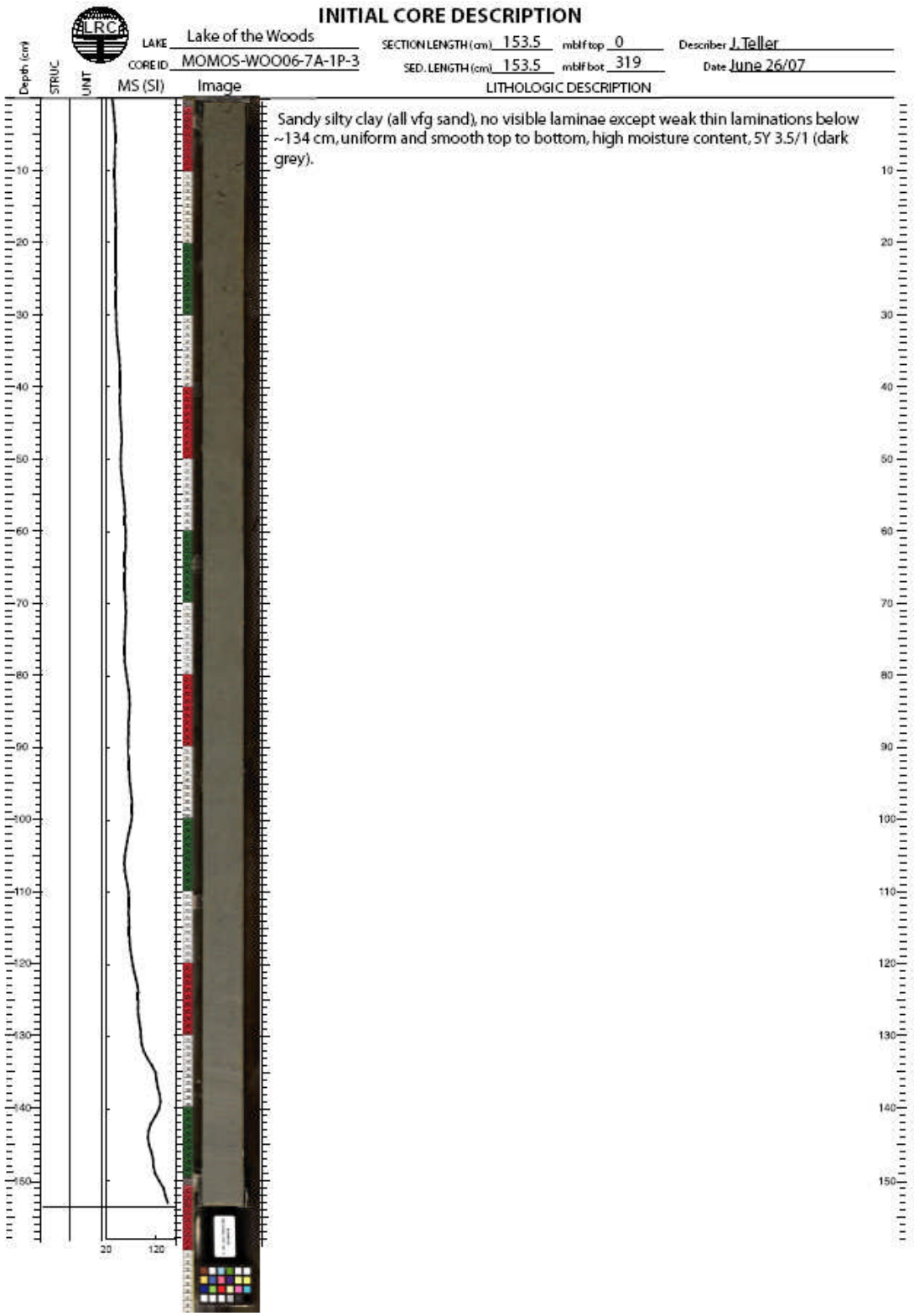

Figure 66. Photographic record and description of WOO06-7A-1P3

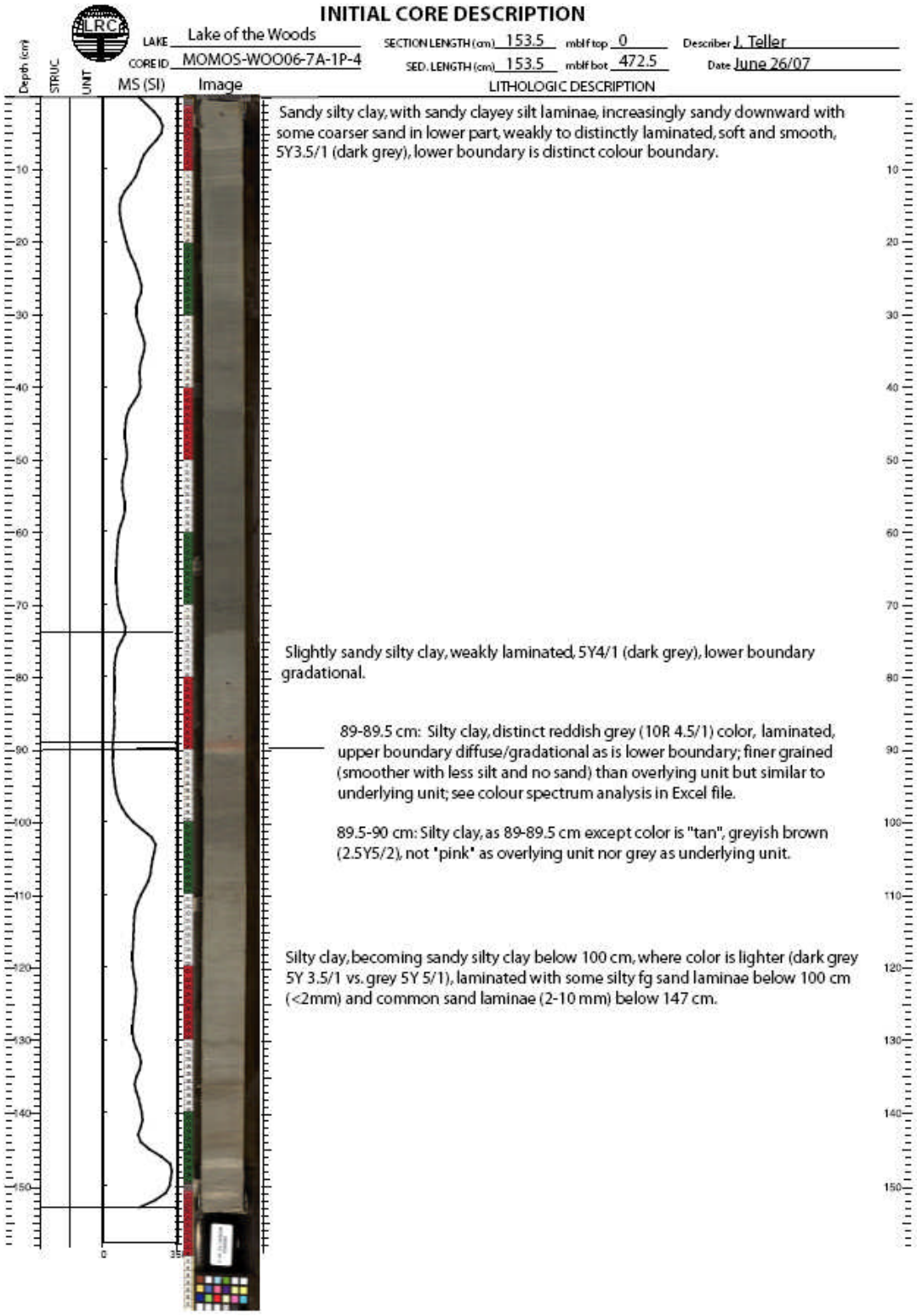

Figure 67. Photographic record and description of WOO06-7A-1P4

4.2.6.3 **Ostracodes**

The ostracode sequence identified in the bottom of the core is composed of an almost exclusive *C. subtriangulata* interval in the bottom ~ 0.8 m of the core, to about 3.9 m (Figure 68). Subsequent ostracode populations are atypical from the other observed cores in that there are primarily only two ostracode species present, *C. subtriangulata* and *C. sharpei,* with one short interval with low population numbers of *L. friabilis* and *F. rawsoni* near the bottom of the core, above a pink clay layer at 4.0 m. The *C. subtriangulata* and *C. sharpei* intervals are separated in time and do not overlap. Additionally, there are four ostracode intervals with three distinct hiatuses, before the last ostracode interval ends at about 1.2 m (Figure 68), which is within the first appearance of thecamoebians. This overlap of ostracode and thecamoebian intervals in the top portion of the core is unique to this core. The *C. subtriangulata* ostracode dominates near and below the pink clay layer in the two ostracode sequences near the bottom of the core, and it briefly reappears in low numbers at about 2.7 m, and then disappears from the record. The *C. sharpei* ostracode appears in low population numbers by itself, above the last incidence of *C. subtriangulata,* and subsequently goes through a hiatus, and then disappears above about 2.2 m.

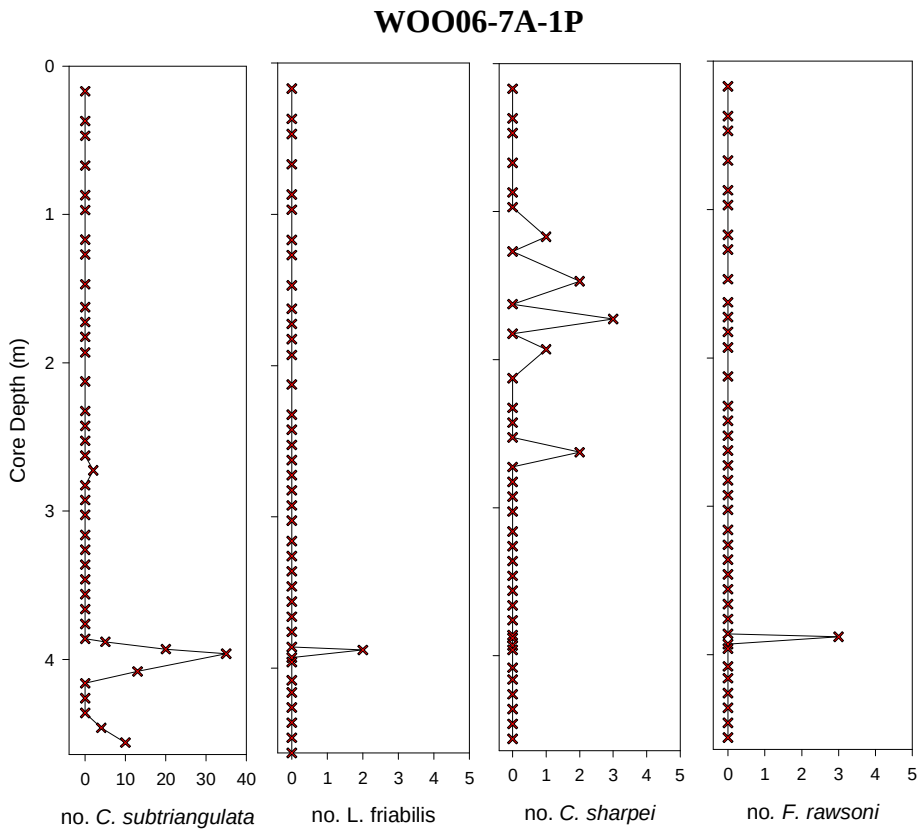

Figure 68. Ostracode population variation from the top of the core to the bottom at 4.65 m. The crosses indicate sample locations. Note the number of ostracodes scale varies, with the *C. subtriangulata* ostracode population much higher than the others.

The last interval of ostracodes begins near an interval dated at 8.310 ^{14}C ka BP (9.350 cal ka BP) (from a twig macrofossil) at about 1.2 m. A date at about 1.1 m just above the end of the ostracodes and below the beginning of the thecamoebians was dated at 6.775 ^{14}C ka BP (7.630 cal ka BP).

Ostracode shells throughout the core are coated, fragile looking, and many are broken. One interval above the pink clay layer had heavily coated shells, and was associated with

the presence of clay balls which appeared in the 20 cm directly above the pink clay. The presence of an articulated ostracode shell was noted near the pink clay bed, indicating reworking near this interval is unlikely.

The lowermost ostracode sequence near and below the pink clay bed which has been associated with the Marquette readvanced, is clearly within the Lake Agassiz period. A hiatus in ostracodes occurred from about 4.4 to 4.1 m after a decline in ostracodes starting from the bottom of the core at 4.65 m, which was followed by a rapid rise in the ostracode population to a maximum at the pink clay bed, at about 4 m.

4.2.6.4 **Thecamoebians**

The early appearance of thecamoebians at 1.5 m, just above the interval dated at 8.265 ^{14}C ka BP (9.235 cal ka BP) is preceded by high insect and plant macrofossils (Figure 69), and is very near the point where LOTWs was estimated to have isolated from Lake Agassiz (Yang and Teller, 2005). The thecamoebians subsequently disappear before reappearing at about 1.0 m, in an interval preceded and followed by relatively high plant, insect and charcoal levels. The appearance of thecamoebians is prior to the end of the last ostracode horizon, which is near a radiocarbon dated interval at 1.1 m of 6.775 ^{14}C ka BP (7.630 cal ka BP).

4.2.6.5 **Other Macrofossils**

Plant and insect macrofossils remained very low until plant material sharply increase about 1.5 m from the bottom of the core at about 3.1 m (about 0.8 m above the pink clay), which is followed by a sharp increase in insects at about 2.6 m (Figure 69). A similar increase in charcoal is noted about the same time as the increase in insects. From the bottom of the core to above the pink clay, there are rare quantities of these biological components to about 3.6 m, where the relative proportion of plant materials increases. Relatively low biotic components continue upwards to about 3.0 m, where plant materials become relatively abundant and insect populations increase.

An insect wing and a grass-like terrestrial plant macrofossil were found at about 3.6 m (Appendix A, Subsection 5.2). High abundance of plant and insect volumes were found below the two radiocarbon dated intervals at about 1.6 m of 8.265 ^{14}C ka BP (9.235 cal ka BP) and 8.310 ^{14}C ka BP (9.350 cal ka BP) (Figure 69). A pelecypod hinge was found at 4.2 m (below the pink clay). Increasing charcoal levels were noted at 2.8 m which become abundant at about 2.5 m (dated nearby at 8.780 ^{14}C ka BP (9.804 cal ka BP).

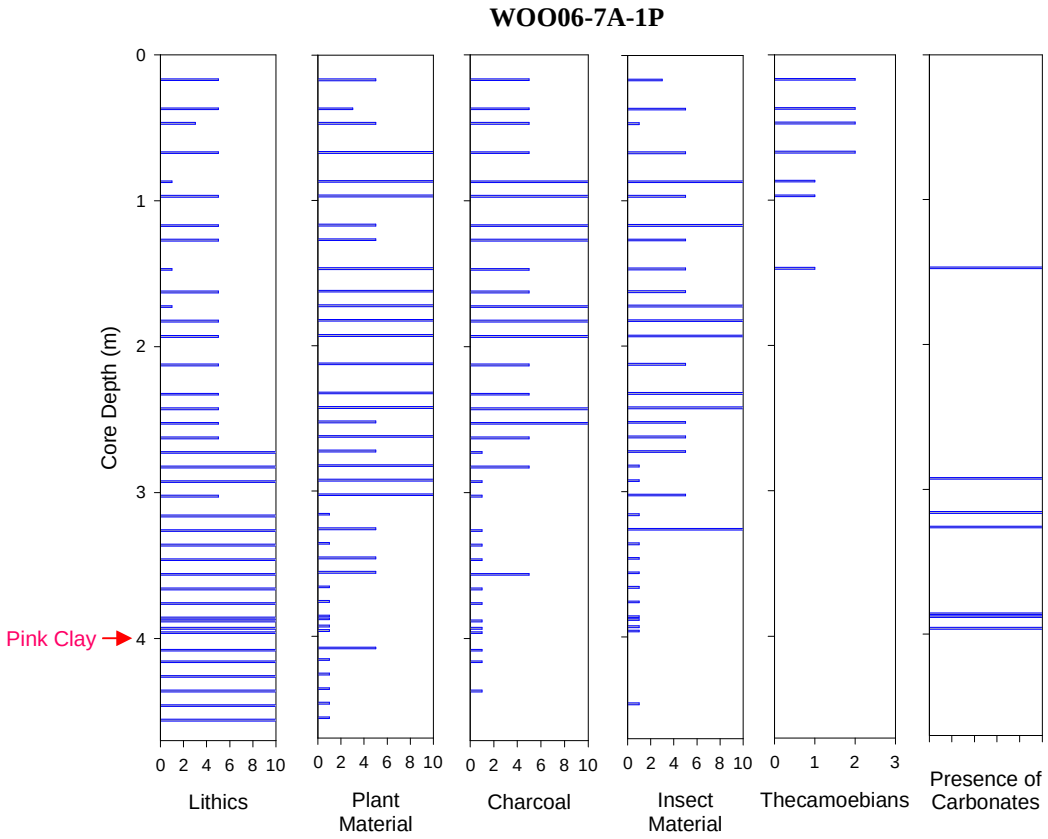

Figure 69. Plots of lithic materials and macrofossils for WOO06-7A-1K from the top to the bottom of the core at 4.65 m. Sampled locations are the same as those in Figure 68. Lithics, plant, charcoal, and insect material were recovered from the subsamples after wet sieving; the high numbers reflect greater abundances in a subsample interval. Presence of thecamoebians and carbonates in a sample are shown by a bar, but do not imply any quantity.

4.2.6.6 **Lithic Grains**

Non disaggregated clay balls occur throughout the core but are most prevalent just above the pink clay. Abundant quartz lithics occur from the bottom of the core to 2.7 m where they drop from abundant to common for most of the remainder of the core, sometimes reaching rare levels (Figure 69). Carbonate lithics and clay balls are noted at and just above the pink clay and at a short interval between about 2.9-3.3 m.

4.2.6.7 **Moisture Analysis**

Moisture data is plotted below in Figure 70. Moisture levels remain relatively consistent throughout the lower portion of the core with moisture levels trending upwards about 1 m from the top of the core. An increase in moisture levels occurs starting above 4 m and corresponds with a dramatic decrease in the ostracodes population and their subsequent disappearance (Figure 68), the presence of carbonate lithics (Figure 69), and a pink clay layer. The increase in moisture at a depth of 1 m also corresponds with the end of the last ostracode interval and the beginning of a continuous zone of thecamoebians in the upper core.

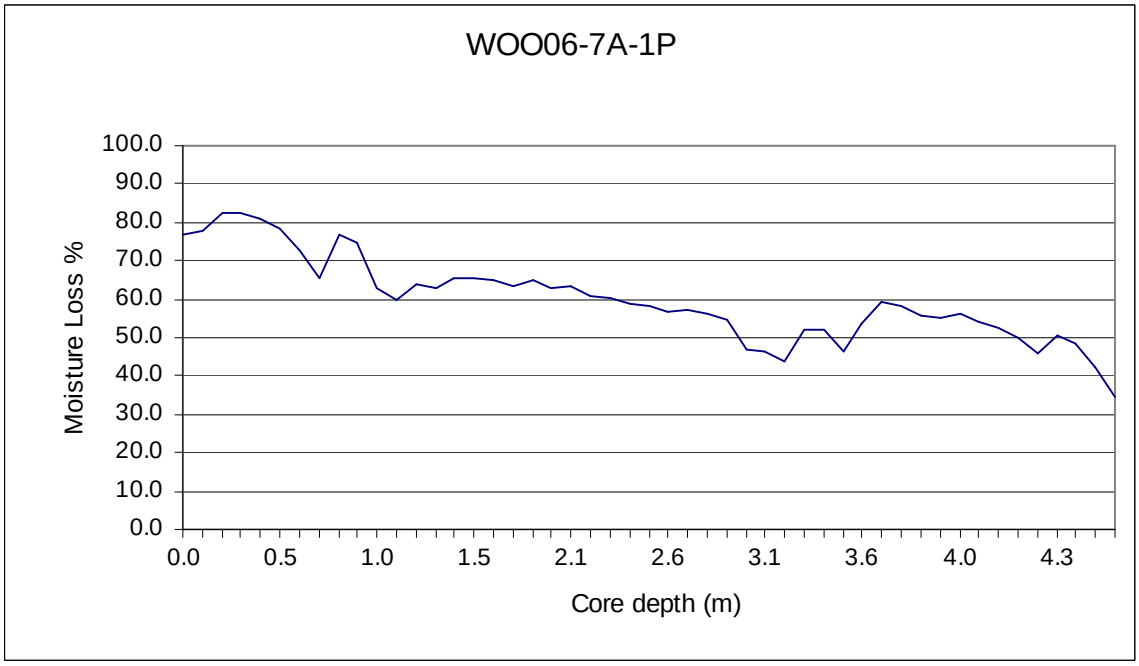

Figure 70. Plot of % moisture loss based on freeze drying of samples, against depth in the WOO06-7A-1P core, with the bottom of the core to the right.

4.2.6.8 **XRD Analysis**

Five broadly spaced samples were taken in the core (refer to Appendix C). Only a very qualitative sampling and data extraction was undertaken in this thesis. Further work including closer sampling intervals and a quantitative assessment of the data would need to be performed to gain further insights. The samples did not appear to show any significant deviation in the general mineralogy of the sediments based on the outputs provided by the Jade program. There was some general variation noted however in the Lake Agassiz sequence above and below the pink clay bed and the lowermost sample appeared unique.

4.2.6.9 **Radiocarbon Dates**

There are two radiocarbon dates at 1.6 m, 8.265 ^{14}C ka BP (9.235 cal ka BP) and 8.310 ^{14}C ka BP (9.350 cal ka BP) in correct chronological sequence. The dates were obtained from twigs (Appendix B, Section 4, Figures B-11 and B-13). One twig did not have bark, and both appeared smooth, however one had the nub of small branch. Subsequently, additional radiocarbon dating from intervals above and below 1.6 m confirmed the stratigraphic sequence was appropriate (Figure 71) with a date from a twig, birch seed, insect parts at about 1.2 m dated to 6.775 ^{14}C ka BP (7.630 cal ka BP) and a date at about 2.4 m on charred conifer needle fragments dated to 8.800 ^{14}C ka BP (9.804 cal ka BP) (Appendix B, Section 5, Figure B-12) and a woody herb tissue 2 cm above at 8.780 ^{14}C ka BP.

A radiocarbon date of 6.060 ^{14}C ka BP (6.930 cal ka BP) from pollen at about 3.3 m and below the older dates from macrofossils appears to be incorrect. A possible sampling or labelling error may have occurred. It did not follow the chronological sequencing of the dated macrofossil materials and is not considered valid.

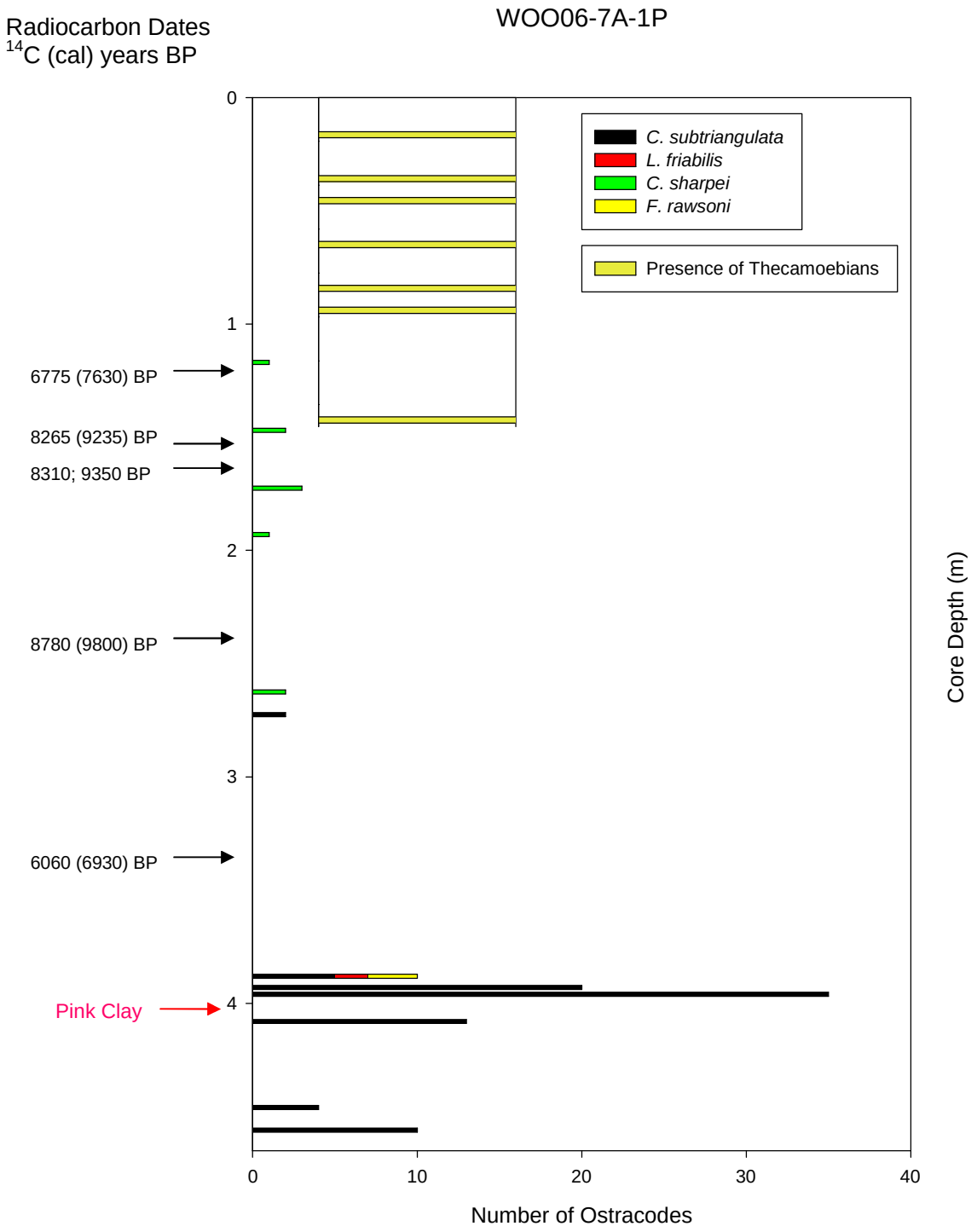

Figure 71. Radiocarbon dates for WOO06-7A-1P showing the ostracode and thecamoebian intervals. Sampled locations are the same as those in Figure 68. The light yellow bars represent the presence of thecamoebians. The unusual radiocarbon date at about 3.3 m is not logical and was not used in core analysis. The total number of ostracodes includes all species as are reported in the details of Figure 68. All dates are from the radiocarbon analysis reports in Appendix B.

4.2.7 Shoal Lake Site - SHO06-2A

4.2.7.1 General

The SHO06-2A-1K coring location, latitude 49.74471^{o} longitude -94.52096^{o}, in the northern portion of SL (Figure 24), is described in Section 2.3.6. The retrieved data are presented in, Subsections 6.1 and 6.2, with detailed photographic images in Appendix A, Subsection 6.3. The SHO06-2A-1K core is located in the narrowing portion of a long bay leading to the northwest portion of the SL about 1 km off shore, in about 9.2 m (30.2 feet) of water. The retrieved length is about 6.85 m.

4.2.7.2 General Stratigraphic Description

The stratigraphy for the WOO06-7A core is described for SHO06-2A-1K1, 1K2, 1K3, 1K4 and 1K5, in Figure 72, Figure 73, Figure 74, Figure 75, and Figure 76. In this core there are two primary stratigraphic units.

Unit 1 is a thinly laminated slightly silty clay with alternating dark and light laminations, from the bottom of the core at 6.84 m, to the top of the unit at about 5.7 m (30 cm in Figure 76), where the laminations disappear and there is a distinct colour change. The unit includes extremely fine organic/algal matter i.e. it is a slightly silty clay gyttja. Unit 1 occurs about 10 cm below the radiocarbon dated interval in Unit 2 dated at 6.685 ^{14}C ka BP (7.554 cal ka BP). Unit 2 starts at about 5.7 m and is a non-laminated clayey silty gyttja with a high moisture content which decreases downward, becoming very soft and

gelatinous. There is an increase in clay content downward from the top of the core to about 2.55 m, where it becomes a smooth soft silty clay. At about 3.75 m it slowly transitions to silty clay with fine organic algal matter below, with intervals of organic detritus along horizontal planes. The silty clay oxidized to a greyer colour over 12 hours implying sulphides are present from here to the bottom of the unit at about 5.7 m.

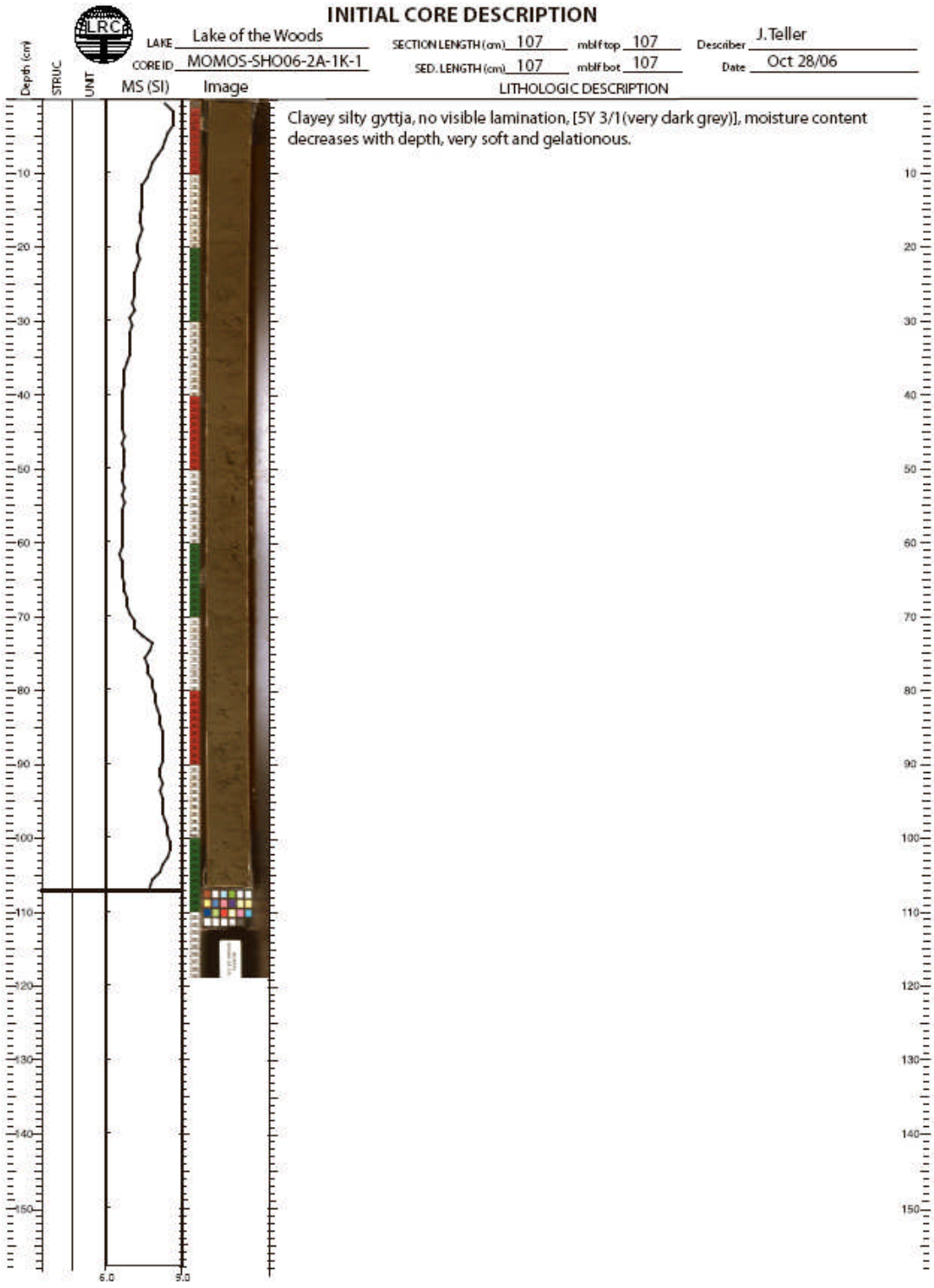

Figure 72. Photographic record and description of SHO06-2A-1K1

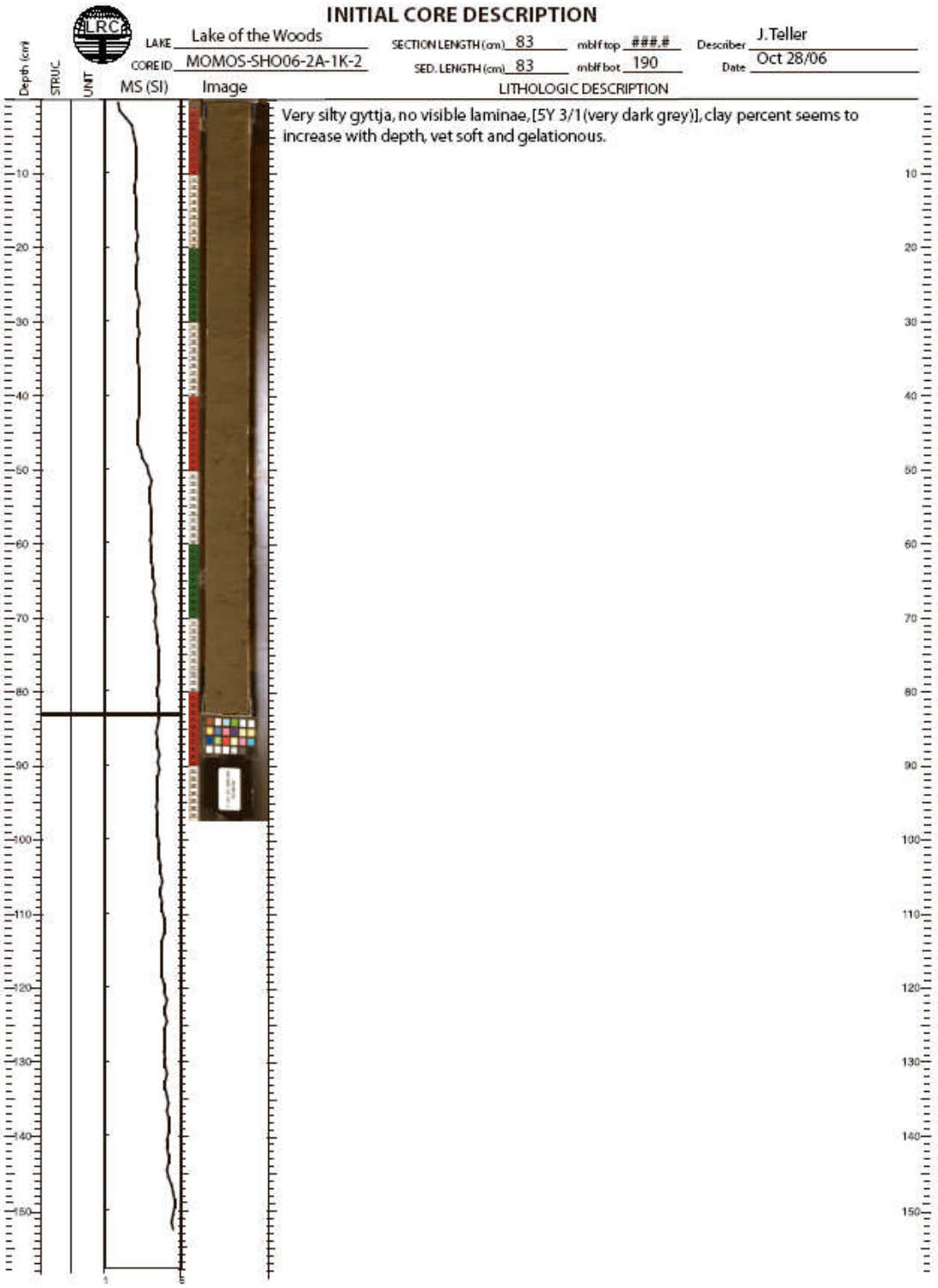

Figure 73. Photographic record and description of SHO06-2A-1K2

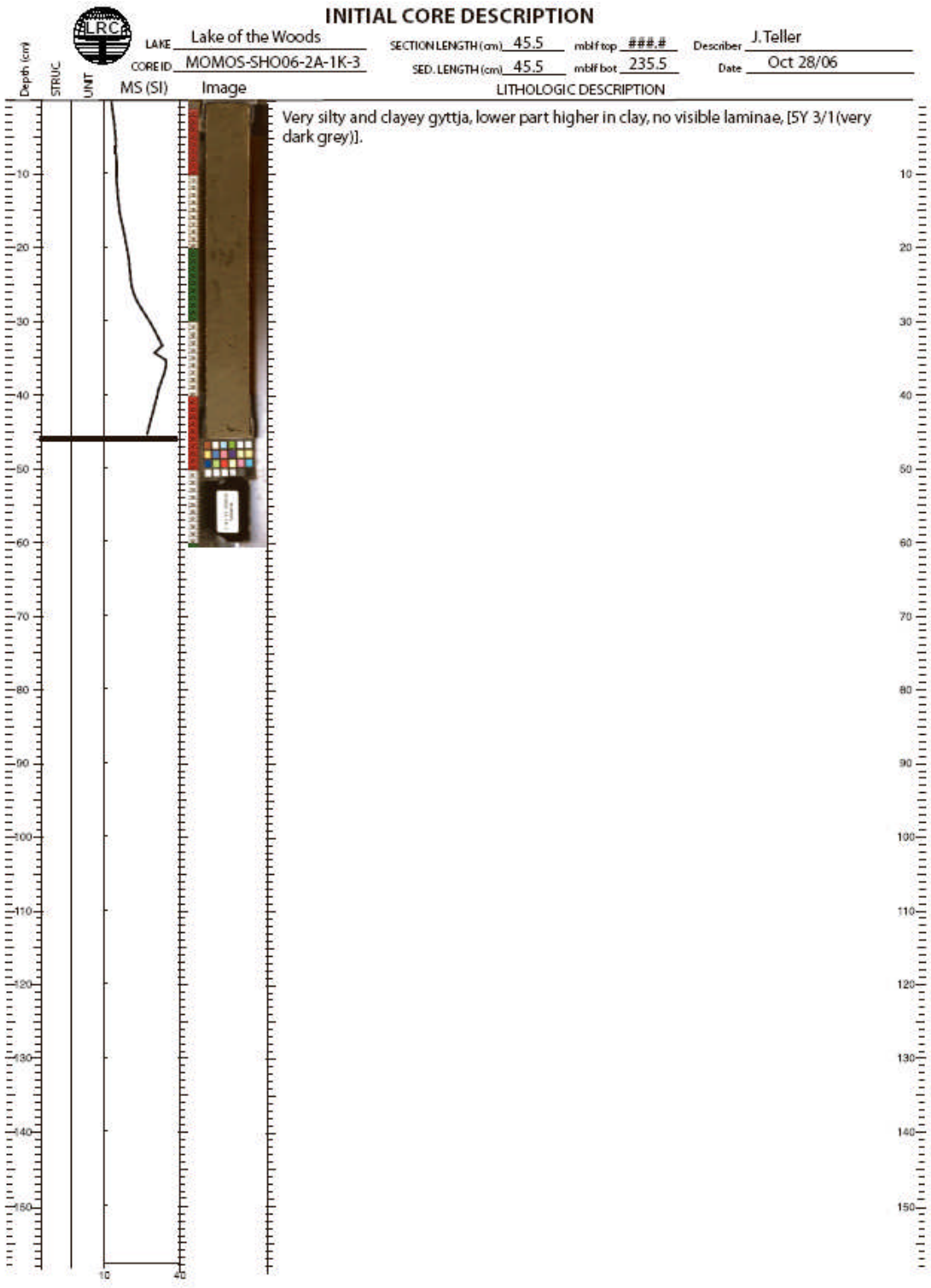

Figure 74. Photographic record and description of SHO06-2A-1K3

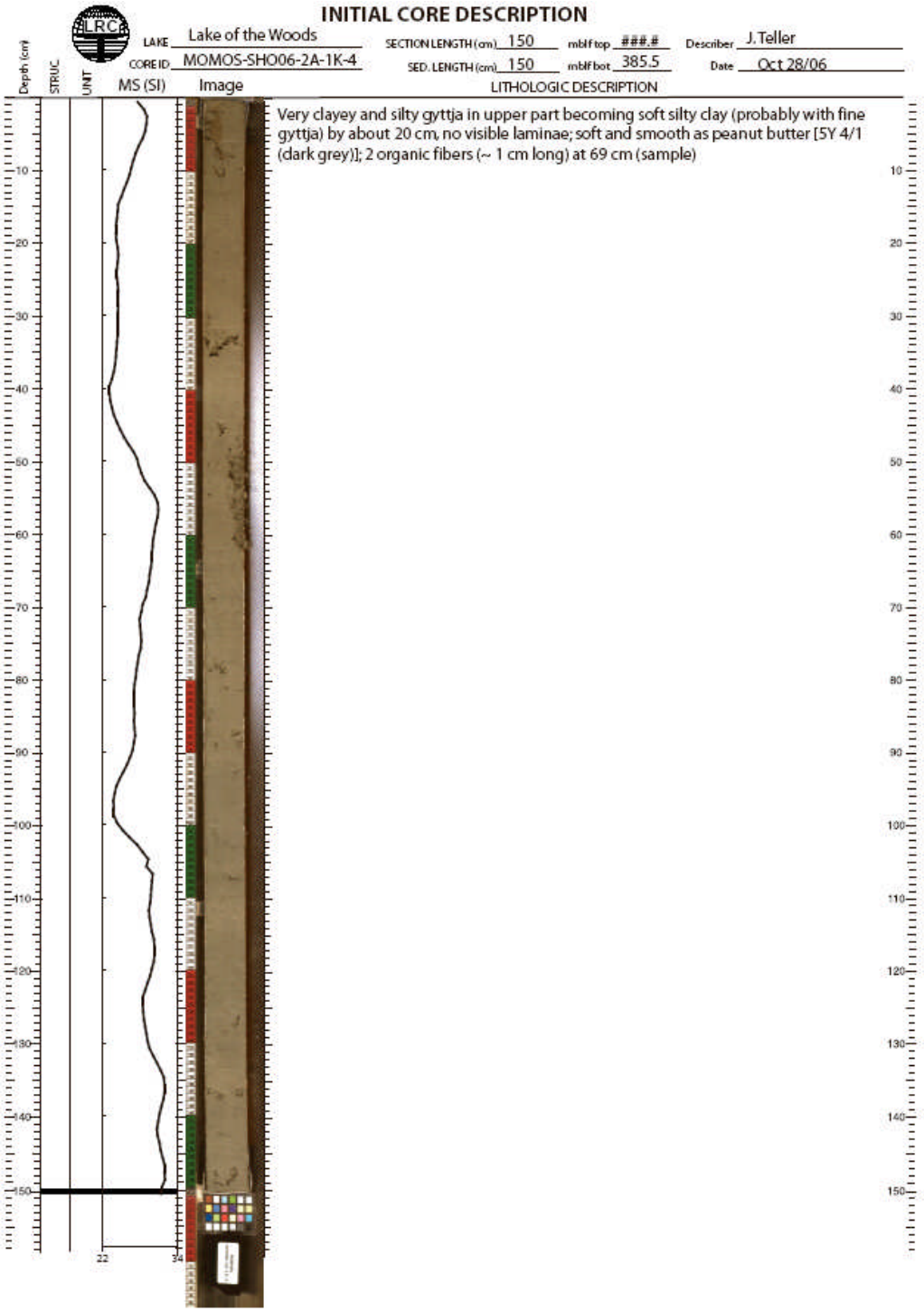

Figure 75. Photographic record and description of SHO06-2A-1K4

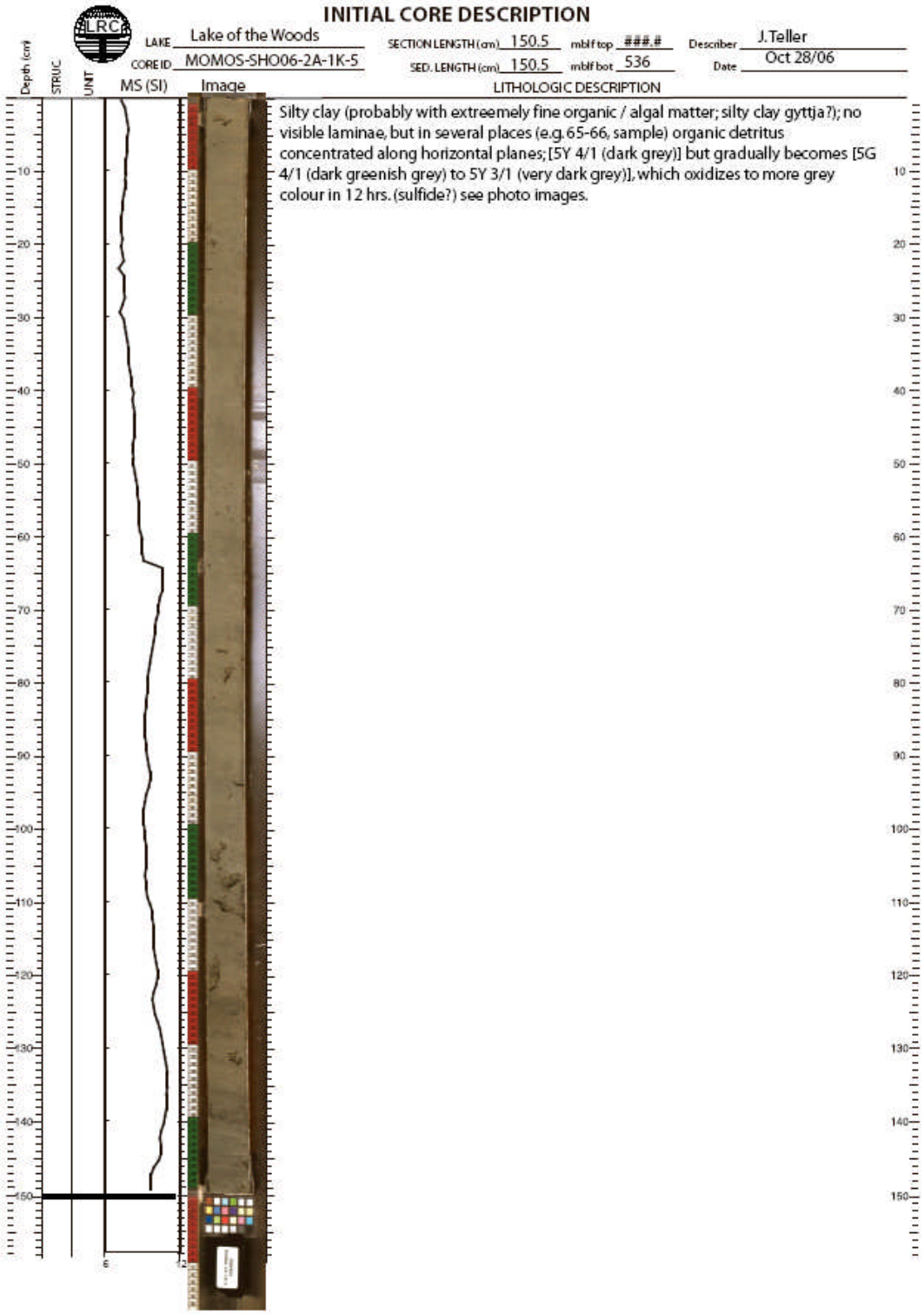

Figure 76. Photographic record and description of SHO06-2A-1K5

4.2.7.3 Ostracodes

The ostracode sequence in this core is like all other cores and ostracodes disappear towards the top of the core (Figure 77). *C. subtriangulata* are present throughout the entire ostracode sequence at the bottom of the core, but are not dominant. Nor do they disappear towards the top of the ostracode sequence as they do in other cores, and actually undergo a peak in population in the top ~ 0.5 m of the ostracode sequence. All four of the ostracode species which were found in the other LOTWs cores are found in the ostracode sequence of this core. This sequence starts at the bottom of the core at 6.84 m to about 3.5 m, with *C. sharpei* dominant. The other two ostracodes *L. friabilis* and *F. rawsoni* are also present in significant numbers with *L. friabilis* more prevalent and spanning a greater range from 6.1 to 3.6 m, with one shell found at the bottom of the core before *L. friabilis* undergoes a long hiatus of about 0.5 m. The upper portion of the *L. friabilis* sequence starts to trend to its final disappearance starting at 3.9 m, at the same time a maximum occurs in *C. subtriangulata.* *F. rawsoni* is much less prevalent, and is intermittently present from about 5.3 to 3.5 m when it disappears with the other ostracode species. Ostracodes disappear about a metre below an interval dated at 7.130 ^{14}C ka BP (7.963 cal ka BP) at about 3 m, however this date does not appear in sequence with other dates and is not likely correct.

The condition of the ostracode shells in this core are quite variable (Appendix A, Subsection 6.2) and range from all species intact, at the bottom intervals of the core, to all mostly intact except *C. subtriangulata.* Articulated ostracode shells are present in

various intervals from the bottom of the core to near the top of the ostracode interval. There was one short interval (5.3-5.6 m) that had ostracode shells that were corroded looking and coated.

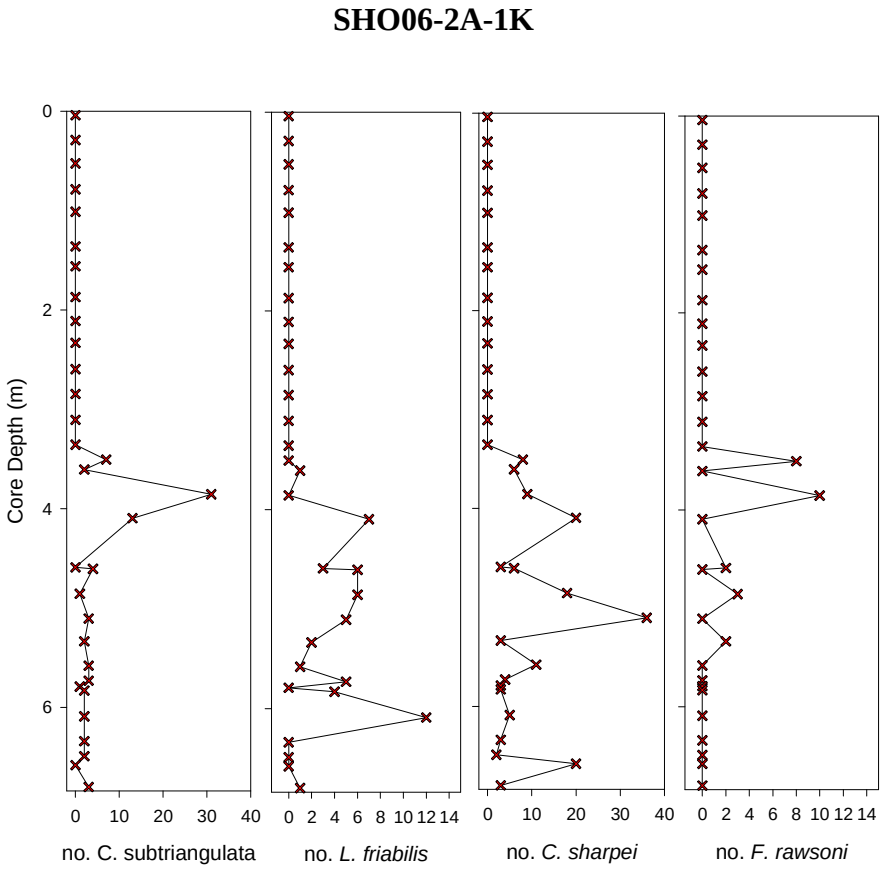

Figure 77. Ostracode population variation for SHO-2A-1K from the top of the core to the bottom at 6.85 m. The crosses indicate sample locations. Note the number of ostracodes scale varies, with the *C. subtriangulata* ostracode population and *C. sharpei* much higher than the others.

4.2.7.4 **Thecamoebians**

Thecamoebians appear at about 6.8-6.6 m and above 2.8 m (Figure 78). The appearance of thecamoebians at the bottom of the core, even in the limited number encountered, is unlike any other core. Additionally, the thecamoebians at the top of the core are continuous within the sampling sequence, and are typically common to abundant in this interval with up to five species identified which are relatively abundant in the interval (Appendix A, Subsection 6.2). The lowermost interval included three species of thecamoebians. Thecamoebians appear above a nearby interval dated at 5.630 ^{14}C ka BP (6.452 cal ka BP), however this date does not appear to be in sequence.

4.2.7.5 **Other Macrofossils**

Plant and insect macrofossils remained relatively high throughout the length of the core (Figure 78). Plant levels were continuously high starting at the bottom of the core, and started decreasing just above the thecamoebian interval at 2.6 m and increased to common and abundant levels at about 1.0 m.

Insect macrofossil abundances were relatively high in the lower portion of the core, and decreased thought the middle portions and then rose to relatively high abundance in the top of the core. Overall insect levels in the core are relatively high, but cycle a number of times from a minimum, rapidly rising to a maximum in the bottom third of the core, then falling to a minimum just before the beginning of thecamoebians before finally rising in

the top 1.5 m of the core. The insect component in the bottom portion of the core is dominated by larvae cases with the upper portions a combination of insect exoskeletons and larvae cases (Appendix A, Subsection 6.2).

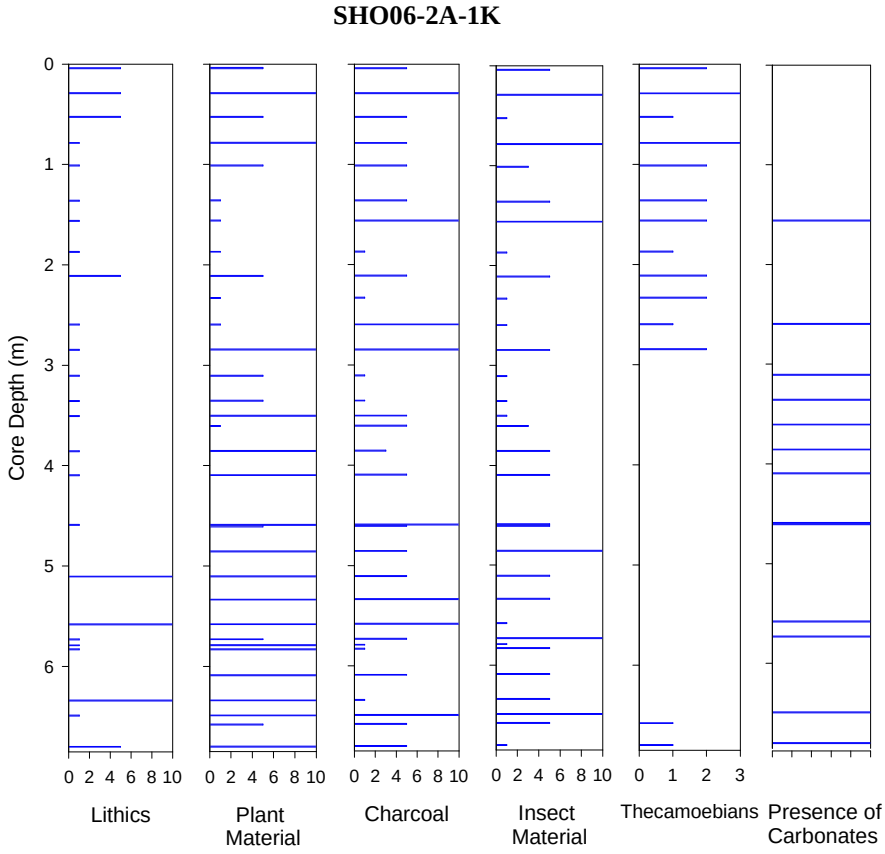

Figure 78. Plots of lithic materials and macrofossils for SHO06-2A-1K, from the top to the bottom of the core at 6.85 m. Sampled locations are the same as those in Figure 77. Lithics, plant, charcoal, and insect material were recovered from the subsamples after wet sieving; the high numbers reflect greater abundances in a subsample interval. Presence of thecamoebians and carbonates in a sample are shown by a bar, but do not imply any quantity.

Charcoal is present starting at the bottom of the core and undergoes numerous fluctuations from rare to abundant throughout the core. Increasing charcoal levels at 2.8 m, including large charcoal fragments, remain relatively high to the top of the core. A

minimum charcoal interval occurs at about 2.3 m after the interval of charcoal abundance and above the first appearance of thecamoebians at 2.8 m. Charcoal levels then rise somewhat before rising to the more abundant levels with large fragments common (Appendix A, Subsection 6.2). Small amorphous charcoal fragments were also noted in some intervals between intervals of large fragments. Large charcoal fragments were noted near the bottom of the core including what appear to be bark fragments. A large (1 cm) charcoal leaf fragment was found at 5.6 m with the interval dated at 6.685 ^{14}C ka BP (7.554 cal ka BP).

Evidence of fish biota is present throughout the core, including the bottom intervals in the core which have a higher incidence. What appear to be fish vertebrae, miscellaneous bones, teeth and scales, are relatively common and significantly more abundant than in LOTWs cores. A gastropod shell at 6.1 m and pelecypod shell at 3.4 m (just beyond the end of ostracodes) were also noted. The pelecypod beyond the ostracode interval correlates with the carbonate lithic evidence found in this interval. This interval is just before the upper thecamoebian interval.

Seeds were present starting at about 2.8 m and became common to about 0.5 m from the top of the core. The seed macrofossils started to appear at the same interval as the beginning of the upper thecamoebian interval. The presence of birch nutlets were noted (Appendix B, Section 4, Figure B-13) at about 1 m, and were dated at 2.525 ^{14}C ka BP (2.636 cal ka BP).

4.2.7.6 **Lithic Grains**

The lithic materials are generally at low levels of abundance although there are some intervals with elevated lithics grains (Figure 78). These are however, primarily non disaggregated clay balls, with only two intervals with elevated quartz lithics (Appendix A, Subsection 6.2). One interval with higher quartz is near the bottom of the core at 6.4 m, and one is near the top (0.3 m). Other than these two intervals, quartz concentrations in this core essentially range from rare to none. An extended interval where carbonate lithic grains including clay balls were observed occurs from about 4.6 to 2.6 m (includes the interval where a pelecypod was observed), with other carbonate grains are interspersed through the core from the bottom to about 1.6 m from the top of the core where they disappear.

4.2.7.7 **Radiocarbon Dates**

Five radiocarbon dates were obtained in this core and are spaced relatively evenly over the length of the core (Figure 79). One date, 7.130 ^{14}C ka BP (7.963 cal ka BP), at 3.0 m, appears to be out of sequence with respect to the adjacent radiocarbon dates, and has been rejected as being too old (by about 3.0 ^{14}C ka). An additional date at the bottom of the core at about 6.8 m which was obtained from a large bulk sample (over a 12 cm interval) was dated at 5.630 ^{14}C ka BP (6.452 cal ka BP) and appears suspect as it is much younger than radiocarbon dates above this interval. The remaining dates are logically sequenced and were used in making the subsequent assessments.

The youngest date 2.525 ^{14}C ka BP (2.636 cal ka BP) at 1 m, was obtained from two birch nutlets and an insect head (*Helodidae*) (Appendix B, Section 5, Figure B-13). This date helps define the beginning of thecamoebians and sedimentation rates in the upper core.

The second oldest valid date of 6.170 ^{14}C ka BP (7.082 cal ka BP) at about 4.5 m was obtained from an aquatic moss (*Drepanocladus* sp) (Appendix B, Section 5, Figure B-14) which can be affected by the hard water effect. It does however appear to chronologically sequenced reasonably well. The lowermost and oldest available valid date at about 5.6 m, was dated at 6.685 ^{14}C ka BP (7.554 cal ka BP) and is the closest viable date to the bottom of the core.

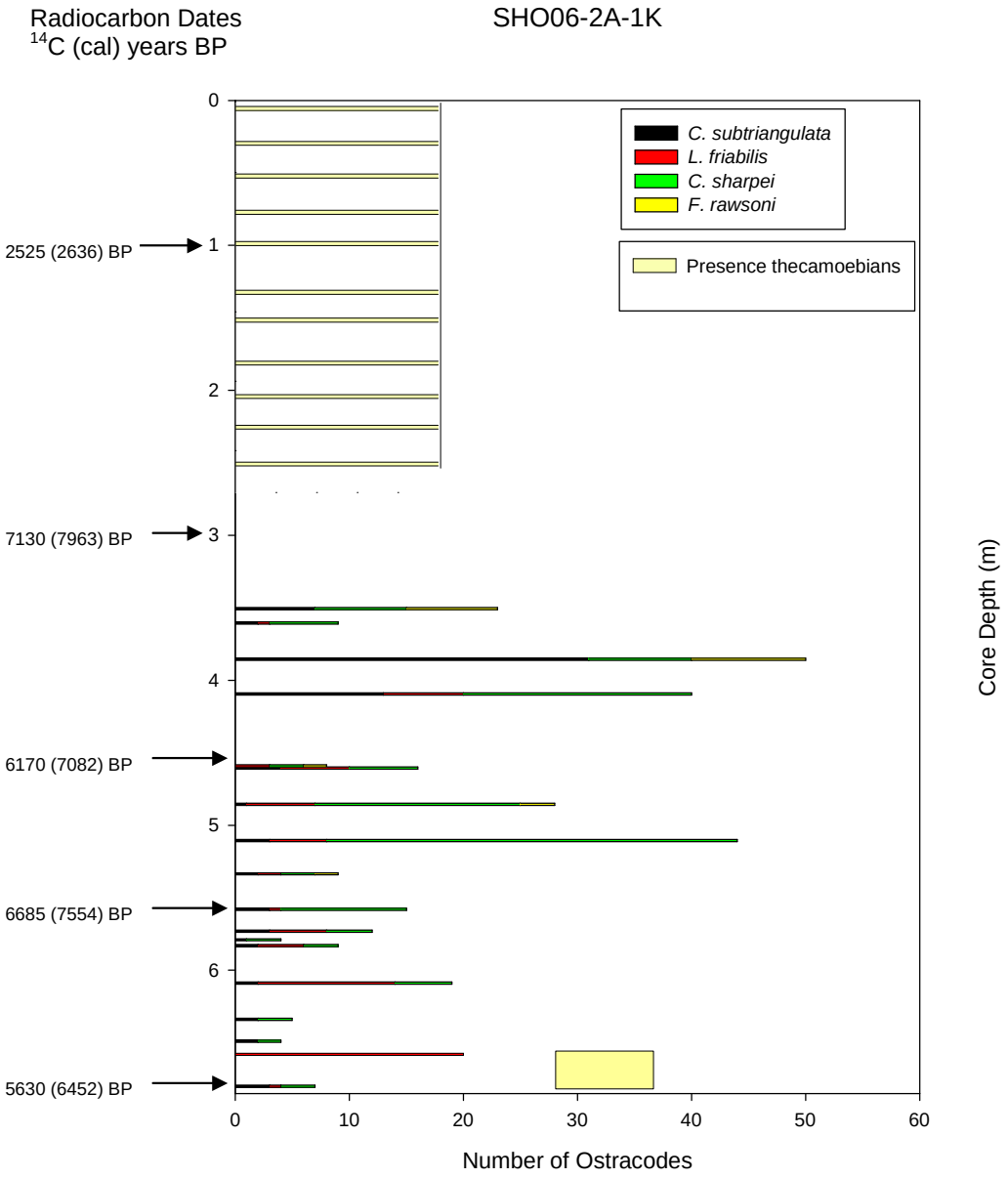

Figure 79. Radiocarbon dates for SHO06-2A-1K showing the ostracode and thecamoebian intervals. Sampled locations are the same as those in Figure 77. The yellow bars represent the presence of thecamoebians at the top of the core and their sample locations; the yellow box indicates the location of the bottom two sample intervals of the lower thecamoebian sequence. The total number of ostracodes includes all species as are reported in the details of Figure 77. All dates are from the radiocarbon analysis reports in Appendix B.

CHAPTER 5 INTERPRETATIONS OF SITE DATA

5.1 Overview

This chapter interprets the data from each individual core in order to assess the paleoconditions at each of the relatively diverse coring sites. In Chapter 6, the interpretations and data from each coring site are then integrated to provide a broader interpretation for the LOTWs and SL region. Some common characteristics became evident while interpreting the data for each coring location and are noted where appropriate, to assist in interpreting data from each coring location. These common characteristics are described in detail in Chapter 6.

5.1.1 Low Abundance and Number of Species of Ostracodes in LOTWs and SL

Only four species of ostracodes were identified in the LOTWs and SL cores, specifically, *Candona subtriangulata*, *Cyclocypris sharpei, Fabaeformiscandona rawsoni*, and *Limnocythere friabilis*. The abundance of ostracodes in the cores was relatively low in many ostracode intervals, with typical concentrations from about 10-25 shells per 15 mL sample, although many samples only had 1-3 shells. Ostracodes were not present throughout the entire length of any of the cores. They were absent in the top portions of all the cores and in most cores generally reduced in overall numbers moving upwards. The lack of modern LOTWs and SL ostracode population analogues makes it difficult to interpret paleo conditions.

The limited number of species may be related to water chemistry within LOTWs and SL. The relatively fresh waters (low TDS) of Lake Agassiz (~ 100 mg/L) (Curry, 1997) are well below the calcite branch point (Figure 33) where ostracode species richness reaches a maximum. Ostracode diversity (species present) increases with increasing TDS levels (De Deckker and Forester, 1988). There was an upwards increase in ostracode diversity in most LOTWs and SL cores (e.g. Figure 68) before the ostracodes disappear from the record. As water TDS level increases above the calcite branch point, ostracode species richness (diversity) drops, but the abundance of the remaining species usually increases as they adapt to these conditions (Smith and Horne, 2002). The low number of ostracode species and their relatively low abundance in most intervals of the LOTWs and SL sequences may reflect low salinity, and non-optimum concentrations of calcium and bicarbonate ions in the water (Smith and Horne, 2002). The specific ostracode species present reflects the available solutes in the water, and are specific to the physical lacustrine conditions at the time (Smith and Horne, 2002).

Decreases in diversity of ostracode species can also be related to decreasing organic nutrient levels and their availability (Burke, 1987), however the presence of thecamoebians in the upper portions of the LOTWs and SL cores, which increases with increasing nutrient levels (Wall et al., 2008), are generally indicative of an increase in primary productivity (movement to more eutrophic conditions). Similarly, increased plant and insect macrofossils were observed in the upper portions of the cores reflecting increases in nutrient levels. This means nutrient levels should have been favourable for

ostracodes toward the top of the core, therefore, lack of sufficient nutrients can be eliminated as a reason for the disappearance of ostracodes.

The chemical conditions in the Lake Agassiz sequence of LOTWs and SL were reflected in the TDS levels and the specific chemical components, which were further reflected by the low diversity of ostracodes in the bottom core sequences, and the dominance of *C. subtriangulata*. These chemical conditions were retained somewhat in the early phases of modern LOTWs and SL due to the input of Lake Agassiz sediments from the new LOTWs and SL watersheds. Since the LOTWs and SL remains relatively low in TDS in the modern lake, the disappearance of ostracodes was not likely caused by changes in TDS, but possibly from the low availability of calcium and bicarbonate ions. However, there may have been intervals when TDS levels fluctuated due to changes in the basin or due to climate induced effects, so some of the ostracode intervals above the basal Lake Agassiz zone may be related to fluctuations in TDS as well as Ca and HCO_3.

The LOTWs watershed slowly evolved towards the modern vegetated watershed as Lake Agassiz disconnected from LOTWs (Figure 8). The overall progression to the modern vegetated LOTWs watershed, likely affected TDS levels. Once the terrestrial terrain stabilized, inputs to the lake would trend away from the Lake Agassiz sediment inputs, and have been influenced by organic rich runoff. Variations in terrestrial conditions around LOTWs and SL, due to isostatic rebound and vegetative response would have influenced the LOTWs generally and perhaps more so at specific sites. Climate change could additionally increase solute through increased precipitation and watershed runoff,

or alternately in drier climatic intervals by increasing evaporation at the lake surface resulting in lower lake levels and increasing proportions of solutes.

Climate induced changes resulting from increases in precipitation and the increased runoff affect acidification of the lakes due to the increased levels of humic acid input and changes in buffering. These climate related changes in pH are another factor affecting ostracode populations and may lead to post diagenetic destruction of carbonate shells.

Although the water chemistry, particularly low bicarbonate levels are important to ostracodes, from the core subsample observations it was noted intervals of carbonate-bearing sediments, and the presence of gastropods and pelecypods, were found near and above the end of the ostracode intervals in the cores. Their presence above these intervals and the lack of any observed trend in damage to their shells, implies low bicarbonate levels and post mortem or post diagenic loss of shell material due to low pH, may not be the primary reasons for ostracodes disappearing from the record.

5.1.2 Radiocarbon Date Inconsistencies

A number of inconsistencies were encountered in radiocarbon dates obtained from the cores, although the dated macrofossil samples were generally consistent and provided a logical and sequential chronology in the cores. AMS radiocarbon dating of pollen was undertaken on a number of cores when limited macrofossil content was encountered in certain intervals, particularly near the bottom of the cores. Some rather large aberrations in radiocarbon dates were encountered when the pollen samples were dated, with the pollen dating from a time when the region was buried deep by the LIS (McMillan et al., 2003; Teller et al., 2008). Pollen intervals, including increased charcoal deposits in nearby WHL, were estimated to have begun from nearby watershed biota about 7.0 cal ka BP (~ 6.1 ^{14}C ka BP), well after Lake Agassiz receded from the region (Teller et al., 2008), hence local pollen should have been relatively young.

Pollen and resuspended microfossils from outside the region can be transported long distances, especially over recently deglaciated terrain with low vegetative cover, and were particularly susceptible to eolian transport including during the Younger Dryas (Birks, 2001; Curry and Yansa, 2004). Long distance transport of pollen causing discrepancies in radiocarbon dates is a well known phenomenon (Bajc et al., 2000).

Transported pollen can create circumstances where pollen and macrofossil radiocarbon dates are not in close agreement due to biasing of the sample towards older dates due to

contamination from older pollen deposits (Bajc et al., 2000), or due to incorporation of older carbon (Nambudiri et al., 1980) in the pollen samples, or in some cases transport or reworking of macrofossils. In view of this, and the possible incorporation of older fine grained carbon into pollen reworked from older sediments (Nambudiri et al., 1980), all the pollen dates were rejected based on their anomalously old ages.

Terrestrial plant macrofossil radiocarbon dates are often considered more reliable than pollen especially if the pollen is degraded (Curry and Yansa, 2004), and more reliable than aquatic macrofossils which can be subject to the hardwater effect. However, in LOTWs, one macrofossil date on a wood fragment (WOO06-5A-1K5 at 37.5 cm) was noted to have been much older than the others and was dated at 15.6 ^{14}C ka BP (18.8 cal ka BP) (Appendix B, Section 2). In this core the abnormally old wood fragment macrofossil is located between two older pollen samples dated at 17.040 ^{14}C ka BP (20.386 cal ka BP) and 17.560 ^{14}C ka BP (20.970 cal ka BP), implying it may have eroded from older sediments and/or had been transported into the region. This radiocarbon date was also rejected.

The macrofossils selected for dating were examined using an optical microscope during processing of the subsamples, or by Paleotec Services during selection of suitable organic materials from additional subsamples (i.e. their appendages were relatively intact). Paleotec Services rejected any macrofossils that indicated they may have been transported, before sending them to the Keck Carbon Cycle AMS Facility for radiocarbon dating. Nonetheless, the possibility exists some macrofossils may have been reworked

from lower (older) Wisconsinian deposits (such as the WOO06-5A-1K5 sample at 37.5 cm), since Wisconsinian deposits have been reported to be close to the surface (< 10 m) in south eastern Manitoba (Matile, 2001), or at the surface due to Lake Agassiz wave actions in regions to the east of the Red River Lowlands (Fenton and Teller, 1980).

Other than the rejected WOO06-5A-1K5 sample radiocarbon dated at 37.5 cm, other macrofossil dates were reasonable and were accepted.

5.2 Coring Site Interpretations General

The interpretation of the individual LOTWs and SL cores provides the means to track paleohydrologic and paleoecologic conditions. However, differential isostatic rebound must also be considered to help in understanding the changing conditions at the coring sites. Seven of the ten cores recovered from LOTWs and SL were examined and subsampled. These cores are the basis for the interpretations of the paleoecological, paleoclimatic and paleohydrological conditions noted in the following sections.

The WOO06-3A-1K core was determined to have deflected sideways and only very limited data was extracted from this core, although its shallower companion core WOO06-4A-1K has provided data suitable for interpretation. The stratigraphic data and the scanned image and core description presented in Chapter 4 are complemented by the data provided in Appendix A for each core. The following paleoecologic and paleohydrologic interpretations are based on those data.

5.2.1 South Basin Site - WOO06-1A

Differential isostatic rebound in this portion of the lake over the interval since LOTWs separated from Lake Agassiz, resulted in the southern basin initially loosing its water (Figure 9). Subsequently, the lake transgressed southward from the northern region near Kenora (Figure 10). The elevation of the northern outlets to the Winnipeg River ultimately controlled the bathymetry of the southern basin. Differential isostatic rebound over time resulted in the northern outlet rising farther above the southern basin elevation, ponding additional water in the large southern basin, and creating a transgression of LOTWs to the south.

The southward transgression into the southern basin would have resulted result in reworking of Lake Agassiz and glacial deposits. This, and the close proximity of the sediment influx from the Rainy River, would likely increase the quantity of lithics in this portion of the LOTWs. The slowly increasing water depths in the south and the proximity to the inflowing Rainy River, would likely result in a unique paleoecology in the southern basin coring site locations, which are about 40 km farther south of the North West Angle area sites, and 90 km farther south of the Kenora outlets. It was anticipated that Lake Agassiz deposits would not be encountered at the WOO06-1A-1K site, however, there is contrary evidence based on the ostracode species identified (Figure 40). In this area, an unconformity likely overlies the Lake Agassiz deposits, as a result of the

southward transgression of LOTWs and reworking of the sediments. This may account for the appearance of the Lake Agassiz type ostracodes (Figure 43) in this core. Alternately, the nearby Rainy River entrance into the southern basin may have created localized compartments of deeper water or deep channels, as the water ponded in the area and supported biota characteristic of Lake Agassiz.

5.2.1.1 **Ostracodes**

The exclusive *C. subtriangulata* interval at the bottom of the core, with a later co-occurrence of *L. friabilis*, implies these sediments were deposited in deep, cold and low salinity (TDS) waters such as those in Lake Agassiz. The later occurrence of *F. rawsoni* implies a transition to higher salinities was underway just before the ostracode record ends. The increase to three species in the core near 2.8 m is an additional indicator of increasing but still relatively low salinity. The presence of carbonate coated shells of all species implies there was sufficient carbonate in the sediments, however thin shells in other nearby intervals may imply these conditions were not consistent. The rapid decrease in ostracode numbers above ~ 2.7 m, without a preceding trend in shell thinning and fragmentation in response to changing environmental conditions may mean a rapid change in paleochemistry may have occurred. This either made the hydrochemistry unsuitable for shell formation, or resulted in dissolution of the shells on the lake floor or within the sediments, which then continued from this point to the top of the core. Alternately, or in conjunction with changing hydrochemistry, a change in food supply may have resulted in the apparent population crash and subsequent end of ostracodes in

LOTWs. A rapid drop in relative abundance of plant materials occurs above ~2.6 m (Figure 43), with a continued low insect proportion, and may be an indication the available food supply became limited, stressing the ostracode population. Interestingly, the first occurrence of thecamoebians occurs at about 1.5 m, and the abundance of plant macrofossils increases, followed by higher abundance of insect macrofossils, indicating the availability of food likely increased at this time. Similarly the increase in plant and insect macrofossils indicates increased lake productivity, supporting changes to more eutrophic conditions as the reason for the increase of thecamoebians in the upper core. The reason for the disappearance of ostracodes therefore is not likely to be the unavailability of food supply.

The ostracode interval identified in the bottom of the core (Figure 40) includes a radiocarbon date of 7.14 ^{14}C ka BP (~ 8.0 cal ka BP) at 3.3 m, with the ostracodes appearing to be a typical Lake Agassiz sequence of ostracodes with an exclusive *C. subtriangulata* interval at the bottom, similar to those observed in the more northerly cores. However, the two radiocarbon dates near the bottom of the core are well after the estimated date Lake Agassiz isolated from LOTWs. An interval further upwards dates to 7.375 ^{14}C ka BP (~ 8.2 cal ka BP) implying this older date above the younger date may be from reworked materials, even though bristles on the dated *Polygonum lapathifolium* seed were intact (Appendix B, Section 2, Table B-1, South Basin Site - WOO06-1A), implying reworking was minimal. Macrofossils in nearby core intervals similarly imply reworking was not significant. Since it is unclear which date is correct, the average of these dates, 7.26 ^{14}C ka BP (8.05 cal ka BP), is used to estimate the end of the ostracode

interval. Nonetheless, both dates are after the date estimated by Yang and Teller for isolation from Lake Agassiz (8.1 ^{14}C ka BP (9.0 cal ka BP)) and do not correspond with the estimated calculated elevation from the paleotopographic maps (Yang and Teller, 2005), which indicate this portion of LOTWs should have been dry at this time (Figure 9).

The ostracode sequence changes to a more mixed population including *L. friabilis* and *F. rawsoni* at about 3.0 to 2.7 m, with ostracode shells disappearing completely at 2.7 m, near the radiocarbon dated sample at 2.9 m, dated at 7.375 ^{14}C ka BP (~ 8.2 cal ka BP). One *C. subtriangulata* shell fragment appears above this point at 2.2 m, which may imply reworking, however, an articulated claw on a bone in this interval, indicates reworking is unlikely.

As noted in Section 5.2.1, there is a strong possibility the sediments in the southern basin were reworked. The ostracode sequence from the cold, deep and low salinity ostracodes species of *C. subtriangulata* and *L. friabilis* evolves upward to the more salinity- tolerant *F. rawsoni*, and is a logical sequence for the hydrochemical evolution of the lake once it became independent from Lake Agassiz. The presence of sub-adult instars in this interval implies the sequence probably was not unduly reworked. Fragmented shells could be an indication some reworking occurred, however, an articulated ostracode shell at 3.0 m and the articulated claw on a bone at 2.2 m, are evidence that reworking in these intervals did not occur or was limited.

Based on the ostracode sequence observed, cold water conditions like that of Lake Agassiz, appear to have existed in the southern basin around 7.3 ^{14}C ka BP (8.1 cal ka BP). Based on the estimated extent of LOTWs and Lake Agassiz by Yang and Teller (2005), and the timing of the isolation of LOTWs from Lake Agassiz this suggests deep compartments existed at this location in the southern basin.

5.2.1.2 **Thecamoebians**

The locations where thecamoebians are present are identified in Figure 41 and detailed thecamoebian observations can be found in Appendix A, Subsection 1.2. Thecamoebians first appear at 1.4 m, corresponding with a high proportion of plant material and generally high abundance of insect macrofossils, suggesting productive lake conditions existed at this time. A radiocarbon date at 1.37 m indicates this first appearance of thecamoebians and the change to more eutrophic conditions at this location occurred at about 1.685 ^{14}C ka BP (1.579 cal ka BP). This is the youngest date for the appearance of thecamoebians in all processed cores (see Chapter 6).

Numerous species of thecamoebians were observed with up to five noted in some intervals (Appendix A, Subsection 1.2), indicating an abundance of food was likely available in this interval. Thecamoebian species including *Difflugia oblonga* and *Centropyxis aculeate* which have been associated with warmer and cooler conditions respectively, indicate thecamoebians may be responding to a changing climate.

5.2.1.3 **Other Macrofossils**

Abundant charcoal in the lower portion of the core and high abundance of plant materials were observed in what would appear to be Lake Agassiz intervals based on the ostracode record. High charcoal and plant abundances in a Lake Agassiz sequence are not typical. This may be an indicator of reworking, but the charcoal does not appear to have been transported based on the many fine fragile looking structures present in the fragments. Numerous mammal molars, an incisor, a claw attached to a bone, and vertebrae were found in the interval from 2.3 to 1.8 m. This is below the thecamoebian zone which was interpreted to be the start of more eutrophic conditions, and about 0.5 m above the end of the ostracode interval. The terrestrial vertebrate macrofossils and presence of terrestrial plant macrofossils are possible indicators of near shore conditions, the articulated claw and bone imply relatively low energy conditions and limited reworking appears to have occurred in this interval. It is possible this interval is either terrestrial, or in a swampy location with the low energy condition implying a swamp-like condition may have existed at this time.

5.2.1.4 **Lithic Grains**

Figure 41 indicates the abundance of lithic grains in the sequence and indicates those locations where carbonate grains were detected. Detailed observations of these lithic grains including presence of clay balls are included in Appendix A, Subsection 1.2. A low volume but high relative abundance of lithic grains is present in the subsamples near the bottom of the core, from 3.3 to 2.2 m. This is similar to Lake Agassiz sequences

observed in the other cores (see Chapter 6). Upward in the core, higher volumes of primarily quartz lithics occur in the subsamples and the abundance of lithics remains high up to 1.1 m. This could possibly be an indication of reworked shorelines as LOTWs transgressed southward, although most organic macrofossils in these intervals do not look to have been transported (Appendix A, Subsection 1.2).

Above 2.0 m, well above the main sequence of ostracodes and about 20 cm above the interval where a single ostracode shell was noted, carbonate lithics were no longer identified. This may indicate a time when a significant hydrological change possibly occurred in this portion of the lake, perhaps due to changes in the drainage basin of the lake, or a time of hydrological/hydrochemical changes. The presence of carbonates corresponds with the intervals where coated ostracode shells were noted, and also includes the 70 cm interval above the ostracode interval. It is possible this may indicate a change to more acidic conditions may have occurred, preventing ostracode shells that may have formed from being preserved with post depositional leaching and destruction of ostracode shells on the lake floor and within the upper sedimentary sequence occurring (Teller, 2009, personal communication).

Lithics were consistently the highest relative proportion of the sieved materials in the lower part of the sequence until about 1.4 m, when conditions in the lake became more productive (Figure 41), as indicated by the increasing macrofossil content including thecamoebians. Maximum lithics sizes were around 4 mm throughout the core decreasing somewhat in the uppermost metre of the core to 2-3 mm. This would be

expected as the initial transgression period probably would have reworked more sediment from the underlying surface.

5.2.1.5 **Sedimentation Rates**

The radiocarbon dates in the core provide the means to estimate sedimentation rates. As discussed previously there are some aberrant dates and these are not included in the sediment rate calculations. The two lower core dates were averaged when the sedimentation rates were estimated. Assuming no losses from the top of the core during recovery, produces an overall sedimentation rate of 0.4 mm/yr [3.0 m / (8228+7973 cal yrs at 3.0 m) / 2) = 0.38 mm/cal yr].

The two upper core radiocarbon dates are in sequence, with the lower date of 1.675 ^{14}C ka BP (1.579 cal ka BP) defining the beginning of the thecamoebian sequence at about 1.4 m. The uppermost radiocarbon date of 1.460 ^{14}C ka BP (1.358 cal ka BP) at about 0.9 m, in conjunction with the lower date, imply two sedimentation rates may have been in effect in the upper part of the core, or some material may have been lost from the top part of the core during recovery.

A sedimentation rate in the top 1.37 m of the core is estimated to be 0.9 mm/yr [(1.37 m / (1579-0) yrs = 0.87 mm/cal yr]. This sedimentation rate corresponds well with modern rates reported by Molot (Molot et al., 1987) of 0.7 mm/yr. In contrast a low overall sedimentation rate of 0.25 mm/yr was observed in the much smaller West Hawk Lake

(Teller et al., 2008) in the 10,000 year period after isolation from Lake Agassiz. This sedimentation rate is consistent with those identified in the Experimental Lakes Area (ELA) since about 8.2 cal ka BP (7.3 ^{14}C ka BP) (Laird and Cumming, 2008). Laird and Cumming reported sedimentation rates as being relatively consistent and based on data from the paper the rate appears to be about 0.16mm/yr over the entire length of the core (ignoring compaction).

In the interval between the upper and lower portions of the core, the sedimentation rate is 0.3 mm/yr [(3.0-1.37 m) / ((8228+7973 yrs) / 2)-1579 yrs) = 0.25 mm/yr]. This sedimentation rate in the intermediate interval of the core is close to those reported others in the LOTWs region.

5.2.1.6 **Discussion and Interpretation of Coring Site Data**

There are a number of conflicting interpretations possible from the data from this core. Initially, based on ostracode sequences, it appears this core extended into Lake Agassiz sediments. However, there are unusually large proportions of charcoal compared to Lake Agassiz sequences in other cores. Perhaps the charcoal is from encroachment of post glacial forests in the region from the south which washed into LOTWs through the Rainy River after Lake Agassiz drained from this area. Mid-core intervals containing terrestrial vertebrate molars and other skeletal components, are noteworthy (Appendix A, Subsection 1.2). Perhaps they indicate a lake had formed in this location of the southern basin, and this coring site was near shore or close to swampy area as discussed earlier.

The uncharacteristically high lithics volume and increased abundance when compared to other cores (see Chapter 6) in the mid-core intervals, and the plant and larger charcoal fragments, including seeds near the bottom of the core in what appears to be a possible Lake Agassiz sequence (Figure 43), are problematic. Based on the other cores, Lake Agassiz sequences typically have low lithics volumes (although a high relative abundance compared to other materials). The lithics volume in this core may be indicative of shoreline erosion, due the subsequent differential isostatic rebound induced southward transgression. The two dates from the lower core indicate the sediments were deposited well after the LOTWs and Lake Agassiz isolation, despite the presence of the deep and cold water C. subtriangulata ostracode. Furthermore, the lowermost radiocarbon dates place the associated sediments in an interval where lacustrine conditions should not have existed in this area (Figure 10). This leads to the possible interpretation of these apparently conflicting data that this part of the LOTWs basin contained small lakes, disconnected from the main body of LOTWs that formed after Lake Agassiz fell below the level of the lake floor.

The sedimentation rate estimates do show some significant changes and the overall sedimentation rate is relatively high at about 0.4 mm/yr, which is about twice the rates from the lake 239 of the ELA, and most of the other cores (see Chapter 6). The upper core sedimentation rate of 0.9 mm/yr is closer to those reported by Molot, but compared to other LOTWs coring sites, it is very high (Molot et al,. 1987).

The relatively high sedimentation rate calculated for the top of the core is of course partially due to less dewatering in the upper core and hence less compaction. The sedimentation rate in the middle core region of about 0.3 mm/yr is close to the overall sedimentation rate and closely reflects the observed ELA and WHL rates, although these lakes are in substantially different watersheds. There is no reliable means to estimate the lower core sedimentation rate with the available radiocarbon dates.

There is some variability in the stratigraphy within the core, with the lower ~ 1.7 m distinctly laminated. A sharp contact at ~ 2.8 m separates a lower moisture interval below with a distinct colour change at this point, from dark grey below, to a dark grey-brown interval above. This point is at the end of the ostracode interval (Figure 40). In view of the distinct contact it is possible that this may be an erosional surface on which a weak soil may have developed (Figure 39). Since the Rainy River inflow is nearby, some of the coarser grains and organics may have been brought into this portion of LOTWs.

The question remains, are the sediments near the bottom of the core either Lake Agassiz or near Lake Agassiz sediments? The ostracode sequence, especially the presence of *C. subtriangulata* and *L. friabilis* indicate that deep, cold, and low TDS paleohydrological conditions existed at least until about 7.3 ^{14}C ka BP (~ 8.1 cal ka BP) at around 3 m (from the averaged two lower dates), shortly above which the ostracode interval ended. The radiocarbon dates however are much later than the estimated separation of LOTWs from Lake Agassiz, and furthermore, this part of the lake should have been dry land according to the paleotopographical data (Figure 9 and Figure 10) from Yang and Teller, 2005. It is

unclear why deep and cold water would have existed at the time the radiocarbon dates suggest, although the dates do appear to be at the beginning of the Hypsithermal possibly prior to the onset of warmer and drier conditions in the region. One possible interpretation is that the inflowing cold Rainy River water flowed into a deep sub-basin within the generally dry southern basin at this coring location.

This independent lake within the southern basin would have remained independent until isostatic rebound caused the main lake to transgress into the southern basin. If this were the case this location would have had a distinctly different history and paleoenvironment than the deep basins to the north, and would have been strongly influenced by the inflowing Rainy River just to the east.

The onset in increased more eutrophic conditions occurred at about 1.685 ^{14}C ka BP (1.579 cal ka BP), with the appearance of thecamoebians above at about 1.4 m. Multiple thecamoebian species are evident throughout most of this part of the sequence, included *D. oblonga* and *C. aculeate*. The appearance of thecamoebians corresponds with increasing plant and insect macrofossils (Figure 41), supporting the interpretation that the appearance of thecamoebians correspond with the onset of more eutrophic conditions in this part of the southern basin.

Summary

The ostracode populations only occur in the bottom portion of the core and they reflect deep, cold, and low TDS conditions typical of Lake Agassiz based on the presence of both *C. subtriangulata* and *L. friabilis*. The radiocarbon dates of 7.140 ^{14}C ka BP (7.973 cal ka BP) and 7.375 ^{14}C ka BP (8.228 cal ka BP) near the bottom of the core are too young however, for these to be Lake Agassiz sediments, so this part of the sequence is interpreted to have been deposited in this location after Lake Agassiz drained from this area about 9-10 cal ka BP. The ostracode species imply there may have been a deep cold compartment in this area, which then trended to more saline conditions during the Hypsithermal.

There is conflicting evidence with respect to reworking of the sediments of the core (Appendix A, Subsection 1.2), making interpretation of paleoconditions challenging. However, a low moisture zone (Figure 39 and Figure 42) at the top of the ostracode bearing sequence at about 2.8 m, suggests that the southern basin may have become dry sometime after about 7 ^{14}C ka BP (~ 7.8 cal ka BP). There is evidence of an erosional surface at 2.8 m and a potential paleosol above. The mid-core sediments above this interval up to the beginning of thecamoebians appear to reflect a nearby low energy shoreline or swampy area existed near this site. The possibility of an erosional surface at the top of the ostracode interval may mean the ostracode bearing sediments were reworked, affecting the ostracode signal and the associated radiocarbon dates which were not sequenced chronologically.

An increase in lake productivity is estimated at 1.685 ^{14}C ka BP (1.579 cal ka), at a point where plant abundance in the lake increases, insect materials increase, and where thecamoebians became part of the record. These data all seem to reflect higher nutrient conditions were established at this time, and have continued to today.

5.3.1 Northwest Angle Site - WOO06-3A

The WOO06-3A-1K coring site is located near an intermediate point in the lake which would have been subject to the long term southward transgression from the more rapidly rebounding northern part of the lake, and would have provided the pathway to the northern outlets from the northward flow of draining waters from the Rainy River watershed and southern basin watershed inflows (Figure 10). The draining of this excess water northward to the Winnipeg River would be through relatively narrow channels in this portion of LOTWs (Figure 24). The Northwest Angle sites are located to the east of a large emerging island within Lake Agassiz (Figure 8) which resulted in a topographic high after separation of Lake Agassiz (Figure 9).

5.3.1.1 **Ostracodes**

No ostracodes were observed in this core.

5.3.1.2 **Thecamoebians**

The uncertainties introduced by the deflection of the core make interpretation of thecamoebian data from this core impossible.

5.3.1.3 **Other Macrofossils**

The uncertainties introduced by the deflection of the core make interpretation of macrofossil data from this core impossible.

5.3.1.4 **Lithic Grains**

Intervals of abundant granitic and quartz lithics were observed throughout the core; however, the uncertainties introduced by the deflection of the core make interpretation of lithic grain data from this core impossible.

5.3.1.5 **Sedimentation Rates**

The uncertainties introduced by the deflection of the core make interpretation data from this core impossible.

5.3.1.6 **Core Chronology**

Only one radiocarbon sample was sent for analysis and it indicated an unusually young radiocarbon date at ~ 7.3 m near the bottom of this 7.47 m core, of 2.915 ^{14}C ka BP (3.070 cal ka BP) (Appendix B, Section 2, Table B-1, NWA - Channel Site WOO06-3A). Establishing a core chronology based on this single radiocarbon date, especially considering the deflection of the core, is not possible.

5.3.1.7 **Discussion and Interpretation of Coring Site Data**

The unusually young date of 2.915 ^{14}C ka BP (3.070 cal ka BP) at about 7.3 m, indicates the WOO06-3A-1K core did not maintain a vertical orientation in the sediments and was significantly deflected when it encountered a hard substrate during its penetration of the sediments. The interpretation that the core underwent a significant deflection is further supported by the processed subsample results. By combining the unusually young date near the bottom of this long core, the observations of thecamoebians at the bottom of the core and their long hiatus from ~ 7 to 1.4 m, and the absence of any ostracodes in the core, it is evident the core barrel had deflected significantly from the vertical. This would also explain the significant difficulty in recovering the core from the sediments to the Kullenberg platform during the core recovery operation.

5.4.1 Northwest Angle Site - WOO06-4A

The WOO06-4A-1K coring site is located near an intermediate point in the lake which would have been subject to the long term southward transgression from the more rapidly rebounding northern part of the lake, and would have provided the pathway to the northern outlets from the northward flow of any water draining from the Rainy River watershed and southern basin watershed inflows (Figure 10). The draining of this excess water northward to the Winnipeg River would be through relatively narrow channels in this portion of LOTWs (Figure 24). The Northwest Angle sites are located to the east of a large emerging island within Lake Agassiz (Figure 8) which resulted in a topographic high after separation of Lake Agassiz (Figure 9).

This LOTWs location is relatively unique in that it is located in a relatively deep narrow channel and would likely have been subject to currents throughout most of its history. It was anticipated sediments in the channel may have differed somewhat from the open basin and that a different paleoenvironment may have prevailed. There is evidence of an indistinct paleosol development (Figure 45) containing pedogenic blocky structures in the sediments of this site and the sediments contain considerable organic accumulations, including evidence of near shore conditions (Appendix A, Subsection 2.2).

This core is the shortest of all cores (about 2 m) however, despite this limited penetration it appears Lake Agassiz sediments may have been encountered. Subsamples from the

bottom of the core have a high relative proportion of lithics, appear relatively barren with low plant and insect contents, and include *C. subtriangulata* ostracodes.

5.4.1.1 **Ostracodes**

Only the *C. subtriangulata* ostracode is found in this core which implies these sediments were deposited in deep, cold, and low salinity (TDS) waters, such as those in Lake Agassiz. The ostracode interval in this core ends about 0.2 m above the bottom of the core at about 1.8 m. The nearby radiocarbon date of 7.655 ^{14}C ka BP (8.443 cal ka BP) from bulrush achenes (*Scirpus validus*), at 1.5 m can be extrapolated downwards to 1.8 m based on a rough estimate of the overall sedimentation rate of 0.23 mm/cal yr (see Section 5.4.1.6). This rough estimate places the end of the ostracode interval in this core at about 8.8 ^{14}C ka BP (9.8 cal years BP) [0.23 mm/yr X (1800 -1500 mm + 8443 = 9747 cal years BP or ~ 8.8 ^{14}C ka BP]. It is important to note this is a very rough estimate as sedimentation rates below the paleosol are not know due to the lack of two available radiocarbon dates below the paleosol, nonetheless it places the end of ostracodes into a Lake Agassiz interval and corresponds reasonably well with the isostatic rebound calculations of Yang and Teller. The presence of the *C. subtriangulata* ostracode species, in conjunction with the high quartz lithics component, and low plant, insect, and charcoal macrofossils, further supports the conclusion the bottom sediments in this core are from Lake Agassiz.

5.4.1.2 **Thecamoebians**

In the first of two thecamoebian intervals in the core at about 0.77 m, two species of thecamoebians were identified. They appear between two lower radiocarbon dated intervals at 0.74 m (6.330 ^{14}C ka BP (7.319 cal ka BP)) and 0.92 m (6.955 ^{14}C ka BP (7.787 cal ka BP)), and therefore, assuming a constant sedimentation rate, the date of first appearance of thecamoebians can be estimated at 6.5 ^{14}C ka BP (7.4 cal ka BP) [(0.77-0.74 m) / (0.92-0.74 m) X (6955-6370 ^{14}C yrs) + 6370 ^{14}C BP = 6.468 ^{14}C ka BP]. This date is the earliest date for the presence of thecamoebians found in the examined LOTWs cores in this area of LOTWs (see Chapter 6), and indicated an early more eutrophic interval in this channel location. This thecamoebian zone is within intervals with abundant large plant and charcoal fragments (Figure 47) (Appendix A, Subsection 2.2).

The second thecamoebian interval at 0.31 m follows a thecamoebian hiatus, and contains four species possibly indicating more eutrophic conditions. The date for this uppermost interval assuming a constant sedimentation rate and using the nearest radiocarbon dated intervals is 3.8 ka BP (4.2 cal ka BP) [(0.31-0.08 m) / (0.74-0.08) X (6370-2495 ^{14}C yrs) + 2495 = 3.845 ^{14}C yrs], which still predates most of the other thecamoebian intervals (see Chapter 6, Table 3). The uppermost appearance of thecamoebians occurs within a zone of high plant and insect macrofossils, and charcoal fragments, which supports the interpretation that the upper portion of the core was productive and hence more eutrophic since about 3.8 ka BP (4.2 cal ka BP).

5.4.1.3 **Other Macrofossils**

Significant changes in environmental conditions are evident in the macrofossil data from this site (Figure 47). The occurrence of fish vertebrae and scales between 0.6 to 0.3 m in the thecamoebian hiatus, and high abundance of plant and charcoal macrofossils, and increased insects material, upward from the black organic rich interval at about 1.5 m, are evidence of these changes (Appendix A, Subsection 2.2). These changes in environmental conditions across the black bed are clearly reflected in Figure 45.

A gradational lower boundary and a sharp boundary at the top of the 5 cm thick distinct black interval, marks the beginning of a transition from a low organic material interval below this point, to a zone of abundant plant and seed macrofossils, and large charcoal fragments within and above this interval. This black organic interval includes an abundance of seeds of terrestrial and near shore plants, such as curlytop knotweed (*Polygonum lapathifolium*) and bulrush (*Scirpus validus*) (Appendix B, Section 4, Figures B-2, B-3 and B-4) and also *Scirpus validus*. These organic rich sediments include insect macrofossils and abundant large charcoal fragments, and are consistent with a near shore paleoenvironment, which reflects the modern configuration of this narrow channel.

5.4.1.4 **Lithic Grains**

Figure 47 indicates the changes in the abundance of lithics within the core, and indicates those subsamples where carbonate lithics were detected. Abundant quartz and mica, and carbonate lithics, in the bottom ~ 0.4 m of the core are similar to the Lake Agassiz sequences observed in the other cores. High abundances of lithic grains including clay balls occur below the distinct black boundary (Figure 45), and are present in conjunction with carbonate lithics and ostracodes. These data appear to be consistent with Lake Agassiz or near Lake Agassiz sediments. The available radiocarbon date confirms these sediments were deposited close to the time estimated for separation of Lake Agassiz from LOTWs. The dramatic appearance of the black organic rich sediments indicates a significant change in the paleoenvironments after the lowermost lithic deposits were laid down.

5.4.1.5 **Core Chronology**

All radiocarbon dates in this core are in chronological sequence (Figure 48) however, the uppermost radiocarbon date of 2.495 ^{14}C ka BP (2.604 cal ka BP) is very near the top of the recovered core at 0.08 m. The closeness of the uppermost radiocarbon dated sample to the top of the core, and its relatively old date, indicates some material was likely lost from the top of the core. The lowermost date of 7.655 ^{14}C ka BP (8.443 cal ka BP) using a *Scirpus validus* (bulrush) seed implies this channel was vegetated shortly after Lake Agassiz withdrew from the region. The two radiocarbon dated samples at 0.74 and 0.92

m of 6.370 ^{14}C ka BP (7.319 cal ka BP) and 6.955 ^{14}C ka BP (7.786 cal ka BP) respectively, were obtained from an interval containing terrestrial plant components such as leaves, stems and seeds, and a near pedogenic sediment (Figure 45). These dates establish the chronology for an interval where this site may have been subject to climate induced changes during a relatively dry interval in the Hypsithermal.

5.4.1.6 **Sedimentation Rates**

Lost material from the top of the core (based on the relatively old radiocarbon date at the top) limits the ability to estimate sedimentation rates in this core. The muck core was also lost at this site. Nonetheless, the overall sedimentation rate was estimated based on the dates from close to the bottom at 1.5 m (7.655 ^{14}C ka BP (8.443 cal ka BP)) and the uppermost radiocarbon date near the top of the recovered core (Figure 48), and is estimated to be about 0.2 mm/yr [(1.5 - .08 m) / (8433 - 2604 cal yrs) = 0.23 mm/yr)]. The rate from the lower mid-core date (6.955 ^{14}C ka BP (7.786 cal ka BP)) to the lowest mid-core date is about 0.9 mm/yr [(1.5 - .92 m) / (8443 - 7786 yrs) = 0.88 mm/yr]. The rate from the upper mid-core date (6.370 ^{14}C ka BP (7.319 cal ka BP)) to the uppermost radiocarbon date near the top of the core date is about 0.1 mm/yr [(.74 -. 08 m) / (7319 - 2604 cal yrs) = 0.14 mm/yr].

The estimated 0.1 mm/yr sedimentation rate in the upper portion of the core is consistent with the overall relatively low sedimentation rate of 0.2 mm/yr, however is much lower than the LOTWs sedimentation rate of 0.7 mm/yr (Molot et al., 1987) and some of those

observed in other cores (see Chapter 6). The loss of material from the top of the core made it necessary to estimate the uppermost sedimentation rate by assuming the rate is similar to the rate from the upper mid-core radiocarbon date to the available upper core date. The higher rate in the mid-core region above the black organic rich bed at 1.5 m, of 0.9 mm/yr, is possibly related to the withdrawal of Lake Agassiz and a change to the arid Hypsithermal climate conditions which caused the channel to shallow. This may have created a higher sedimentation rate than average across the core in this interval.

5.4.1.7 **Discussion and Interpretation of Coring Site Data**

The *C. subtriangulata* ostracode species in the lowermost part of the core interval and lack of any other ostracode species, implies the cold, deep and low TDS conditions of Lake Agassiz existed in the bottom portion of the core. The *C. subtriangulata* ostracodes, high relative proportion of quartz lithics, and presence of carbonates, all imply Lake Agassiz conditions prevailed at the bottom of this core. The available radiocarbon date of 7.655 ^{14}C ka BP (8.443 cal ka BP) confirms the bottom of the core is likely within the Lake Agassiz sequence (Figure 48). The disappearance of ostracodes roughly estimated at 8.8 ^{14}C ka BP (9.8 cal years BP) appears to be close to the time when LOTWs became isolated from Lake Agassiz.

The observed change of lithology at the black organic rich bed at a sharp contact just below 1.5 m (Figure 45) indicates a dramatic change in conditions above this interval. Perhaps this contact marks the time when isostatic rebound and possibly a dry climate

markedly changed the environment within this channel completing the transition from a Lake Agassiz dominated paleoenvironment, to a LOTWs influenced environment. A drop in moisture content was also noted below 1.5 m. It is also possible the sharp upper contact of organic materials may be indicative of a localized shallow fluvial deposit within the channel creating an unconformity. Both possibilities indicate a fundamental change occurred about this time.

The unit above the black organic rich bed to about 0.8 m which is dated at 6.955 ^{14}C ka BP (7.786 cal ka BP), ranges from well laminated to poorly laminated, with a fine angular blocky pedogenic like layer at the top of the interval (Figure 45). The inclusion of two distinct black beds above the black organic bed at 1.5 m, and other smaller ones within this sedimentary unit, imply a shallowing near shore environment, with blocky structures indicating a near paleosol condition down to about 1.3 m. The processed subsamples (Appendix A, Subsection 2.2) confirm the observations in the core descriptions, with abundant plant and charcoal fragment intervals prevalent throughout the unit, and with clay balls and ball fragments near the top at about 0.8 m.

Although there are variations in the observed lithology in the core above 1.5 m, the processed samples have a limited variability except at about 0.74 m, where carbonate lithics reappear and then disappear above (Figure 47). The abundance of insect material drops at this interval, and the processed subsample is primarily a mat of plant materials, including seeds and large charcoal fragments, which are continuous from the black organic rich bed to this point. The pedogenic structures and large volumes of organics

imply a paleosol and/or terrestrial conditions occur from the black bed to just below 0.77 m, which is dated at 6.370 ^{14}C ka BP (7.319 cal ka BP). The first thecamoebians appear at 0.77 m indicating a change in the environment in the channel at this point, and then they disappear as they undergo a hiatus above to 0.31 m.

The pedogenic and near pedogenic lithology and terrestrial conditions, likely indicate arid Hypsithermal paleoenvironmental conditions. Two dated samples, one dated at 6.370 ^{14}C ka BP (7.319 cal ka BP) at 0.74 m, and the other at 6.955 ^{14}C ka BP (7.786 cal ka BP) at 0.92 m, were obtained from this pedogenic/terrestrial interval providing times when these dry climatic conditions occurred. The thecamoebians indicate local eutrophic conditions likely occurred within this channel perhaps as a result of reduced flows in the channel due to dry conditions.

The reduction of overall volume of organic and large charcoal components in the processed samples above 0.74 m and the thinly laminated interval above, which grade to non-laminated at the boundary of the uppermost gyttja unit at 0.08 m, are likely in response to increasing water depth. The presence of fish vertebrae and scales in the uppermost portions of the core similarly may indicate increasing depth. The effects of differential isostatic rebound may have slowly deepened the waters within the channel as a result of the transgression, in conjunction with increased precipitation as the climate eventually became less arid post Hypsithermal. The re-occurrence of multiple types of thecamoebians near the top of the core may signal increased eutrophic conditions that are

prevalent within the LOTWs in the uppermost portions of all examined cores, including the nearby cores in the open basin near the Northwest Angle (see Chapter 6).

The large amount of organic material and abundant charcoal at 1.5 m at the black organic rich bed, suggest a period of shallow water conditions, or terrestrial conditions. The abundant large charcoal fragments in this unit, implies the region was arid and fires were nearby, similar to the other Northwest Angle sites. The fluvial conditions within this channel in LOTWs may have resulted in higher concentrations of large charcoal deposits at this site, as charcoal materials were transported by wind and wave action into this channel from the dry basin sites of the Northwest Angle at this time. These materials may have been amplified by shedding of materials from the large Lake Agassiz island and subsequent highlands to the west (Figure 8 and Figure 9). This influx of materials may be recorded as the black organic rich bed.

Dramatic increases in insect macrofossils at 0.74 m, above the last paleosol interval were noted. These occurred just prior to the increased thecamoebian interval and the subsequent drop in the insect component. This is similar to characteristics in both of the Northwest Angle basin sites (discussed in Chapter 6). There appears to be an increase in productivity in this part of the LOTWs, based on the plant and insect materials and thecamoebian signals.

The short sediment length in this core (~ 1.5 m) from the top of the core to Lake Agassiz sediments may have been the result of current flow through the channels in this region

and possibly erosion of sediments (note as indicated earlier some material was lost from the top of this core).

Summary

Based on the radiocarbon dates of the paleosol intervals in this core, it appears these intervals may have been associated with dry Hypsithermal conditions. The formation of shallow water conditions and paleosols within the channel appear to have occurred between the black bed dated at 7.655 ^{14}C ka BP (8.443 cal ka BP) at 1.5 m and 6.370 ^{14}C ka BP (7.319 cal ka BP) at 0.74 m. Although the paleotopographic maps indicate this region should have been terrestrial at 8.1 ^{14}C ka BP (9.0 cal ka BP) (Yang and Teller, 2005), this part of the LOTWs would have received transgressive waters from the north basin of LOTWs due to differential isostatic rebound and have received the runoffs from the ponding of waters in the south basin area supplied by the Rainy River. It appears this channel site was in operation from the time of the retreat of Lake Agassiz, through the period of time when this region of LOTWs was predicted to have been dry, however its operation appears to have been interrupted as indicated by the formation of a paleosol interval.

Based on the available radiocarbon date at the black bed at 1.5 m, the bottom of the core appears to be well within the Lake Agassiz sequence. Ostracodes and these Lake Agassiz like sediments continued to be deposited in this region at least up until the end of the

ostracode interval roughly estimated at 8.8 ^{14}C ka BP (9.8 cal years BP) which corresponds well with the paleotopographic maps.

Thecamoebians appeared in two separate intervals (Figure 47); the first one at about 6.468 ^{14}C ka BP (7.397 cal years BP) is earlier than most of the other processed cores (see Chapter 6). The second interval 3.845 ^{14}C ka BP (4.247 cal ka BP) is still much earlier than most of the other LOTWs sites. An increased insect component noted even earlier than this thecamoebian date appears to indicate an increase in productivity, possibly due to localized conditions within this narrow channel. The high charcoal and plant macrofossil contents in these sediments from the black organic rich bed at 1.5 m to the gyttja interval at the very top of the recovered core, implies nearby surrounding terrestrial biota and possibly the introduction of terrestrial materials from the nearby Northwest Angle basin area which may have been dry at his time from differential isostatic rebound and possibly due to drying climatic conditions at this time. The presence of terrestrial and near shore plants in the sediments of the channel would likely be strongly influenced by the narrowness of the channel, making it difficult to use these indicators to assess paleohydrologic conditions. Nonetheless, there appears to be a consistent signal from the various proxies in this area which reflect the changing paleohydrologic conditions since Lake Agassiz isolated, including changes introduced by differential isostatic rebound, drying conditions in the Hypsithermal, and the changes from increasingly productive conditions in the modern lake in this region.

5.5.1 Northwest Angle Site - WOO06-5A

The WOO06-5A-1K coring site is located at the north/south mid-point of modern LOTWs (Figure 24) and would have been subject to the long term southward transgression from the more rapidly rebounding northern part of the lake (Figure 10). Differential isostatic rebound in this northern part of the southern LOTWs basin, resulted in this basin accumulating water flowing in from the main inlet from the Rainy River and the LOTWs watershed, with the elevation of the northern outlet to the Winnipeg River ultimately controlling the bathymetry of the southern basin (Figure 10). The Northwest Angle sites are located to the east of a large emerging island within Lake Agassiz (Figure 8) which resulted in a topographic high after separation of Lake Agassiz (Figure 9).

The relative shallowness of this part of the northern basin region and distance from the Rainy River inlet, would likely make this region more responsive to aridity during climate warming cycles and due to the effects of differential isostatic rebound. Sedimentary evidence and macrofossil evidence from this core provide evidence of paleosol formation from the early Holocene through the mid-Holocene. Sediments at the bottom of the core appear to have been deposited during a phase of Lake Agassiz. This core was extensively subsampled and radiocarbon dated.

5.5.1.1 **Ostracodes**

An exclusively *C. subtriangulata* interval in the bottom metre of the core implies these sediments were deposited in deep, cold and low salinity waters (TDS), such as those in Lake Agassiz. Changes to a more mixed ostracode sequence (Figure 54), including the *L. friabilis* interval from 4.5 to 4.1 m, continues to be consistent with deep, cold and low TDS conditions. The disappearance of *C. subtriangulata* at about 3.8 m, with *L. friabilis* dominating in an interval from about 3.9 - 3.4 m, which also contains *C. sharpei* and *F. rawsoni* is consistent with increasing TDS levels and warmer water conditions.

The presence of ostracodes within the paleosol does not at first appear reasonable (Figure 80), however, it is possible these ostracodes were present in the overlying lacustrine environment, and then were incorporated into the paleosol when it formed. Paleosol horizons form downward (personal communication J. Teller) and the presence of ostracodes within the upper and lower paleosols may have resulted from the paleosol working downward into the lake sequence deposits (and the associated ostracode bearing sediment). It appears these ostracode intervals within the paleosol were not significantly reworked based on the articulated ostracode shells in the first soil horizon. Above 3.4 m, dated at about 8.3 - 8.4 ^{14}C ka BP (9.3 - 9.5 cal ka BP) near the end of the lowermost paleosol (PS3), *C. sharpei* and *F. rawsoni* reappear (at about 3.3 m) in a lacustrine interval between the 2nd (PS2) and the uppermost paleosol (PS3) (Figure 57 and 80).

This lacustrine interval appears to occur near the two dated intervals (Figure 57), at about 7.4 to 7.6 ^{14}C ka BP (~ 8.2 to 8.4 cal ka BP). The dominance of *C. sharpei* indicates this lacustrine interval was shallower, warmer and had higher TDS levels. Ostracodes then reappear in a lacustrine sequence above the PS2 paleosol interval which is dominated by *L. friabilis* and *F. rawsoni.* The ostracode sequence ends above 2.7 m within the uppermost paleosol, with *L. friabilis* disappearing, but with the other three ostracode species present including *C. subtriangulata*. In the preceding lacustrine interval *C. sharpie* disappears and *F. rawsoni* reappears joined by *L. friabilis,* possibly implying there was a deepening sequence between the PS2 paleosol and the PS3 paleosol, and less saline waters. However, the large percentages of plant, charcoal and insect material (Figure 55) in this interval implies relatively shallow conditions occurred at this time, although these materials may have been washed into the basin from the elevated terrain to the west.

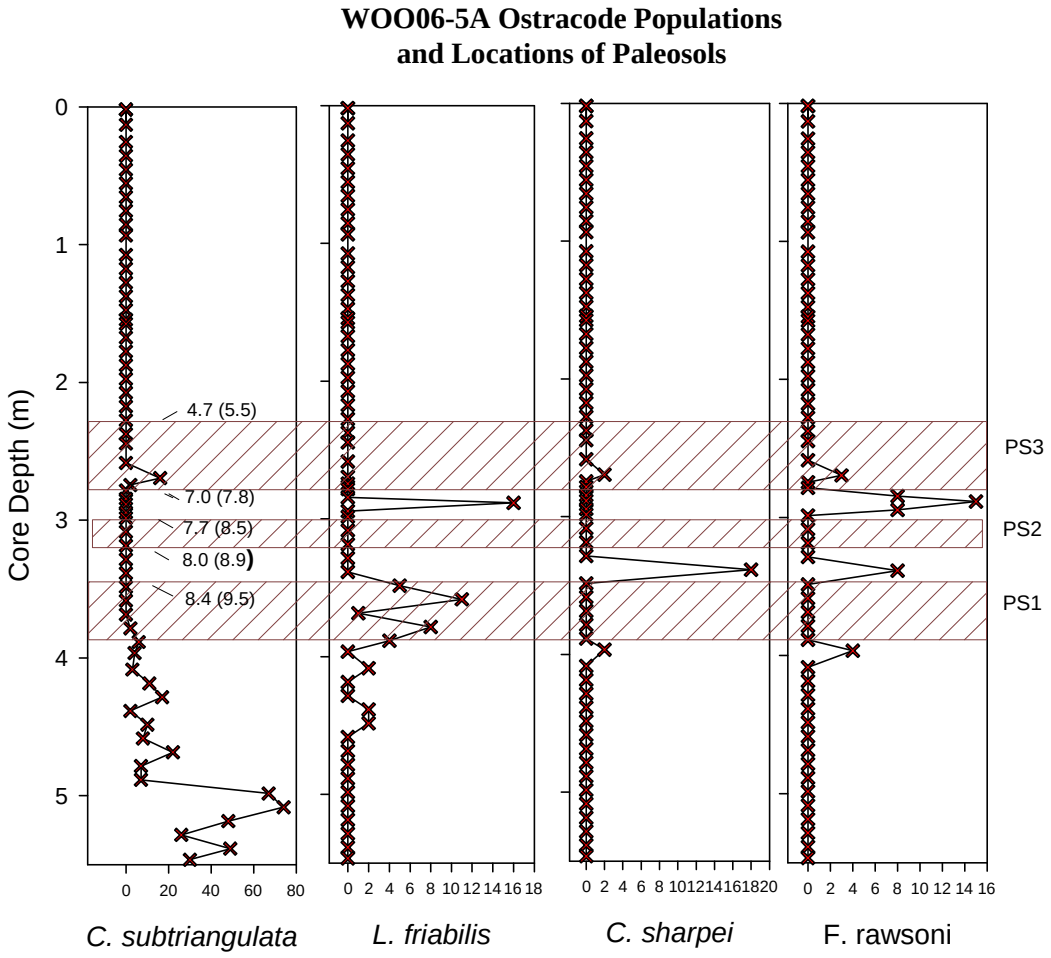

Figure 80. Ostracode population variation (from Figure 54) from the top of the core to the bottom at 5.49 m with the approximate locations of paleosols (PS1, PS2 and PS3) indicated by brown hachured lines. The estimated time (see Section 5.5.1.5) for the beginning and end of the paleosols are indicted in ka ^{14}C BP (calendar years in brackets). The crosses indicate sample locations. Note the number of ostracodes scale varies, with the *C. subtriangulata* ostracode population much higher than the others.

The appearance and domination of *C. subtriangulata* within the PS3 paleosol in conjunction with the reappearance of *L. friabilis* in the lake sequence just below, suggests there was a possible deepening trend before the PS3 paleosol formed. This occurred sometime after about 7.4 - 7.6 ^{14}C ka BP (8.2 - 8.4 cal ka BP) near the beginning of the Hypsithermal.

Estimating the date for the end of the ostracode interval is difficult due to their disappearance within the PS3 paleosol. Nonetheless, the top of the paleosol is estimated at 4.7 ^{14}C ka BP (5.5 cal ka BP) (refer to Section 5.5.1.5 below). Using the dates from the lacustrine interval below, the disappearance of ostracodes within and near the bottom of the last paleosol would be after the date estimated for the bottom of the paleosol, which was estimated at 7 ^{14}C ka BP (7.8 cal ka BP) (refer to Section 5.5.1.5 below). The disappearance of ostracodes in the upper portions of the core repeats a similar pattern found in other cores reflecting ecological and chemical changes within the basin.

The condition of the ostracode shells in this core appear to have been affected by paleochemical conditions, diagenetic changes and/or paleosol formation. Ostracode shells near the paleosol horizons appear crushed implying freeze/thaw conditions occurred, in shallow water or in soils. Below the first soil horizon ostracode shells are mostly broken and thin and have a corroded appearance, possibly reflecting chemical conditions in the lake or sediments, or perhaps a combination of mechanical stresses associated with sediment reworking or paleosol formation.

5.5.1.2 **Thecamoebians**

The appearance of thecamoebians at about 0.8 m in an interval already abundant in plant and insects macrofossils (Figure 55) indicates an increase in lake productivity occurred about this time in this part of the core. The closest available radiocarbon date of 2.080

^{14}C ka BP (2.071 cal ka BP) is 0.1 m above the interval where thecamoebians first appeared. The date of first appearance is roughly estimated to be about 2.3 ^{14}C ka BP (~ 2.3 cal ka BP) based on the nearby date.

5.5.1.3 **Other Macrofossils**

Relatively large volumes of plant and the presence of charcoal were observed in the lower portion of the core (Figure 55) within what otherwise appears to be a typical cold and deep water Lake Agassiz sequence based on the lithics and ostracode sequences. This apparent Lake Agassiz interval should have been a relatively barren ecological zone. The emerging island to the west and subsequent topographic high may be the source of these plant macrofossils and charcoal materials.

The macrofossils and lithics in processed subsamples (Appendix A, Subsection 3.2) confirmed the existence paleosols which were evident from the blocky and granular appearance of the sediments in the split core (Figure 51, Figure 52 and Figure 53). The subsample observations helped to constrain the paleosol locations identified in the visual examinations of the core. The presence of well endurated clay pellets, and a high abundance of plant material, particularly seeds and charcoal materials, are indicative of terrestrial, or near terrestrial shallow water conditions, and were also used to identify the location of the paleosol. Thick mats of organic material in the subsamples were noted in paleosol locations.

The abundant seeds within and near the second (the thinnest) paleosol horizon, include the shallow water plant S*cirpus validus,* and near shore terrestrial plants such as *Rumex maritimus* and *Chenopodium sp.*, all indicating shallow water and likely near shore terrestrial conditions were present, and support the observations of paleosols in the split core. Based on the type of seeds in the interval between the lowermost and uppermost paleosols, the environment between the lower and upper paleosols were not likely deep water environments. The birch nutlets in the uppermost paleosol (PS3) suggest terrestrial conditions at this time. The zones between the paleosol horizons include seeds, twigs, and abundant gastropod and pelecypod shells, and indicate an overall shallow water environment. The interval between the PS2 to the uppermost PS3 paleosol horizon also contains abundant charcoal, implying arid conditions existed.

Below and within the PS1 paleosol, there appears to be considerable sediment reworking in some intervals. The presence of deep and cold water *C. subtriangulata* ostracodes within abundant plant material zones, and horizons containing charcoal are somewhat problematic. The aberrant radiocarbon dates below the first paleosol horizon imply that much older macro and microfossil components are present, and also imply the sedimentary inputs to this area may have experienced considerable reworking and possibly subaerial exposure before re-deposition. Terrestrial sediments shed from the topographical high to the west, or redeposition of eolian deposits from this nearby landform, may explain the aberrant radiocarbon dates in the lower portions of the core and what appear to be an unusually high organic components in Lake Agassiz vintage sediments.

5.5.1.4 **Lithic Grains**

Quartz lithics are abundant from the bottom of the core (Figure 55) upwards to the beginning of the first soil horizon (PS1) at about 3.9 m. This dominance of quartz lithics in this interval is interpreted as being due to the deposition of sediments from Lake Agassiz. The presence of *C. subtriangulata* provides evidence of the cold and deep conditions in the glacial lake existed at the time of deposition of these sediments.

In this core iron stained carbonate lithics, and carbonate clay pellets and balls, dominate the bottom 0.5 m of the core above which quartz lithics become the dominant lithic up to the first paleosol horizon. The reason(s) for this unique characteristic in this core is not clear. The high abundance of carbonate lithics may be the result of deposits from a region of Lake Agassiz rich in carbonates, possibly from wave driven erosion along the eastern shore of Lake Agassiz and/or shed deposits from the emerging Lake Agassiz island and subsequent high topography (Figure 8).

5.5.1.5 **Core Chronology**

Generally the radiocarbon dates of the macrofossil seeds and terrestrial plants resulted in dates that were well sequenced (Figure 57). The radiocarbon date of a well rounded twig however, appeared to have been reworked and transported, as it dated at 15.62 ^{14}C ka BP (18.8 cal ka BP), which is long before Lake Agassiz formed at the melting glacial front

around 11.7 ^{14}C ka BP (13.6 cal ka BP) (Teller and Leverington, 2004). This twig was within the *C. subtriangulata* ostracode sequence which means it should have dated to an interval within the Lake Agassiz period. Subsequent pollen analysis bounding this interval also indicated unusually old dates 17.56 ^{14}C ka BP (20.97 cal ka BP) and 17.04 ^{14}C ka BP (20.36 cal ka BP). This confirms there are older than Lake Agassiz period components in the sediments. The pollen samples imply the pollen was from a period after the last glacial maximum 23.0 cal ka BP, or that old carbon components were not separated from the pollen samples, and contaminated the pollen samples, resulting in older and erroneous radiocarbon dates (Nambudiri, et al., 1980; Mybro, A.E., 2009). All three of these unusually old radiocarbon dates were rejected and not used to establish core chronology.

A radiocarbon date of 7.510 ^{14}C ka BP (8.308 cal ka BP) at 2.9 m was obtained between the middle paleosol (PS2) and the upper paleosol (PS3) (Figure 80). This date is close to what appears to be the bottom of the upper paleosol (at about 2.8 m). Based on this date an estimated date for the bottom of the uppermost paleosol of about 7 ^{14}C ka BP (7.8 cal ka BP) seems reasonable. To establish the date for the top the upper paleosol, the sedimentation rate between the upper available radiocarbon dates (3.910 and 2.080 ^{14}C ka BP at 1.78 m and 0.66 m respectively) was used and extrapolated downward to the top of the paleosol at 2.38 m (i.e. 0.5 m below interval at 3.910 ^{14}C ka BP). A date for the top of the upper paleosol of about 4.7 ^{14}C ka BP (5.5 cal ka BP) was estimated [(3910-2080) / (1.78-0.66) X (2.28-1.78) = 1634 X 0.5 = 817 yrs; 3910 + 817 = 4.726 ^{14}C ka BP].

The lacustrine interval between the PS3 and PS2 paleosols based on the nearby radiocarbon dates appears to be from about 7.7 to 7 ^{14}C ka BP (8.5 to 7.8 cal ka BP). The lacustrine interval after the first paleosol (PS1) started near the radiocarbon dated interval at about 3.3 m and is dated at 8.405 ^{14}C ka BP (9.437 cal ka BP) and lasted until sometime after the dated interval at 3.25 m of 8.065 ^{14}C ka BP (9.008 cal ka BP). This is very near the estimated time for LOTWs isolation from Lake Agassiz based on differential isostatic rebound calculations (Yang and Teller, 2005).

5.5.1.6 **Sedimentation Rates**

Calculating lacustrine sedimentation rates within or across the paleosol intervals would need to account for these interruptions and hence it was not possible to determine sedimentation rates in the interval between the lower and upper paleosols. The two sets of dates within lake sequences between paleosols may provide some information but they are close together in the core, and errors would be difficult to quantify, and therefore sedimentation rate estimates were not undertaken. The rate above the two uppermost dates, which are above the last paleosol (Figure 57) are suitable dates for estimating sedimentation rates, assuming a relatively consistent sedimentation rate, and recognising the compaction of older/deeper sediments would give lower sedimentation rates than the upper non compacted (i.e. dewatered) sediments.

The sedimentation rate from the top to the deeper of the two radiocarbon dates dated at 3.91 ^{14}C ka BP, at 1.78 m (above the last paleosol) is 0.4 mm/yr (1780 mm / 4343 cal yrs = 0.41 mm/yr). The rate between the two dated intervals at 4.343 and 2.071 cal ka BP at 1.78 m and 0.66 m respectively is 0.5 mm/yr [(1780-660 mm / (4343-2071 yrs) = 0.49 mm/yr]. These sedimentation rates are comparable and therefore increase the confidence that the estimated sedimentation rates are reasonable.

5.5.1.7 **Discussion and Interpretation of Coring Site Data**

The *C. subtriangulata* shells below the lowermost paleosol had thin and broken shells with a corroded appearance, implying they may have been subject to reworking and/or diagenetic changes. Broken and crushed ostracode shells appear within the intervals of the core at about 3.7 to 3.3 m, and through the other paleosol horizons, suggesting reworking of these paleosols may have taken place, and/or freeze thaw cycles may have occurred. Contrary to these data, the presence of articulated ostracode shells leads to the conclusion reworking was not significant if it occurred at all. Nonetheless the presence of ostracodes within the lowermost (PS1) and uppermost paleosol (PS3) horizons (Figure 80) implies reworking of these sediments may have taken place as a result of shallowing waters.

Below the uppermost paleosol (PS3) the ostracode population was mostly dominated by *L. friabilis and F. rawsoni*. The presence of *C. subtriangulata* and *L. friabilis* in and near the paleosol implies the water may have been deepening somewhat before the formation of the last paleosol, with *C. sharpei* and *F. rawsoni* inferring a period of increasing TDS levels and warming/shallowing waters. This interval was also noted to have contained significant quantities of seeds leading to the interpretation that shallow water conditions or near shore conditions existed. The presence of these conflicting data near the same interval may be rationalized based on the possibility that the paleosol was reworked, bringing the former lake intervals to near the same paleosol horizon as a result of initial reworking as the water shallowed.

The large amount of organic material and abundant charcoal in the short interval between the lowermost PS1 and PS2 paleosols (Figure 80), indicate a short period of near shore very shallow water conditions occurred. These high relative abundances of charcoal throughout the paleosol interval and within the sediments in the lake interval between paleosols, imply the region was arid with nearby fires. Large charcoal fragments in these intervals (Appendix a, Subsection 3.2) lead to the conclusion nearby fires existed during the early Hypsithermal, both near the time of withdrawal of Lake Agassiz from this location, sometime between the PS1 and PS2 paleosols (8.405 ^{14}C ka BP (9.437 cal ka BP) to 8.065 ^{14}C ka BP (9.008 cal ka BP), and subsequently after the withdrawal of Lake Agassiz from the Northwest Angle region of LOTWs in the PS2 to PS3 uppermost paleosol intervals around 7.7 to 7 ^{14}C ka BP (8.5 to 7.8 cal ka BP).

The formation of a paleosol in what appears to be a Lake Agassiz period is noteworthy. The rising Lake Agassiz island to the west due to isostatic rebound is likely the reason for paleosol formation (Figure 8 and Figure 9), causing this region to rise above the lake level within Lake Agassiz before 8.405 ^{14}C ka BP (9.437 cal ka BP). The coring site then appears to have returned to a shallow lake sequence before a second paleosol formed (Figure 80). This time the driving force for the paleosol formation and duration may have been strongly influenced by a drying climate, sometime during the early Hypsithermal after 8.405 ^{14}C ka BP (9.437 cal ka BP). The abundant and large charcoal fragments present in the sediments (Figure 55 and Appendix A, Subsection 3.2) support this as a possibility. A further climate change appears to have returned the site to

lacustrine conditions before a last paleosol period occurred sometime after 7.0 ^{14}C ka BP (7.8 cal ka BP), possibly due to drying climatic conditions in conjunction with differential isostatic rebound. The site finally returned to lacustrine conditions sometime around 4.7 ^{14}C ka BP (5.5 cal ka BP) and continued as a lake sequence to the present. This change may have occurred as a result of a wetter climate.

Above the last paleosol horizon there are intervals of common to abundant charcoal which generally reduces to rare in the top ~ 0.5 m of the core (Figure 55). An interval of common to abundant charcoal with relatively large charcoal fragments from about 1.0 to 0.5 m (Appendix A, Subsection 3.2), implies nearby fires existed at this time (about 2.2 to 1.5 cal ka BP), and the climate in the region was likely dry.

Dramatic increases in insect macrofossils above the last soil horizon are evident, with abundant to common insect intervals throughout the upper part of the core (Figure 55). Only one interval dropped to rare levels, which interestingly corresponds to an interval with no thecamoebians around 0.5 m. The apparent change to more oligotrophic conditions in this portion of the core is clear, but the reasons for this change are not apparent, although the subsequent drop in charcoal levels also implies wetter conditions may have become prevalent.

The lack of insect macrofossils in the core prior to the first paleosol supports the interpretation that Lake Agassiz conditions prevailed at this time. The abundance of plant macrofossils however at the same time is problematic. It is possible however the

abundant plant material may have resulted from materials been shed into the lake from the large island / high topography to the west, and/or eolian transport may have taken place. The relatively shallow and protected LOTWs configuration as LOTWs became independent (Figure 8), may however also have been a factor.

Summary

The lowermost paleosol in this core appears to correspond with the withdrawal phase of Lake Agassiz. The lowermost radiocarbon date of 8.405 ^{14}C ka BP (9.437 cal ka BP) is very close to the top of the lowermost paleosol (Figure 80), which indicates its initial formation must have been even earlier and much earlier than anticipated for terrestrial conditions in this region. An initial formation date for this paleosol is not available. Shed sediments from the large emerging Lake Agassiz island and subsequent elevated topography to the west may have in-filled the basin, and differential isostatic rebound may have combined with this effect to form this early paleosol in this region of LOTWs. It is also possible the paleosol formation may have been influenced by an early arid Hypsithermal interval.

Isostatic rebound in the northern portion of LOTWs at the outlets to the Winnipeg River in conjunction with a wetter climate may have caused an interval of deeper water in the Northwest Angle area, interrupting the initial paleosol formation. The return of colder water ostracode species such as *L. friabilis,* support the interpretation that deeper water conditions returned. This deeper water interval may have been interrupted by drier

conditions in the unstable Hypsithermal period, forming two further paleosols and subsequent returns to lacustrine conditions, as climate varied between wet and dry conditions and as LOTWs continued to experience the effects of differential isostatic rebound. The last paleosol started forming sometime after 7.0 ^{14}C ka BP (7.8 cal ka BP) (Figure 80). The transgression of waters from the north due to differential isostatic rebound, in conjunction with a wetter climate likely reflooded this region ending the formation of the uppermost paleosol at around 4.7 ^{14}C ka BP (5.5 cal ka BP). The lacustrine interval above the last paleosol includes indications of changing ecological conditions, such as changes in abundance of plant and insect macrofossils, and the abundance of charcoal (Figure 55).

The end of ostracodes in this core was estimated to be about at about 7 ^{14}C ka BP (7.8 cal ka BP) at 3.3 m within the last paleosol. Thecamoebians appeared at about 2300 cal years BP (Figure 57) which is very close to the date estimated for the shallow water companion site of about 2400 cal years (see next section). This places the beginning of a more eutrophic interval at about 2300 cal years BP. A peak in plant material at this time and continued high insect levels supports this timing for the beginning of more productive lake conditions. The high charcoal contents in these sediments up to and above this interval, including the presence of large charcoal fragments just prior to the interval, implies nearby surrounding terrestrial biota may have been subject to the dry climatic conditions.

5.6.1 Northwest Angle Site - WOO06-6A

The WOO06-6A-1K coring site is located at the north/south mid-point of the modern LOTWs (Figure 24) and would have been subject to the long term southward transgression from the more rapidly rebounding northern part of the lake (Figure 10). Differential isostatic rebound in this northern part of the southern LOTWs basin, resulted in this basin accumulating water flowing in from the main inlet from the Rainy River and the LOTWs watershed, with the elevation of the northern outlet to the Winnipeg River ultimately controlling the bathymetry of the southern basin. The Northwest Angle sites are located to the east of a large emerging island within Lake Agassiz (Figure 8) which resulted in a topographic high after separation of Lake Agassiz (Figure 9).

The relative shallowness of this part of the northern basin region and distance from the Rainy River inlet would likely make this region more likely to form paleosols during periods of aridity and due to the effects of differential isostatic rebound. Sedimentary evidence and macrofossil evidence from this core and its companion core (WOO06-5A-1K) provide evidence of paleosol formation in the early Holocene. Sediments at the bottom of the core provide evidence these lowermost sediments were deposited during a phase of Lake Agassiz.

5.6.1.1 **Ostracodes**

C. subtriangulata dominate at the bottom of the core (~ 2m) to about 1.8 m from the top of the core where a transition from the well laminated to weakly laminated sediments, and the observed paleosol occurs (based on hard 1-3 mm granules). The ostracode sequence identified in the bottom of this core implies these sediments were deposited in deep, cold and low TDS conditions, such as those in Lake Agassiz. In this core however, there is a mixed sequence of ostracodes from the bottom of the core to about 2.8 m including *L. friabilis* and one rare interval of *C. sharpei, a*lthough *C.* s*ubtriangulata* was dominant. The presence of *L. friabilis* in conjunction with *C.* s*ubtriangulata* in the deepest parts of the core, confirms deep cold conditions with low TDS levels existed, which is consistent with a Lake Agassiz sequence. The short interval of *C. Sharpei* in conjunction with the decrease in *C.* s*ubtriangulata* and *L. friabilis* ostracode populations implies a short interval of possibly shallower and higher TDS conditions may have existed before conditions returned to deeper, cooler and perhaps lower TDS conditions. This change in conditions may indicate a change in conditions within Lake Agassiz occurred, and/or the emergence of the large island to the west which appears at about 10.0 cal ka BP (Figure 8), was influencing local conditions with possible additional affects from an arid climatic condition.

The end of the ostracode interval in this core at about 1.9 m, is very close (8 cm below) the radiocarbon dated interval of 6.760 ^{14}C ka BP (7.616 cal ka BP). The absence of

ostracodes in the upper portions of the core repeats a similar pattern present in other cores.

Ostracode shells within the paleosol horizon appear crushed which suggests freeze/thaw periods occurred in shallow water conditions or in exposed soils. *C. subtriangulata* shells are typically broken and thin and have a corroded appearance, possibly reflecting chemical conditions at the time, or perhaps a combination of mechanical stresses associated with sediment reworking and/or post diagenetic chemical changes. However, the presence of two intervals below the paleosol with articulated ostracode shells implies the shells were not transported or significantly disturbed despite the crushed appearance of some *L. friabilis* ostracodes. This may mean they may have undergone a freeze/thaw process near a paleosol or in shallow low energy water and not have been significantly reworked.

The lack of mechanical damage or corroded appearance of ostracode shells in the bottom ~ 0.4 m provides evidence of what appears to be a different paleoenvironment in the bottom portion of the core. Perhaps this interval is closer to the deep and cold Lake Agassiz environment, although the relatively high population of *L. friabilis* in the ostracode sequence implies a somewhat shallower condition existed, perhaps as a result of the emerging western island.

5.6.1.2 **Thecamoebians**

The appearance of thecamoebians at about 1.3 m follows an interval of increasing abundance of plant, insect and charcoal materials (Figure 62), and confirms productivity was increasing towards more eutrophic conditions in LOTWs. Although a detailed thecamoebian species analysis was not performed, up to four species were noted (Appendix A, Subsection 4.2). This thecamoebian interval is about 0.6 m above the end of the paleosol. Nearby radiocarbon dates of 3.245 ^{14}C ka BP (3.481 cal ka BP) at about 1.5 m, and a second dated interval at 1.0 m of 2.11 ^{14}C ka BP (2.091 cal ka BP), provide the means to estimate the first appearance of thecamoebians. Assuming the sedimentation rate was relatively constant, appearance of thecamoebians is estimated to be about 2.8 ^{14}C ka BP (2.9 cal ka BP) [(3245-2110) X (1.3-1.0)/ (1.5-1.0) +2110 = 2796 ^{14}C years BP (2899 cal ka BP)].

5.6.1.3 **Other Macrofossils**

Relatively large volumes of plant and charcoal (Figure 62) in the lower portion of the core, within what appears to be a Lake Agassiz sequence, based on the available radiocarbon date and presence of the cold and deep water *C. subtriangulata* ostracode species, are problematic. The same characteristics, however, occurred in the deeper companion site (WOO06-5A-1K). The presence of large plant and charcoal macrofossils, along with the presence of a *C. sharpie* ostracode while the *C. subtriangulata* population fell dramatically and *L. friabilis* was falling around 3.3-3.2 m, may reflect a shallowing was underway in this portion of Lake Agassiz. At 10.0 cal ka

BP a large island within Lake Agassiz had been rebounding (Figure 8 and Figure 9) such that this portion of LOTWs was dry land about 1000 years before Lake Agassiz fully withdrew from the LOTWs basin. This leads to the conclusion that the Northwest Angle sites were terrestrial or shallow, before Lake Agassiz fully withdrew from LOTWs (see Section 5.5.1.7). This could have affected the type of Lake Agassiz sediments in this location as Lake Agassiz became shallower. This may explain why the lower core interval in this core does not reflect what should be a relatively barren Lake Agassiz interval and instead includes relatively abundant plant, charcoal, and insect macrofossils possibly shed from the large Lake Agassiz island to the west, and from the subsequent presence of shallow water environmental conditions.

A paleosol horizon was identified during core logging (Figure 59) and this was supported by observations from the associated subsamples (Appendix A, Subsection 4.2). The location of the paleosol horizon in this core appears to be between 2.0 and 1.8 m based on visual observations and the data from processed subsamples. Large quantities of plant materials were present throughout the paleosol horizon and helped to constrain the extent of the paleosol. A shallow water zone below the observed paleosol interval is evident in this core, with high volumes of plant materials, large fragments of charcoal, and gastropod shells, all supporting an interpretation that a shallow near shore condition prevailed prior to the formation of the paleosol. The presence of *C. subtriangulata* in this zone may be due to reworking of earlier deeper water sediments in a higher energy shallow water environment. The presence of carbonate lithic components at the soil horizon is consistent with the presence of a bivalve in this paleosol interval. Above the

paleosol plant materials, charcoal and insect materials increased dramatically, indicating shallow water conditions may have prevailed for some time after the end of the paleosol.

The presence of a bivalve within the soil horizon indicates the reason for the end of the ostracode interval was not likely related to the availability of carbonate. It is interpreted that the disappearance of ostracodes is more likely due to a changing paleoclimate and the effects of differential isostatic rebound, which changed the paleoecological conditions within Lake Agassiz.

5.6.1.4 **Lithic Grains**

In the deeper portions of the core the dominant lithic component is quartz, which is typical of the deep sediments in other cores, but this dominance only occurs in the bottommost ~ 0.3 m of the core. Based on the type of lithics and the available radiocarbon date of 6.760 ^{14}C ka BP (7.616 cal ka BP) these lowermost sediments are interpreted as being from Lake Agassiz.

Iron stained carbonate rich pellets are common from near the bottom of the core and through the paleosol (Appendix A, Subsection 4.2). The frequent occurrence of clay pellets and balls above these Lake Agassiz deposits up to the paleosol and above it, is another indication of changing depositional and diagenetic conditions in this core. The presence of *C. subtriangulata* ostracodes and coated ostracode shells may indicate these pellets are products of diagenesis and reworking of Lake Agassiz deposits. It is unclear

why some of the pellets appear to be iron stained but these pellets are typically composed of carbonates, whereas non stained pellets are not. Nonetheless, the presence of these pellets and the carbonates, appear to be associated with Lake Agassiz sediments, in this case likely reworked, as this region shallowed and dried from the effects of differential isostatic rebound and possibly a drying climate.

5.6.1.5 **Core Chronology**

The radiocarbon date at 1.9 m of 6.760 ^{14}C ka BP (7.616 cal ka BP) is very near the top of the paleosol at 1.8 m and may be a possible means to establish a date for the top of this paleosol, and additionally provides a date shortly after the ostracode interval (Figure 63). Although it is the closest date to the bottom of the core it is still almost 2 m above the bottom of the core, and hence does not provide the means to accurately date the bottom of the core, especially since it is within the paleosol and the core may be missing material due to the paleosol formation and reworking below the paleosol. It is likely however, the bottom of the core is within a Lake Agassiz sequence based on this date and other observations.

The two other radiocarbon dates are above the paleosol; 2.11 ^{14}C ka BP (2.091 cal ka BP), at 1.0 m and 3.245 ^{14}C ka BP (3.481 cal ka BP), at 1.5 m. These dates provide the means to estimate the beginning of the thecamoebians at 1.3 m which is estimated to be about 2.8 ^{14}C ka BP (2.9 cal ka BP). This estimated date places the beginning of a more eutrophic condition within this part of the lake, at about 2.8 ^{14}C ka BP (2.9 cal ka BP),

when thecamoebians first appeared, although more productive conditions were already underway based on the sharp increase in insects and plant macrofossils just below the radiocarbon date of 3.245 ^{14}C ka BP (3.481 cal ka BP).

Based on the available radiocarbon dates above the paleosol and extrapolating downward, the date for the top of the paleosol is 4.4 ^{14}C ka BP (4.9 cal ka BP) [(1.5-1.0 m) / (3245-2110 ^{14}C yrs) = 0.27 mm/yr; 0.27 X (3245-2110) + 3245 = 4355 ^{14}C years BP]. This is a much later date than the date indicated within the paleosol. This indicates considerable reworking or erosion took place in the paleosol, which is supported by broken ostracode fragments near this interval.

From Figure 9, the drying of the terrain at this location would have initiated prior to 10 cal ka BP and should have remained dry until sometime between 6-7 cal ka BP depending on the type of climate (Figure 10). The infilling of the Northwest Angle region with shed deposits form the emerging landform to the west may have made this occur even earlier, especially if the climate was arid. The estimated date for the end of the paleosol of 4.4 ^{14}C ka BP (4.9 cal ka BP) indicates a return to lake conditions occurred much later, possibly as a result of the infilling of sediments and an arid climate at the end of the paleosol interval.

5.6.1.6 **Sedimentation Rates**

The overall sedimentation rate from the paleosol upwards is about 0.21 mm/yr [1.86 m / 4900 cal yrs = 0.21 mm/yr]. The rate between the two upper radiocarbon dates (Figure 63) is also about 0.2 mm/yr [(1.32 -1.01 m) / (3481-2091 cal yrs) = 0.22]. This rate is about half of the sedimentation rate observed in its companion core (WOO06-5A-1K). The sedimentation rate below the paleosol is indeterminate since the available radiocarbon date of 6.760 ^{14}C ka BP (7.616 cal ka BP) is within the paleosol and cannot be accurately extrapolated downward.

5.6.1.7 **Discussion and Interpretation of Coring Site Data**

The ostracodes species in the lower part of the core interval infer cold Lake Agassiz conditions existed, however their thin and broken shells and corroded appearance imply they may have been subject to reworking and/or diagenetic changes, that differ from the deep core intervals of other sites. They look very similar to the WOO06-5A-1K companion site ostracode shells. The crushed/distorted appearance of some ostracode shells near the paleosol implies these shells may have been exposed to freeze/thaw cycles in shallow water or have been subjected to drying in the paleosol. Broken and crushed ostracode shells appear from the intervals of the core below the paleosol horizon, implying reworking of soil horizons may have taken place, and/or freeze thaw cycles may have occurred.

The ostracode horizon (Figure 61) includes a transition from deep water *C. subtriangulata* and *L. friabilis*, and very rarely *C. sharpie* indicating a possible shallowing interval and movement to higher TDS conditions. The ostracode interval extends from the bottom of the core into the paleosol zone. The presence of *C. subtriangulata* and *L. friabilis* ostracodes implies a deeper and colder environment at the bottom of the core. Nonetheless, the disappearance of the last ostracode horizon at the paleosol (Figure 63) seems to be reasonable, as the soil horizon may have worked downward into the underlying lake sequence and the associated ostracode sediments, without significantly reworking the sediments, as indicated by the articulated ostracodes near the upper soil horizon. The presence of a bivalve in the soil horizon is noteworthy. This means the conditions in the lake had changed, but the chemistry still favoured the development of $CaCO_3$ shells, hence the reason for disappearance of the ostracodes was not likely related to paleochemistry, but rather paleoenvironmental changes, that no longer favoured the ostracodes, particularly *C. subtriangulata*.

The radiocarbon date at 1.9 m of 6.760 ^{14}C ka BP (7.616 cal ka BP) near the top of the paleosol (near 1.8 m) (Figure 63) is much earlier than the date estimated by extrapolating downward 4.4 ^{14}C ka BP (4.9 cal ka BP), using the two dated intervals above the paleosol (Section 5.6.1.5). This much earlier date than the date within the paleosol indicates considerable reworking may have taken place within the paleosol which is also indicated by broken ostracode fragments within the paleosol. The 4.4 ^{14}C ka BP (4.9 cal ka BP) estimated date for the top of the paleosol seems more appropriate.

The sediment after the last paleosol interval indicates this is a continuous lake sequence, with variations productivity evident through variations in the plant and insect components and the occurrence of thecamoebians in the upper portion of the core (Figure 62). The high abundance of charcoal after the paleosol interval starting at about 1.6 m to about 1.4 m implies the region was dry, and based on the presence of large charcoal fragments (Appendix A, Subsection 4.2) suggests fires were nearby. An estimated start date for this dry interval, is close to the radiocarbon dated interval at 1.5 m of about 3.245 ^{14}C ka BP (3.481 cal ka BP), which lasts until the thecamoebians appeared at 2.8 ^{14}C ka BP (2.9 cal ka BP). Intervals of common to abundant charcoal, generally reduces above this point to rare, in the top ~ 0.5 m of the core indicating conditions may have become wetter.

Dramatic increases in insect macrofossils above the soil horizon are evident with abundant to common insect intervals to about 1.2 m, where they trend lower (Figure 62). These characteristics are similar to the WOO06-5A-1K companion core. Plant materials in the core above the paleosol, increase and remain abundant to the top of the core. The change to more productive conditions in this portion of the LOTWs is clear, based on the plant and insect materials, and ultimately the appearance of thecamoebians.

The primarily low levels of insect macrofossils in the core prior to the paleosol, suggests Lake Agassiz conditions or similar conditions may have prevailed up to this time. The associated higher than expected plant macrofossils, similar to the WOO06-5A-1K core, may have been shed, or eolian transport may have taken place, from the large island to the west. This may be the reason for the high relatively high plant content of the

sediments below the paleosol. The very bottom of the core has less plant material and may be closer to Lake Agassiz conditions. The subsample plant materials observed in these lower intervals, were primarily aquatic suggesting non Lake Agassiz conditions prevailed in this interval.

Summary

A radiocarbon date within the paleosol in this core of 6.760 ^{14}C ka BP (7.616 cal ka BP) provides a reasonable estimate for the date where ostracodes disappeared. This disappearance occurred when there was evidence of carbonates in the paleosol indicating a lack of carbonates was not the reason for the end of the ostracode interval.

It appears the paleosol was formed into Lake Agassiz sediments as a result of differential isostatic rebound and remained considerably later than would have been predicted by the paleotopographic maps (Figure 10). The delayed return of lake conditions in this area may be due to sediment in-filling of the region from the large rebounding Lake Agassiz island to the west of the Northwest Angle area and possibly due to a dry interval in the Hypsithermal. Similarly, this part of LOTWs may have isolated earlier from the influences of Lake Agassiz, but the unavailability of radiocarbon dates in the lower parts of the core means this cannot be verified. The sediments in the lacustrine interval above the last paleosol indicate some variability in paleoenvironment which is reflected by plant and insect macrofossils, and charcoal signals (Figure 62). The estimated date for the top of the paleosol obtained by extrapolating downward from the two dated intervals above

the paleosol indicates the top of the paleosol and hence the return to lacustrine conditions occurred at about 4.4 ^{14}C ka BP (4.9 cal ka BP) at 1.8 m.

Thecamoebians appeared at about 2900 cal years BP, which is earlier than, but comparable to the deeper water companion site (dated at about 2300 cal years BP). Indications of increasing productivity preceded the beginning of thecamoebians (increasing plant and insect materials) with the beginning of thecamoebians at about 2.8 ^{14}C ka BP (2.9 cal ka BP) possibly signalling a shift to more eutrophic conditions (Figure 62). The high charcoal contents in these sediments from the paleosol to the thecamoebian interval, implies nearby surrounding terrain may have been subject to drying conditions. The age for the start of this dry interval which begins at about 1.6 m, is provided by the nearby dated interval at 1.5 m of 3.245 ^{14}C ka BP (3.481 cal ka BP). This interval extends to around 1.3 m when the thecamoebians appeared at 2.8 ^{14}C ka BP (2.9 cal ka BP).

5.7.1 Kenora Site - WOO06-7A

This coring site is located near the location where LOTWs drains into the Winnipeg River system in a complex channel connecting to more open waters to the south (Figure 24). Differential isostatic rebound in this area over the interval since Lake Agassiz separated from LOTWs, resulted in this deep northern basin being initially depressed even further with respect to the modern elevations of LOTWs, due to its more recent

proximity to the retreating LIS ice margin. The relatively rapid isostatic rebound compared to the remainder of the lake to the south, and southeast, raised the northern outlets and caused a transgression to the south. This part of LOTWs had always been relatively deep (Figure 9) and water level variations would not likely have been as significant to the lacustrine paleoenvironment in this location, as those in the shallow portions of the modern lake. This makes the paleoenvironment generally less subject to change and less responsive to climatic variations. Nonetheless, since this portion of the lake receives inputs from the Rainy River basin and inputs from the surrounding LOTWs watershed, paleoenvironment changes in the LOTWs basins and the drainage basin may be visible in the changes in lake productivity and chemical conditions. The presence of a pink clay bed at about 4 m in this core reflects significant change in Lake Agassiz paleohydrology.

5.7.1.1 **Ostracodes**

The almost exclusive *C. subtriangulata* interval in the bottom of the core, to about 3.9 m (Figure 68) is similar to Lake Agassiz sequences observed in most of the cores. The appearance of a dominant albeit low population of *C. sharpei* upwards of about 2.1 m is atypical compared to other cores. This trend from the cold, deep, and low TDS preferring *C. subtriangulata* to the higher TDS and water temperature tolerant *C. sharpei* tracks a dramatic change in conditions at this site even prior to the estimated time when Lake Agassiz separated from LOTWs (Yang and Teller, 2005).

The one short interval with low population numbers of *L. friabilis* and *F. rawsoni* near the bottom of the core above a pink clay bed at 4.0 m, in an otherwise exclusively *C. subtriangulata* interval, may reflect the changing conditions at the time of deposition of the pink clay bed in Lake Agassiz, including conditions shortly thereafter when the ostracode population entered a hiatus for about 1 m in the core. It is possible the hiatus was related to a deepening sequence, which was less favourable to ostracodes in this part of Lake Agassiz and disrupted the lacustrine niche preferred by these ostracodes.

The three distinct ostracode hiatuses in the core are clear indicators of dramatic changes occurring in the coring area, before a final environmental change at about 1.2 m resulted in the disappearance of ostracodes from the record. Within the last ostracode sequence thecamoebians appear providing further evidence of a dramatic change in conditions. This overlap of ostracode and thecamoebian intervals in the top portion of the core is unique to this core.

The deep and cold water *C. subtriangulata* ostracode dominated near and below the pink clay layer in the two ostracode sequences near the bottom of the core, and it briefly reappears in low numbers at ~ 2.7 m, and then disappears from the record. At the bottom of the core, dropping population numbers for *C. subtriangulata* indicate conditions were becoming unfavourable possibly due to shallowing water levels in Lake Agassiz, before they began to rise below the pink clay, with *L. friabilis* and *F. rawsoni* ostracodes appearing with them before they all disappeared above the pink clay bed. The *C. sharpei* ostracode appears in low population numbers by itself, above the last incidence of *C.*

subtriangulata, and subsequently goes through a hiatus, before reappearing in low numbers and then finally disappearing above about 1.2 m, following the appearance of thecamoebians.

The coated, fragile looking, and broken ostracode shells (Appendix A, Subsection 5.2) appear to reflect changing paleoconditions in the region of this core and possibly changes in preservation conditions. The heavily coated shells in an interval above the pink clay bed were associated with the presence of clay balls. An articulated ostracode shell noted near the pink clay bed indicates reworking near this interval was not significant and was not likely the reason for broken ostracode shells nearby.

The lowermost ostracode sequence is unusual, in that it is clearly within a Lake Agassiz period, as reflected by their presence near and below the pink clay bed. This pink clay bed is estimated by others to have been deposited between about 10.1 to 9.4 ^{14}C ka BP as a result of the Marquette readvance over the eastern Lake Agassiz outlets which flooded water westward over the height of land and into the LOTWs region (Teller and Leverington, 2004; Teller et al., 2005). The hiatus in ostracodes from about 4.4 to 4.1 m may have been due to changes in Lake Agassiz, and the location of the ice margin prior to the Marquette readvance, possibly due to the Younger Dryas climatic changes at 10.9 ^{14}C ka BP (12.8 cal ka BP), and changes in Lake Agassiz during the Herman, Norcross and Tintah stages (Teller et al., 2005).

The rapid rise in the ostracode population to a maximum at the pink clay layer is also noteworthy. It appears conditions in the region became optimal for ostracodes during the time when Lake Agassiz received inputs from the transgression initiated by the Marquette readvance. This may have been due to a change in chemistry, hydrology, or a change to increased productivity within Lake Agassiz due to increased food supply from flooded terrain.

The last interval of ostracodes begins about 20 cm below the sample at about 1.7 m, dated at 8.310 ^{14}C ka BP (9.350 cal ka BP). This is just before the time when LOTWs was estimated to have disconnected from Lake Agassiz (Figure 9), at about 8.1 ^{14}C ka BP (9.0 cal ka BP), based on differential isostatic rebound calculations assuming LOTWs hydrology was at the level of the northern outlets. The final disappearance of ostracodes occurs after the separation of Lake Agassiz from LOTWs. The exclusive *C. sharpie* ostracodes in this portion of the core at this time, when deep Lake Agassiz conditions should still have prevailed, implies changing water chemistry may have been a factor, along with other paleoenvironmental conditions that may also have changed. However, the disappearance of *C. subtriangulata* well before the independence of LOTWs suggests the reason for disappearance of ostracodes in this area was not likely water chemistry but perhaps other paleoenvironmental conditions. The change to the warmer and shallower water and higher TDS tolerant *C. sharpie* ostracodes may reflect significant changes in the local environment even prior to the complete isolation from Lake Agassiz. These changes in the ostracode populations are very different from the other cores.

Conditions at the time of the exclusive *C. sharpie* ostracode interval would appear to have favoured deep and cold water species. Closer examination of Figure 8 however, shows an emerging large Lake Agassiz island to the west, and a nearby complex island to the north of this coring site. These rebounding terrains possibly changed the local ecological conditions due to changes in the hydrology at this location, affecting the bathymetry and possibly creating strong local currents as the LOTWs watershed flowed towards the receding Lake Agassiz. This coring location is near the northern outlets and the modern configuration is in a complex channel system supporting this possibility.

5.7.1.2 **Thecamoebians**

The early appearance of thecamoebians at 1.5 m, just above the interval dated at 8.265 ^{14}C ka BP (9.235 cal ka BP) at 1.6 m, is preceded by high insect and plant macrofossils (Figure 69), and indicates an early change to more productive conditions in this core. This thecamoebian presence appears to be within or very near the point where LOTWs was estimated to have become isolated from Lake Agassiz based on isostatic rebound calculations. The associated presence of large charcoal fragments, prior to and following the first thecamoebians, indicates drier conditions existed at this time, likely from the climatic variations of the early Hypsithermal. The appearance was short lived and they only appeared in small numbers, before they reappeared at 1.0 m, above the interval at 1.2 m dated at 6.775 ^{14}C ka BP (7.630 cal ka BP), and then continued to the top of the core.

This second interval of thecamoebians appeared prior to the end of the last ostracode horizon shortly after ostracodes disappeared after 6.775 ^{14}C ka BP (7.630 cal ka BP). The relatively early date for appearance of thecamoebians places the onset of more productive ecological conditions before the arid Hypsithermal period, but close to a time when emerging islands to the west and north were appearing, implying these rebounding nearby terrains were having significant effects on the paleoecology of this site.

5.7.1.3 **Other Macrofossils**

The Lake Agassiz phase of this core in the lower metre of the core, except for a sharp increase in plant material just prior to the pink clay bed, has very limited abundances or no observed quantities of plant, insect, and charcoal. This short lived spike may be due to the influx of waters from the east, which transported aquatic plant materials and wood fragments from the flooded shoreline due to the blocking of the eastern outlets. A pelecypod hinge at 4.2 m (below the pink clay) may indicate a shallowing in Lake Agassiz in this region before the influx of the waters from the Marquette readvance.

The increases in plant and insect macrofossils from these very low levels until plant materials sharply increase at about 3.1 m, and the subsequent sharp increase in insects and charcoal at about 2.5 m (Figure 69), reflect significant changes in Lake Agassiz from the typically low levels of biota. A short increase of plant and charcoal at an interval near 3.6 m within the Lake Agassiz sequence reflects additional short duration changes in Lake Agassiz or its environs. Moving upwards in the core to about 3.3 m, plant and

insect components increase becoming even more uncharacteristic of Lake Agassiz sediments. The insect wing and a grass-like terrestrial plant macrofossil found at about 3.6 m (Appendix A, Subsection 5.2) implies changing conditions were underway in nearby terrestrial environments, with the increasing plant components also increasing above this interval to abundant above 3 m. From here upwards plant and insect abundances fluctuate somewhat but remain generally high. The same general characteristic also applies to charcoal levels which start at about 2.8 m. A notable change in the lithics indicates the presence of carbonates starting about 3.3 m corresponds with this interval of increasing macrofossils. The high abundances of plant, insect and charcoal below the two radiocarbon dated intervals at about 1.6 m, of 8.265 ^{14}C ka BP (9.235 cal ka BP) and 8.310 ^{14}C ka BP (9.350 cal ka BP), does not seem consistent with the estimated isolation date of LOTWs from Lake Agassiz based on isostatic rebound. The presence of high abundances of carbon macrofossils starting around 3.0 m, well below an interval dated at 8.780 ^{14}C ka BP (9.804 cal ka BP) and which appear to be well within the Lake Agassiz interval, all indicate the conditions within Lake Agassiz at this location had become more productive which is uncharacteristic of the relatively sterile conditions of a large proglacial lake.

Increasing charcoal levels at 2.8 m which become abundant at about 2.5 m (dated nearby at 8.780 ^{14}C ka BP (9.804 cal ka BP), possibly indicate increasing aridity in the region particularly locally, as large fragments of charcoal are common, indicating nearby fires. This increase in charcoal fragments is prior to the unstable warm climate of the Hypsithermal. However, Figure 8 and Figure 9 indicate the appearance of an emerging

island to the west, and a larger and closer one to the north and east of the site, and these rising terrains may provide a source of charcoal relatively near to this coring site.

5.7.1.4 **Lithic Grains**

The occurrence of carbonate lithics within and just above the pink clay bed, are another indication of the dramatic changes in conditions at this time in Lake Agassiz (Figure 69) (Appendix A, Subsection 5.2).

The abundance of quartz lithics remains high from the bottom of the core to 2.7 m where they drop from abundant to common for most of the remainder of the core, sometimes reaching rare levels, as the biota become the major component in the subsamples. The decrease in abundance of the quartz lithic component above 2.7 m is about 0.3 m below the dated interval of 8.780 ^{14}C ka BP (9.804 cal ka BP) at 2.4 m. This change in the abundance of lithics may reflect changes in the configuration of Lake Agassiz at this location, which is also supported by subsequent increases in plant, insect and charcoal macrofossils. The nearby emerging Lake Agassiz islands Figure 8 indicate significant topographic changes were underway near this location within Lake Agassiz.

5.7.1.5 **XRD Analysis**

Although the broadly spaced qualitative XRD sampling and analyses did not appear to show any significant deviation in the mineralogical signatures of the sediments (refer to

Appendix C), there was a variation noted in the mineralogy across the pink clay bed in the Lake Agassiz sequence. The sample nearest to and above the bed was unique with conditions above this sample returning to the same general signature observed below the bed. This variation likely reflects the different source of sediments that were input into the LOTWs region of Lake Agassiz by the damming of the eastern outlets and the movement of sediments westward as a result of the flooding produced by the Marquette glacial readvance at about 10.1 to 9.4 ^{14}C ka BP (Teller and Leverington, 2004; Teller et al., 2005). The qualitative XRD sampling and analysis further confirms what is evident from the core descriptions and from the observed subsample biota.

The relatively consistent XRD plots in Appendix C, other than above and below the pink clay, imply the Lake Agassiz sediments and LOTWs sediments were similar over the entire period when the sediments were deposited (within the limitations of the sampling program). It seems the Lake Agassiz depositions and subsequent transportation of these sediments from terrestrial locations surrounding the lake basin, after LOTWs isolated from Lake Agassiz, continued to dominate the sediments of LOTWs. A reason for the lack of ostracode macrofossils in the upper portions of the core was not evident from the qualitative XRD analysis.

5.7.1.6 **Core Chronology**

The two Radiocarbon dates of 8.265 ^{14}C ka BP (9.235 cal ka BP) and 8.310 ^{14}C ka BP (9.350 cal ka BP) at approximately 1.6 m, which are near the top of the core and it

appears that some material may be missing or that these dates are too old. Additionally, a pollen date at about 3.3 m of 6.060 ^{14}C ka BP (6.930 cal ka BP) brought these dates into question. It was noted however the dates are chronologically sequenced and two dated samples above and below are also chronologically sequenced (Figure 71) restoring confidence that these dates are appropriate. The pollen date was rejected based on the series of four macrofossil dates which are chronologically correct, and noting the pollen dated interval at 3.3 m was relatively near the pink clay bed which is estimated to have been deposited much earlier and well within a Lake Agassiz sequence.

With this aberrant pollen date removed from the sequence, the overall chronological sequence appears logical, although the late date of 6.775 ^{14}C ka BP (7.630 cal ka BP) at 1.1 m is close to the top of the core. Nonetheless the upper date provides an estimate for both the disappearance of the ostracodes and the beginning of the thecamoebians.

5.7.1.7 **Sedimentation Rates**

The overall sedimentation rate from the oldest date to the top of the core is about 0.2 mm/yr [2.4 m / 9804 cal yrs = 0.245 mm/yr]. The uppermost sedimentation rate is estimated at 0.1 mm/yr [1.1 m / 7630 cal yrs = 0.144].

The sedimentation rate in the middle portions of the core, from the lowest radiocarbon date at 2.4 m dated at 8.780 ^{14}C ka BP (9.804 cal ka BP) to the uppermost date of 6.775 ^{14}C ka BP (7.630 cal ka BP) at 1.1 m, is estimated as 0.6 mm/yr [(2.4 - 1.1 m) / (9804 -

7630 cal yrs) = 0.598 mm/yr]. Based on the assumption the pink clay layer is around 10.1 to 9.4 ^{14}C ka BP, the sedimentation rate to the lowest radiocarbon date at 8.780 ^{14}C ka BP, is similar to the higher rate observed between the upper and lowermost radiocarbon date, of approximately 0.6 mm/yr.

5.7.1.8 **Discussion and Interpretation of Coring Site Data**

The pink clay bed appears to be associated with the inflows over the height of land from the Superior Basin caused by the Marquette readvance and the associated covering of the eastern outlets by the LIS. Unfortunately, there are insufficient macrofossils near this interval, and the LOTWs pollen samples have proven to be unreliable. Projecting down in the core from 2.4 m, assuming the sedimentation rate between the uppermost and lowermost dates is constant, an estimate of the date for deposition of the pink clay can be made. Using the 0.598 mm/yr sedimentation rate over the core interval from the pink clay at 4.0 m to the dated interval at 2.4 m, provides an estimated date of 12.5 cal ka BP (10.5 ^{14}C ka BP) [(4.0 - 2.4 m) / 0.598 mm/yr + 9800 cal yrs = 2675 + 9800 = 12476 cal yrs]. This date is somewhat older than the estimated time of the Marquette readvance, but is sufficiently close to the estimated deposition dates of between about 10.1 to 9.4 ^{14}C ka BP (Zoltai, 1963; Teller and Thorleifson, 1983; Teller and Leverington, 2004; Teller et al., 2005), to confirm the lowermost macrofossil radiocarbon date used for this estimate is reasonable.

The reasons for the ostracode hiatus intervals, which initially appear to be within the Lake Agassiz sequence, are unclear. Similarly, the reason for the end of *C. subtriangulata* just above the pink clay layer within a Lake Agassiz sequence is not clear. Although the overall characteristics of *C. subtriangulata* sequence in the lower portion of the core is similar to the other cores, the early disappearance of *C. subtriangulata* in this core sequence is very different than all the other cores. This part of the core is, however, in an earlier Lake Agassiz sequence, and temporally is very different from the other cores. The lack of *C. subtriangulata* in what should have been the beginning of the LOTWs sequence however is also somewhat problematic. This portion of the LOTWs should have been the deepest part of LOTWs and its environment should have been conducive to both *C. subtriangulata* and *L. friabilis*. *C. subtriangulata* did reappear in small numbers for a short time at about 2.6 m, but the sequence died out. The re-emergence of *C. sharpie* in an intermittent population and in small numbers around 2.0 m, well within what should have been a Lake Agassiz sequence, implies conditions in the coring site were not deep or cold at the time. The emerging nearby islands and landforms in this complex portion of the connection between Lake Agassiz and LOTWs would appear to have been dominant factors in the environment at this coring site at this time.

From Figure 8, it appears this portion of the LOTWs had shallowed somewhat to 0 to 40 m, and the connection to Lake Agassiz through this portion of LOTWs at 10,000 cal yrs BP was a winding narrow, although deep channel. The emerging terrain near this Kenora site and the narrowing channel may have effectively isolated LOTWs at this time from the influences of Lake Agassiz. The deep cold conditions preferred by the *C.*

subtriangulata ostracode may have been terminated prior to the complete isolation of LOTWs from Lake Agassiz. This would explain the ostracode sequence and their disappearance before Lake Agassiz fully isolated sometime around 9000 cal years BP (Figure 9). The uplift of the surrounding terrain in the region, would also account for the early rise in plant, insect and thecamoebians, as well as high charcoal levels due to a relatively early establishment of terrestrial biota nearby.

From the macrofossil data around 3 m (Figure 69), a shallowing sequence appears to be underway, although this is long before the isolation from Lake Agassiz. The insect wing and apparent grass macrofossil around 3.6 m may indicate shallower conditions in Lake Agassiz in this region. An earlier pelecypod macrofossil at 4.2 m, from below the pink clay layer, may reflect the shallowing sequence in this portion of Lake Agassiz before the Marquette readvance. The emerging Lake Agassiz islands and terrain near this Kenora coring site (Figure 8) may be the source of the apparent shallowing and subsequent changing paleoenvironmental conditions reflected in the sediments.

Similarly, charcoal increases at 2.8 m, becoming abundant at about 2.5 m (Figure 69), possibly indicate increasing local aridity at a time when Lake Agassiz conditions should have been present. Once again the specific location of this site within Lake Agassiz may have been affected by the emerging islands and terrain near the coring site. The presence of large charcoal fragments prior to and following the first thecamoebians at about 1.6 m dated at 8.265 ^{14}C ka BP (9.235 cal ka BP), may indicate drier conditions, possibly from

the early climatic variations of the Hypsithermal. This may also mean LOTWs may have operated below the sill of the northern outlets at this time.

Similarly the very early appearance of thecamoebians at 1.5 m just above the dated interval at 1.6 m, of 8.265 ^{14}C ka BP (9.235 cal ka BP), which is preceded by high insect and plant macrofossils, all indicate a very early change to more productive ecological conditions in this core, and point to the emerging terrain as the likely source of significant paleoecological changes. The onset of these conditions occurred prior to the end of the last ostracode horizon, which is near to a radiocarbon dated interval of 6.775 ^{14}C ka BP (7.630 cal ka BP) at 1.1 m.

Summary

The paleoenvironmental conditions of this core are very different from the other LOTWs cores and the lower portions of this core reaches the furthest into the Lake Agassiz sequence, which is confirmed by the appearance of a pink clay bed about 0.9 m above the bottom of the core. The core contains the earliest evidence of thecamoebians at approximately 8.2 ^{14}C ka BP (9.2 cal ka BP) which significantly precedes the ultimate ostracode disappearance at 6.8 ^{14}C ka BP (7.6 cal ka BP). Variability in paleoconditions is evident from the early presence of thecamoebians and subsequent hiatus, a number of hiatuses of ostracodes, and the relatively high abundances of charcoal and insect macrofossils in what should be Lake Agassiz period sediments. The proximity of this location to the complex interconnections between LOTWs and Lake Agassiz and the

emerging landforms, likely resulted in materials being washed from the emerging islands and nearby terrain, through the interconnecting channels (Figure 8). This complexity and the variability in environments at this site make it more difficult to interpret the data from this core.

The early appearance of thecamoebians and disappearance of ostracodes in conjunction with early increases in abundance of plant and insect macrofossils and charcoal Figure 69, may reflect dry conditions in the region and operation of LOTWs below the nearby northern outlets to the Winnipeg River.

5.8.1 Shoal Lake Site - SHO06-2A

This coring site is located in SL in a narrowing portion of a long bay leading to the northwest portion of the SL, in 9.8 m (32.2 ft) of water (Figure 24). Differential isostatic rebound in this area over the interval since LOTWs separated from Lake Agassiz, would be very similar to the deep northern basin near Kenora as it is close to the same line of equal isostatic rebound (Figure 7).

The SL connection to LOTWs is to the southwest of the Kenora outlets so a minor difference in differential rebound of the Shoal Lake connection to LOTWs would occur, but overall the northern basin in LOTWs and Kenora would share a very similar isostatic rebound history. The effect of any difference in the differential isostatic rebound

between the SL to LOTWs interconnection at the shallow Ash Rapids sill, would be a rise in the SL sill elevation, increasing its relative elevation to the LOTWs northern basin (Figure 10) and its interconnection to the Winnipeg River sill. This elevation difference would have reduced due to the slowly equalizing effects of differential isostatic rebound. The modern interconnect was subject to anthropogenic changes which deepened and widened the narrow interconnecting channel, essentially equalizing the lake levels (Shoal Lake Watershed Management Plan, 2001).

SL and the northern LOTWs basin have always been relatively deep (Figure 8), and water level variations since the isolation from Lake Agassiz, would not likely have been as significant to the lacustrine paleoenvironment, as those in the shallow portions of the modern LOTWs (note: the bathymetry data for SL in Figure 10 was not fully available and the paleotopographic maps for this lake should show a bathymetry history similar to the deep northern basin of LOTWs). Its relatively deep bathymetry and its limited connectivity to LOTWs may make the paleoenvironment in SL less subject to change and less responsive to the regional climatic variations than much of LOTWs. Variations in regional evaporation and precipitation were likely the primary means to change the paleohydrology, since its watershed is limited and there are no major fluvial inputs, as there are in the LOTWs. Since SL was, and is today, at a slightly higher elevation than LOTWs it has essentially operated independently and would have different paleoecological conditions after it was essentially separated from LOTWs by its narrow and shallow connection, with only conditions of extreme high water levels in the LOTWs resulting in any exchange of water from LOTWs. Overall the water budget would be

much simpler and more subject to the climatic variations of the evaporation/precipitation balance than LOTWs.

5.8.1.1 **Ostracodes**

The ostracode sequence identified in the bottom of the core does not have the dominant *C. subtriangulata* sequence observed in LOTWs cores although, like the other cores, ostracodes do disappear towards the top of the core (Figure 79). *L. friabilis* and *C. sharpei* populations trend downward starting at 4.1 m to their final disappearance from the record around 3.4 m, at the same time a maximum occurs in *C. Subtriangulata* at 3.9 m. This implies conditions may have moved away from the more saline and warmer conditions preferred by *C. sharpei*, to the deeper, cooler and lower TDS condition preferred by *C. subtriangulata* and usually tolerated by *L. friabilis.* Why *L. friabilis* disappear while *C. subtriangulata* were increasing is not clear, but the disappearance of *C. subtriangulata* and all ostracodes by 3.4 m after a brief increase in all ostracodes indicates conditions were changing at this time. Using a radiocarbon date at 4.5 m of 6.170 ^{14}C ka BP (7.082 cal ka BP) and the date at 1.0 m of 2.525 ^{14}C ka BP (2.636 cal ka BP), the end of ostracodes can be estimated as 5.1 ^{14}C ka BP (5.8 cal ka BP) [(3.5-1.0) / (4.5-1.0 m) X (6170-2525) + 2525 = 5113 ^{14}C BP]. The oldest dated ostracode sequence at about 5.8 m is dated at 6.685 ^{14}C ka BP (7.554 cal ka BP). This estimated date for the disappearance of ostracodes places this interval within the unstable climate conditions of the Hypsithermal and is very much later than other LOTWs sites.

Other fluctuations in ostracode populations occur throughout the ostracode intervals indicated by numerous trends sometimes simultaneous, or out of sequence, or in opposite directions. Clearly there are changing environmental conditions but there is not a clear signal, other than environmental changes were occurring within the lake during the Hypsithermal. The presence of carbonate lithics immediately below and above the last ostracode sequence (Appendix A, Subsection 6.2) implies that chemical changes related to lack of carbonate in the water, was not likely responsible for the disappearance of ostracodes.

The variability in the condition of the *C. subtriangulata* ostracode shells may also represent an indirect climate signal as TDS levels in the lake may have been fluctuating with climate aridity cycles (Appendix A, Subsection 6.2). The other ostracode shells vary from all intact at the bottom, to mostly intact. The fluctuations in *C. subtriangulata* shell conditions throughout most of the core from thin and often broken, to intact may be related to this ostracode being close to its ecological limit, while the other ostracodes are apparently flourishing.

The presence of articulated ostracode shells in various intervals from the bottom of the core to near the top of the ostracode interval, suggest sediments throughout most of the ostracode range were not reworked. The lowermost ostracode sequence does not appear to be within a Lake Agassiz sequence based on the radiocarbon date of 6.685 ^{14}C ka BP (7.554 cal ka BP) at 5.6 m, and the presence of the warmer and shallow water *C. sharpei*

ostracode near the bottom of the core along with low levels of *C. subtriangulata* and *L. friabilis*.

5.8.1.2 **Thecamoebians**

The two thecamoebians intervals, one at the bottom of the core between 6.8-6.6 m and another larger interval above at about 2.8 m, differ from most other LOTWs cores which generally only have thecamoebians in the upper parts of the core. The beginning of the upper interval in this core at about 2.8 m, is estimated to be at about 4.4 ^{14}C ka BP (4.9 cal ka BP) [(2.8-1.0) / 4.5-1.0)] x (6170-2525) + 2525 = 4384]. It was noted the upper thecamoebian interval is preceded by an almost continuously high plant levels although plant materials fell after the beginning of thecamoebians until they returned nearer the top of the core (Figure 78). Insect macrofossils increased after the first thecamoebians were observed. The increasing plant macrofossils indicate the lake was becoming more productive, with the appearance of thecamoebians and subsequent increase in insect macrofossils supporting this interpretation. The high abundance of thecamoebians in the subsamples of the upper interval (Appendix A, Subsection 6.2) and presence of five species may indicate increasingly eutrophic conditions towards the top of the core reflecting a similar pattern observed in the LOTWs cores.

The presence of thecamoebians in two sampled intervals at the bottom of the core is unique to this examined SL core. The lower portion of the core is undated due to lack of suitable macrofossils and an invalid date near the bottom of the core, however based on

the lowermost viable dated sample (6.685 ^{14}C ka BP (7.082 cal ka BP), it appears to be about 7.2 ^{14}C ka BP (8.0 cal ka BP) (see Section 5.8.1.5). The lowermost interval included three types of thecamoebians with a relatively rare abundance level. Nonetheless, their appearance suggests productivity at this time was relatively high. High plant and insect levels at this time confirm this interpretation.

5.8.1.3 **Other Macrofossils**

The relatively high levels of plant and insects in the core and the presence of thecamoebians starting at the bottom, indicates this lake has been productive throughout most of the cored length. The high abundance of both plant and insect macrofossils prior to, and through, the upper thecamoebian interval starting at 2.6 m (Figure 78) support the interpretation that the lake was becoming more eutrophic. The decrease in plant materials after the interval when the upper thecamoebian interval occurred seems somewhat contrary to what would be expected with increasing eutrophication, however the subsequent general increase in abundance of the insect component and abundant thecamoebians seems to infer shallower water and productive environment existed.

The insect component in the bottom portion of the core is dominated by larvae cases with the uppermost portions a combination of insect exoskeletons and larvae cases (Appendix A, Subsection 6.2). It is not clear why this characteristic exists, other than perhaps indicating slightly deeper conditions when only larvae cases are noted, which may have

been washed into the deeper water due to their relatively small size or floated over and sank in deeper water.

Increasing charcoal levels, including larger charcoal fragments starting at the beginning of the upper thecamoebian level, may be an indicator of more arid conditions in the SL and LOTWs region, which may also have created lower lake levels and possibly more eutrophic conditions at this location in the lake. The sharp increase in charcoal levels at 2.8 m dated at about 4.4 ^{14}C ka BP (4.9 cal ka BP) which remain relatively high to the top of the core, include large charcoal fragments. These large charcoal fragments infer nearby fires and indicate drier climatic conditions may have prevailed at various times.

The trend in charcoal abundance seems to correspond with apparent increases in the lake productivity. The minimum charcoal interval at about 2.3 m above the first appearance of thecamoebians then rises somewhat before falling and once again rising to the more abundant levels which may be indicative of a change in climatic to drier conditions (Figure 78). Large charcoal fragments in the upper core interval (Appendix A, Subsection 6.2) indicate nearby fires and possibly increasing aridity in the region. Small amorphous charcoal fragments in some intervals, indicate the fires were more distal, and several intervals varying from distal to more proximal locations were noted. Large charcoal fragments near the bottom of the core, including what appear to be bark fragments, imply there was a nearby forest at this time. This further confirms the bottom of this core was not in a Lake Agassiz sequence along with the large (1 cm) charcoal leaf fragment found at 5.6 m which was dated at 6.685 ^{14}C ka BP (7.554 cal ka BP). High

aquatic plant levels were also noted in the earliest parts at the bottom of the core providing additional evidence of non Lake Agassiz conditions.

The presence of fish macrofossils throughout the core, including high incidence of these biota in bottom intervals of the core, in conjunction with high plant and insect components at this time, imply the paleolacustrine conditions may have been more productive throughout the period represented by this core. The presence of these vertebrate macrofossils throughout the core further confirms the bottom of the core is not a Lake Agassiz sequence.

The gastropod shell at 6.1 m and pelecypod shell at 3.4 m (just beyond the end of ostracodes) in conjunction with carbonate lithic evidence found in this interval, confirms the existence of appropriate chemical conditions for ostracode shell development, after the interval in which they disappeared. The presence of these macrofossils and carbonate lithics as noted earlier, implies changes in paleochemistry related to $CaCO_3$ levels, were not responsible for the disappearance of ostracodes.

The presence of seeds starting at about 2.8 m with levels becoming increasingly more common to about 0.5 m, implies changes in the nearby surrounding terrestrial conditions were underway. The birch nutlets found at 1 m and dated to 2.525 ^{14}C ka BP (2.636 cal ka BP) indicates modern deciduous forests were present at this time.

5.8.1.4 **Lithic Grains**

Lithic grains in this core are generally in low abundance (Figure 78), with some intervals elevated in the abundance of non disaggregated clay balls, and only two intervals with elevated quantities of quartz lithics. This is very different from the LOTWs cores. Perhaps the relatively small watershed including the lack of a major river system running through it, are responsible for this characteristic. Additionally, it is unlikely any significant reworking of glacial deposits occurred in SL, as this lake was not subject to the differential isostatic rebound induced transgression evident in the southern basin of LOTWs.

The high levels of clay balls in certain intervals, primarily occurring near the bottom and close to the top, may be due to difficulties experienced in disaggregating subsamples in this core, although one interval at 5.1 m did have high levels of large clay pellets with deep blue staining (possibly vivianite). This implies the presence of carbonate clay balls were not just a result of difficulties in processing the subsamples. The extended interval of carbonate lithics from 4.6 to 2.6 m encompasses the interval where a pelecypod was found. As noted earlier, the presence of carbonate lithics immediately below and above the last ostracode sequence, and the pelecypod (Appendix A, Subsection 6.2), further supports the premise that chemical changes related to lack of carbonate in the water, were not likely responsible for the ostracode sequence ending.

5.8.1.5 **Core Chronology**

Of the five radiocarbon dates obtained in this core two were rejected. The chronology is based on the remaining three dates and all are well sequenced (Figure 79). The youngest date of 2.525 ^{14}C ka BP (2.636 cal ka BP) at 1 m, is used in conjunction with the next lower valid date to estimate the beginning of thecamoebians at about 4.4 ^{14}C ka BP (4.9 cal ka BP) and was used to estimate sedimentation rates in the upper portion of the core. The two oldest valid dates of 6.170 ^{14}C ka BP (7.082 cal ka BP) at about 4.5 m and the date closest to the core bottom 6.685 ^{14}C ka BP (7.554 cal ka BP) at 5.6 m, are well within the estimated LOTWs (SL) isolation date from Lake Agassiz. Extrapolating from the lowermost date, the bottom of the core is estimated to be about 7.2 ^{14}C ka BP (8.0 cal ka BP) [(6685 - 6170 ^{14}C yrs) / (5.6 - 4.5 m) = 468 ^{14}C yrs x 6.9 - 5.6 m = 562 yrs + 6685 = 7247 ^{14}C yrs BP (8032 cal yrs BP)].

The validity of the estimated date for the bottom of the core is supported by the macrofossils in this portion of the core, specifically the higher plant and insect macrofossils, and high charcoal levels including large charcoal fragments (Appendix A, Subsection 6.2). Additionally, the bottom ostracode interval of the core is not dominated by *C. subtriangulata*, and thecamoebians are present at the bottom of the core.

5.8.1.6 **Sedimentation Rates**

The overall sedimentation rate based on the oldest radiocarbon date available of 6.685 ^{14}C ka BP (7.554 cal ka BP) at 5.6 m, to the top of the core, is about 0.7 mm/yr [5.6 m /

7554 cal yrs = 0.741 mm/yr]. The uppermost sedimentation rate is estimated at 0.4 mm/yr [1.0 m / 2636 cal yrs = 0.379 mm/yr].

The sedimentation rate in the middle portions of the core, from the lowest available radiocarbon date of 6.685 ^{14}C ka BP (7.554 cal ka BP), to the uppermost date of 2.525 ^{14}C ka BP (2.636 cal ka BP) at 1.0 m, is estimated at 0.9 mm/yr [(5.6 - 1.0 m) / (7554 - 2636 cal yrs) = 0.935 mm/yr]. The sedimentation rate in the middle portion of the core is high, but comparable to some other LOTWs mid-core sedimentation rates, however, it has a relatively high overall rate of 0.7 mm/yr. The reasons for such a high sedimentation rate when compared to LOTWs and other regional lakes such as ELA Lake 239, are not immediately evident. It is possible the relatively small modern SL watershed, may have been larger in the past, with possible inflows through Falcon Creek from the Falcon and High Lake watersheds may have input sediments but the relatively few quartz lithics intervals do not seem to support this. Based on the long gyttja sequences observed in the core, it is possible the biota within SL including high levels of cyanobacteria, may have resulted in high sedimentation rates, especially during climate induced eutrophic intervals.

5.8.1.7 **Discussion and Interpretation of Coring Site Data**

The ostracodes species in the lower part of the core (Figure 77) do not correspond with the typical Lake Agassiz sequence dominated by the *C. subtriangulata* ostracode that were observed in the other cores, indicating the bottom of this core is not into Lake

Agassiz sediments. This is confirmed by the extrapolation downward from the lowermost valid radiocarbon date to obtain an estimated date of about 7.2 ^{14}C ka BP (8.0 cal ka BP) for the bottom of the core (Section 5.8.1.5). The low quartz lithic, high charcoal abundances including large fragments, abundant plant and insect components, and presence of thecamoebians (Appendix A, Subsection 6.2), all indicate the bottom of the core is not a Lake Agassiz sequence (Figure 78). The bark fragments and a leaf fragment in conjunction with abundant charcoal in subsamples near the bottom of the core, also suggest there was a nearby vegetated terrain and arid conditions, which in combination with evidence of fish, provide further evidence these sediments are not likely Lake Agassiz sediments.

The fluctuations in the ostracode species populations up until they disappear at about 3.5 m at about 5.1 ^{14}C ka BP (5.8 cal ka BP) appear to be related to changing bathymetric and climatic conditions during the unstable Hypsithermal period. Their abrupt disappearance at 3.5 m may be related to a significant environmental change at this time, which is also reflected in the plant and insect macrofossils (Figure 78). The presence of carbonate lithics immediately below and above the last ostracode sequence and the presence of a pelecypod shell at 3.4 m (Appendix A, Subsection 6.2), directly above the end of the ostracodes, implies that chemical changes related to lack of carbonate in the water, was not likely responsible for the ostracode sequence ending.

The presence of *C. subtriangulata* throughout most of the lower part of the, core although mostly in low numbers, implies conditions in the lake were relatively deep, cold and had

low TDS levels. Variations in temperature and TDS levels are indicated by changes in the other ostracodes. A peak in *C. subtriangulata* near the top of the ostracode interval indicates a possible deepening and with cooler water conditions still available in a deeper water environment, likely below the thermocline. Decreasing plant and insect levels at this time appear to support the possibility conditions could have been cooling.

The higher levels of more saline tolerant ostracodes at the bottom of the core (*C. sharpie* and *F. rawsoni*) indicate the initial phase of the core, may have had relatively high TDS levels. The limited number of insect exoskeleton fragments at the bottom of the core, while larvae cases remain high, may also be an indicator of deeper waters near the bottom of the core although both of the deeper colder ostracodes (*C. subtriangulata* and *L. friabilis)* were in decline. Fragile and broken *C. subtriangulata* shells near the bottom imply this species of ostracode may have be at its ecological limit in this interval, perhaps responding to warming, shallowing and higher trending TDS levels. The presence of articulated ostracode shells near broken *C. subtriangulata* shell intervals, and intact shells of other ostracode species, confirms shell damage is not due to transport or reworking of ostracode shells.

The almost continuously high plant levels prior to the upper thecamoebian interval (Figure 78), implies conditions were becoming more eutrophic, with the appearance of thecamoebians supporting this interpretation. The high abundance of thecamoebians in the subsamples of the upper interval and presence of five species (Appendix A, Subsection 6.2), also indicates an increase to more eutrophic conditions towards the top

of the core. There is a decrease in plant materials after the initiation of the upper thecamoebian interval contradicting the interpretation of increases in productivity, however the increase in insect levels above the thecamoebian interval does support a shallower water and more productive environment interpretation. Towards the top of the core an increase plant macrofossils indicates lake productivity was increasing.

Conditions from the end of the ostracode interval at about 5.1 ^{14}C ka BP (5.8 cal ka BP) appear to be trending to a shallower, or a warmer water interval, based on the beginning of thecamoebians at 2.8 m dated at about 4.4 ^{14}C ka BP (4.9 cal ka BP), and the generally increasing plant and insect levels. The increase in charcoal at the beginning of thecamoebians at 2.8 m also provides evidence of a drier local climate at this time. The trend in charcoal abundance to a minimum after the interval of charcoal abundance possibly indicates a short wetter interval occurred at this time before charcoal levels increased indicating a return to drier climate conditions in the upper part of the core. A simultaneous maximum in plant, insect, charcoal and thecamoebians at 0.3 m indicates a relatively recent dry period occurred before a return to a lower level of productivity at the top of the core. Using the uppermost radiocarbon date and assuming a constant sedimentation rate, this arid interval can be estimated to have occurred at 0.8 ^{14}C ka BP (0.7 cal ka BP [0.3 / 1.0 X 2525 ^{14}C BP = 757.5 ^{14}C BP (~ 687 cal BP)] which appears to correspond with the end of Medieval Warm Period.

The presence of fish biota and the high plant and insect components, throughout the core, imply the paleolacustrine conditions may have been more productive in SL than LOTWs.

This is further supported by the sedimentology of the core. The long 5.75 m sedimentary unit of the top unit of the core which is primarily a clayey silty gyttja, and the lower slightly laminated slightly silty clay, are very different from LOTWs cores. The unusually high sedimentation rates in the SL are also very different than LOTWs and may have been influenced by the high productivity in the lake including periods where cyanobacteria were abundant which may have further increased sedimentation rates and the formation of gyttja deposits. The high productivity in SL throughout the history of this core indicates the connection to LOTWs was either not a significant interconnection, or perhaps not in play at all over long intervals, allowing Shoal Lake to be more or less independent from LOTWs for most of its lifetime.

Summary

Evidence from the bottom of this core, including the presence of ostracode species not normally found in Lake Agassiz sediments, a low quartz component in the sediments, high plant and insect components, high charcoal levels, presence of thecamoebians, and common fish macrofossils, all indicate that this core does not extend into Lake Agassiz sediments despite it being the longest examined core. This is further confirmed by radiocarbon dating which places the bottom of the core at about 7.2 ^{14}C ka BP (8.0 cal ka BP) (Section 5.8.1.5).

Throughout the core, the relatively high incidence of aquatic plant, insect and fish macrofossils, and the sedimentology, all indicate the sediments in this core were

deposited during relatively eutrophic conditions compared to LOTWs, and the lake likely operated independently from LOTWs.

CHAPTER 6 CORE DATA INTEGRATION AND INTERPRETATION

6.1 GENERAL

In Chapter 5 the interpretation of the history at each coring site in LOTWs and SL (Figure 24) was performed based on the data from each specific core, while the effects of differential isostatic rebound at each site were considered. The various regions (subbasins) in LOTWs (southern basin, Northwest Angle basin, Northwest Angle channel and the outflow sites at Kenora) and SL, each experienced somewhat different histories due to their topography, elevation, and the effects of differential isostatic rebound. Many of these subbasins of LOTWs were not always connected during the Holocene because lake levels (due to isostatic rebound and/or climate) did not always rise over thresholds separating one basin from another. Studying the coring sites individually, provided the means to establish the paleohydrology at each site and more easily differentiate climate driven changes from those of differential isostatic rebound, without unduly complicating the interpretations due to spatial and temporal variations in this complex lake. To more fully understand the paleohydrology of LOTWs and SL and the paleoclimate of the LOTWs region, data from the six available cores now need to be integrated. Additionally, the data from the two Northwest Angle companion cores (WOO06-5A and WOO06-6A), come from two different nearby locations and can be compared to help trend the changing water depths in this region of LOTWs. To a limited degree site comparisons were made to assist in individual site interpretation in Chapter 5, however, a broader examination is required and is presented in this Chapter.

Data from the coring sites are integrated and discussed in the following sections based on ostracode, thecamoebian, charcoal macrofossil, and sedimentation rate data, while considering the nature and composition of the sediment, radiocarbon dates and variations of the macrofossils and lithic grains identified in the subsamples. Once these data are integrated, broader interpretations can be made to help to develop an overall history of LOTWs and SL which is summarized in Chapter 7.

In order to integrate the data from the cores, a number of figures have been developed. Figure 81 is a composite of stratigraphic sections of LOTWs and SL cores and includes radiocarbon dates. The locations of paleosols, an important organic-rich bed inWOO06-4A, and a pink clay bed in WOO07-7P are indicated. Figure 82 builds on Figure 81 and includes the ostracode and thecamoebian data. Figure 83 overlays abundance of charcoal data.

Some broad observations and conclusions are reached which were common to most cores. The ostracode and thecamoebian macrofossils do not range the entire core length and the timing of their appearance and disappearance provides important markers within the cores. In addition variations in the charcoal content and the size of the charcoal fragments may reflect climatic changes in the region. Variations in plant and insect biota also provide the means to track changes in the lake ecosystems and help to identify changes in lake productivity due to warming climatic conditions. The abundance and types of lithic grains in the cores also provided information on changing sedimentary

conditions in the cores, and helped to further discriminate the locations of paleosols in some cores, identify the transition from Lake Agassiz to LOTWs, and identify potential changes in the availability of carbonates. All of these data provided the means to identify hydrologic changes in the lakes and changes in regional climatic and are located in Appendix A, Subsection 2 for each core (i.e. Appendix A, Subsections 1.2, 2.2, 3.2, 4.2, 5.2 and 6.2).

Figure 81 shows the overall core stratigraphy including the location of the paleosols and indicates the location of the radiocarbon dates which were obtained for the cores. Not all radiocarbon dates were used, with suspect dates rejected for various reasons as discussed earlier.

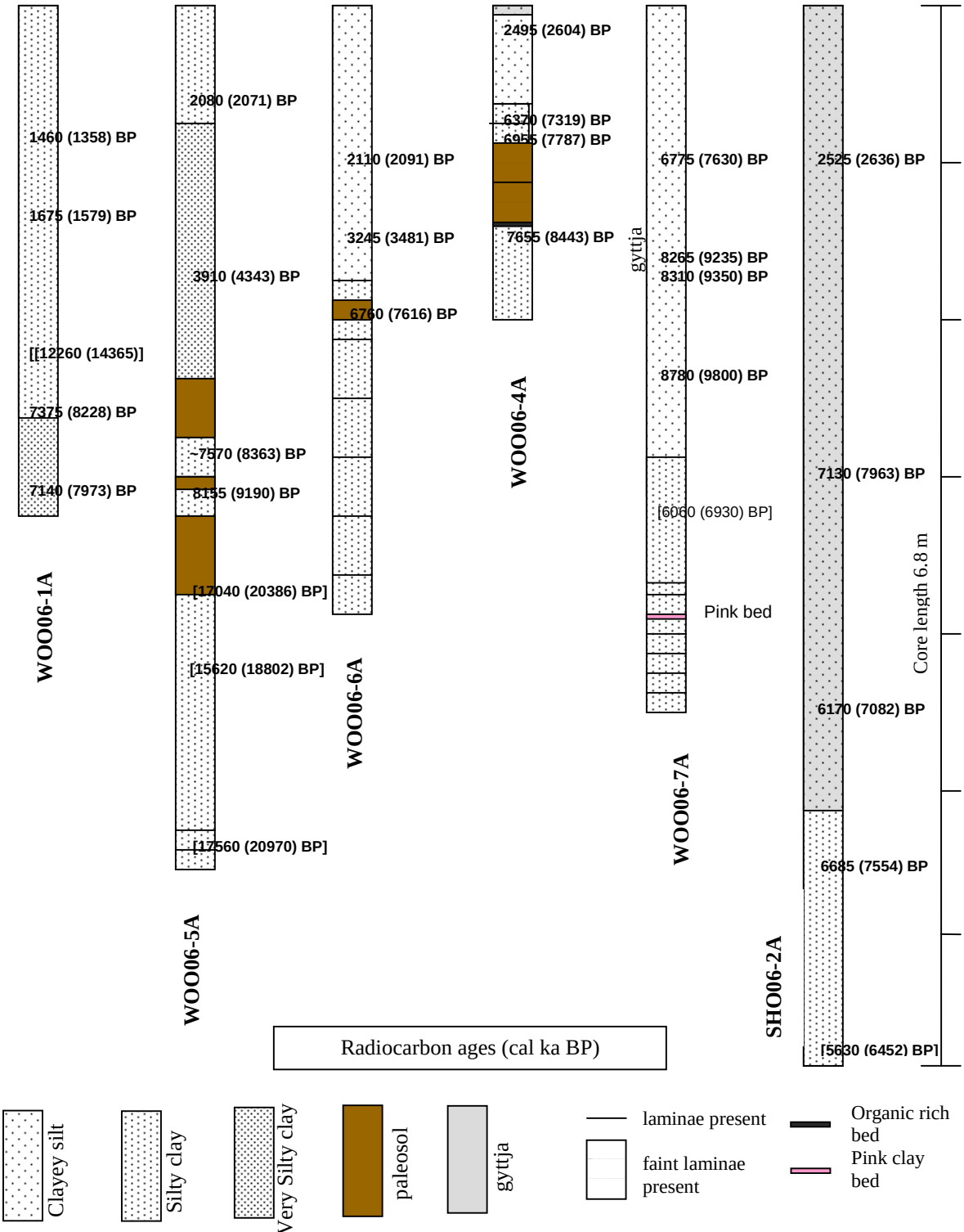

Figure 81. Schematic stratigraphic sections of LOTWs and SL cores. Radiocarbon dates are indicated [aberrant dates in square brackets]. Locations of paleosols, an organic-rich bed (WOO06-4A), and a pink clay bed (WOO06-7A) are shown. Ages between paleosols in WOO06-5A are averaged. A scale with metre intervals is provided on the right. LOTWs cores are arranged starting on left from south to north.

6.2 OSTRACODE DATA – INTEGRATION AND INTERPRETATIONS

6.2.1 General

The ostracode populations in LOTWs cores are highly variable, reflecting the ecological complexity in LOTWs as it separated from Lake Agassiz, and the effects of differential isostatic rebound and the changing climate exerted their influence. The most notable characteristic is that ostracodes disappear in the upper portions of the cores (Figure 82). Ostracode populations also become more diverse upward in the sequence before disappearing, except in WOO06-4A where only *C. subtriangulata* is present, and in SHO06-2A which has a relatively diverse population throughout the ostracode interval. The increase in diversity upwards may reflect increasing TDS levels (Figure 33). The lowermost part of the ostracode zone is almost exclusively *C. subtriangulata* in most cores, inferring deep, cold, and low TDS conditions. The exception is in the SHO06-2A core where *C. subtriangulata* doesn't become dominant until close to the top of the ostracode interval (Figure 77), indicating a significantly different paleoenvironment in SL. SL appears to have moved from relatively shallower and warmer conditions near the bottom to a deeper phase with *C. subtriangulata,* suggesting they were possibly living in colder water environments below the thermocline.

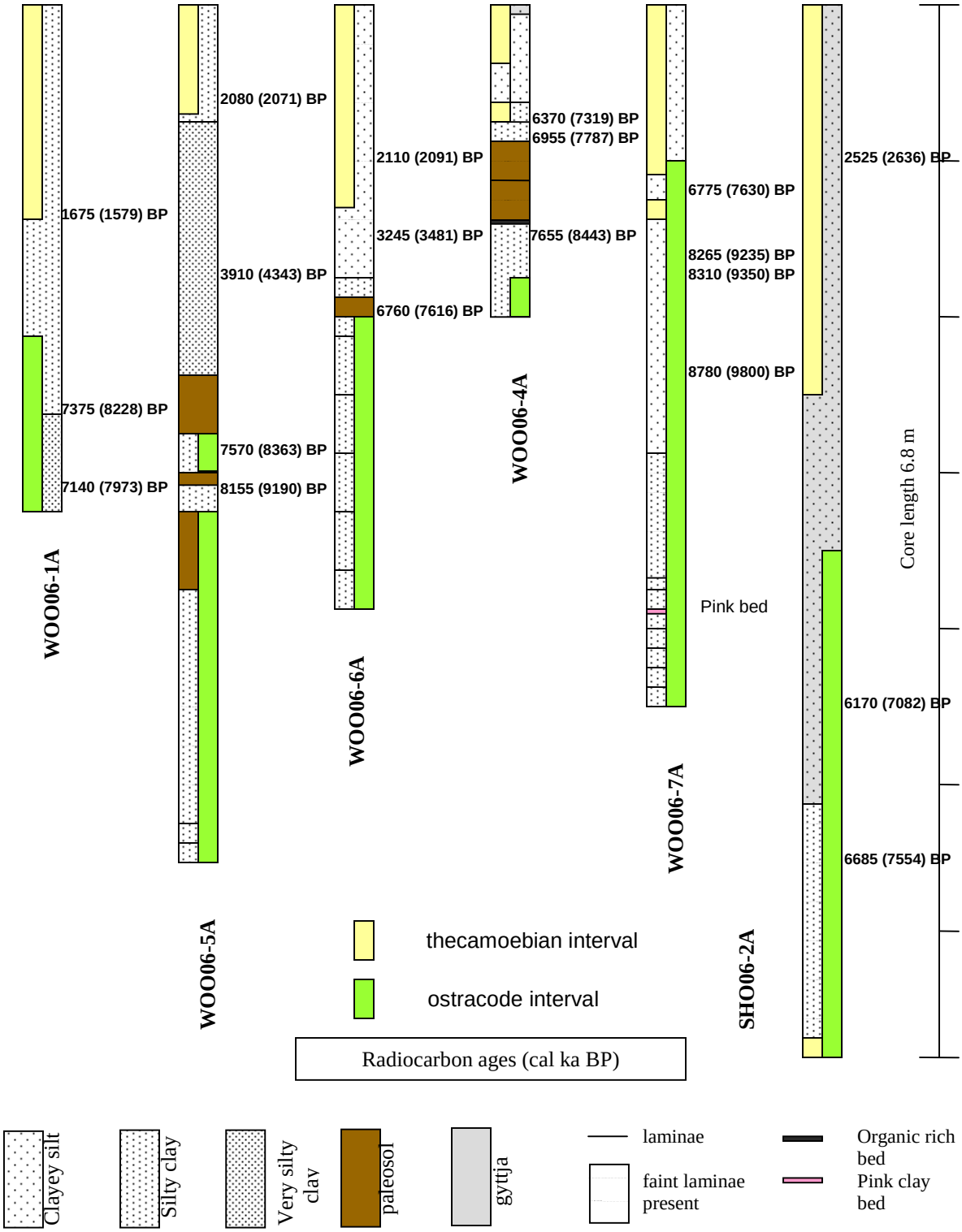

Figure 82. Location of ostracode and thecamoebian intervals of LOTWs and SL cores. The intervals are superimposed on the schematic stratigraphic sections with key radiocarbon ages indicated and aberrant dates removed for clarity; note the two radiocarbon dates between the paleosols in WOO06-5A are presented here as an average. A scale with metre intervals is provided on the right.

6.2.2 Possible Reasons for the Disappearance of Ostracodes

The disappearance of ostracodes (Figure 82) and other organisms with $CaCO_3$ shells in the upper parts of all cores, probably reflects a change in the chemistry of the lakes, and may be related to the lack of the bicarbonate or calcium ions necessary for shell production. Furthermore, low levels of Ca and CO_3 may result in re-solution of carbonate shells through diagenetic changes on the lake floor or within the sediments. The presence of well preserved pelecypods and gastropods above the end of the ostracode intervals, and the presence of carbonate lithics and calcareous clay balls within and above these intervals in a number of cores, imply that this chemical change is an unlikely candidate to explain the disappearance of ostracodes from the record, since Ca and CO_3 were clearly available. Additionally, although in some cores the ostracode shells (particularly *C. subtriangulata*) appeared broken and thin near the time they disappeared, some *C. subtriangulata* and other species in the same interval were observed to be intact and showed no sign they were thinning due to chemical re-sorption (Appendix A, Subsections 1.2, 2.2, 3.2, 4.2, 5.2 and 6.2). No specific trend indicating decreasing shell thickness was observed in the cores as the ostracode interval terminated.

In some cores, ostracode shells seemed to be coated with what appeared to be carbonate deposits. It is possible a leaching process could have occurred within the sediments and have been related to increasing acidity in the lakes. However, no coatings were observed on the ostracode shells in SL or in the WOO06-5A-1K core, while in other LOTWs cores like the Kenora core (WOO06-7A-1P), coatings spanned much of the ostracode interval. It seems more likely lower pH levels may have interfered with the production of

ostracode shells, although some shells could have been eliminated from the record due to post diagenetic changes as was discussed in Section 3.2.3 (Chemical Influences on the Presence of Ostracodes). The presence of more acid-tolerant thecamoebians in the upper part of the cores, which generally increase in abundance upward, seems to support the idea that pH in the lakes may have been increasing, making ostracode shell production and preservation more difficult. Increasing acidity may have been due to the continued terrestrial inputs into the LOTWs basin, including an increasing humic acid component from the influences of post glacial terrestrial biota. This, and the reduction of inputs of some incoming ions such as bicarbonate, as the watershed became more stable and as soil production reduced carbonate availability by erosion of glacial drift, may also have contributed to increased acidity (J. Teller, 2009, personal communication).

The presence of ostracode species in the lower portions of all six of the cores implies paleochemical conditions were similar in the various coring locations around LOTWs. As discussed above, the disappearance of ostracodes in the upper portions of all cores indicates there was a change in conditions throughout the LOTWs region that affected the viability and/or the preservation of ostracodes. From the radiocarbon ages in Figure 82 this indicates the chemical conditions in LOTWs suitable for ostracodes changed somewhere between 6.8 and 7.3 ^{14}C ka BP (7.6 and 8.0 cal ka BP) (Sections 5.5.1.1 and 5.6.1.1), with the WOO06-4A-1K Northwest Angle core occurring much earlier at 8.8 ^{14}C ka BP (9.8 cal ka BP) (5.4.1.1) and SL much later at 5.1 ^{14}C ka BP (5.8 cal ka BP) (Section 5.8.1.1). The underlying geology of the region of course did not change, but overland inputs from the watershed would have changed due to the warming post-glacial

climate and the stabilizing effect of the colonizing terrestrial biota. In addition, the availability of the calcareous component from Lake Agassiz sediments would reduce over time as the watershed vegetated, and carbonate availability was primarily limited to those carbonate bearing components within LOTWs. The increased terrestrial cover in the region and an associated increase in humic acidic inputs and subsequent reduction in bicarbonates in the lakes, were likely a primary driving force for the disappearance of ostracodes in LOTWs and SL in the upper cores.

Over time, the input from calcareous drift and Lake Agassiz deposits in the watershed and reworked Lake Agassiz deposits slowly decreased as the watershed was stabilized by vegetation and exposed deposits at the shoreline were no longer available. This could have further reducing the availability of these inputs, and subsequently changed the chemical conditions in the lakes until these conditions no longer supported ostracodes. The 990,000 year sediment sequence in nearby West Hawk Lake does not have suitable conditions for production and preservation of ostracode and bivalve shells, due to the slightly basic conditions and low alkalinity of ~ 24 mg/L ($CaCO_3$) (Teller et al., 2008). Mean alkalinity in LOTWs today is about double at 44.5 mg/L ($CaCO_3$) and is also slightly basic with a mean pH of 7.8 (Pla et al., 2005), and remains well below the calcite branch point (typically ~ 250 mg/L (Forester, 1987). TDS levels are estimated to have been typically about 100 mg/L in Lake Agassiz (Curry, 1997) implying there have been significant changes from the historical periods of the LOTWs. These changes and the movement to more acidic conditions induced by the influx of humic acid runoff into the LOTWs basin, may have tipped the balance and changed the niche the ostracodes had

occupied to less favourable conditions, and decreased the probability that survivors would be preserved in the sediments.

6.2.3 Ostracode Populations; The Transition From Lake Agassiz to LOTWs

The lacustrine paleochemical conditions may have slowly changed after LOTWs became isolated from Lake Agassiz and fresher meteoric sourced inputs replaced the turbid glacial-melt input. The Lake Agassiz sediments consist of fine grain sediments suspended in the turbid melt waters coming from the LIS and from wave resuspension of those previously-deposited lacustrine and glacial sediments (Teller et al., 2008). The paleochemistry in LOTWs and SL continued to be strongly influenced by Lake Agassiz through its reworked sediments in LOTWs and its watershed, even after the lakes became isolated from Lake Agassiz. Reworking of previously deposited sediments, including calcareous lacustrine sediment and glacial drift, within the smaller LOTWs basin and along the shorelines, as well as erosional inputs from the Rainy River watershed would have continued to contribute ions to the lake, including bicarbonate, although this contribution would have diminished as the watershed and water levels became more stable. This means hydrochemical conditions in the LOTWs basin may have remained similar during the early post Lake Agassiz period, continuing to provide a suitable environment for ostracodes.

Variability in climate during the unstable Hypsithermal would induce further changes beyond the general trend from the warming post glacial climate and the waning effects of Lake Agassiz. Changes in groundwater, fluvial, and the overland inputs into the basin

would probably induce periodic changes in water chemistry impacting ostracodes. Aridity, which was documented just to the west of LOTWs in the bordering grasslands, would have influenced the LOTWs region, affecting the evaporation/precipitation ratios and resulting in higher TDS levels in LOTWs and SL. Drier periods caused decreases in terrestrial plant biota (see Teller et al., 2008) and forest fires in forested areas, and would change watershed erosional inputs further increasing TDS beyond those which are induced as a result of increased evaporation. Exposure of lake sediments in periods of low water levels would also result in re-suspension of the minerals laid down in an earlier time (Risberg et al., 1999) reintroducing calcareous sediments from earlier deposits and also increase TDS levels. The introduction these sediments would contribute to increased TDS levels and may change the percentage of calcium and bicarbonate, and calcite may even precipitate if it exceeded the calcite branchpoint (Figure 32) (Curry, 1999; Smith and Horne, 2002). The calcite branchpoint is fundamental to ostracode species diversity and abundance (Figure 33).

The changes in the paleochemistry in conjunction with changes to paleoecological conditions would result in changes in the ostracode species observed in LOTWs and SL sediments as they progressed towards modern conditions. A fundamental change in hydrochemistry appears to have resulted in ostracodes eventually disappearing as the influences of Lake Agassiz and its sediments waned and the LOTWs and SL moved to more modern conditions.

6.2.4 Integrating and Interpreting the Ostracode Record

The dates for the disappearance of ostracodes from the record are relatively consistent throughout most of LOTWs given the inherently poor discrimination in interpolating and extrapolating from the available radiocarbon dates, with most cores indicating a disappearance of ostracodes (Refer to Sections 5.2.1.1, 5.4.1.1, 5.5.1.1, 5.6.1.1, 5.7.1.1 and 5.8.1.1) by about 6.8 to 7.3 ^{14}C ka BP (7.6 to 8.0 cal ka BP) (Figure 82). Table 3 summarizes these dates and for completeness provides additional data related to thecamoebians and sedimentation rates. In the Northwest Angle core (WOO06-4A) ostracode disappearance was much earlier at about 8.8 ^{14}C ka BP (9.8 cal ka BP) indicating this channel site was very different from the open basin locations near this site.

The disappearance of ostracodes from the SHO06-2A core dated at about 5.1 ^{14}C ka BP (5.8 cal ka BP), is much later than the others. This difference in timing for the end of the ostracode interval and the characteristically different ostracode sequences in SL, are prime indicators that this lake had a different and probably mainly isolated paleoecological environment from that of LOTWs, despite its very similar bedrock geology. However, the changing hydrological conditions around the LOTWs, was much more complex due to the larger LOTWs watershed and effects of differential isostatic rebound. The diversity of ostracode species in SL may have been affected by the shedding of terrestrial materials from the Lake Agassiz island to the west (Figure 8) which has a very different surface geology (Figure 16); the TDS levels and ionic composition may therefore have been different than those in LOTWs.

Table 3. Interpretation Summary of Ages of Disappearance of Ostracodes and Appearance of Thecamoebians, and Estimated Sedimentation Rates in LOTWs and SL Cores

Core #	Last ostracode interval	First appearance thecamoebians	Sedimentation Rates (mm/yr)			Comments
			overall	mid-core	upper	
WOO06-1A	7.3 (8.0)	1.7 (1.6)	0.4	0.3	0.9	This core is unique; has the latest date for disappearance of ostracodes and latest appearance of thecamoebians, and a high sedimentation rate including the highest upper core rate.
WOO06-4A	8.8 (9.8)	6.5 (7.4)	0.2	0.9	0.1	Material was lost from the top of the core during core recovery so this estimate does not include the uppermost part of core.
WOO06-5A	<7.0 (7.8)	2.3 (2.3)		0.4	0.5	The presence of multiple paleosols make estimates of the overall sedimentation rate difficult and likely unreliable.
WOO06-6A	6.8 (7.6)	2.8 (2.9)	0.2	0.2	0.2	The presence of a paleosol and lack of radiocarbon dates below the paleosol, reduce the accuracy of the overall sedimentation rate.
WOO06-7A	6.8 (7.6)	8.2 (9.2)	0.2	0.6	0.1	The early appearance of thecamoebians overlapping the ostracode interval is unique.
SHO06-2A	5.1 (5.8)	4.4 (4.9) 7.0 (7.8)	0.7	0.9	0.4	The two thecamoebian intervals are unique to this core.

All dates are approximate, with some projected from the available radiocarbon dates, and are expressed as ka BP, with calendar years following in brackets.

The lack of significant tributaries and the cul de sac morphology of SL with its historic inflow into LOTWs (Shoal Lake Watershed Management Plan, 2001) means SL was not likely influenced by changes in fluvial inputs or overland inflow changes, as much as the much larger LOTWs watershed. Perhaps for this reason, ostracodes do not disappear in SL for more than 1500 years after they disappeared from LOTWs. The evaporation/precipitation ratio would be the same in both of these essentially hydrologically independent lakes, so the difference in the size of the two basins may have helped determine the viability of ostracodes in these lakes and accounts for the differences observed between SL and LOTWs.

The ostracode interval in the southern basin WOO06-1A core is dominated by *C. subtriangulata* which infers cold, deep and low TDS conditions existed up until about 7.3 ^{14}C ka BP (8.0 cal ka BP) (Figure 43) when the ostracodes disappeared, however, lake reconstructions based on isostatic rebound indicate this location would have emerged from Lake Agassiz by about 10.0 cal ka BP and not yet have become part of the expanding LOTWs water body (Figure 9). As can be seen from Figure 9, the WOO06-1A site would have been inundated by expanding LOW by 6000-7000 years ago, suggesting that an independent lake existed in the southern part of the basin during the early post-Agassiz period. In fact, in this core ostracodes were present at the bottom of the core and were estimated to have disappeared at around 7.3 ^{14}C ka BP (8.0 cal ka BP), which is the 2nd earliest time of disappearance and 500 years before their disappearance in other locations (Table 3). One explanation for this discrepancy may be that a deep compartment (lake) within the southern basin in this region was supplied by the Rainy

River drainage system. A wetter climate in the Rainy River watershed and LOTWs watershed may also have maintained deep lakes in the southern basin of LOTWs.

The ostracode signals all show a similar upward increase in the number of species indicating a similar overall change to higher TDS conditions which were likely driven by a drier climate. Support for the interpretation that the change in TDS level was driven by a drier climate is provided by paleosol formation in the cores of the Northwest Angle at this time. The multiple paleosols in the WOO06-5A indicates there may have been a number of dry climate periods, although other factors may have been at play in the formation of the earliest paleosol. One possibility may be that sediments shed from the emerging island to the west (Figure 8) caused associated infilling of the Northwest Angle area and/or a low level phase occurred in Lake Agassiz due to a change in an outflow location at the eastern outlets. The shed materials may also have influenced timing of the formation of the other paleosols based on Figure 8 and Figure 9 as this part of the basin infilled and shallowed.

The unique exclusive *C. subtriangulata* population in the WOO06-4A core and the available radiocarbon date supports the interpretation this ostracode interval was within a Lake Agassiz sequence at this site. A rough estimate for disappearance of ostracodes at this site is about 8.8 ^{14}C ka BP (9.8 cal ka BP), and is well within a late Lake Agassiz sequence (Figure 8) for this location and is the earliest date identified for ostracode disappearance. Figure 9 predicts this area was dry at about 8.1 ^{14}C ka BP (9.0 cal ka BP) which is much later than the disappearance date. It is unclear why *C. subtriangulata*

ostracodes disappeared at his time, but may have been influenced by the factors noted above.

Ostracodes are present in sediments below the uppermost paleosol in the nearby Northwest Angle basin site WOO06-5A core, and are roughly estimated to have continued until they disappear at about 7.0 ^{14}C ka BP (7.8 cal ka BP) (Figure 80), although ostracodes within the above paleosol indicates they continued sometime after this. Ostracodes in the WOO06-6A core are estimated to have disappeared at 6.8 ^{14}C ka BP (7.6 cal ka BP) (Section 5.6.1.1). This confirms the presence of lake conditions until about this time. In WOO06-4A, a shallowing sequence above the ostracode interval at 7.655 ^{14}C ka BP (8.443 cal ka BP) indicated by the black organic rich bed and subsequent paleosol, corresponds reasonably well with the beginning of the upper paleosol in nearby WOO05-5A and the paleosol in WOO06-6A (Figure 82) which ended this lake sequence in the Northwest Angle region of LOTWs. This indicates the timing of the terrestrial conditions indicted in Figure 9 does not correspond with the paleohydrology in this part of LOTWs at this time. Lake conditions at the Northwest Angle basin sites appear to have continued about 1000 years after the indicated terrestrial conditions from the isostatic rebound calculations. Wetter climatic conditions and operation above the outflow elevation prior to this time may be the reason for this non correlation.

The ostracode interval in the Kenora core (WOO06-7A) core disappears at about 6.8 ^{14}C ka BP (7.6 cal ka BP) (Section 5.7.1.1). This is similar to most other cores but in this case extends well into the thecamoebian interval (Figure 71) which is unique in the

examined cores.

6.2.5 Summary of Ostracode Data Interpretations and Integrations

Complications from the differential isostatic rebound and the very complex morphology and ecology of LOTWs, and the differing ostracode data encountered in the various cored regions of LOTWs, some possibly related to unconformities, makes it very difficult to extract both paleoclimate and paleohydrologic signals. Furthermore, the limited number of radiocarbon dates in some cores and uncertainties due to aberrant dates, make it difficult to correlate with the paleotopographic maps of Lake Agassiz and LOTWs produced by Yang and Teller (2005). Despite the uncertainties and the gaps in the radiocarbon dating of the cores, and the incomplete ostracode record in the upper portions of the cores, a pattern of the paleohydrology was extracted. Not unexpectedly, in order to gain additional discrimination in both the paleohydrology and paleoclimate signals, other proxies need to be considered in addition to ostracodes.

6.3 THECAMOEBIAN DATA – INTEGRATION AND INTERPRETATIONS

Thecamoebians occur primarily in the upper portions of all cores. The SL core is unique as it has thecamoebians present at the bottom of the core (Figure 79) which then underwent a subsequent long hiatus, with the upper sequence then following a pattern and timing somewhat similar to the other sites. The Kenora core was also unique with an overlapping of the thecamoebian and ostracode intervals (Figure 71). The appearance of

thecamoebians in the upper parts of the cores is interpreted as being associated with increasing productivity in LOTWs and SL and may also be linked to increasing acidity and the ability of thecamoebians to tolerate more acidic conditions. However, the overlap of ostracode and thecamoebian intervals in the Kenora core implies they both were able to occupy a similar hydrochemical niche in LOTWs at this time. This implies the ultimate disappearance of ostracodes may not be related to low pH conditions alone.

Thecamoebians in the southern basin site (WOO06-1A) (Section 5.2.1.2) and Northwest Angle basin coring sites (WOO06-5A and 6A) (Sections 5.5.1.2 and 5.6.1.2) appeared relatively late around 2 ^{14}C ka BP (2 cal yrs BP) (Table 3). These three sites appeared to have shared a relatively similar set of ecological and hydrological conditions at this time. Any earlier records containing the fragile tests of thecamoebians may have been eliminated in these regions of LOTWs during the differential isostatic rebound induced transgression, paleosol formation and reworking of the southern shoreline.

The first appearance of thecamoebians in the Northwest Angle channel (WOO06-4A) (Section 5.4.1.2), the SL (SHO06-2A) (Section 5.8.1.2), and Kenora (WOO06-7A) (Section 5.7.1.2) coring sites all had a much earlier appearance of thecamoebians in the sedimentary record than the other sites (Figure 82) (Table 3). The Kenora core thecamoebians appear at 8.2 ^{14}C ka BP (9.2 cal ka BP), which is near the estimated time of isolation from Lake Agassiz based on differential isostatic rebound estimates. It appears this early appearance of thecamoebians may indicate LOTWs operated below the sill to the Winnipeg River creating lower and warmer water conditions which increased the productivity. Other observed data from this core, including ostracode data, do not

support the conclusion that Lake Agassiz or near Lake Agassiz conditions still existed at the estimated time of separation of Lake Agassiz from LOTWs of about 8.1 ^{14}C ka BP (9.0 cal ka BP). The complexities of the hydrologic interconnections to Lake Agassiz and increasing complexities in this area induced by differential isostatic rebound in conjunction with climatic induced operation below the sills to the Winnipeg River, likely produced conditions very different from those of Lake Agassiz which is evident in the sediments. The sedimentary record including both ostracodes and thecamoebians, and other proxies discussed below indicate the isolation effectively occurred earlier.

Similarly, the early appearance of thecamoebians in WOO06-4A, and SHO06-2A of 6.5 ^{14}C ka BP (7.4 cal ka BP) and 7.0 ^{14}C ka BP (7.8 cal ka BP), indicate warm Hypsithermal conditions had affected the paleohydrology and paleoenvironmental in the channel WOO06-4A site, and in the SL basin near the same time (Table 3) (Figure 82). This likely caused lower water levels and warmer water environments conducive to increased productivity and higher populations of thecamoebians. The early presence of thecamoebians at the bottom of the SL core estimated at about 7.0 ^{14}C ka BP (7.8 cal ka BP) (Section 5.8.1.2), implies the sediments below the core, may also have contained thecamoebians, with a first appearance possibly similar to the Kenora core which is estimated to have occurred after 8.2 ^{14}C ka BP (9.2 cal ka BP) (Section 5.7.1.2). This early appearance of thecamoebians in this northern deep part of the LOTWs watershed supports the interpretation that the lakes in this interval were relatively productive at this time, and this may be related to a dry climate interval and operation below the outlets to the Winnipeg River. The atypical long hiatus in thecamoebians in the SL core (Section

5.8.1.2) once again indicates the SHO06-2A coring site is unlike the others, although short hiatuses in the WOO06-7A and WOO06-4A cores are noteworthy (Sections 5.5.1.2 and 5.6.1.2) and possibly related. The hiatus interval may be a climate signal, and indicate a possible deepening in the SL core with a return to more productive conditions at about 4.4 ^{14}C ka BP (4.9 cal ka BP) with the WOO06-4A channel site returning to more eutrophic conditions about 3.8 ^{14}C ka BP (4.2 cal ka BP) (Section 5.4.1.2), and the Kenora site returning to these conditions sometime after 6.8 ^{14}C ka BP (7.6 cal ka BP) (Section 5.7.1.2). This may mean the WOO06-7A core higher productivity conditions may have been related to other than climatic driven changes, with the isostatic rebound and the elevation of the Winnipeg River sill a complicating factor.

Overall the more northerly sites all indicate more productive conditions existed well before the southern basin sites (Table 3) with the deep channel Northwest Angle site (WOO06-4A) the youngest of this grouping possibly reflecting the reintroduction of waters from the transgression into the south basin, and the role of this channel in interconnecting the deep northern basin and the deepening south basin. There appears to be an anomaly in the thecamoebian record for the Northwest Angle basin and southern basin sites. This region would have shallowed during the initial phases of the withdrawal of Lake Agassiz from the region, and shallow and warm conditions should have existed for a period of time, especially in the Northwest Angle basin sites. This shallowing would have been conducive to the development of a thecamoebian population. However, as was noted earlier, fragile thecamoebian tests may not have been preserved in the sedimentary record as this region was subject to paleosol formation in the Northwest

Angle sites and reworking from the subsequent transgression. This portion of the thecamoebian record shortly after Lake Agassiz became isolated and conditions shallowed appears to be missing.

6.4 CHARCOAL MACROFOSSIL DATA – INTEGRATION AND INTERPRETATIONS

Figure 83 provides an indication of the abundance of charcoal observed in LOTWs and SL cores, superimposed on the stratigraphic, ostracode, thecamoebian and radiocarbon dating data. These charcoal signals provide additional information to assist in interpreting the paleoclimate conditions in the core.

In the Kenora core (WOO06-7A), an unusually high charcoal signal (Figure 69) was noted at about 2.4 m which dated to 8.8 ^{14}C ka BP (9.8 cal ka BP) (Section 5.7.1.3), in an interval that should be in the Lake Agassiz sequence. The occurrence of high levels of charcoal in the relatively sterile sediments of a proglacial lake seems very anomalous. However, from Figure 8, it is apparent the hydrological interconnections between LOTWs and Lake Agassiz were very complex. The source of the charcoal may be from emerging land to the west, east and north of the Kenora core area. The high abundance of charcoal at a time when Lake Agassiz was in the region confirms this area had a complex paleoenvironment at this time.

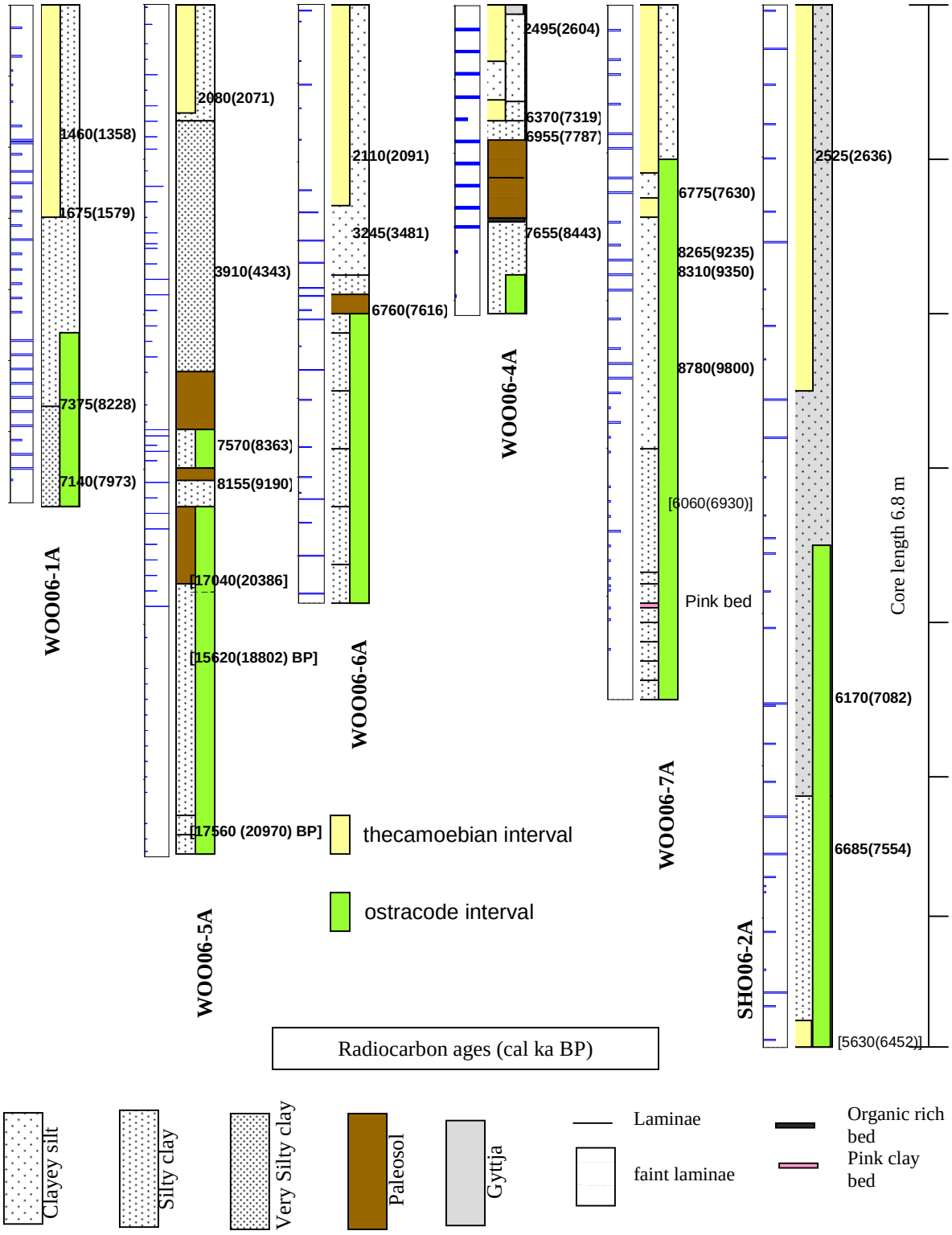

Figure 83. Charcoal relative abundance in LOTWs and SL cores; indicated by the length of the small bars to the left of cores (from Appendix A, Subsample Data table for each core). Stratigraphic sections, ostracode and thecamoebian data, and important radiocarbon ages are indicated (including rejected dates enclosed in square brackets. A scale with metre intervals is provided on the right.

The WOO06-4A core (at 1.5 m) and WOO06-5A and 6A cores include intervals containing large and abundant charcoal fragments (Appendix A, Subsection 3.2 and 4.2) (Figure 83) which has been interpreted by others (McMillan et al., 2003) to indicate fires were located nearby. These intervals of abundant and large charcoal, start near the beginning of the first paleosol in WOO06-5A, and extend part way into the upper paleosol after 7.5 ^{14}C ka BP (8.4 cal ka BP). Similarly in WOO06-6A, high relative charcoal levels (Figure 83) were noted around the paleosol about 6.8 ^{14}C ka BP (7.6 cal ka BP) with high charcoal levels appearing in WOO06-4A about 7.7 ^{14}C ka BP (8.4 cal ka BP). These estimated dates of high relative charcoal levels are similar in age and suggest warmer and drier conditions in the Northwest Angle area during the mid-Holocene Hypsithermal period. The rising terrain around these sites may also have introduced charcoal into the sediments from runoff in addition to aerial inputs of charcoal from nearby forests which would have recently colonized the area as the land emerged from Lake Agassiz. This terrain would then have been subject to forest fires particularly during drier climatic conditions.

A similar interval of high charcoal abundance and large charcoal fragments (Appendix A, Subsection 5.2), dated to about 6.8 ^{14}C ka BP (7.6 cal ka BP) at about 1.2 m in the WOO06-7A core (Figure 83), further supports the interpretation of relatively dry climate conditions at that time with nearby fires. Incidences of high relative amounts of charcoal were also present in the SL core with two intervals dating to about 6.2 ^{14}C ka BP (7.1 cal ka BP) and 6.7 ^{14}C ka BP (7.6 cal ka BP) (Figure 83); these also contained abundant and

large charcoal fragments (Appendix A, Subsection 6.2). The 6.7 ^{14}C ka BP (7.6 cal ka BP) date in SL closely corresponds with the WOO06-7A core dates, and is reasonably close although somewhat later than the other cores.

The incidence of relatively high charcoal abundance and the presence of large charcoal fragments in LOTWs cores between 6.8 and 6.2 ^{14}C ka BP (7.6 to 7.1 cal ka BP) (Figure 83) indicate the LOTWs region was undergoing a dry climate interval around this time. This is further supported by the timing of the beginning of the paleosol horizons in the Northwest Angle area core paleosols of WOO06-4A and WOO06-6A, and the upper paleosol of WOO06-5A which indicate the paleosols formed sometime around 7.7 to 6.7 ^{14}C ka BP (8.4 to 7.6 cal ka BP) (Figure 80 and Figure 83). The apparent dry intervals in WOO06-7A and SL cores, which corresponds reasonably close to the beginning of the Northwest Angle paleosols, suggests a climatic component in addition to the effects of differential isostatic rebound may have been in play at this time (see Section 6.6).

Other intervals of relatively abundant charcoal in the WOO06 5A and WOO06-6A cores (Figure 83) (Appendix A, Subsections 3.2 and 4.2) occur prior to the thecamoebian interval, indicating there were fires in the region after the last paleosol interval ended in the WOO06-5A core about 4.8 ^{14}C ka BP (5.5 cal ka BP) (Figure 80) to about 2.8 ^{14}C ka BP (2.9 cal ka BP) when the first thecamobians appeared in this core (Table 3). In the WOO06-6A core large charcoal fragments (Appendix A, Subsection 4.2) indicates nearby region fires occurred about 3.2 ^{14}C ka BP (3.5 cal ka BP) (Section 5.6.1.5). In the WOO06-5A core near the radiocarbon dated interval at 1.8 m dated at 3.910 ^{14}C ka BP

(4.343 cal ka BP) (Figure 80), intervals of relatively high charcoal levels also occur (Appendix A, Subsection 3.2). The SL core contains high charcoal, plant, and insect components which vary in abundance throughout the core (Appendix A, Subsection 6.2), indicating variable climatic conditions occurred within this relatively stable basin. An interval of charcoal in the SL core just prior to the beginning of thecamoebians around 4.4 ^{14}C ka BP (4.9 cal ka BP) included a burnt twig (Appendix A, Subsection 6.2). Although the SL sampled intervals were broadly spaced in this part of the core, short increases in charcoal indicate varying and sometimes dry climatic conditions. From these cores, the data suggests dry climate conditions at around 4.0 ^{14}C ka BP (4.5 cal ka BP).

Based on charred seed pods and wood fragments (Appendix A, Subsection 6.2) near the radiocarbon dated interval of about 2.5 ^{14}C ka BP (2.6 cal ka BP) at 1m in the SL core (Figure 83), another dry climate interval appears to have occurred. High abundance of charcoal including a charred needle in WOO06-5A at about the same time, in conjunction with common charcoal and blackened stems in WOO06-6A all support the interpretation that relatively dry conditions prevailed around 2.5 ^{14}C ka BP (2.6 cal ka BP) (Figure 80).

6.5 SEDIMENTATION RATE DATA – INTEGRATION AND INTERPRETATIONS

Sedimentation rates were roughly estimated from the available radiocarbon dates with some rates estimated by extrapolating or interpolating the available dates. Estimates of the sedimentation rates were made for the overall rate, a mid-core rate and upper rate, in most cores (Sections 5.2.1.5, 5.4.1.6, 5.5.1.6, 5.6.1.6, 5.7.1.7, and 5.8.1.6). Lower core

sedimentation rates were mostly unavailable due to a lack of reliable radiocarbon dates in the lower portions of the cores and only overall, mid-core and upper core sedimentation rates were estimated and are summarized in (Table 3). The effects of sediment compaction were ignored, but qualitative sedimentation rate comparisons between cores over similar locations in the cores, should be reasonably comparable. The overall rate from the WOO06-5A core could not be obtained due to the numerous paleosols.

Sedimentation rates in the cores are variable and range from about 0.1 to a maximum of 0.9 mm/yr (Table 3). The available estimated rates in the WOO06-5A core (Section 5.5.1.6) were more than double those of its companion core WOO06-6A (Section 5.6.1.6), likely reflecting its position deeper in the basin. The highest sedimentation rate cores were the SL core (SHO06-2A) (Section 5.8.1.6), and the southern basin core (WOO06-1A) (5.2.1.5). The SL core is the only coring site that likely had relatively unchanging lake basin paleoconditions, with its sedimentation rates remaining relatively high throughout its history. The high rates in the southern basin site (WOO06-1A) are likely related to the transgression onto the southern basin shoreline, with the highest rates in the upper part of the core possibly reflecting the continuing erosion along the southern shoreline and addition of that sediment to the offshore record as the south basin waters deepened and transgressed to the southwest. The Northwest Angle channel site (WOO06-4A) (Section 5.4.1.6) and the Kenora (WOO06-7A) (Section 5.7.1.7) sites both had high mid-core sedimentation rates, while overall and upper core sedimentation rates were the lowest (0.1 mm/yr). The lower upper core rates may reflect deep channels and high currents at these locations during these intervals, reducing sediment deposition.

Caution is required when considering the data collected from the cores. Based on the typical subsample length along the core of 2 cm, and the deposition rates from Table 3, the subsamples represent intervals that vary between 10 to 100 years of sedimentation. This does not take into account the effect of increased compaction of sediments at the bottom of the core, which increases the time period represented by the subsample. The discrimination available for the data therefore generally varies from the top to the bottom of the core, and decreases downward based on compaction. The typical inter-sample interval of between 10 to 20 cm, can represent a range of 100 to 1000 years, or 200 to 2000 years, respectively. The discrimination available from the subsamples and their sample intervals is therefore limited. The accuracy of the interpretations from the climate and hydrologic proxies therefore varies considerably and must be kept in mind.

The data available from each core is affected by the differing sample intervals, with some cores sampled extensively such as the WOO06-5A core, while others were only broadly sampled such as the SL core. Additionally, sampling intervals along the core were not consistent, with the sampling frequency increasing around stratigraphic features of interest, such as the paleosols in WOO06-5A. The sampling intervals and variabilities in sedimentation rates between and within the cores, introduces uncertainties. Despite these uncertainties, the general trend in the changing sedimentation rates in the cores can be discerned and interpretations related to the paleohydrology and paleoclimate were made. To improve inter-core sedimentation rate comparability a different sampling strategy

would be required accounting for the highly variable sedimentation rates, and additional radiocarbon dates would be required.

6.6 PALEOSOL DATA – INTEGRATION AND INTERPRETATIONS

Paleosol horizons within the cores are key markers for low water levels at those sites and indirectly possibly reflect drier climatic conditions. The first two of three paleosol horizons within WOO06-5A are however likely to have appeared for differing reasons. The radiocarbon dates place the first paleosol (PS1) (Figure 80) within a Lake Agassiz timeframe with this paleosol ending around 8.4 ^{14}C ka BP (9.5 cal ka BP) and may have been influenced at this time by isostatic rebound, in particular the influence of the rising terrain associated with the large Lake Agassiz island to the west (Figure 8) and associated sediment transport and basin infilling. Alternately, or in cojunction with high sedimentation into the Northwest Angle area, it is possible a low level phase in Lake Agassiz occurred from opening of lower elevation Lake Agassiz outlets to the east, with a possible subsequent higher level phase prior to LOTWs occupying the region.

The reasons for the formation of the second paleosol (PS2) (Figure 80) may be a mixture of the continuing rebound and shedding of sediments, plus early Hypsithermal climatic variations since this paleosol ended at about 7.7 ^{14}C ka BP (8.5 cal ka BP). The paleosol may have formed when drying conditions occurred when the terrain was uplifting and lake sediments including materials which were previously shed from the island the west, were exposed. The timing and possibly duration of this paleosol may have been

influenced by the uplifting terrain and the shed sediments. The formation of the upper paleosol (PS3) (Figure 80) was possibly more strongly influenced by a drying climate than the PS2 since the age of the paleosol of about 7.0 ^{14}C ka BP (7.8 cal ka BP) to about 4.7 ^{14}C ka BP (5.5 cal ka BP), spans the relatively warm and dry Hypsithermal period. The corresponding abundant charcoal intervals with large charcoal fragments in the WOO06-7A and SL cores near the time when the paleosols formed around 6.8 to 6.2 ^{14}C ka BP (7.6 to 7.1 cal ka BP) (Section 6.4), indicate the LOTWs region was undergoing a drier climate around this time possibly significantly influencing paleosol timing and duration.

The estimated termination of the upper PS3 paleosol of 4.7 ^{14}C ka BP (5.5 cal ka BP) (Figure 80) signals the return to lacustrine conditions and corresponds closely with the date for return to these conditions in its shallower companion core WOO06-6A estimated at about 4.4 ^{14}C ka BP (4.9 cal ka BP) (see section 5.6.1.5). The correlation is even closer when taking into consideration that the shallower coring site would not see the return to lake conditions until sometime after its deeper companion core. The return of lake conditions corresponds well with the paleotopographic maps of Yang and Teller, 2005 (Figure 10) including about a 600 year delay in the return of water to the WOO06-6A site.

The radiocarbon date from sediment overlying the upper paleosol in the WOO06-4A channel site of 6.955 ^{14}C ka BP (7.787 cal ka BP) does not correlate well with the end of paleosols of the Northwest Angle basin sites (Figure 80). This much older date indicates

a return to lacustrine conditions at this site would be about 2300 to 2900 years earlier than the end of the uppermost paleosol in nearby Northwest Angle sites. The estimated date of formation of this paleosol just below the paleosol of 7.655 ^{14}C ka BP (8.443 cal ka BP) (Figure 82) does however correspond reasonably well with the estimated date of formation of the upper paleosol in the WOO06-5A core of 7.0 ^{14}C ka BP (7.8 cal ka BP) (Figure 80) and the formation of the paleosol in the WOO06-6A core of sometime prior to the dated interval within the paleosol of 6.760 ^{14}C ka BP (7.616 cal ka BP) (Figure 82).

The WOO06-4A paleosol horizon is not distinct and hence the associated ages of formation and termination are not well constrained. The paleosol likely formed at a time when lake levels in this region of LOTWs were primarily shallow. The intervals of pedogenic structures, hard gray pellets, abundant plant materials and charcoal (Appendix A, Subsection 2.2) within sediment that is part of this paleosol horizon, may be interpreted as a reflection of drier intervals immediately prior to when the lake began to form the main paleosol. Alternately, the soil formation may have formed in the interval following independence of the basin from Lake Agassiz when it became dry, but before differential isostatic rebound caused the site to be reflooded (Figure 10). Similar to the upper paleosol interpretations for the Northwest Angle basin sites, the reasons for the paleosol formation in this channel may reflect dry climatic conditions during the Hypsithermal or possibly.

6.7 OTHER DATA – INTEGRATION AND INTERPRETATIONS

Other macrofossil and lithic data from the subsamples were used in developing the paleohydrology and paleoclimate interpretations in LOTWs and SL. Much of these data have been incorporated in the interpretations in the above sections, and were presented in the lithic materials and macrofossil plots for each core in Chapter 5. In addition to these supporting lithic and macrofossil data, other macrofossil data from the subsamples (Appendix A, Subsections 1.2, 2.2, 3.2, 4.2, 5.2 and 6.2) were used to assist in the interpretations. These data included the presence of pelecypods and gastropods, identification of seeds in many cores which indicated terrestrial or near shore conditions, the presence of aquatic/terrestrial plants and insects, and other information such as fish scales and vertebrae (in addition to providing material to obtain radiocarbon dates). These data and radiocarbon dates were used to support individual core interpretations and were extensively used with the final integration of these interpretations presented in this chapter. Since most of the data from macrofossils and lithic grains were used in the core by core interpretations, this detailed information is not repeated here. These data assisted in integrating and interpreting the sediment data necessary to develop the history of the LOTWs and SL, which is presented in Chapter 7.

The lithic grain data from the subsamples helped to assess the paleolacustrine conditions, with clay pellets used to help in further defining the end of paleosol horizons. The presence of carbonate rich clay balls and carbonate lithics were used to define core intervals where carbonates were present, and hence were used in investigating the reasons

for disappearance of ostracodes. The pink clay bed in the WOO06-7A core was also confirmed through the examination of lithics, with carbonate lithics appearing within and directly above the bed (Appendix A, Subsection 5.2).

There were no other pink sediments such as those in the WOO06-7A core in any of the other cores, and this is interpreted to mean that no other cores penetrated as deeply as the Kenora core. Based on the interpretation of others (Zoltai, 1963; Teller and Thorliefson, 1983; Teller and Leverington, 2004) this pink bed was deposited in other places in Northwestern Ontario about 9.9 ^{14}C ka BP (11.3 cal ka BP), as a result of overflow into Lake Agassiz from the Superior basin where red coloured bedrock and glacial drift is found. In the WOO06-7A core a rough estimate extrapolated from the available radiocarbon dates, indicates this clay was deposited about 10.5 ^{14}C ka BP (12.5 cal ka BP), which is somewhat older than the date established by others. In view of the uncertainties in the radiocarbon dates and variabilities in the sedimentations rates in LOTWs cores, the relatively close proximity of this roughly estimated date to the estimates of others is remarkable and confirms the available radiocarbon dates in the lower part of the WOO06-7A core are valid.

The abundance of SL macrofossil data (Appendix A, Subsection 6.2) and their primarily lacustrine nature throughout the length of the core is distinct and unlike many others does not contain paleosols. The SL macrofossil data is discussed in detail in Section 5.8.1.3.

CHAPTER 7 SUMMARY AND CONCLUSIONS

7.1 SUMMARY

7.1.1 Stratigraphic Correlations and Summary of Core Data Interpretations and Integration

This section summarizes many of the interpretations and subsequent integrations from the previous chapter. Figure 84 proposes stratigraphic correlations for ostracodes, paleosols, and thecamoebian intervals which are superimposed on the stratigraphic sections, and show the interpreted age for the end of ostracodes, end of the uppermost paleosol, and the beginning of thecamoebians which were discussed extensively in Chapter 6. The approximate chronological dates associated with these stratigraphic events were estimated, when necessary, by extrapolating or interpolating, and using the roughly calculated sedimentation rates (refer to Chapters 5 and 6).

The end of the ostracode intervals correlate reasonably well for most of the LOTWs coring sites with most locations ending about 6.8 to 7.0 ^{14}C ka BP (7.6 to 7.8 cal ka BP) (Figure 84). The southern basin ostracodes disappeared earlier at about 7.3 ^{14}C ka BP (8.1 cal ka BP) (Section 5.2.1.1). Ostracodes in the WOO06-4A channel site differ significantly and disappear much earlier at about 8.8 ^{14}C ka BP (9.8 cal ka BP) while in SL the ostracode interval ends much later at about 5.1 ^{14}C ka BP (5.8 cal ka BP) (Section 5.8.1.1), reflecting the generally differing paleoenvironment in SL.

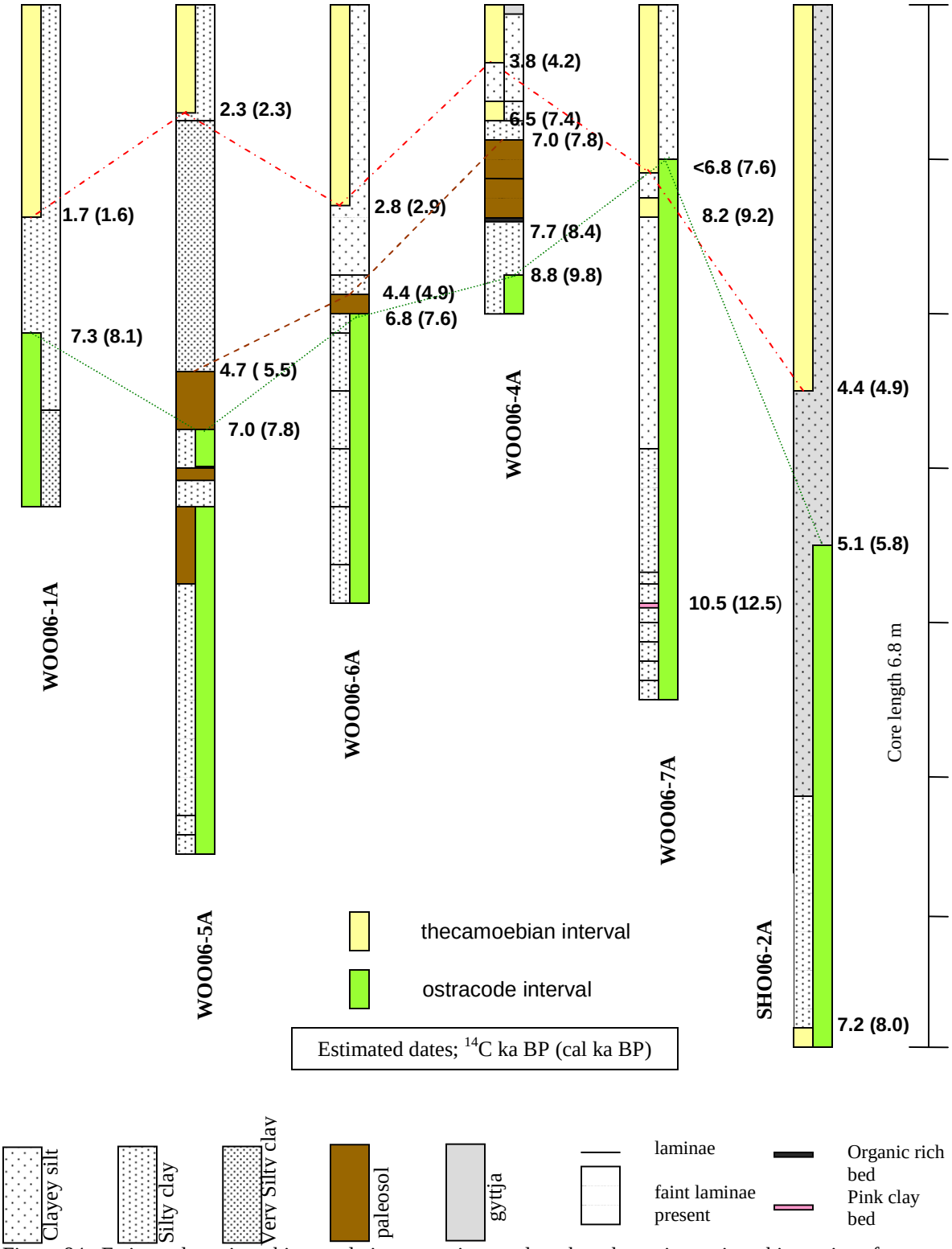

Figure 84. Estimated stratigraphic correlations superimposed on the schematic stratigraphic sections for the end of ostracode intervals (green dotted lines), beginning and end of the upper paleosol (brown dashed lines), and beginning of upper thecamoebian intervals (red dashed lines). Dates for beginning of the first thecamoebian interval are also shown. The dates are based on estimates from available radiocarbon dates.

The end of the paleosol horizons in the companion cores WOO06-5A and WOO06-6A appropriately reflect the 600 cal yr chronological offset in the return to lacustrine conditions in the higher elevation WOO06-6A core, and correlate well with the paleotopographic map reconstructions (Figure 10). The paleosol within the narrow WOO06-4A channel site is dated from about 7.655 ^{14}C ka BP (8.443 cal ka BP) to 6.955 ^{14}C ka BP (7.787cal ka BP), based on these available radiocarbon dates near the end and beginning of the paleosol, and corresponds reasonably well with the beginning of the upper paleosol of WOO06-5A which occurs sometime after 7.0 ^{14}C ka BP (7.8 cal ka BP) and the WOO06-6A paleosol starting sometime before about 6.8 ^{14}C ka BP (7.6 cal ka BP) (Figure 84).

The end of the WOO06-4A paleosol, however, does not correlate well with the end of the paleosols in the basin sites. It occurs about 2300 years earlier than the WOO06-5A core and 2900 years earlier than the WOO06-6A core. This is possibly due to the nature of this channel site which helps to direct the northward flow from the Rainy River towards the northern outlets near Kenora, and also provides part of the pathway for the differential isostatic rebound induced transgression which reflooded the southern basin. These factors, the narrowness of the channel and the relatively near shore location of this core could result in temporal differences in the paleosol formation and its termination, when compared to the paleosols in the nearby Northwest Angle basin sites.

From the radiocarbon dating of LOTWs and SL cores (Figure 81 and Figure 82) some significant differences were noted when comparing these to the paleotopographic maps

prepared by Yang and Teller, in 2005 (Figure 9 and Figure 10) which were generated from differential isostatic rebound calculations. Specifically, deep lacustrine conditions were identified at the southern basin WOO06-1A site prior to the estimated end of the ostracode interval at about 7.26 ^{14}C ka BP (8.05 cal ka BP) near the bottom of the core (Figure 84), whereas the paleotopographic maps indicate this portion of the LOTWs should have been terrestrial at this time. Lacustrine conditions were also observed in the Northwest Angle area WOO06-5A core between 8.4 to 8.0 ^{14}C ka BP (9.5 to 8.9 cal ka BP) after the end of an earlier paleosol, and at about 7.7 to 7.0 ^{14}C ka BP (8.5 to 7.8 cal ka BP) (Figure 80 and Figure 82), whereas Figure 9 and Figure 10 indicate terrestrial conditions started at about 9000 years BP and continued until about 6000 years BP. However, the return to lacustrine conditions after the upper paleosol in the WOO06-5A core and at the end of the paleosol in the WOO06-6A core, which are estimated at about 4.7 and 4.4 ^{14}C ka BP respectively (5.5 and 4.9 cal ka BP) (Figure 84), correlates very well with the paleotopographic map (Figure 10).

The lacustrine conditions in the southern basin and Northwest Angle basin sites at a time when the paleotopographic map predicted terrestrial conditions may have been the result of climatic effects which caused LOTWs to operate at or above above the sill to the Winnipeg River at this time. This may have created lake conditions in small compartments around an otherwise relatively dry lake basin which may have been connected from Rainy River inflows and/or as differential isostatic rebound reflooded this region. The southern basin and Northwest Angle sites may have been particularly susceptible to the formation of small lakes or development of channels in the lake, either

due to the proximity to of the WOO06-1A core to the Rainy river inlet, or due to the location of WOO06-5A and WOO06-6A cores near the interconnecting region between the southern basin and deep northern basin. This may account for the spatial and temporal differences between the paleotopographic maps produced by isostatic rebound calculations and the observations and interpretations based on the core sediments.

The timing of the Lake Agassiz isolation from LOTWs based on the paleotopographic maps, does not appear to be reflected in the Kenora core sedimentary data and by the available radiocarbon dates. Both an early thecamoebian interval and abundant quantities of charcoal, predate the isolation of LOTWs from Lake Agassiz (Figure 8 and Figure 9), and suggest these sediments may not have been deposited during a Lake Agassiz phase. The high abundance of charcoal may reflect the forest cover developing on the nearby uplifted terrain and possibly a dry climate induced by the warming post Lake Agassiz climate. The sediments in the lower part of the Kenora core do not appear to be the typical deep water Lake Agassiz sediments and indicate LOTWs may have started isolating from Lake Agassiz earlier. This may also indicate LOTWs had effectively been isolated earlier and operated below the Winnipeg River outlets shortly after separation, creating more productive conditions at the WOO06-7A coring site than would be possible in Lake Agassiz.

The SHO06-2A core, although the longest of the recovered cores, did not reach Lake Agassiz sediments with the bottom of the core estimated to be about 7.2 ^{14}C ka BP (8.0 cal ka BP) (Figure 84). The paleotopographic maps (Figure 9 and Figure 10) do not

reflect the lacustrine conditions found in the SHO06-2A core sediments, with these maps indicating the lake should have been dry, starting about 9000 cal years BP and should have remained dry until around 4000 cal years BP.

In SL a charcoal interval at about 2.5 m (Figure 83) included a burnt twig (Appendix A, Subsection 6.2) near an interval estimated to be about 4.4 ^{14}C ka BP (4.9 cal ka BP) near the beginning of thecamoebians, corresponds well with other climate proxies in LOTWs cores (refer to Section 6.4), indicating dry climate conditions occurred between about 4.5 to 4.0 ^{14}C ka BP. In addition charred seed pods and wood fragments about 2.5 ^{14}C ka BP (2.6 cal ka BP) in the SL core, correspond well with WOO06-5A and WOO06-6A cores (refer to Section 6.4), indicating another dry climatic interval at about this time.

The differing ecological conditions within LOTWs and its morphological complexities make comparisons between LOTWs and SL difficult. The timing of the disappearance of ostracodes and appearance of thecamoebians (Figure 84) in the SL core does not correlate well with LOTWs cores (Table 3), however, some of the later Hypsithermal dry cycles noted above, are reasonably consistent with those in the nearby Northwest Angle area of LOTWs. Additionally, there also appears to be some similarities in the timing of charcoal abundances and large charcoal fragments between the SL and Kenora WOO06-7A cores and the Northwest Angle WOO06-4A channel site during the early Hypsithermal with the SL and Kenora cores closely corresponding at about 6.7 ^{14}C ka BP (7.6 cal ka BP) and 6.8 ^{14}C ka BP (7.6 cal ka BP) respectively (refer to Section 6.4). The WOO06-4A Northwest Angle channel site charcoal abundances and fragment size also

correlate somewhat with these cores, although it dates somewhat earlier around 7.7 ^{14}C ka BP (8.4 cal ka BP). These similarities are possibly related to the common paleoclimate conditions in these LOTWs and SL cores.

7.1.2 History of LOTWs and SL

Based on the studied proxies and radiocarbon dates from the southern basin core (WOO06-1A), this location was in a lacustrine environment from about 7.3 ^{14}C ka BP (8.1 cal ka BP) up to the present (see Section 5.2.1.1), although there is evidence that an erosional surface may have existed with a possible paleosol above, perhaps indicating this coring location may have been exposed and dried for a period of time. Based on the effects of isostatic rebound depicted in the paleotopographic maps (Figure 9 and Figure 10), the region should have been dry from around 9.0 cal ka BP to 6.0 cal ka BP, and LOTWs should not have been present here at this time. There are however lacustrine sediments in this core that dated earlier than this and they aren't all glacial Lake Agassiz sediments. This suggests the coring location may have been in a local lacustrine compartment (lake) supplied by the nearby Rainy River, which was suitably cold and deep enough to continue to sustain a Lake Agassiz like ecological environment. This entire region then eventually flooded as a result of the southward transgression in LOTWs, although the date for this transition could not be determined from the characteristics of the sediments.

The Northwest Angle basin sites on the north side of the southern basin, indicate the bottom of these cores reached Lake Agassiz sediments. The Lake Agassiz sequence and subsequent LOTWs sequence were interrupted by paleosol formation. In the deeper WOO06-5A core, the first paleosol formed during the Lake Agassiz phase prior to 8.4 ^{14}C ka BP (9.5 cal ka BP) and then three lacustrine intervals with two intervening paleosols formed (Figure 80). The formation of these later paleosols, particularly the uppermost one, appears to have been primarily caused by dry Hypsithermal intervals with the last paleosol interval ending with the return to lacustrine conditions about 4.7 ^{14}C ka BP (5.5 cal ka BP) (Figure 84). The isostatically-driven transgression (Figure 10) and likely wetter climatic conditions as the dry Hypsithermal period waned, were likely the reason for the timing of this return to lacustrine conditions. The shallower companion site returned to lacustrine conditions about 600 years later at 4.4 ^{14}C ka BP (4.9 cal ka BP) as the transgression and possibly wetter climate flooded this site located closer to the edge of the basin.

The Northwest Angle channel site (WOO06-4A) appears to have been occupied by Lake Agassiz as late as 8.1 ^{14}C ka BP (9.0 cal ka BP). The lacustrine/riverine sequence was interrupted by an interval of paleosol formation between about 7.7 to 7 ^{14}C ka BP (8.4 to 7.8 cal ka BP), then the channel appears to have been flooded around 7 ^{14}C ka BP (7.8 cal ka BP) (Figure 84). This ended the paleosol forming episode in WOO06-4A which corresponds with the lacustrine interval in the deeper Northwest Angle basin site core (WOO06-5A) (Figure 80), with WOO06-4A appearing to have remained in a flooded state throughout the uppermost paleosol interval in the WOO06-5A and in the WOO06-

6A cores, although it was likely subject to low water level intervals. The span of the paleosol of about 7.7 to 7 ^{14}C ka BP (8.4 to 7.8 cal ka BP) also indicates WOO06-4A may have been subject to the effects of drying climates during dry periods of the early Hypsithermal at this time. However, the location of this channel in the interconnecting channels between the south basin and north basin may be the reason for what appears to be mostly riverine conditions in this channel site, in an apparently otherwise dry portion of LOTWs. This part of the lake would have received the inputs from the Rainy River to the south as its waters flowed northwards and would have been subject to the deepening effects of the differential isostatic rebound induced transgression from the rising northern outlets.

The Kenora core (WOO06-7A) appears to have been in a highly complex environment in both its late Lake Agassiz and LOTWs phases. This core was clearly well within the Lake Agassiz sequence which is reflected by the pink clay bed marker bed (Figure 67) introduced from the Marquette readvance. The complexity of the ostracode and thecamoebian proxies, the presence of abundant charcoal and plant materials in Lake Agassiz vintage sediments, and the complexity of the interconnection to Lake Agassiz (Figure 8) make interpretations from this core difficult. However, it appears this location in the northern portion of the LOTWs had high charcoal levels (Figure 83) about 8.8 ^{14}C ka BP (9.8 cal ka BP) well before the time when LOTWs became isolated from Lake Agassiz (based on the paleotopographic maps). However, the early appearance of thecamoebians (Figure 84) at 8.2 ^{14}C ka BP (9.2 cal ka BP) and already abundant plant and insect macrofossils (Appendix A, Subsection 5.2) and charcoal (Figure 83) all imply

an earlier separation from Lake Agassiz occurred somewhere around 9.0 ^{14}C ka BP (10.0 cal ka BP). This may have resulted from a drop in Lake Agassiz as a result of opening of an eastern outlet and/or operation below the Winnipeg River sills. Subsequently it appears the north basin may have operated below these outlets until about 6.8 ^{14}C ka BP (7.6 cal ka BP) (Figure 83 and Figure 84) when abundant and large charcoal fragments occurred (Appendix A, Subsection 5.2), and dry conditions were observed in the region with paleosols present in the Northwest Angle basin sites (Figure 84), implying possibly drier climatic conditions.

If the deep northern basin in LOTWs did operate below the northern outlets and/or effectively became isolated around 9.0 ^{14}C ka BP (10.0 cal ka BP) possibly due to a low water Lake Agassiz phase, then why is there evidence of Lake Agassiz sediments in the Northwest Angle area after this time? From Figure 8 it appears a connection to Lake Agassiz through the Northwest Angle inlet area could have been in operation after 9.0 ^{14}C ka BP (10.0 cal ka BP). If a connection existed this may be the source of the apparent Lake Agassiz like conditions in the Northwest Angle area after the date when it appears the Kenora location of LOTWs had isolated from Lake Agassiz. It may also explain why the Southern Basin lakes may have existed beyond the time when the basin was expected to be dry. A flow channel possibly ran from the Rainy River inlet through the Northwest Angle region supplying water to maintain deep compartments in this region. The channel may have then infilled with sediments after the southward transgression erasing any obvious evidence of the existence of the channel. Clearly more work is required to explore this possible explanation.

SL was lacustrine for the entire interval in the recovered core. The presence of thecamoebians at the bottom of the core around 7.2 ^{14}C ka BP (8.0 cal ka BP) (Figure 84), in addition to high organic materials (Figure 83), supports the interpretation that an early Hypsithermal dry period occurred which corresponds with a similar signal from the Kenora core, indicating the LOTWs operated below the Winnipeg River outlet sills.

7.1.3 Summary of LOTWs and SL Regional Paleoclimate

Century-scale duration cycles of extreme drought occurred in the northern U.S. plains and Canadian prairie (Laird et al., 2003), including 600 year droughts experienced around 7.2 ^{14}C yr BP (8.0 cal ka BP) (Clark et al., 2002). Studies of Lake Winnipeg, 240 km to the northwest, indicate that a mid-Holocene drought from about 7.5 to 4.0 ^{14}C yr BP (8.4 to 4.5 cal ka BP) dramatically affected its level, and runoff was reduced such that the lake stopped overflowing (Lewis et al. 2001). The Wampum lagoon site very near to the south basin of LOTWs experienced a dry interval between about 6.2 to 4.0 ^{14}C ka BP (7.1 to 4.5 cal ka BP) (Teller et al., 2000). At Lake 239 about 50 km to the northeast of LOTWs, lake levels fluctuated up to 8 m indicating an unstable and intermittent arid period in the mid-Holocene about 8.0 to 4.0 ^{14}C ka BP (8.9 to 4.4 cal ka BP) (Laird and Cummings, 2008).

These mid-Holocene dry conditions appear to correspond to some of the dry intervals identified in the mid-Holocene portion of LOTWs. In particular they correspond to the

conditions noted in the WOO06-7A core after isolation from LOTWs and the apparent operation below the Winnipeg River outlets. These reported dry conditions also align reasonably well with the SL core thecamoebian and high charcoal intervals at the bottom of the core. Additionally, they also correspond well with the dates of formation of the upper Northwest Angle paleosol sites and charcoal intervals which indicated nearby fires. The paleosol intervals appear around 7.7 to 6.8 ^{14}C ka BP (8.4 to 7.6 cal ka) (Figure 84). A similar interval of high abundance of charcoal in the WOO06-7A core, around 6.8 ^{14}C ka BP (7.6 cal ka BP) (Figure 83), contained large charcoal fragments (Appendix A, Subsection 5.2), indicating relatively dry conditions and nearby fires may have existed and correlates well with the Northwest Angle site data (Appendix A, Subsections 3.2 and 4.2), indicating a LOTWs regional aridity existed.

Late Holocene conditions in the northern Great Plains region at Devils Lake, North Dakota, were determined to be wet from 4.5 to 3.5 cal ka BP with more saline lake (dry) conditions returning at about 3 cal ka BP (Haskell et al., 1996). These drying conditions were noted by Fritz et al., 2000, and were likely reflected in lakes just to the north on the Canadian prairies. Farther east in Minnesota, nearly synchronous droughts are recorded (Haskell et al., 1996). At Lake 239 conditions in the last 3000 years had become drier and more stable (Laird and Cummings, 2008). Bog moisture variability studies have found that over the past 2000 years in sites in southern Michigan and north central Minnesota, intervals of extreme drought in both regions have occurred (Booth and Jackson, 2003; Booth et al., 2006).

In LOTWs the Northwest Angle sites WOO06-6A indicates there were nearby fires from about 4.8 ^{14}C ka BP (5.5 cal ka BP) to 2.8 ^{14}C ka BP (2.9 cal ka BP), with large charcoal fragments indicating nearby fires around 3.2 ^{14}C ka BP (3.5 cal ka BP) (Section 6.4). In the WOO06-5A core at approximately 3.9 ^{14}C ka BP (4.3 cal ka BP) intervals of relatively high charcoal levels occur (Figure 83). An interval of charcoal in the SL core around 4.4 ^{14}C ka BP (4.9 cal ka BP) (Section 5.8.1.3) indicates dry conditions occurred at this time which corresponds well with the WOO06-6A site. A second interval about 2.5 ^{14}C ka BP (2.6 cal ka BP) in the SHO06-2a, WOO06-5A and WOO06-6A cores all indicate that dry conditions occurred about this time (Section 6.4).

7.1.4 Mid-Holocene Climate; Analogy to Current Warming Climate?

Lake level variations back into the highly variable and often drier climatic conditions of the mid-Holocene (Lewis et al., 2001; Laird and Cumming, 2008), infer similar future unstable climate conditions could have dramatic effects on LOTWs and SL, and on the regional watersheds. In the LOTWs the effects of differential isostatic rebound is now much reduced (Yang and Teller, 2005) as the isostatic rebound slows and approaches equilibrium, and the natural ability to raise the northern outlets and increase the holding capacity of the LOTWs and SL is very much reduced. In the future, the southeastward transgression within the LOTWs will no longer play a major role in preferentially expanding the areal extent of the lake southwards. Any increase in the inventory of LOTWs due to a wetter climate would be distributed evenly around the basin and flows into the Winnipeg River would increase. Similarly, extended dry climate intervals would

result in levels falling in all basins of LOTWs without the compensating effects of deepening in the southern basin from differential isostatic rebound.

LOTWs levels are now controlled by the power stations at the northern outlet channels, and are subject to international regulation rather than those of natural processes. However, prolonged wet intervals would increase shoreline erosion particularly in the southern basin which is surrounded by glacial and older lacustrine deposits and is susceptible to wind induced wave erosion particularly during storms. Prolonged droughts would result in lower levels in LOTWs and an end to overflow into the Winnipeg River from LOTWs. In SL, levels would increase in wetter climates with increasing LOTWs levels above the elevation of the connection through the deepened Ash Rapids channel which now ties these two lakes together as part of international regulation. In a prolonged drier climate conditions SL would become independent should the level of the LOTWs drop below the relatively shallow connecting ledge at Ash Rapids. From this point onwards SL water levels would continue to fall with a prolonged drought. In essence there would be little difference from the natural uncontrolled state with drought duration determining whether lake level could be controlled.

It has been suggested that the effects of future climatic changes might be reflected by those in the past (e.g. Alley and Augustsdottir, 2005). Past variations in LOTWs hydrology have been very significant with some basins drying or flooding, however the effects of differential isostatic rebound tended to mask or enhance the effects of climate changes recorded in the sediments, making it difficult to determine which effect was

predominant. Nonetheless, climate variabilities have had dramatic impacts on lake levels and the surrounding vegetation, which were identified in the sediments of LOTWs and SL, and future climate fluctuations would induce changes that would likely be similar. However, using the mid-Holocene Hypsithermal climate as an analog to predict future climate instabilities in the LOTWs region, induced by the effects of increasing anthropogenic CO_2 emissions, needs to consider the moderating affects that the receding and disintegrating LIS had on the past climate change. Future climate variabilities in this region will not be influenced by an ice sheet to the north (Figure 1 and Figure 2) or Lake Agassiz until it drained into Hudson Bay at about 8.2 cal ka BP (Figure 6). This could mean, based on the same degree of climate forcing, future climate instabilities may be more pronounced than those experienced in the Hypsithermal and the response of the region to similar climate fluctuations to those of the early mid-Holocene, would not likely be directly applicable.

Without the moderating effect of the LIS to the north which affects the location of the Arctic high, the magnitude and frequency of climate variations may be significantly different. In the past, the ice sheet tended to moderate changes until the ice sheet moved sufficiently far from the region, or disintegrated sufficiently to reduce its climatic impact (Forester et al., 1987). The moderating effect of Lake Agassiz would similarly have in effect provided resistance in the climate system to climate fluctuations before it finally drained. In the past some dramatic regional scale changes were induced by fluctuations in the location of the zonal and meridional patterns in the region (Harrison and Metcalfe, 1985) which were strongly affected by the presence of the LIS and Lake Agassiz, and

they continued to be influenced even when these resistive components were far to the north. Furthermore, regional climatic variabilities were influenced by more global weather changes affecting the interplay of the Arctic high, Pacific and maritime tropical air masses (Figure 19).

The climate instabilities in the Hypsithermal in North America were possibly the result of the loss of these resistive climate influences over time, after the draining of Lake Agassiz and as the ice sheet completed its retreat to its modern locations. An anthropogenic induced CO_2 forcing will not be restrained by the influence of these temperature-moderating climate components. In addition, the impact of the rapid warming predicted and being experienced in the far north due to the positive feedback from the melting Arctic sea ice and subsequent dramatic decrease in albedo, was not in play during the Hypsithermal. The effect of this temperature gradient on the location of the east-west temperature line reflecting the collision between the Polar air mass with the Pacific and maritime tropical air masses (Figure 19), will likely be that this line will be much farther north. Predicting the location of the north/south line which reflects the collision zone of the Pacific and maritime tropical air masses, will be even more difficult. The locations of these two collision zones are very important to predicting the impact of any climate warming. In the past the influences of the location of these collision zones on region climate had significant impacts on the central portion of North America including the LOTWs region.

In summary, the mid-Holocene climate fluctuations of the past and what appears to be the current primarily anthropogenic induced warming may have very different characteristics, however climate instability seems likely. In the past, the instabilities of the Hypsithermal had dramatic impacts on the LOTWs and SL and the surrounding terrain. Nothing less should be expected if the climate system becomes unstable.

7.2 CONCLUSIONS

Through the use of ostracode, thecamoebian and other macrofossil data from the sediments of LOTWs and SL, and the study of the core stratigraphy, a picture of the paleohydrology and paleoclimate of the LOTWs region was developed. The complex morphology and watershed of LOTWs and additional complications introduced by differential isostatic rebound, made the sedimentary data challenging to interpret. Difficulties in obtaining radiocarbon dates, especially in the lowermost portions of the LOTWs core sequences where organic materials were very limited or absent, created further challenges. The two primary macrofossil proxies (ostracodes and thecamoebians) which were used to interpret paleoclimate and paleohydrology, did not span the core lengths and introduced uncertainties in the interpretations, although their disappearance and appearance in certain portions of the core provided the means to interpret changing conditions.

To overcome some of the difficulties in interpreting the ostracode and thecamoebian data, other proxies were used. Additional observations from the subsamples related to the type

of lithic grains, plant materials, size and shape of charcoal fragments and presence of vertebrate and invertebrate macrofossils were also used. Through the use of these proxies the Holocene hydrologic history of LOTWs and SL was reconstructed and related to changes in regional paleoclimate.

The presence of a pink clay bed in the Kenora core (WOO06-7A) provides evidence of the intrusion of the Lake Agassiz sediments into the LOTWs region from the Superior Basin as a result of the Marquette glacial readvance. This confirmed the lower portions of the WOO06-7A core were well into Lake Agassiz sediments.

The LOTWs appears to have operated below its northern outlets during the early Holocene indicating the LOTWs may have effectively isolated earlier from Lake Agassiz at around 9.0 ^{14}C ka BP (10.0 cal ka BP) when compared to the predictions of the paleotopographic maps generated from differential isostatic rebound calculations. This may have been due to a drop in Lake Agassiz level through the opening of overflow outlets to the east and possibly an early Holocene drier climate interval. Based on these maps, variations in lake level in the cored regions of LOTWs were expected and the data reflected these variations. Lake Agassiz like paleoecological conditions were evident from macrofossils in the bottom of cores from the southern regions of the LOTWs, even after the time the Kenora region of LOTWs appears to have become isolated from Lake Agassiz, suggesting that Lake Agassiz may have been connected to these other locations after the northern basin dropped below the modern northern outlets and isolated from

Lake Agassiz. It's possible a connection through the Northwest Angle inlet to Lake Agassiz may have been in operation.

The paleosols in the NW Angle region provide evidence of the affects of the changing paleoclimate. SL remained immune from most of the effects of differential isostatic rebound and provides a clearer picture of changes in the paleoclimate for the interval covered by this core.

REFERENCES

Adams, J., Maslin, M., and Thomas, E., 1999. Sudden climate transitions during the Quaternary, Progress in Physical Geography, vol. 23, no. 1, p. 1-36.

Alley, R.B., 2000. The Younger Dryas cold interval as viewed from central Greenland, Quaternary Science Reviews, vol. 19, issues 1-5, pg. 213-226.

Alley, R.B., and Augustsdottir, A.M., 2005. The 8k event: cause and consequences of a major Holocene abrupt climate change, Quaternary Science Reviews, vol. 24, p. 1123-1149.

Barber, D.C., Dyke, A., Hillaire-Marcel, C., Jennings, A.E., Andrews, J.T., Kerwin, M. W., Bilodeau, G., McNeely, R., Southon, J., Morehead, M.D., and Gagnon, J.M., 1999. Forcing of the cold event of 8,200 years ago by catastrophic drainage of Laurentide lakes, Nature, vol.400, no. 6742, p. 344-348.

Bajc, A.F., Schwert, D.P., Warner, B.G., Williams, N.E., 2000. A reconstruction of Moorhead and Emerson Phase environments along the eastern margin of glacial Lake Agassiz, Rainy River basin, northwestern Ontario, Canadian Journal of Earth Sciences, vol. 37, p. 1335-1353.

Balch, D.P., Cohen, A.S., Schnurrenberger, D.W., Haskell, B.J., Valero Garces, B.L.,

Beck, J.L., Cheng, H., Edwards, R.L., 2005. Ecosystem and paleohydrological response to Quaternary climate change in the Bonneville Basin, Utah, Palaeogeography, Palaeoclimatology, Palaeoecology, vol. 221, p. 99-122.

Benson, R.H., 2003. The ontogeny of an ostracodologist, The Paleontological Society Papers, vol. 9, p. 1-8.

Birks, H.H., 2001. Plant Macrofossils. In: Tracking environmental change using lake sediments, Volume 3, Terrestrial, algal, and siliceous indicators, Smol, J.P., Birks, H.J.B., and Last, W.M., (Eds.), Kluwer Academic Publishers, p. 49-74.

Booth, R.K., and Jackson, S.T., 2003. A high-resolution record of late-Holocene moisture variability from a Michigan raised bog, U.S.A, The Holocene vol. 13, p. 863-876.

Booth, R.K., Notaro, M., Jackson, S.T., and Kutzbach, J.E., 2006. Widespread drought episodes in the western Great Lakes region during the past 2000 years: Geographic extent and potential mechanisms, Earth and Planetary Science Letters, vol. 242, p. 415-427.

Broecker, W.S., Kennett, J., Flower, B., Teller, J.T., Trumbore, S., Bonani, G., and Wolfli, W., 1989. Routing of meltwater from the Laurentide Ice Sheet during the Younger Dryas cold episode, Nature vol. 341, p. 318–321.

Brown, K.J., Clark, J.S., Grimm, E.C., Donovan, J.J., Mueller, P.G., Hansen, B.C.S., and Stefanova, I., 2005. Fire cycles in North American interior grasslands and their relation to prairie drought, Proceedings of the National Academy of Sciences, vol. 102, no. 25, p. 8865-8870.

Burke, C.D., 1987. The effects of Late-Quaternary climatic changes and glacioisostatic rebound on lake level fluctuations and benthos of Lake Michigan, Palaios, vol. 2, p. 514-522.

Camill, P., Umbanhowar Jr., C.E., Teed, R., Geiss, C.E., Aldinger, J., Dvorak, L., Kenning, J., Limmer, J., and Walkup, K., 2003. Late-glacial and Holocene climatic effects on fire and vegetation dynamics at the prairie–forest ecotone in south-central Minnesota, Journal of Ecology, vol. 91, p. 822–836.

Chivas, A.R., De Decker, P., and Shelley, J.M.G., 1986. Magnesium and Strontium in non-marine ostracode shells as indicators of paleosalinity and paleotemperature, Hydrobiologia, vol. 143, p. 135-142.

Clark, P.U., Marshall, S.J., Clarke, G.K.C., Hostetler, S.W., Licciardi, J.M., and Teller, J.T., 2001. Freshwater forcing of abrupt climate change during the last glaciation, Science, vol. 293, issue 5528, p. 283-287.

Clark, J.S., Grimm, E.C., Donovan, J.J., Fritz, S.C., Engstrom, D.R., and Almendinger, J.E., 2002. Drought cycles and landscape responses to past aridity on prairies of the Northern Great Plains, U.S.A, Ecology, vol. 83(3), p. 595-601.

Clarke, G.K.C., Leverington, D.W., Teller, J.T., and Dyke, A.S., 2004. Paleohydraulics of the last outburst flood from glacial Lake Agassiz and the 8200 BP cold event Quaternary Science Reviews, vol. 23, no. 3-4, p. 389-407.

Cohen, A.S., 2003. Paleolimnology: The history and evolution of lake systems, Oxford University Press, p. 1-448.

Cook, E.R., Seager, R., Cane, M.A., Stahle, D.W., 2007. North American drought: Reconstructions, causes, and consequences, Earth-Science Reviews, vol. 81, p. 93-134.

Curry B.B., 1997. Paleochemistry of Lakes Agassiz and Manitoba based on ostracodes; Canadian Journal of Earth Sciences, vol. 34, p. 699-708.

Curry B.B., 1999. An environmental tolerance index for ostracodes as indicators of physical and chemical factors in aquatic habitats, Palaeogeography, Palaeoclimatology, Palaeoecology vol. 148, p. 51-63.

Curry, B.B., 2003. Linking ostracodes to climate and landscapes in "Bridging the Gap: Trends in the Ostracode Biological and Geological Sciences" ed. L. Park and A. J. Smith, the Paleontological Society Papers, vol. 9, p. 223-246.

Curry, B.B., Delorme, D., 2003. Ostracode-based reconstruction from 23,300 to about 20,250 cal yr BP of climate, and paleohydrology of a groundwater-fed pond near St. Louis, Missouri, Journal of Paleolimnology, vol. 29, p. 199–207.

Curry, B.B., and Yansa, C.H., 2004. Evidence for stagnation of the Harvard sublobe (Lake Michigan lobe) in Northeastern Illinois, U.S.A., from 24000 to 17600 BP and subsequent tundra-like ice-marginal paleoenvironments from 17600 to 15700 BP, Geographie physique et Quaternaire, vol. 58, no. 2-3, p. 305-321.

Davis, J.W., Smith, A.J., Palmer, D.F., Forester, R.M., and Curry, B.B., 2003. Environmental constraints on ostracode habitats in springs, wetlands, and streams of the United States, 2003 Seattle, Annual Meeting (November 2–5, 2003) Paper No. 49-5.

Dean, W.E., 1997. Rates, timing, and cyclicity of Holocene eolian activity in north-central United States: evidence from varved lake sediments, Geology, vol. 25, p. 331-334.

Dean, W.E., Forester, R.M., and Bradbury J.P., 2002. Early Holocene change in atmospheric circulation in the Northern Great Plains: an upstream view of the 8.2 ka cold event, Quaternary Science Reviews, vol. 21, issues 16-17, p. 1763-1775.

De Deckker, P., and Forester, R.M., 1988. The use of ostracodes to reconstruct continental paleoenvironmental records. In: Ostracoda in the Earth Sciences, De Deckker, P., Colin, J.P., and Peypouquet, J.P., (Eds.), p. 175-199.

De Deckker, P., 2002. Ostracode paleoecology, in Ostracode. In: The Ostracoda, Applications in Quaternary Research, Holmes, J.A., and Chivas, A.R., (Eds.), Geophysical Monograph 131, American Geophysical Union, p. 125-132.

Delorme, L.D., 1969. Ostracodes as Quaternary paleoecological indicators, Canadian Journal of Earth Science, no. 6, p. 1471-1476.

Delorme, L.D., 1970a. Freshwater ostracodes of Canada, Part III: family Candonidae; Canadian Journal of Zoology, vol. 48, p. 1099-1127.

Delorme, L.D., 1970b. Freshwater ostracodes of Canada, Part II: subfamily Cypridopsinae, and Herpetocypridinae, and farmily Cyclocyprididae; Canadian Journal of Zoology, vol. 48, p. 253-266.

Delorme, L.D., 1970c. Freshwater ostracodes of Canada, Part I: subfamily Cypridinae; Canadian Journal of Zoology, vol. 48, p. 153-168.

Delorme, L.D., 1970d. Freshwater ostracodes of Canada, Part IV: families Ilyocyprididae, Notodromadidae, Darwinulidae, Cytherideidae, and Entocytheridae; Canadian Journal of Zoology, vol. 48, p. 1251-1259.

Delorme, L.D., 1971a. Freshwater ostracodes of Canada, Part V; families Limnocytheridae, Loxoconchidae; Canadian Journal of Zoology, vol. 49, p. 43-64.

Delorme, L.D., 1971b. Paleoecology of Holocene sediments from Manitoba using freshwater ostracodes, Geological Association of Canada, Special Paper, no. 9, p. 301-304.

Delorme, L.D., 1971c. Paleoecological determinations using freshwater ostracodes, Bulletin, Centre Rech., Pau-SNPA 5 supplement, p. 341-347.

Delorme, L.D., and Zoltai, S.C., 1984. Distribution of an Arctic ostracode fauna in space and time, Quaternary Research, vol. 21, p. 65-73.

Delorme, L.D., 1989. Freshwater ostracodes. In: Methods in Quaternary ecology, Warner, B.G., (Ed), Geoscience Canada, Reprint Series 5. 1990, p. 93-100.

Delorme, L.D., 2001. Chapter 20 Ostracodes, In Thorp, J.H., and Covich, A.P., (Eds.)

Ecology and Classification of North American Freshwater Invertebrates, 2nd Edition, Academic Press, p. 811-848.

Dettman, D.L., Smith, A.J., and Lohmann, K.C., 1995. Glacial meltwater in Lake Huron during early postglacial time as inferred from single-valve analysis of oxygen isotopes in ostracodes, Quaternary Research, vol. 43, p. 297-310.

Digerfeldt, G., 1986. Studies on past lake-level fluctuations, in Berglund, B.E. (Ed.), Handbook of Holocene Palaeoecology and Palaeohydrology, John Wiley & Sons Ltd., p. 127-143.

Digerfeldt, G., Almendinger, J.E., Björck, S., 1992. Reconstruction of past lake levels and their relation to groundwater hydrology in the Parkers Prairies sandplain, west-central Minnesota, Palaeogeography, Palaeoclimatology, Palaeoecology vol. 94, p. 99-118.

Donovan, J.J., and Grimm, E.C., 2007. Episodic struvite deposits in a Northern Great Plains flyway lake: indicators of mid-Holocene drought?, The Holocene, 17, 8 (2007), p. 1155-1169.

Donovan, J.J., Smith, A.J., Panek, V.A., Engstrom, D.R., and Emi, I., 2002. Climate-driven hydrologic transients in lake sediment records: calibration of groundwater conditions using 20th Century drought, Quaternary Science Reviews, vol. 21, issues 4-6, p. 605-624.

Dyke, A.S., 2005. Late Quaternary vegetation history of northern North America based on pollen, macrofossil, and faunal remains, Géographie Physique et Quaternaire vol. 59, p. 211-262.

Fisher, T.G., 1996. Sand-wedge and ventifact palaeoenvironmental indicators in North-West Saskatchewan, Canada, 11 ka to 9.9 ka BP, Permafrost and Periglacial Processes, vol. 7, p. 391-408.

Forester, R.M., Delorme, D.D., and Bradbury, J.P., 1987. Mid-Holocene climate in Northern Minnesota, Quaternary Research, vol. 28 p. 263-273.

Forester, R.M., Smith, A.J., Palmer, D.F. and Curry, B.B., 2005. NANODe: North American Non-marine Ostracode Database, v. 1, (www.kent.edu/NANODe, Kent State University, Kent, Ohio, USA).

Fritz, S.C., Engstrom, D.R., and Haskell, B.J., 1994. "Little Ice Age" aridity in the North American Great Plains: a high-resolution reconstruction of salinity fluctuations from Devils Lake, North Dakota, U.S.A, The Holocene, vol. 4, no. 1, p. 69-73.

Fritz, S.C., Ito, E., Yu, Z., Laird, K.R., and Engstrom, D.R., 2000. Hydrologic variation in the Northern Great Plains, Quaternary Research vol. 53, p. 175-184.

Grimm, E.C., 2001. Trends and palaeoecological problems in the vegetation and climate history of the Northern Great Plains, U.S.A, Biology and Environment: Proceedings of the Royal Irish Academy, vol. 101b, no. 1-2, p. 47-64.

Harrison, S.P., and Metcalfe, S.E., 1985. Variations in lake levels during the Holocene in North America: an indicator of changes in atmospheric circulation patterns, Géographie Physique et Quaternaire, vol. 34, no. 2, p. 141-150.

Haskell, B.J., Engstrom, D.R., and Fritz, S.C., 1996. Late Quaternary paleohydrology in the North American Great Plains inferred from the geochemistry of endogenic carbonate and fossil ostracodes from Devils Lake, North Dakota, U.S.A, Palaeogeography, Palaeoclimatology, Palaeoecology vol. 124, p. 179-193.

Holmes, J.A., 2001. Ostracoda. In: Tracking Environmental Change Using Lake Sediments, vol. 4, Zoological Indicators, J.P., Birks, H.J.B., and Last, W.M., 2001 (Eds.), Kluwer Academic Publishers, Dordrecht, the Netherlands, p. 125-151.

Horne, D.J., Cohen, C., and Martens, K., 2002. Taxonomy, morphology and Biology of Quaternary and Living ostracodes. In: The Ostracoda, Holmes, J.A., and Chivas, A.R., (Ed.), Applications in Quaternary Research, Geophysical Monograph 131, American Geophysical Union, p. 5-36.

Hostetler, S.W., Bartlein, P.J., Clark, P.U., Small, E.E., and Solomon, A.M., 2000. Simulated influences of Lake Agassiz on the climate of central North America 11,000 years ago, Nature vol. 405, p. 334-337.

Hu, F.S., Ito, E., Brown, T.A., Curry, B.B., and Engstromi, D.R., 2001. Pronounced climatic variations in Alaska during the last two millennia, PNAS, vol. 98, no. 19, p. 10552-10556.

IPCC, 2007. Summary for policy makers. In: The physical science basis, Contribution of Working Group I to the Fourth Assessment Report of the Intergovernmental Panel on Climate Change, Climate change 2007, Solomon, S., Qin, D., Manning, M., Chen, Z., Marquis, M., Averyt, K.B., Tignor, M., Miller, H.L (Eds.), Cambridge University Press, Cambridge, United Kingdom and New York, New York, U.S.A.

Ito, E., 2002. Mg/Ca, Sr/Ca and ^{13}C chemistry of Quaternary lacustrine Ostracode shells from the North American continental interior. In: The Ostracoda, Applications in Quaternary Research, Holmes, J.A., and Chivas, A.R., (Ed.), Geophysical Monograph 131, American Geophysical Union, p. 267-278.

Kehew A.E., and Teller J.T., 1994. History of late glacial runoff along the southwest margin of the Laurentide Ice Sheet, Quaternary Science Reviews, vol. 13, p. 859-877.

Kennett, D.J., West, A., Mercer, C., Que Hee, S.S., Bement, L., Bunch, T.E., Sellers, M., and Wolbach, W.S., 2009. Nanodiamonds in the Younger Dryas boundary sediment layer, Science, vol. 323, p. 94.

Laird, K.R., Cumming, B.F., Wunsam, S., Rusak, J.A., Oglesby, R.J., Fritz, S.C., and Leavitt. P.R., 2003. Lake sediments record large-scale shifts in moisture regimes across northern prairies of North America during the past two millennia, Proceedings of the National Academy of Sciences, vol. 100, p. 2483-2488.

Laird, K.R., and Cumming, B.F., 2007. Reconstruction of Holocene lake level from diatoms, chrysophytes and organic matter in a drainage lake from the Experimental Lakes Area (northwestern Ontario, Canada), Quaternary Research, vol. 69, p. 292-305.

Last, W.M., Teller, J.T., and Forester, R.M., 1994. Paleohydrology and paleochemistry of Lake Manitoba, Canada: the isotope and ostracode records, Journal of Paleolimnology vol. 12, p. 269-282.

Leroy S.A.G., and Coleman, S.M., 2001. Coring and drilling equipment and procedures for recovery of long lacustrine sequences. In: Tracking Environmental Change Using Lake Sediments, vol. 1, Basin Analysis Coring, and Chronological Tecniques, Last, W.M., and Smol, J.P., 2001 (Eds.), Kluwer Academic Publishers, Dordrecht, the Netherlands, p. 107-136.

Leverington, D.W., and Teller, J.T., 2003. Paleotopographic reconstructions of the eastern outlets of glacial Lake Agassiz. Canadian Journal Earth Sciences, vol. 40, p. 1259-1278.

Lewis, C.F.M., Forbes, D.L., Todd, B.J., Nielsen, E., Thorleifson, L.H., Henderson, P.J., McMartin, I., Anderson, T.W., Betcher, R.N., Buhay, W.M., Burbidge, S.M., Schröder-Adams, C.J., King, J.W., Moran, K., Gibson, C., Jarrett, C.A., Kling, H.J., Lockhart, W.L., Last, W.M., Matile, G.L.D., Risberg, J., Rodrigues, C.G., Telka, A.M., Vance, R.E., 2001. Uplift-driven expansion delayed by middle Holocene desiccation in Lake Winnipeg, Manitoba, Canada. Geology, vol. 29, p. 743-746.

Lewis, C.F.M., and Thorleifson, L.H., 2003. Empirical modeling of regional glacio-isostatic warping for evaluating drainage system development in Red River valley and Lake Winnipeg basin, In Brooks, G.R., George, S.S., Lewis, C.F.M., Medioli B.E., Nielsen, E., Simpson, E., and Thorleifson, L.H., 2003 Geoscience insights into Red River flood hazards in Manitoba, The final report of the Red River flood project. Natural Resources Canada.

Limaye, R.B., Kumaran K.P.N., Nair K. M., and Padmalal, D., 2007. Non-pollen palynomorphs as potential palaeoenvironmental indicators in the Late Quaternary sediments of the West coast of India, Current Science, vol. 92, no. 10, p. 1370-1382.

LWCB Brochure, 2002. Managing the water resources of the Winnipeg River drainage basin, Lake of the Woods Control Board, 2002/11, p. 1-20.

Manitoba Hydro Brochure, ~ 1991. Lake Winnipeg Erosion and Water Levels.

Mann, J.D., 1999. Using ostracodes and sediments in paleolagoons Behind the Upper Campbell Beach of glacial Lake Agassiz to reconstruct its History during the Emerson Phase, master of science thesis, University of Manitoba, p. 1-293.

Matile, G., 2001. Email communication Matile, G., to Teller, J.T., August 27, 2001.

McMillan, K., Boyd, M., Teller, J., King, J., and Schnurrenberger, D., 2003. Physical sedimentology of West Hawk Lake, Manitoba –implications for paleohydrology and paleoclimate, CANQUA annual meeting, 2003, Halifax, Nova Scotia, poster.

Medioli, F.S., and Scott, D.B., 1988. Lacustrine thecamoebians (mainly Arcellaceans) as potential tools for palaeolimnological interpretations. Paleogeography, Paleoeclimatology, Paleoecology, vol. 62, p. 361-386.

Medioli, F.S.L., Scott, D.B., and Medioli, B.E., 2003. The Thecamoebian Bibliography, 2nd, Palaeontologia Electronica 6(5): 107, (http://palaeo-electronica.org/paleo/2003_1/biblio/issue1_03.htm).

McAndrews, J.H., 1982. Holocene environment of a fossil bison from Kenora, Ontario. Ontario Archaeology, vol. 37, p. 41-51.

Minning, G.V., Cowan, W.R., Sharpe, D.R., and Warman, T.A., 1994. Quaternary geology and drift composition, Lake of the Woods region, Northwestern Ontario, Geological Survey of Canada, Memoir 436, p. 1-239.

Mitchell, J.F.B., 1990. Greenhouse warming: is the Mid-Holocene a good analogue?, Journal of Climate, vol. 3, p. 1177-1192.

Molot, L., 1987. Re: Lake of the Woods Progress Report, B.A.R. Environmental letter to Nicholls, K., Water Resources Branch, Ontario Ministry of Environment, April 15, 1987, p. 1-15.

Molot, L.A., Trick, C.G., and Zimmerman, A.P., 1987. A paleolimnological investigation of algal pigments in Lake-of-the-Woods: recent changes in trophic status near Donald Duck and Smith Islands, Report for Ontario Ministry of Environment and Energy, p. 1-40.

Morgan, A.V., and Morgan, A., 1990. Beetles. In: Methods in Quaternary Ecology, Warner, B.G., (Ed.), Geoscience Canada, Reprint Series 5, p. 113-126.

Mybro, A.E, 2009. Personal email communication Mybro, A.E, to Teller, J.T., re LOW pollen ages, March 09, 2009.

Nambudiri, E.M.V., Teller, J.T., and Last, W.M., 1980. Pre-Quaternary microfossils a guide to errors in radiocarbon dating, Geology, vol. 8, p. 123-126.

Pair, D.L., and Rodrigues, C.G., 1993. Late Quaternary deglaciation of the southwestern St. Lawrence Lowland, New York and Ontario; with Suppl. Data 9321, GSA Bulletin, vol. 105, no. 9, p. 1151-1164.

Parent, M., and Occhietti, S., 1999. Late Wisconsinan deglaciation and glacial lake development in the Appalachians of southeastern Québec, Géographie physique et Quaternaire, vol. 53, no. 1, p. 117-135.

Patterson, R.T., and Kumar A., 2000. Assessment of arcellacean (thecamoebian) assemblages, species, and strains as contaminant indicators in James Lake, Northeastern Ontario, Canada, Journal of Foraminiferal Research, vol. 30, no. 4, p. 310-320.

Patterson, R.T., and Kumar A., 2002. A review of current testate rhizopod (thecamoebian) research in Canada, Palaeogeography, Palaeoclimatology, Palaeoecology vol. 180, p. 225-251.

Pla, S., Paterson, M., Smol, J.P., Clark, B.J., and Ingram, R., 2005. Spatial variability in water quality and surface sediment diatom assemblages in a complex lake basin: Lake of the Woods, Ontario, Canada, International Association Great Lakes Resources, vol. 31, 2005, p. 253-266.

Pfaff, L.J., 2004. Using non-marine ostracodes to reconstruct Quaternary plaeoenvironments, Emporia University, Kansas, p. 1-7, (http://www.emporia.edu/earthsci/student/pfaff2/ostracode.htm).

Risberg, J., Sandren, P., Teller, J.T., and Last, W.M., 1999. Siliceous microfossils and mineral magnetic characteristics in a sediment core from Lake Manitoba: Canada a remnant of glacial Lake Agassiz, Canadian Journal of Earth Sciences, vol. 36, no. 8, p. 1299-1314.

Ruddiman, W.F., 2002, Earth's Climate Past and Future, New York, W. H. Freeman and Company, p.1-465.

Ruhland, K., 2006. Personal email communication Ruhland, K., to Teller, J.T., re Lake of the Woods carbonate, April 17, 2006.

Sado, E.V., Fullertton, D.S., Goebel, J.E., and Ringrose, S.M., 1995. Quaternary Geologic Map of the Lake of the Woods 4^{o} x 6^{o} Quadrangle, United States and Canada, Quaternary Geologic Atlas of the United States, Miscellaneous Investigations Series Map I-1420, NM-15, U.S Department of the Interior, U.S. Geologic Survey.

Schindler, D.W., 1997. Widespread effects of climatic warming on freshwater ecosystems in North America. Hydrological Processes, vol. 11, p. 1043-1067.

Schindler, D.W., Bayley, S.E., Parker, B.R., Beaty, K.G., Cruikshank, D.R., Fee, E.J., Schindler, E.U., Stainton, M.P., 1996. The effects of climatic warming on the properties of boreal lakes and streams at the Experimental Lakes Area, northwestern Ontario, Limnology and Oceanography, vol. 41, p. 1004-1017.

Scott, D.B., Medioli, F.S., and Schafer, C.T., 2001. Monitoring in coastal environments using foraminifera and thecamoebian indicators, New York, Cambridge University Press, p. 94-168.

Shoal Lake Watershed Management Plan, 2001. A report to governments by the Shoal Lake Watershed Working Group, final working group draft prepared for public review, p. 1-145.

Shuman, B., Webb, T., Bartlein, P., and Williams, J.W., 2002. The anatomy of a climatic oscillation: vegetation change in eastern North America during the Younger Dryas chronozone, Quaternary Science Reviews, vol. 21, p. 1777-1791.

Smith, A.J., 1991. Lacustrine ostracodes as hydrochemical indicators in Holocene lake records of the north-central United States, Brown University, thesis, 1991, p. 1-306.

Smith, A.J., 1993. Lacustrine ostracodes as hydrochemical indicators in lakes of the north-central United States, Journal of Paleolimnology, vol. 8, p. 121-134.

Smith, A.J., Delorme, L.D., and Forester, R.M., 1992. A lake's solute history from ostracodes: comparison of methods. In: Proceedings of the 7th International Symposium on Water-Rock Interaction, Kharaka, Y.K., and Maest, A.S., WRI-7 / Park City, Utah, U.S.A, July 1992, p. 677-680.

Smith, A.J., and Horne, 2002. Ecology of marine, marginal marine, and non marine ostracodes. In: The Ostracoda, Applications in Quaternary Research, Holmes, J.A., and Chivas, A.R., (Ed.), Geophysical Monograph 131, American Geophysical Union, p. 37-64.

St. George, S., and Nielsen, E., 2002. Hydroclimatic changes in southern Manitoba since A.D. 1409 inferred from tree rings. Quaternary Research, vol. 58, p. 103-111.

St. George, S., 2006. Streamflow in the Winnipeg River basin, Canada: Trends, extremes and climate linkages, Journal of Hydrology, p. 1-16.

St. Jacques, J., Cumming, B.F., and Smol, J.P., 2008. A 900-year pollen-inferred temperature and effective moisture record from varved Lake Mina, west-central Minnesota, U.S.A, Quaternary Science Reviews, vol. 27, p. 781-196.

St. Jacques, J., Cumming, B.F., and Smol, J.P., 2009. A 900-yr diatom and chrysophyte record of spring mixing and summer stratification from varved Lake Mina, west-central Minnesota, USA, The Holocene, 19, 4, p. 537-547.

Taylor, K.C., Lamorey, G.W., Doyle, G.A., Alley, R.B., Grootes, P.A., Mayewski, P.A., White, J.W.C., and Barlow, L.K., 1993. The "flickering" switch of the late Pleistocene climate change, Nature, vol. 361, p. 432-436.

Teller, J.T., 1985. Glacial Lake Agassiz and its influence on the Great Lakes, Quaternary Evolution of the Great Lakes, Geological association of Canada, paper 30, p. 1-12.

Teller J.T., and Fenton, M.M., 1980. Late Wisconsinan glacial stratigraphy and history of southeastern Manitoba, Canadian Journal of Earth Science, vol. 17, p. 19-35.

Teller J.T., and Last, W.M., 1982. Pedogenic zones in postglacial sediment of Lake Manitoba, Canada, Earth surface processes and landforms, vol. 7, p. 367-379.

Teller, J.T., and Clayton, L., 1983. An introduction to glacial Lake Agassiz. In: Glacial Lake Agassiz, Teller, J.T., Clayton, L. (Eds.), Geological Association of Canada, St John's, Newfoundland, p. 3-5.

Teller, J.T., and Thorleifson, L.H., 1983. The Lake Agassiz-Lake Superior connection. In: Glacial Lake Agassiz, Teller, J.T., Clayton, L. (Eds.), Geological Association of Canada, Special Paper 26, p. 261-290.

Teller, J.T., Risberg, J., Matile, G., and Zoltai, S., 2000. Postglacial history and Paleoecology of Wampum, Manitoba, a former lagoon in the Lake Agassiz basin, GSA Bulletin 112, p. 943-958.

Teller, J.T., Leverington, D.W., and Mann, J.D., 2002. Freshwater outbursts to the oceans from glacial Lake Agassiz and their role in climate change during the last deglaciation. Quaternary Science Reviews 21, p. 879-887.

Teller J.T., and Leverington D.W., (2004) Glacial Lake Agassiz: a 5000-year history of change and its relationship to delta ^{18}O record of Greenland. Bulletin, American Geological Society, vol. 116, p. 729-742

Teller, J.T., Boyd, M., Yang, Z., Kor, P.S.G., Fard, A.M., 2005. Alternative routing of Lake Agassiz overflow during the Younger Dryas: new dates, paleotopography, and a re-evaluation, Quaternary Science Reviews vol. 24 p. 1890-1905.

Teller, J.T., Yang, Z., Boyd, M., Buhay, W.M., McMillan, K., Kling, H.J., and Telka, A.M., 2008. Postglacial sedimentary record and history of West Hawk Lake crater, Manitoba, Journal of Paleolimnology, vol. 40, p. 661-688.

Tolonen, K., 1986. Chapter 31, Rhizopod analysis. In: Handbook of Holocene Palaeoecology and Palaeohydrology, Berglund, B.E., (Ed.), John Wiley & Sons Ltd., p. 645-666.

Von Grafenstein, U., Eicher, U., Erlenkeuser, H., Ruch, P., Schwander, J., and Ammann, B., 2000. Isotope signature of the Younger Dryas and two minor oscillations at Gerzensee (Switzerland): palaeoclimatic and palaeolimnologic interpretation based on bulk and biogenic carbonates, Palaeogeography, Palaeoclimatology, Palaeoecology, vol. 159, p. 215-229.

Wall, A., Magny, M., Gilbert, D., Millet, L., Vannière, B., and Ruffaldi, P., 2008. Subfossil thecamoebians response to climate variations during the transition lateglacial / Holocene: a case study from Lake Lautrey (Jura, France), EGU General Assembly 2008, Geophysical Research Abstracts, vol. 10, EGU2008-A-00755, SRef-ID: 1607-7962/gra/EGU2008-A-00755.

Warner, B.G., 1990. Plant Macrofossils. In: Methods in Quaternary Ecology, Warner, B.G., (Ed.), Geoscience Canada, Reprint Series 5, p. 53-63.

Williams, J.W., Webb, T., Richard, P.H, and Newby, P., 2000. Late Quaternary biomes of Canada and the eastern United States, Journal of Biogeography, vol. 27, no. 3, p. 585-607.

Yang, Z., and Teller, J.T., 2005. Modeling the history of Lake of the Woods since 11,000 cal yr B.P. using GIS. Journal of Paleolimnology, vol. 33, p. 483-498.

Yansa, C.H., Dean, W.E., and Murphy, E.C., 2007. Late Quaternary paleoenvironments of an ephemeral wetland in North Dakota, U.S.A, Journal of Paleolimnology, vol. 38, no. 3, p. 441-457.

Wasylikowa, K., 1986. Analysis of fossil fruit and seeds. In: Handbook of Holocene Palaeoecology Palaeohydrology, Berglund, B., (Ed.), John Wiley & Sons Ltd., p. 571-590.

Whitlock, C., and Larsen, C., 2001. Charcoal as a fire proxy. In: Tracking environmental change using lake sediments, Volume 3, Terrestrial, algal, and siliceous indicators, Smol, J.P., Birks, H.J.B., and Last, W.M., (Eds.), Kluwer Academic Publishers, p. 75-97.

Willard, D.A., Bernhardt, C.E., Brooks, G.R., Cronin, T.M., Edgar, T., and Larson, R., 2007. Deglacial climate variability in central Florida, U.S.A, Palaeogeography, Palaeoclimatology, Palaeoecology, vol. 251, p. 366-382.

Wolfe, S.A., Huntley D.J., and Ollerhead, J., 2004. Relict Late Wisconsinan dune fields of the northern Great Plains, Canada, Geographie physique et Quaternaire, vol. 58, no. 2-3, p. 323-336.

Woodhouse, C.A., 2004. A paleo perspective on hydroclimatic variability in the western United States. Aquatic Sciences 66, 346-356.

Xia, J., Haskell, B.J., Engstrom, D.R., and Ito, E., 1995. Holocene climate reconstructions from tandem trace-element and stable isotope composition of ostracodes from Coldwater Lake, North Dakota, U.S.A, Journal of Paleolimnology, vol. 17, p. 85-100.

Zoltai, S.C. 1961. Glacial history of part of northwestern Ontario, Proceedings of Geological Association of Canada, vol. 13, p. 61-83.

Zoltai, S.C., 1963. Glacial features of the Canadian Lakehead area. Canadian Geographer 7, p. 101–115.

INTERNET SITES

Aber, J.S., Ostracode morphology, web page, Earth Science 767, Quaternary Geology, Emporia State University, Emporia, Kansas, http://images.google.com/imgres?imgurl=http://www.emporia.edu/earthsci/student/pfaff2/ostracode_morphology.jpg&imgrefurl=http://www.emporia.edu/earthsci/student/pfaff2/ostracode.htm&h=459&w=800&sz=60&hl=en&start=1&usg=__TSO5XhI2h8Zk5d1xvzqVEWTMEdg=&tbnid=i9StRbTXrPE_tM:&tbnh=82&tbnw=143&prev=/images%3Fq%3Dsite:www.emporia.edu%2BCandona%2Brawsoni%26hl%3Den

CalPal-2007online, 2009, software by Danzeglocke, U., Jöris, O., Weninger, B., http://www.calpal-online, calibration data set CalPal-2007Hulu.

NANODe Version 1, www.kent.edu/NANODe, (http://www.kent.edu/CAS/Geology/nanode/).

Illustration of Piston Corer, (http://esp.cr.usgs.gov/info/lacs/piston.htm).

Satellite Image of Lake of the Woods, (http://www.virtualnorth.net/satimp/).

Appendix B, Section 4 modern analogue images in following figures:

Figure B-2 (www.delawarewildflowers.org).

Figure B-3 (http://search.creativecommons.org/?q=Polygonum+lapathifolium+images&sourceid=Mozilla-search).

Figure B-4 (http://plants.ifas.ufl.edu/images/scival/sciva101.jpg).

.

APPENDICES

APPENDIX A: Core Subsample Data and Core Images

1. WOO06-1A-1K

1.1 WOO06-1A-1K: Subsample Ostracode Data:

Table A-1: Ostracode Data - Lake of the Woods South Basin Site 1A (WOO06-1A-1K)

sample code	Core Length (m)	*C. subtriangulata*	*L. friabilis*	*C. sharpei*	*F. rawsoni*
top of core	0.00	0	0	0	0
1K1 09-10	0.06	0	0	0	0
1K1 19-21	0.16	0	0	0	0
1K1 39-41	0.36	0	0	0	0
1K1 49-51	0.46	0	0	0	0
1K1 59-61	0.56	0	0	0	0
1K-2 2-4	0.68	0	0	0	0
1K-2 19-21	0.85	0	0	0	0
1K-2 29-31	0.95	0	0	0	0
1K-2 31-33	0.97	0	0	0	0
1K-2 39-41	1.05	0	0	0	0
1K-2 51-53	1.17	0	0	0	0
1K-2 59-61	1.25	0	0	0	0
1K-2 69-71	1.35	0	0	0	0
1K-2 79-81	1.45	0	0	0	0
1K-2 89-91	1.55	0	0	0	0
1K-2 99-101	1.65	0	0	0	0
1K-2 109-111	1.75	0	0	0	0
1K-3 3-4	1.86	0	0	0	0
1K-3 9-11	1.92	0	0	0	0
1K-3 19-21	2.02	0	0	0	0
1K-3 29-31	2.12	0	0	0	0
1K-3 39-41	2.22	**1**	0	0	0
1K-3 49-51	2.32	0	0	0	0
1K-3 59-61	2.42	0	0	0	0
1K-3 69-71	2.52	0	0	0	0
1K-3 79-81	2.62	0	0	0	0
1K-3 89-91	2.72	**1**	**1**	0	0
1K-3 99-101	2.82	**18**	**4**	0	**6**
1K-3 109-111	2.92	**25**	0	0	0
1K-3 119-121	3.02	**17**	**1**	0	0
1K-3 129-131	3.12	**24**	0	0	0
1K-3 139-141	3.22	**26**	0	0	0
1K-3 147-149	3.30	**23**	0	0	0

1.2 WOO06-1A-1K Subsample Lithic and Macrofossil Data, and Observations

Table A-2: WOO06-1A-1K Subsample Data

Sample Code	depth (m) Note 1	Lithic Note 1	plant mat'l. Note 1	charcoal * Note 1	insect mat'l. Note 1	carbonates (presence) Note 2	Thecam. (presence) Note 2	moisture estimate **	Sample volume estimate**	Observations
top of core	0.0									no sample
1K1 09-10	0.1	1	10					3	2	sample missing.
1K1 19-21	0.2	5	10	5	5	0	1	3	2	lith-com, qtz to 3mm, rre mica; insect-com.(exoskel & larvae cases, abn daphnia); charc-com, wood frags, misc frags. incl lves. to 5mm incl spruce needle, stems; pln't mat'l-abn, lves, stems, wood frags; theca-abn, 4 types incl spiney & cannon-like.
1K1 39-41	0.4	10	10	5	1	0	1	1	2	lith-com, qtz to 4mm, fibrous white min; insect-com.(exoskel & larvae cases, mostly daphnia); charc-com, lves & stems; pln't mat'l-abn, aquatic; theca-com, 5 types incl spiney, cannon-like & flat.
1K1 49-51	0.5	1	10	1	10	0	1	2	2	lith-rre, qtz to 2mm; insect-com.(exoskel & larvae cases, mostly daphnia); charc-rre, stems&amorphous; pln't mat'l-abn, aquatic; theca-abn, 5 types incl spiney, & 2 varieties of flat.
1K1 59-61	0.6	5	10	1	5	0	1	2	2	lith-rre, qtz to 3mm; insect-com.(exoskel & larvae cases, mostly daphnia); charc-rre, lge frags; pln't mat'l-abn, aquatic + seed pods; theca-abn, 2 types of spiney vases (short and tall).
1K-2 2-4	0.7	1	10	1	5	0	1	2	3	lith-rre-com (2%), qtz to 2mm; insect-com.(exoskel & larvae cases); charc-rre (1%), stems(not transptd) & terr. lves; pln't mat'l-abn, aquatic & terr + seed; theca-abn, 5 types incl spiney & 2 flat varieties + brn vase).
1K-2 19-21	0.9	5	10	5	1	0	1	3	2	lith-com, qtz to 4mm, fibrous wht min; insect-rre. (exoskel & larvae cases); charc-rre-com(1-2%), thin stems(not transptd) & terr. lves; pln't mat'l-abn, aquatic? Lge lves to 2 cm; theca-rre-com, 2 types short/tall vase + brn vase); periostracum bivalve frag. dated 1460 (1358) C^{14} (Cal) yrs. BP.
1K-2 29-31	1.0	5	10	10	5	0	0	3	2	lith-com, mostly non deaggr. clay, qtz to 1mm; insect-com. (exoskel & larvae cases); charc-abn, terr. large frags to 1cm, fenestral frags; pln't mat'l-abn, long hollow stem (grass?); theca-none.

Sample Code	depth (m) Note 1	Lithic Note 1	plant mat'l. Note 1	charcoal * Note 1	insect mat'l. Note 1	carbonates (presence) Note 2	Thecam. (presence) Note 2	moisture estimate **	Sample volume estimate**	Observations
1K-2 31-33	1.0	1	10	10	1	0	1	2	2	lith-rre, qtz to 2mm; insect-rre. (exoskel & larvae cases); charc-abn, terr. Lve frags, hollow stems to 8mm, non transported; pln't mat'l-abn, aquatic + darkened lves/stems to 1cm x 1mm; theca-abn, 2 varieties incl with rim spikes, various sizes.
1K-2 39-41	1.1	10	1	5	1	0	1	3	2	lith-abn, qtz to 4mm; insect-rre. (exoskel & larvae cases); charc-rre-com (1-2%), leaf frags 5-7mm, non transported; pln't mat'l-rre, aquatic; theca-rre, vase, brn vase, larvae encasement 5 mm.
1K-2 51-53	1.2	10	10	10	5	0	1	2	2	lith-abn, qtz to 3mm rre darker min; insect-com. (exoskel & larvae cases); charc-abn, twigs & bark (not transported), pieces of wood to 4mm, fenestral frags; pln't mat'l-abn, aquatic; theca-com, common vase variable sizes, 1 elongate, + brn. vase.
1K-2 59-61	1.3	10	1	10	10	0	1	2	1	lith-abn, qtz to 3mm, fibrous wht min; insect-abn. (exoskel & larvae cases); charc-abn, thin stems, lves, large frags. (not transported); pln't mat'l-rre, aquatic; theca-rre-com, 4 vase variable sizes incl flat, flat spiny, & brn. vase, 6mm insect frag (leg)?.
1K-2 69-71	1.4	10	5	5	5	0	1	3	1.5	lith-abn, qtz to 3mm; insect-com. (exoskel & larvae cases); charc-rre-com(1-2%), stems, leaf frags to 4mm; pln't mat'l-com, aquatic; theca-rre-com, 1 type (vase), + brn. vase. One conifer seed wing (no seed) & beetle elytron (1) nearby at 69-71 cm, processed at Paleotec & dated. 1675 (1579) C^{14} (Cal) yrs. BP.
1K-2 79-81	1.5	10	1	5	1	0	1	3	2	lith-abn, qtz to 3mm; insect-rre. (exoskel & larvae cases); charc-rre-com (2%), twigs, stems, wood, & leaf frags, datable; pln't mat'l-rre; theca vase shaped rre, & brn vase.
1K-2 89-91	1.6	10	1	5	1	0	0	3	2	lith-abn, qtz to 4mm; insect-rre. (exoskel & larvae cases); charc-rre-com (2%), twigs, leaf frags, seed cases (to 3mm), datable; pln't mat'l-rre, aquatic; no theca.
1K-2 99-101	1.7	10	1	10	1	0	0	3	2	lith-abn, qtz to 3mm, fibrous wht min; insect-rre. (exoskel & larvae cases); charc-abn, twigs, leaf frags (to 4mm), stems, datable; pln't mat'l-rre, aquatic; no theca except brn vase.

Sample Code	depth (m) Note 1	Lithic Note 1	plant mat'l. Note 1	charcoal * Note 1	insect mat'l. Note 1	carbonates (presence) Note 2	Thecam. (presence) Note 2	moisture estimate **	Sample volume estimate**	Observations
1K-2 109-111	1.8	10	1	5	1	0	0	2	2	lith-abn, qtz to 4mm, fibrous wht min; insect-rre. (exoskel & larvae cases); charc-rre-com (3%), stems, lge. leaf frags. & wood frags, fenestral; frags, datable; pln't mat'l-rre, aquatic + wood frag; molar 3-4 mm blk.
1K-3 3-4	1.9	10	1	5	1	0	0	2	2	lith-abn, qtz to 4mm, fibrous wht min; insect-rre. (exoskel & larvae cases); charc-rre-com (2%), stems, lge. frags, seeds & cases, leaf frags; datable; pln't mat'l-rre, aquatic incl spiral leaf & stem; brn vase.
1K-3 9-11	1.9	10	1	5	1	0	0	3	2	lith-abn, qtz to 3mm, wht fluffy min; insect-rre. (exoskel & rre. larvae cases); charc-rre-com (2%), stem & leaf frags, wood frags; look transported; pln't mat'l-rre, aquatic.
1K-3 19-21	2.0	10	1	5	1	1	0	3	3	lith-abn, qtz to 5mm, carbonates; insect-rre. (exoskel & rre. larvae cases); charc-com (3%), stem, wood & leaf frags; not transptd; pln't mat'l-rre, aquatic; vertebrae, molars.
1K-3 29-31	2.1	10	1	5	1	1	0	3	0.5	lith-abn, qtz to 3mm, fibrous wht min (carbonate); insect-rre. (larvae cases only); charc-com, sml stems, wood & amorphous frags; not transptd; pln't mat'l-rre, aquatic; insect appendage.
1K-3 39-41	2.2	10	1	10	5	0	0	3	0.5	lith-abn, qtz to 3mm, fibrous wht min; insect-com (2%), (exoskel & larvae cases); charc-abn, sml frags stems, wood & lves; not transptd; pln't mat'l-rre, aquatic; molars, 1 broken ostra (ST) possible outlier or reworked?, incisor and molar?, claw attached to bone (implies no reworking).
1K-3 49-51	2.3	10	1	10	10	1	0	3	2	lith-abn, qtz to 4mm, wht snow flake min (carbonate); insect-rre, (exoskel & larvae cases); charc-abn, lge. leaf, stem, wood frags, seed (4mm, shiny blk); not transptd; pln't mat'l-rre, aquatic;
1K-3 59-61	2.4	10	1	10	1	1	0	3	1	lith-abn, qtz to 4mm, wht fibrous min (carbonate); insect-rre, (exoskel & larvae cases); charc-abn, lge. wood frags to 5mm, lves, stems not transptd; pln't mat'l-rre, aquatic. Radiocarbon date using pollen at 2.45 m. 12260 (14365) C^{14} (Cal) yrs. BP.
1K-3 69-71	2.5	10	1	10	1	1	0	2	1	lith-abn, qtz to 3mm, rre calcarious min; insect-rre, (exoskel & larvae cases); charc-abn, wood, stems, leaf frags, not transptd; pln't mat'l-rre, aquatic.

Sample Code	depth (m) Note 1	Lithic Note 1	plant mat'l. Note 1	charcoal * Note 1	insect mat'l. Note 1	carbonates (presence) Note 2	Thecam. (presence) Note 2	moisture estimate **	Sample volume estimate**	Observations
1K-3 79-81	2.6	10	5	10	5	1	0	1	0.5	lith-abn, qtz to 3mm, rre opaque wht. Min, carbonates; insect-rre, (exoskel (incl. leg parts, & larvae cases); charc-abn (40%), sml. amorphous gry/blk frags, wood frags (not transptd); pln't mat'l-abn, aquatic.
1K-3 89-91	2.7	10	10	10	1	1	0	1	0.5	lith-abn, qtz/fsp to 3mm, some rust coloured, rre fibrous wht. min. & carbonate min; insect-rre, (exoskel & larvae cases); charc-abn (70%), sml frags) sml. amount wood, stems, leaf frags (not transptd); pln't mat'l-rre, seed; aquatic; ostra (ST,F) coated. two 89-91 samples processed.
1K-3 99-101	2.8	10	5	10	0	1	0	1	1	lith-abn, qtz/fsp to 3mm, abn carbonate; insect-none; charc-abn (10%), leaf frags 6mm seeds *Polygonal lapathifolium* (not transptd); pln't mat'l-rre, non char leaf & wood frags; frag. gastropod; ostra ((ST, F, & R) often coated, some frags. 7375 (8228) C^{14} (Cal) yrs. BP**.**
1K-3 109-111	2.9	10	5	10	0	1	0	1	1	lith-abn, qtz to 4mm, calcarious min, lge abn non disaggr. gry clay; insect-none; charc-abn, wood, stems, leaf frags, not transptd, seeds (appear burnt) *Polygonal lapathifolium*; pln't mat'l-abn, aquatic & seeds; ostra (ST) thin shelled & coated, possible vertebrae.
1K-3 119-121	3.0	10	1	5	0	1	0	1	1.5	lith-abn, qtz to 4mm, turquoise min, carbonate min, abn. non disaggr. clay; v rre. Insect (larvae case); charc-com, stems, leaf frags, not transptd; pln't mat'l-rre, aquatic & seeds, Polygonal lapathifolium; ostra (ST, F) coated, one articulated.
1K-3 129-131	3.1	10	1	10	1	1	0	1	1	lith-abn, qtz to 4mm, wht. opaque min, carbonates; rre. Insect (larvae cases); charc-com, stems, lge to 8mm leaf & wood frags, not transptd; pln't mat'l-rre, aquatic; ostra (ST, F) thin & coated. Two samples processed.
1K-3 139-141	3.2	10	10	10	1	1	0	1	1	lith-abn, qtz to 4mm, wht. opaque min, carbonates; rre. Insect (exoskel & larvae cases); charc-abn, seeds, lves & stem frags, not transptd; pln't mat'l-rre, aquatic; ostra (ST) coated, some broken. 2 139-141 samples processed. *Polygonum lapathifolium* seeds (4) found nearby (141-144) at 3.25 m and dated. 7140 (7973) C^{14} (Cal) yrs. BP**:**

Sample Code	depth (m) Note 1	Lithic Note 1	plant mat'l. Note 1	charcoal * Note 1	insect mat'l. Note 1	carbonates (presence) Note 2	Thecam. (presence) Note 2	moisture estimate **	Sample volume estimate**	Observations
1K-3 147-149	3.3	10	5	1	0	1	0	1	1	lith-abn, qtz to 3mm, com blk & red min, non deagrreg. clay granules to 5mm,clear min, carbonates; Insect, none; charc-rre, leaf frags; pln't mat'l-rre, aquatic; ostra (ST) coated, some broken.

Note 1: For lithics, plant material, charcoal, and insect material: 1=rare; 5=common; 10=abundant.

Note 2: For carbonates and thecamoebians; 1=present, 0=not present (relative % were not estimated).

* note abundance of charcoal of 10, means its subsample volume was > 5%
** volume of material and moisture estimates based on scale 1=low (rare); 2=common; 3=high
ostra = ostracodes; ST=*C. subtriangulata*, F=*L. friabilis*; S=*C. sharpie*; R=*F. rawsoni.*

1.3 WOO06-1A-1K Scanned Core Images and Core Lithologic Descriptions

The following scanned core images WOO06-1A-1K1, 1K2, and 1K3; provide a view of the sedimentology in the core. The coloured bars at the bottom of the scanned core are each 10 cm long. Core Lithologic descriptions of these scanned images are provided on the following 3 pages.

1K1

1K2

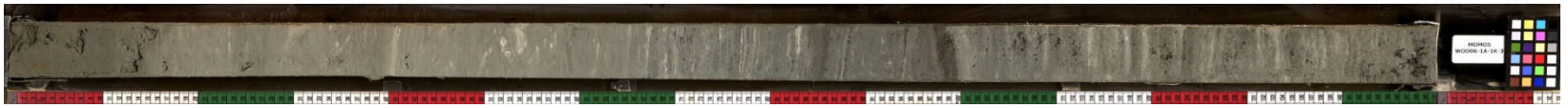

1K3

2. WOO06-4A-1K

2.1 WOO06-4A-1K: Subsample Ostracode Data:

Table A-3: Ostracode Data - LOTWs Northwest Angle Channel Site 4A (WOO06- 4A-1K)

sample code	Core Length (m)	*C. subtriangulata*	*L. friabilis*	*C. sharpei*	*F. rawsoni*
top core	0.00				
1K1 7-9	0.08	0	0	0	0
1K1 15-17	0.16	0	0	0	0
1K1 30-32	0.31	0	0	0	0
1K1 45-47	0.46	0	0	0	0
1K2 10-12	0.62	0	0	0	0
1K2 22-23	0.74				
1K2 25-27	0.77	0	0	0	0
1K2 40-42	0.92	0	0	0	0
1K2 55-57	1.07	0	0	0	0
1K2 70-72	1.22	0	0	0	0
1K2 85-87	1.37	0	0	0	0
1K2 99-100	1.50	0	0	0	0
1K2 115-117	1.67	0	0	0	0
1K2 130-132	1.82	**2**	0	0	0
1K2 145-147	1.97	**12**	0	0	0
1K-2 99-101	2.01				

2.2 WOO06-4A-1K: Subsample Lithic and Macrofossil Data, and Observations

Table A-4: WOO06-4A-1K Subsample Data

Sample Code	depth (m)	Lithic Note 1	plant mat'l. Note 1	charcoal * Note 1	insect mat'l. Note 1	carbonates (presence) Note 2	Thecam. (presence) **	moisture estimate **	Sample volume estimate**	Observations
top of core	0.00									
1K1 7-9	0.08									Paleotec sample, dated; bulrush *Scirpus validus* seeds, no attached bristles, some opened. **2495 (2604) C14 (Cal) yrs. BP.**
1K1 15-17	0.16	5	10	10	1	0	1	2	3	lith-com, qtz typically <0.5mm; insect-rre (larvae cases); charc-abn, abn lge wood frags to 3mm, + sml frags wood and amorphous; pln't mat'l-abn, lves, stems, wood frags, seeds (multiple types, including bulrush (*Scirpus validus)* to 7-8 mm, pine cone frags?; theca-rre, 3 types incl flat spiney.
1K1 30-32	0.31	1	10	10	10	0	3	3	2	lith-rre, qtz & mica to 3mm; insect-com.(exoskel & larvae cases); charc-abn, abn lge. wood frags; pln't mat'l-abn (75%), lves, stems, wood frags, seeds to 3mm (2 types, incl (*Polygonum lapathifolium*)curlytop knotweed)); theca-abn, 4 types incl mostly flat, & rimless.
1K1 45-47	0.46	1	10	10	10	0	0	2	1.5	lith-rre, qtz, micas, grn min. to 3mm; insect-abn. (exoskel & larvae cases); charc-abn, stems incl. branch to 6mm, long fenestral frags; pln't mat'l-abn, aquatic rre seeds; theca-none, fish bone? larvae encasement; not transpt'd.
1K2 10-12	0.62	5	10	10	5	0	0	2	2.5	lith-com, qtz & abn. micas to 3mm; insect-com.(exoskel & larvae cases); charc-abn, lge frags incl blk. seeds 5mm, stems (2-3mm); pln't mat'l-abn, multiple variety of stems, lves, etc, 3 types seeds to 8mm, some blackn'd, possible pine cone frag; theca-none, fish scale frag; org. not transpt'd.
1K2 22-23	0.74									Paleotec sample, dated, wood fragment 1 cm long. 6370 (7319) **C^{14} (Cal) yrs. BP.**

Sample Code	depth (m)	Lithic Note 1	plant mat'l. Note 1	charcoal * Note 1	insect mat'l. Note 1	carbonates (presence) Note 2	Thecam. (presence) **	moisture estimate ** 	Sample volume estimate**	Observations
1K2 25-27	0.77	5	10	5	1	1	1	1.5	3	lith-com, qtz & micas 1-2mm, carbonate lithics; insect-com.(exoskel & rre. larvae cases); charc-com, wood & twig frags; pln't mat'l-abn (80%) thick mat, lves, stems, lge. wood pieces (one lge transprt'd to 1cm), seeds & seed pods, pine cone frags?, to 8mm; theca-rre, 2 types incl. flat type, larvae encasement, org. mostly not transpt'd.
1K2 40-42	0.92	1	10	10	1	0	0	1.5	3	Paleotec sample (42-43), dated 1 cm wood frag: lith-rre (<1%), qtz to 2mm; insect-com.(rre-exoskel & larvae cases); charc-abn (50%), stems, seeds, amorphous frags; pln't mat'l-abn (50%), seeds lge & sml, lge wood frags. to 5x4mm; theca-none visible could not sieve due to matted plant mat; not transpt'd. Dated 4 wood frags to 1 cm long **6955 (7787) C14 (Cal) yrs. BP.**
1K2 55-57	1.07	5	10	10	1	0	0	1.5	3	lith-com, qtz typically 1 mm + non deaggr. clay balls, insect-rre. (exoskel & larvae cases); charc-rre-abn(5%), charc frags long (some look transpt'd; pln't mat'l-abn (90%), lge frgmts wood & lves, some wood not transpt'd; thick organic mat not sieved.
1K2 70-72	1.22	1	10	10	1	0	0	2	3	lith-rre, mostly hard gry clay pellets to 4mm; insect-rre. (v-rre-exoskel & larvae cases); charc-abn (5%), sml twigs & wood frags not transptd; pln't mat'l-abn (95%), lves, stems, wood frags, lge. & sml. seeds to 5mm, 2 types (incl. bullrush & curlytop knotweed); long hollow wood frag.
1K2 85-87	1.37	1	10	10	1	0	0	0.5	3	lith-rre, qtz to 5mm; insect-rre. (exoskel, incl. dapnia, & larvae cases); charc-abn (5%), lge plant mat'ls in a mat, blackened seeds, sml. amorphous charc; pln't mat'l-abn (90%), aquatic & terr. all types plant mat'l, sml-lge. seeds to 5mm (incl. bullrush), dark and light coloured, not transpt'd.
1K2 99-100	1.50	0.5	10	10	3	0	0	0.5	3	lith-v-rre; insect-com. (exoskel & larvae cases); charc-abn (25%), lge pieces of wood to 10mm; pln't mat'l-abn (70%), terr. & aquatic, seeds and seed cases to 8 mm, 2 types (incl. bulrush & curlytop knotweed), stems & lves; org. not transpt'd. Dated *scirpus* achenes **7655 (8443) C14 (Cal) yrs. BP.**

Sample Code	depth (m)	Lithic Note 1	plant mat'l. Note 1	charcoal * Note 1	insect mat'l. Note 1	carbonates (presence) Note 2	Thecam. (presence) **	moisture estimate **	Sample volume estimate**	Observations
1K2 115-117	1.67	10	1	1	1	1	0	1	1.5	lith-abn, qtz & micas/granitic to 1mm, rre carbonates; insect-rre (exoskel & larvae cases); charc-rre, sml frags, (transported); pln't mat'l-rre, aquatic.
1K2 130-132	1.82	10	1	0	1	1	0	1.5	1	lith-abn, qtz & micas, rre carbonates, some clay balls (react to HCl) to 2; mm, opaque min; insect-rre (exoskel & larvae cases); charc-none; pln't mat'l-rre, aquatic; ostra (ST), lightly coated, broken.
1K2 145-147	1.97	10	0.5	0.5	0.5	1	0	0.5	3	lith-abn, qtz, non deaggr. clay balls to 3mm, brn min, carbonate; insect-v-rre. (exoskel & larvae cases); charc-v-rre; pln't mat'l-abn (aquatic), long thin stems; ostra (ST), thin & fragmnt'd.

Note 1: For lithics, plant material, charcoal, and insect material: 1=rare; 5=common; 10=abundant.
Note 2: For carbonates and thecamoebians; 1=present, 0=not present (relative % were not estimated).

* note abundance of charcoal of 10, means its subsample volume was > 5%
** volume of material and moisture estimates based on scale 1=low (rare); 2=common; 3=high
ostra = ostracodes; ST=*C. subtriangulata*, F=*L. friabilis*; S=*C. sharpie*; R=*F. rawsoni.*

2.3 WOO06-4A-1K Scanned Core Images and Core Lithologic Descriptions

The following scanned core images WOO06-4A-1K1 and 1K2 provide a view of the sedimentology in the core. The coloured bars at the bottom of the scanned core are each 10 cm long. Core lithologic descriptions of these scanned images are provided on the following 2 pages.

1K1

1K2

3. WOO06-5A-1K

3.1 WOO06-5A-1K: Subsample Ostracode Data:

Table A-5: Ostracode Data - LOTWs Northwest Angle Basin Site 5A (WOO06- 5A-1K)

sample code	Core Length (m)	*C. subtriangulata*	*L. friabilis*	*C. sharpei*	*F. rawsoni*
top core	0.00				
1K1 12-14	0.02	0	0	0	0
1K1 22-24	0.13	0	0	0	0
1K2 2-4	0.02	0	0	0	0
1K2 09-11	0.26	0	0	0	0
1K-2 19-21	0.36	0	0	0	0
1K-2 29-31	0.46	0	0	0	0
1K-2 39-41	0.56	0	0	0	0
1K-2 49-51	0.66	0	0	0	0
1K-2 59-61	0.76	0	0	0	0
1K-2 69-71	0.86	0	0	0	0
1K-2 78-80	0.94	0	0	0	0
1K-3 9-11	1.08	0	0	0	0
1K-3 19-21	1.18	0	0	0	0
1K-3 29-31	1.28	0	0	0	0
1K-3 39-41	1.38	0	0	0	0
1K-3 49-51	1.48	0	0	0	0
1K-3 55-57	1.55	0	0	0	0
1K-3 59-61	1.58	0	0	0	0
1K-3 69-71	1.68	0	0	0	0
1K-3 79-81	1.78	0	0	0	0
1K-3 89-91	1.88	0	0	0	0
1K-3 99-101	1.98	0	0	0	0
1K-3 109-111	2.08	0	0	0	0
1K-3 119-121	2.18	0	0	0	0
1K-3 129-131	2.28	0	0	0	0
1K-3 139-141	2.38	0	0	0	0
1K-3 147-149.5	2.45	0	0	0	0
1K-4 9-11	2.59	0	0	0	0
1K-4 20-22	2.70	**16**	0	**2**	**3**
1K-4 25-27	2.75	**2**	0	0	0
1K-4 29-31	2.79	0	0	0	0
1K-4 35-37	2.85	0	0	0	**8**
1K-4 39-41	2.89	0	**16**	0	**15**
1K-4 45-47	2.95	0	0	0	**8**

sample code	Core Length (m)	*C. subtriangulata*	*L. friabilis*	*C. sharpei*	*F. rawsoni*
1K-4 49-51	2.99	0	0	0	0
1K-4 59-61	3.09	0	0	0	0
1K-4 69-71	3.19	0	0	0	0
1K-4 75-77	3.25				
1K-4 79-81	3.29	0	0	0	0
1K-4 82-83	3.31				
1K-4 82-83	3.31				
1K-4 89-91	3.39	0	0	**18**	**8**
1K-4 99-101	3.49	0	**5**	0	0
1K-4 109-111	3.59	0	**11**	0	0
1K-4 119-121	3.69	0	**1**	0	0
1K-4 129-131	3.79	**2**	**8**	0	0
1K-4 139-141	3.89	**6**	**4**	0	0
1K-4 147-149	3.97	**4**	0	**2**	**4**
1K-5 9-11	4.09	**3**	**2**	0	0
1K-5 19-21	4.19	**11**	0	0	0
1K-5 29-31	4.29	**17**	0	0	0
1K5-5-37.5	4.36				
1K-5 39-41	4.39	**2**	**2**	0	0
1K-5 49-51	4.49	**10**	**2**	0	0
1K-5 59-61	4.59	**8**	0	0	0
1K-5 69-71	4.69	**22**	0	0	0
1K-5 79-81	4.79	**7**	0	0	0
1K-5 89-91	4.89	**7**	0	0	0
1K-5 99-101	4.99	**67**	0	0	0
1K-5 109-111	5.09	**74**	0	0	0
1K-5 119-121	5.19	**48**	0	0	0
1K-5 129-131	5.29	**26**	0	0	0
1K-5 139-141	5.39	**49**	0	0	0
1K-5 147-149	5.47	**30**	0	0	0
bottom core	5.48				

3.2 WOO06-5A-1K Subsample Lithic and Macrofossil Data, and Observations

Table A-6: WOO06-5A-1K Subsample Data

Sample Code	depth (m)	Lithic Note 1	plant mat'l. Note 1	charcoal * Note 1	insect mat'l. Note 1	carbonates (presence) Note 2	Thecam. (presence) **	moisture estimate **	Sample volume estimate**	Observations
top of core	0.00									Sample core depths adjusted to compensate for 10 cm of foam to obtain top of recovered core.
1K1 12-14	0.02	5	1	1	5	0	1	3	2	lith-com, qtz; insect-com. (rre exoskel; com larvae cases); charc-rre; org pln't mat'l-com; theca-rre.
1K1 22-24	0.13	1	1	3	10	0	2	3	2	lith-com, qtz; com insect-com (rre exoskel); charc-rre; org pln't mat'l-com; theca-com (2 types).
1K2 2-4	0.02	1	5	1	5	0	1	3	1	lith-rre, qtz; insect-com (rre exoskel); charc-rre; pln't mat'l.- rre; theca-rre (1 type, flat rimless), brn vase.
1K2 09-11	0.26	3	5	1	5	1	1	3	2	lith- rre-com, qtz, carbonate lithics; insect-com (rre exoskel;); charc-rre; pln't mat'l-rre; theca-rre (vase), brn vase.
1K-2 19-21	0.36	1	1	1	5	0	1	3	2	lith-rre, qtz to 2mm; insect-com. (rre exoskel) plnt-com (rre seeds); charc-com (some lge frags); theca-rre (vase).
1K-2 29-31	0.46	1	1	5	1	0	0	3	0.5	lith-rre qtz (com non disaggr. clay balls); insect-rre (l lge piece 3mm; larvae cases); charc-com; pln't mat'l-rre (rre seed); no theca; fish bone.
1K-2 39-41	0.56	1	5	1	1	1	0	3	1	lith-rre, qtz, carbonate lithics; insect-rre.(exoskel & larvae cases); charc-rre; org pln't mat'l-com; no theca, brn vase.
1K-2 49-51	0.66	5	1	5	5	0	2	3	1	lith-com, qtz; insect-com.(exoskel & larvae cases); charc-com (8mm blk needle, larch); org pln't mat'l-rre; theca-com (short vase). C14 date from 49-61 (conifer seed wing, beetle *elytron. Ant* mandible) **2080 (2071) C^{14} (Cal) yrs. BP.**

Sample Code	depth (m)	Lithic Note 1	plant mat'l. Note 1	charcoal * Note 1	insect mat'l. Note 1	carbonates (presence) Note 2	Thecam. (presence) **	moisture estimate **	Sample volume estimate**	Observations
1K-2 59-61	0.76	7.5	10	5	7.5	0	1	3	1	lith-com/abn, qtz; insect-com.(exoskel & larvae cases); charc-com (up to lge 3mm); pln't mat'l-abn; theca-rre (vase), brn vases; org mat'l not tranpt'd. 2 samples processed, one FD.
1K-2 69-71	0.86	1	5	5	10	0	0	3	0.5	lith -rre, opaque min.; insect-abn.(exoskel & larvae cases); char-com. to 2mm; plant mat'l-com; no theca; mat'ls not transpt'd.
1K-2 78-80	0.94	5	1	5	5	0	0	3	0.5	lith-com, qtz; insect-com. (exoskel & larvae cases); charc-com (to 2-3 mm) pln't mat'l-rre; no theca.
1K-3 9-11	1.08	1	1	1	10	0	0	3	1	lith-rre, qtz, opq. min; insect-com.(exoskel & larvae cases); charc-rre; pln't mat'l-rre (1 sml seed, birch nutlet); no theca; fish tooth?
1K-3 19-21	1.18	1	5	7.5	10	1	0	3	0.5	lith-rre, qtz, opaque min (carbonate); insect-abn.(exoskel & larvae cases); charc-com/abn (not transpt'd); pln't mat'l-com (blk lichen?); brn vase frag, 1 ST (contam? not counted).
1K-3 29-31	1.28	1	5	5	5	0	0	3	1	lith-rre, qtz; insect-com.(exoskel & rre larvae cases); charc-com; pln't mat'l-com.
1K-3 39-41	1.38	1	1	1	10	0	0	3	1	lith-com, qtz; insect-abn.(exoskel & larvae cases); charc-rre; pln't mat'l-rre.
1K-3 49-51	1.48	5	5	5	5	0	0	3	1	lith-com, qtz & fsp; insect-com.(exoskel & larvae cases); charc-com; pln't mat'l-com.
1K-3 55-57	1.55	0.5	1	5	10	0	0		1	FD sample; lith-v rre; qtz, amorphous white min.; insect-abn (exoskel & larvae cases); charc-com (not transpt'd); pln't mat'l-rre.
1K-3 59-61	1.58	0.5	1	5	10	0	0	3	1	porcessed in Champaign, Ill; sample missing (refer to nearby sample above) used same values with moisture and vol. est. from below.
1K-3 69-71	1.68	5	1	5	5	0	0	3	1	lith-com, qtz; insect-com.(exoskel & rre larvae cases); charc-com; pln't mat'l-rre; no theca, brn vase - 2mm.

Sample Code	depth (m)	Lithic Note 1	plant mat'l. Note 1	charcoal * Note 1	insect mat'l. Note 1	carbonates (presence) Note 2	Thecam. (presence) **	moisture estimate **	Sample volume estimate**	Observations
1K-3 79-81	1.78	1	1	10	10	0	0	3	1	lith-rre, qtz; insect-abn.(exoskel & larvae cases); charc-abn; pln't mat'l-rre. C14 date from 78-90 Dated grass seed and misc insect parts **3910 (4343) C14 (Cal) yrs. BP.**
1K-3 89-91	1.88	5	1	10	5	0	0	3	1	lith-com, qtz; insect-com.(exoskel & larvae cases); charc-abn; pln't mat'l-rre.
1K-3 99-101	1.98	1	1	5	10	0	0	3	2	lith-rre, qtz (opaque min.); insect-abn.(exoskel & larvae cases); charc-com; pln't mat'l-rre; ostra. broken ST, contam?
1K-3 109-111	2.08	1	3	5	5	0	0	3	1	lith-rre, qtz (opaque min.); insect-com.(rre exoskel, & com. larvae cases); charc-com; pln't mat'l-rre/com.
1K-3 119-121	2.18	1	3	3	10	0	0	3	1	lith-rre, qtz, com non disaggr. clay balls; insect-abn.(exoskel & larvae cases); charc-rre (1-2 mm blk lichen); pln't mat'l-rre (common sml seeds); organics not transpt'd; supplmt FD sample (1K-3 115-117) indicted carbonate & char leaf & twigs; + coated F(1) ostrac? (not counted), contam?
1K-3 129-131	2.28	1	5	5	5	0	0	3	2	lith-rre, qtz; insect-com.(rre exoskel & com larvae cases); charc-com; pln't mat'l-com (rre sml seeds) larvae encasement.
1K-3 139-141	2.38	10	3	1	3	0	0	3	1.5	lith-abn pellets (blk/red-up to 5-6mm), rre qtz; opaque min; insect-rre. (exoskel & larvae cases); charc-rre; pln't mat'l-rre/com (aquatic); suppl FD sample 136-137 also used.
1K-3 147-149.5	2.45	10	0	0	0.5	1	0	2	2	lith-abn, clay pellets, blue -vivianite? lithics (most abn), opaque min. (carbonate), no qtz; insect-rre. (one larvae case); charc-0; pln't mat'l-0; fish bones.
1K-4 9-11	2.59	10	10	1	5	0	0	1	2	lith-abn clay pellets (brn exterior), rre-qtz; insect-com.(exoskel & larvae cases); charc-rre; pln't mat'l (aquatic leaves)-abn, + numerous *scirpus* seeds (birch nutlets).

Sample Code	depth (m)	Lithic Note 1	plant mat'l. Note 1	charcoal * Note 1	insect mat'l. Note 1	carbonates (presence) Note 2	Thecam. (presence) **	moisture estimate **	Sample volume estimate**	Observations
1K-4 20-22	2.70	5	5	1	10	0	0	1	3	lith-com, clay pellets blue (vivianite?) rre qtz; insect-abn.(exoskel & larvae cases); charc-rre; pln't mat'l-com (incl sml stems); ostra (ST,S,R): many broken & thin.
1K-4 25-27	2.75	10	10	10	5	1	0		1	FD sample: lith-abn, clay pellets, wht fibrous min. (carbonate); insect-com (exoskel & larvae cases); charc-com (2-3 mm leaf frags & fenestral & amorphous frags); pln't mat'l-abn aquatic; ostra (ST?), all thin & broken, ttl # est. from frags; organics not transpt'd; white feather-like 2mm object?
1K-4 29-31	2.79	1	1	10	10	0	0	1	0.5	lith-very rre, qtz; insect-abn.(rre exoskel & com larvae cases); charc-abn; pln't mat'l-rre (seeds to 3 mm); v-rre ostra frags not tallied; suppl FD sample 25-27 included.
1K-4 35-37	2.85	1	10	5	10	0	0		1	FD sample: lith-rre, orange clay pellets only; insect-abn (exoskel & larvae cases); charc-com (1-2 mm non transpt'd twigs); pln't mat'l-abn aquatic; ostra (R), all thin & broken one distinct R, ttl # est. from frags.
1K-4 39-41	2.89	1	5	10	10	0	0		1	Processed at Champaign, Ill. (no additional data); many Ostr (F) crushed… nearby soil? est.data from FD sample 35-37 above. **7510 (8308) C14 (Cal) yrs. BP.**
1K-4 45-47	2.95	1.5	5	5	10	0	0		1	Date confirms above date. Nearby sample 49-51 used to est. data**. 7630 (8419) C14 (Cal) yrs. BP.**
1K-4 49-51	2.99	3	5	0	7.5	0	0	1	2	lith-com clay pellets, rre qtz; insect-com.(exoskel & larvae cases, eye cover); charc-0; pln't mat'l-com (com seeds to 4 mm lves, stems, wood frags); no ostra.

Sample Code	depth (m)	Lithic Note 1	plant mat'l. Note 1	charcoal * Note 1	insect mat'l. Note 1	carbonates (presence) Note 2	Thecam. (presence) **	moisture estimate ** 	Sample volume estimate**	Observations
1K-4 59-61	3.09	1	10	10	3	0	0	1	3	lith-com, clay pellets, opaque min, rre qtz; insect-rre/com.(exoskel & larvae cases); char-abn; pln't mat'l-abn. (leaves stems & seeds incl *scirpus* (bullrush-); no ostrac; wht. deposits on seeds; org mat'ls not transpt'd.
1K-4 69-71	3.19	1	10	5	5	0	0	1	2	lith-rre, clay pellets, very rre qtz; insect-com.(exoskel & larvae cases); charc-com; pln't mat'l-abn (abn lge seeds to 4 mm, various types incl. *Polygonum lapathifolium* curlytop knotweed, & banna shaped seed), sml vertebrae; organics not transpt'd.
1K-4 75-77	3.25									Date confirms sequence. **8065 (9008) C14 (Cal) yrs. BP.**
1K-4 79-81	3.29	1	10	10	5	0	0	1	3	lith-rre, qtz; insect-com.(larvae cases); charc-abn; pln't mat'l-abn nearby fire?, (abn lrg & sml seeds; incl bananna shaped & *scirpus* (bullrush-), organics not transpt'd, not sieved due to organic matting.
1K-4 82-83	3.31									This sample & below sample from same interval processed at Keck lab differently with 100 yr difference likely the process. **8285 (9317) C14 (Cal) yrs. BP.**
1K-4 82-83	3.31									This sample & above sample from same interval this 100 yr older uses same process as all other samples. **8405 (9437) C14 (Cal) yrs. BP.**
1K-4 89-91	3.39	1	10	10	1	1	0	1	3	lith-rre, clay pellets & qtz; insect-very rre; charc-abn; pln't mat'l-abn (abn lge seeds to 4 mm (bullrush-scirpus), & wood frags); gastropod & bivalve frags, abnt (carbonate), ostra R & S (some articulated).
1K-4 99-101	3.49	1	10	5	0.5	1	0	1	2	lith-rre, non disaggr. clay balls & qtz, carbonate frags; insect v-rre; charc-com; pln't mat'l-abn (lge to 5mm, terr/aquatic?) ostra (F), etched; sample bubbled vigorously when boiling water added.

Sample Code	depth (m)	Lithic Note 1	plant mat'l. Note 1	charcoal * Note 1	insect mat'l. Note 1	carbonates (presence) Note 2	Thecam. (presence) **	moisture estimate **	Sample volume estimate**	Observations
1K-4 109-111	3.59	5	5	5	1	1	0	1	1	lith-rre, opaque min. & qtz, carbonate frag.; insect-very rre.(larvae case); charc-com; pln't mat'l-com; charc-com; ostra (F) distorted.
1K-4 119-121	3.69	1	5	5	1	0	0	1	2	lith-rre, sml brn fine grained clay & qtz; insect-rre.(larvae cases); charc-com (blk round fine, rre wood frags.); ostra (F) (1) distorted; Sample bubbled vigorously when boiling water added. Pollen sample: 17040 (20386)) C14 (Cal) yrs. BP.
1K-4 129-131	3.79	5	1	5	5	1	0	1	2	lith-com, clay balls opaque min. & qtz, carbonate; insect-com.(larvae cases); charc-com; pln't mat'l-rre; ostra. (F & instar ST) (counted as adults).
1K-4 139-141	3.89	1	1	10	1	0	0	1	2	lith-rre, qtz; insect-rre.(larvae cases); char-abn (sml & round); pln't mat'l-rre; ostra (F (1 articulated) & ST (5 A-2 instar; count'd as adult)), thin & corroded (white patches and opaque), sample bubbled vigorously when boiling water added
1K-4 147-149	3.97	5	1	0	1	0	0	1	0.5	lith-v-rre, qtz & fsp to 2mm; insect-rre.(1-exoskel); char-0; pln't mat'l-rre; ostra (thin shells, many broken) ST & R (mostly A-1; some A-2, not counted) & S.
1K-5 9-11	4.09	10	5	1	1	1	0	1	1	lith-abn, qtz, opaque min (carbonate); insect-rre. (larvae cases); char-rre (1, 2mm piece); pln't mat'l-com (1 seed); ostra (ST & F, ST poor cond.)
1K-5 19-21	4.19	10	5	0	0	0	0	1	1	lith-abn, clay pellets, qtz & fsp; insect-0; char-0; pln't mat'l-com (datable); ostra ST (many broken).
1K-5 29-31	4.29	10	1	1	0	0	0	1	1	lith-abn, qtz, clay pellets; insect-0; char-rre; pln't mat'l-rre (aquatic); ostra (ST; many broken).
1K5-5-37.5	4.36									Wood fragment; likely old carbon**. 15620 (18802) C14 (Cal) yrs. BP.**
1K-5 39-41	4.39	10	5	1	1	0	0	1	1	lith-abn, qtz, opaque min.;insect-rre (larvae cases); charc-rre (sml amorphous); pln't mat'l-com (stem piece noted); ostra ST eroded and corroded, crushed; F (intact); organics not transpt'd.

Sample Code	depth (m)	Lithic Note 1	plant mat'l. Note 1	charcoal * Note 1	insect mat'l. Note 1	carbonates (presence) Note 2	Thecam. (presence) **	moisture estimate **	Sample volume estimate**	Observations
1K-5 49-51	4.49	5	1	1	1	1	0	1	1	lith-com, qtz & clay balls, carbonate; insect-rre (larvae cases).; charc-rre (sml amorphous); pln't mat'l-rre (aquatic); broken ostra shells (F,ST), F & sml ST intact, large ones mostly broken.
1K-5 59-61	4.59	10	10	1	1	1	0	3	1	lith-abn, qtz, opaque min, carbonate; insect-rre.(larvae cases); charc-rre; pln't mat'l-abn (aquatic); ostra ST, sml mostly intact, large oned broken; organics not transpt'd.
1K-5 69-71	4.69	10	1	1	1	1	0	2	1	lith-abn, qtz to 2 mm, carbonate; insect-0; charc-rre (sml amorphous); pln't mat'l-rre (aquatic); ostra ST, mostly intact.
1K-5 79-81	4.79	10	5	1	1	1	0	2	1	Processed at Champaign Ill., assumed similar to below sample.
1K-5 89-91	4.89	10	5	1	1	1	0	2	1	lith-abn, qtz,fsp, wht opaque (carbonate); insect-rre (larvae case); charc-rre (sml amorphous); pln't mat'l-com (aquatic); ostra ST, (A and A-1 intact), adults broken.
1K-5 99-101	4.99	10	5	1	0	1	0	1	1	lith-abn, qtz, carbonate lithics; insect-0; charc-rre (sml amorphous); pln't mat'l-com (incl. 2-3 mm leaflets); ostra (ST) plentiful, gen. intact.
1K-5 109-111	5.09	10	10	1	0	1	0	2	1	lith-abn, qtz & iron stained clay pellets (react HCl), carbonate lithics; insect-0; charc-rre (one 3mm sq. bark?); pln't mat'l-abn (aquatic, 3mm leaflet); ostra. (ST) plentiful, gen. intact rre thin or corroded.
1K-5 119-121	5.19	10	5	0	0	1	0	3	1	lith-abn, qtz & iron stained/blk clay pellets (carbonate); insect-0; charc-0; pln't mat'l-com (aquatic leaflets and broad lves); fish tooth; moisture estimate missing.
1K-5 129-131	5.29	10	5	1	0	1	0	3	1	lith-abn, qtz & iron stained clay pellets (carbonate); insect-0; charc-rre (lge frags 1-2 mm); pln't mat'l-com (aquatic leaves & stems); ostra A & A-1, + plentiful A-2's; shell thin but intact, some lge. broken.

Sample Code	depth (m)	Lithic Note 1	plant mat'l. Note 1	charcoal * Note 1	insect mat'l. Note 1	carbonates (presence) Note 2	Thecam. (presence) **	moisture estimate **	Sample volume estimate**	Observations
1K-5 139-141	5.39	10	10	1	0	1	0	1	1	lith-abn, qtz & clay pellets (carbonate); insect-0; charc-rre (sml amorphous); pln't mat'l-abn (aquatic); ostra ST, thin shells, some broken (lrg.) & corroded. Pollen sample: **17560 (20970) C14 (Cal) yrs. BP.**
1K-5 147-149	5.47	10	1	1	0	1	0	1	2	lith-abn, qtz & iron stained clay pellets (carbonate); insect-0; charc-rre (sml amorphous to 1 mm); pln't mat'l-rre (aquatic); ostra ST, thin shells.
bottom of core	5.48									

Note 1: For lithics, plant material, charcoal, and insect material: 1=rare; 5=common; 10=abundant.

Note 2: For carbonates and thecamoebians; 1=present, 0=not present (relative % were not estimated).

* note abundance of charcoal of 10, means its subsample volume was > 5%
** volume of material and moisture estimates based on scale 1=low (rare); 2=common; 3=high
ostra = ostracodes; ST=*C. subtriangulata*, F=*L. friabilis*; S=*C. sharpie*; R=*F. rawsoni.*

3.3 WOO06-5A-1K Scanned Core Images and Core Lithologic Descriptions

The following scanned core images WOO06-5A-1K1 to 1K5 provide a view of the sedimentology in the core. The coloured bars at the bottom of the scanned core are each 10 cm long. Core lithologic descriptions of these scanned images are provided on the following 5 pages.

1K1

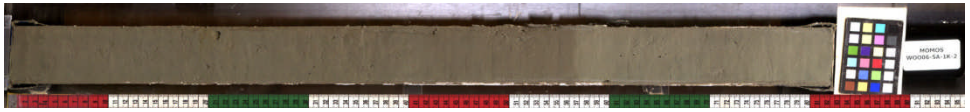

1K2

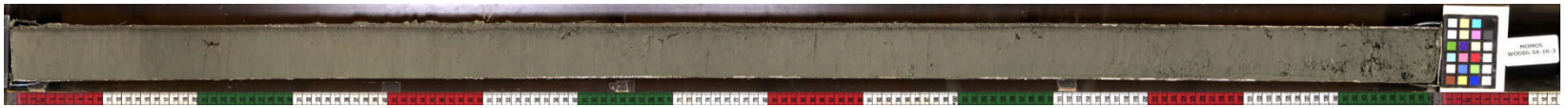

1K3

1K4

1K5

4. WOO06-6A-1K

4.1 WOO06-6A-1K: Subsample Ostracode Data:

Table A-7: Ostracode Data - LOTWs Northwest Angle Basin Site 6A (WOO06-6A-1K)

sample code	Core Length (m)	*C. subtriangulata*	*L. friabilis*	*C. sharpei*	*F. rawsoni*
Top of Core	0				
1K1 3-5	0.04	0	0	0	0
1K1 10-12	0.11	0	0	0	0
1K1 35-37	0.36	0	0	0	0
1K1 50-52	0.51	0	0	0	0
1K1 65-67	0.66	0	0	0	0
1K1 85-87	0.86	0	0	0	0
1K2 11-12	1.01				
1K2 27-29	1.18	0	0	0	0
1K2 42-44	1.32	0	0	0	0
1K2 60-62	1.50	0	0	0	0
1K2 74-76	1.64	0	0	0	0
1K2 89-91	1.80	0	0	0	0
1K2-95-96	1.85	0	0	0	0
1K2-97	1.86				
1K2 104-105	1.94	**3**	0	0	0
1K2 111-112	2.00	**3**	0	0	0
1K2 127-128	2.17	**1**	0	0	0
1K3 3-5	2.32	**17**	0	0	0
1K3 21-22	2.51	**11**	0	0	0
1K3 51-53	2.81	**11**	**2**	0	0
1K3 71-72	3.00	**5**	0	0	0
1K3 79-81	3.10	0	0	0	0
1K3 84-86	3.14	**22**	0	**1**	
1K3 99-101	3.29	**15**	**3**	0	0
1K3 120-122	3.50	**23**	**2**	0	0
1K3 141-144	3.71				
1K3 146-148	3.74	**36**	**9**	0	0
Bottom of Core					

4.2 WOO06-6A-1K: Subsample Lithic and Macrofossil Data, and Observations

Table A-8: WOO06-6A-1K Subsample Data

Sample Code	depth (m)	Lithic Note 1	plant mat'l. Note 1	charcoal * Note 1	insect mat'l. Note 1	carbonates (presence) Note 2	Thecam. (presence) **	moisture estimate **	Sample volume estimate **	Observations
top core	0.0									Sample core depths not adjusted to compensate for 1 cm of foam (insignificant).
1K1 3-5	0.0	5	10	1	5	0	2	2	3	lith-com, qtz; insect-com.(exoskel; larvae cases ?); charc-rre; abn pln't mat'l; theca-com (2 types, narrow and broad mouth vase).
1K1 10-12	0.1	1	10	5	1	1	0	3	3	lith-rre, qtz to 2mm, clay balls, wht fibrous & opaque lithics (carbonates); insect-rre (exoskel & mostly larvae cases); charc-rre (wood frags 10-15 mm, & coated stem pieces); pln't mat'l-abn (aquatic leaves).
1K1 35-37	0.4	1	10	5	5	0	2	2	3	lith-rre, qtz; insect-com (exoskel & larvae cases); charc-rre (sml frags); org pln't mat'l-abn (lves, stems (6-7mm), seed husk); theca-com (4 types, vase & flat, many in population sml); brn vase; organics not transpt'd.
1K1 50-52	0.5	5	10	1	5	1	1	3	3	lith-com, qtz, carbonate lithics; insect-com (exoskel & larvae cases); charc-rre; pln't mat'l-abn; theca-rre (est. from nearby samples).
1K1 65-67	0.7	1	10	1	1	0	2	2	3	lith-rre, qtz & mica; insect-rre (exoskel & larvae cases); charc-rre (sml amorphous frags); org pln't mat'l-abn (aquatic), (lves, stems, & wood frags); theca-com (2 types, flat & rimless); brn vase.
1K1 85-87	0.9	1	10	5	1	0	1	2	3	lith-rre, qtz & granitic; rre insect-com (exoskel & larvae cases, eye covers); charc-com (blackened stems to 2mm, sml frags incl amorphous); pln't mat'l-abn (aquatic); theca rre/com (4 types, incl vase and flat); fish vertebrae; organics not transpt'd.
1K2 11-12	1.0									Within thecamoebian interval. Dated blackened organics **2110 (2091) C14 (Cal) yrs. BP.**

Sample Code	depth (m)	Lithic Note 1	plant mat'l. Note 1	charcoal * Note 1	insect mat'l. Note 1	carbonates (presence) Note 2	Thecam. (presence) **	moisture estimate **	Sample volume estimate **	Observations
1K2 27-29	1.2	5	10	5	5	0	1	2	2	lith-com, qtz to 2 mm; insect-com (exoskel & larvae cases); charc-com (sml 2mm & stem to 4mm, sml amorphous frags); pln't mat'l-abn (aquatic leaves, & stems and wood frags); theca-rre some ornamented (4 types).
1K2 42-44	1.3	7.5	10	10	5	0	1	2	1	lith-abn, qtz; insect-com.(exoskel & larvae cases); charc-abn (twig and amorphous frags); pln't mat'l-abn (aquatic lves & seed 2mm); theca-rre vase (1 type); organic mat'l not transpt'd.
1K2 60-62	1.5	10	5	10	5	0	0	3	2	Sample at Paleotec: lith-abn, qtz & clay balls; insect-com.(exoskel incl leg piece, & larvae cases); charc-abn (frags); pln't mat'l-abn (aquatic leaves). Dated beetle parts **3245 (3481) C14 (Cal) yrs. BP.**
1K2 74-76	1.6	10	10	10	10	0	0	2	1	lith-abn, qtz, orange pellets (not carbonate); insect-abn.(rre exoskel & abn larvae cases); charc-abn (stems, bark to 4 mm & amorphous frags); pln't mat'l-abn (aquatic leaves broad & seed 2mm); organics not transpt'd.
1K2 89-91	1.8	10	1	1	1	1	0	2	3	lith-abn; qtz, abn red/orange clay pellets to 10mm (carbonate); insect-rre (exoskel & larvae cases); charc-rre; pln't mat'l-rre (aquatic).
1K2-95-96	1.9	10	1	0	1	1	0	1	2	lith-abn; qtz, brownish clay pellets to 4mm (react to HCl); insect-rre (larvae cases); charc-rre; pln't mat'l-rre; gastropod frag.
1K2-97	1.9									Dated shell debris. **6760 (7616) C14 (Cal) yrs. BP.**
1K2 104-105	1.9	5	5	0	0	0	0	1	1	lith-com; qtz & non disaggr. clay balls, wht opaque min, to 2mm, insect-0; charc-0; pln't mat'l-com (aquatic); ostra (ST) frags.
1K2 111-112	2.0	10	5	0	1	0	0	1	1	lith-abn, qtz & clay pellets to 3mm; insect-rre (exoskel); charc-0; pln't mat'l-com (leaflets to 3mm), ostra ST.
1K2 127-128	2.2	1	10	5	0	0	0	1	1	sample 50% full; lith-rre, mica; insect-0; charc-com; pln't mat'l-abn (matted); one ostra frag ST (broken).

Sample Code	depth (m)	Lithic Note 1	plant mat'l. Note 1	charcoal * Note 1	insect mat'l. Note 1	carbonates (presence) Note 2	Thecam. (presence) **	moisture estimate **	Sample volume estimate **	Observations
1K3 3-5	2.3	10	10	3	0.5	1	0	1	1	lith-abn, clay pellets (rusty), carbonate lithics & qtz/micas; insect -v-rre (larvae case); charc-rre/com (sml frags); pln't mat'l-abn (aquatic plus dark brn mat'l & branched stems (not transpt'd, some coated), wood frags; ostra (ST), coated, Adults fragmt'd others intact.
1K3 21-22	2.5	5	10	5	0	0	0	1	1	lith-com, qtz, opaque min. fibrous; insect-0; charc-com; pln't mat'l-abn; ostra ST incl. 2 A frags; moisture & quantity est. from nearby.
1K3 51-53	2.8	5	10	10	1	1	0	1	2	lith-com, clay pellets (rusty) react HCl, qtz; insect-rre (exoskel & larvae cases); charc-abn (stems & leaves); pln't mat'l-abn (aquatic leaves) ostra (F,ST), ST A's broken, F crushed & articilated, other tests intact; organics not trqanspt'd.
1K3 71-72	3.0	5	10	5	0	0	0	1	2	lith-com, clay pellets & qtz; insect-0; charc-com (including blackened needle, not transpt'd); pln't mat'l-abn (aquatic leaflets); ostra (ST).
1K3 79-81	3.1	1	1	10	10	0	0	1	1	lith-very rre, qtz; insect-abn.(rre exoskel & com larvae cases); charc-abn; pln't mat'l-rre (seeds to 3 mm); v rre ostra frags not tallied.
1K3 84-86	3.1	10	10	5	1	1	0	1	1	lith-abn, clay pellets (blk & reddish brn), qtz, & carbonates; insect-rre (exoskel & larvae cases); charc-abn (lge frags & stems to 2mm); pln't mat'l-abn (aquatic leaves); ostra (S,ST), ST A's broken, some coated and thin, instars mostly intact, 1 articulated.
1K3 99-101	3.3	5	10	5	0.5	1	0	1	1	lith-com, qtz, carbonate pellets; insect-rre (larvae cases); charc-com (frags not transported); pln't mat'l-abn (aquatic leaves, 3 mm stem with lves.) ostra (F,ST).
1K3 120-122	3.5	10	5	1	5	0	0	1	1	lith-abn, qtz; insect-com (exoskel & larvae cases); charc-rre; pln't mat'l-abn; ostra (F,ST) good cond.
1K3 141-144	3.7									Paleotec sample; no datable organics; 19 ostracode valves (species not identified, likely ST).

Sample Code	depth (m)	Lithic Note 1	plant mat'l. Note 1	charcoal * Note 1	insect mat'l. Note 1	carbonates (presence) Note 2	Thecam. (presence) **	moisture estimate **	Sample volume estimate **	Observations
1K3 146-148	3.7	10	3	5	0.5	1	0	1	1	lith-abn, qtz/micas, carbonate lithic; insect-v-rre (larvae cases); charc-abn (stems not transported & bark frags); pln't mat'l-abn (aquatic leaves & stems) ostra (F,ST), lightly coated, thin, some broken.

Note 1: For lithics, plant material, charcoal, and insect material: 1=rare; 5=common; 10=abundant.
Note 2: For carbonates and thecamoebians; 1=present, 0=not present (relative % were not estimated).

* note abundance of charcoal of 10, means its subsample volume was > 5%
** volume of material and moisture estimates based on scale 1=low (rare); 2=common; 3=high
ostra = ostracodes; ST=*C. subtriangulata*, F=*L. friabilis*; S=*C. sharpie*; R=*F. rawsoni.*

4.3 WOO06-6A-1K Scanned Core Images and Core Lithologic Descriptions

The following scanned core images WOO06-6A-1K1, 1K2 and 1K3, provide a view of the sedimentology in the core. The coloured bars at the bottom of the scanned core are each 10 cm long. Core lithologic descriptions of these scanned images are provided on the following 3 pages.

1K1

1K2

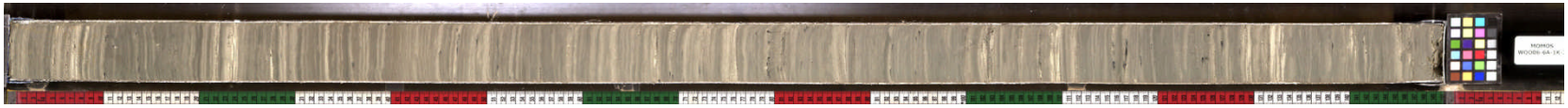

1K3

5. WOO06-7A-1P

5.1 WOO06-7A-1P: Subsample Ostracode Data

Table A-9: Ostracode Data - LOTWs Kenora site (WOO06-7A-1P)

sample code	depth	subtriangulata	friabilis	sharpi	rawsoni
top core	0				
1P-1 14-16	0.07				
1P-1 24-27	0.17	0	0	0	0
1P-1 44-46	0.37	0	0	0	0
1P-1 54-56	0.47	0	0	0	0
1P-1 74-76	0.67	0	0	0	0
1P-2 4-6	0.87	0	0	0	0
1P-2 14-16	0.97	0	0	0	0
1P-2 34-36	1.17	0	0	**1**	0
1P-2 44-46	1.27	0	0	0	0
1P-2 64-66	1.47	0	0	**2**	0
1P-2 75	1.57				
1P-3 4-6	1.63	0	0	0	0
1P-3 14-16	1.73	0	0	3	0
1P-3 24-26	1.83	0	0	0	0
1P-3 34-36	1.93	0	0	**1**	0
1P-3 54-56	2.13	0	0	0	0
1P-3 74-76	2.33	0	0	0	0
1P-3 84-86	2.43	0	0	0	0
1P-3 94-96	2.53	0	0	0	0
1P-3 104-106	2.63	0	0	**2**	0
1P-3 114-116	2.73	**2**	0	0	0
1P-3 124-126	2.83	0	0	0	0
1P-3 134-136	2.93	0	0	0	0
1P-3 144-146	3.03	0	0	0	0
1P-4 4-6	3.16	0	0	0	0
1P-4 14-16	3.26	0	0	0	0
1P-4 24-26	3.36	0	0	0	0
1P-4 34-36	3.46	0	0	0	0
1P-4 44-46	3.56	0	0	0	0
1P-4 54-56	3.66	0	0	0	0
1P-4 64-66	3.76	0	0	0	0
1P-4 74-76	3.86	0	0	0	0
1P-4 76-78	3.88	**5**	**2**	0	**3**
1P-4 81-83	3.93	**20**	0	0	0
1P-4 84-86	3.96	**35**	0	0	0
1P-4 96-98	4.08	**13**	0	0	0
1P-4 104-106	4.16	0	0	0	0
1P-4 114-116	4.26	0	0	0	0
1P-4 124-126	4.36	0	0	0	0
1P-4 134-136	4.46	**4**	0	0	0
1P-4 144-146	4.56	**10**	0	0	0

5.2 WOO06-7A-1P: Subsample Lithic and Macrofossil Data, and Observations

Table A-10: WOO06-7A-1P Subsample Data

Sample Code	depth (m)	Lithic Note 1	plant mat'l. Note 1	charcoal * Note 1	insect mat'l. Note 1	carbonates (presence) Note 2	Thecam. (presence) **	moisture estimate **	Sample volume estimate **	Observations
top of core	0.0									
1P-1 14-16	0.1									no sample
1P-1 24-27	0.2	5	5	5	3	0	2	3	2	lith-abn-50%, qtz & brn non disaggr. clay; insect-com-10%.exoskel & larvae cases); charc-abn-15% (frags); pln't mat'l-abn-35% (aquatic lge lves& seed cases); theca-com 4 types.
1P-1 44-46	0.4	5	3	5	5	0	2	3	2	lith-abn-60%, brn non disagg. clay rre qtz; insect-com-20%.exoskel & larvae cases); charc-abn-15% (plant frags & seed cases) pln't mat'l-com-15% (aquatic plus seed cases); theca-com 3 types.
1P-1 54-56	0.5	3	5	5	1	0	2	2	1	lith-com-10%, qtz; insect-rre-<1%. (exoskel & larvae cases); charc-abn-15% (lrg plant frags); pln't mat'l-com-75% (seeds, husks lves,stems); theca-com 2 types.
1P-1 74-76	0.7	5	10	5	5	0	2	2	2	lith-com, qtz to 3mm, white fibrous min; insect-com. (exoskel & larvae cases); charc-com; pln't mat'l-abn (aquatic and terr.) lves, stems (lge) wood frags. seed husks to 4 mm; theca-com. 2 types; possible feather frag.
1P-2 4-6	0.9	1	10	10	10	0	1	3	2	lith-abn, qtz & micas to 2mm; insect-abn. (exoskel & larvae cases); charc-abn; pln't mat'l-abn, aquatic & lge terr. lves (2-6mm), stems (lge) not transptd; theca-v rre. 1 only, broken vase.

Sample Code	depth (m)	Lithic Note 1	plant mat'l. Note 1	charcoal * Note 1	insect mat'l. Note 1	carbonates (presence) Note 2	Thecam. (presence) **	moisture estimate **	Sample volume estimate **	Observations
1P-2 14-16	1.0	5	10	10	5	0	1	3	0.5	2 samples: lith-com, qtz to 3mm, white fibrous min; insect-com. (exoskel - mostly daphnia & larvae cases); charc-abn (lge. Lves & stems); pln't mat'l-abn (aquatic and terr.) lves, stems (lge) wood frags. - to 1cm, seed husks; theca-rre. 4 types; Paleotec samples: 1/3 Rumex seed (12-14), birch seed (16-18).
1P-2 34-36	1.2	5	5	10	10	0	0			lith-com, qtz; insect-abn. (exoskel & larvae cases); charc-abn (plant frags incl. lves & datable twigs, seeds); pln't mat'l-com; ostra, 1 (S?) Dated from 24-30 cm misc insect parts and org. frags. **6775 (7630) C14 (Cal) yrs. BP.**
1P-2 44-46	1.3	5	5	10	5	0	0	3	2	lith-com, qtz & mica to 1-5mm; insect-com. (exoskel & larvae cases); charc-abn (lge. leaf frags to 2.5 cm & seed); pln't mat'l-com (aquatic & terr.) seeds (lge & partly burnt) lge leaflets & hollow stem with lves.
1P-2 64-66	1.5	1	10	5	5	1	1	2	1	lith-rre, qtz & other min. <1mm, carbonate grn lithics; insect-com. (exoskel & larvae cases); charc-com (lge. leaf frags & lge seed 5mm); pln't mat'l-abn (aquatic); theca v-rre (1); ostra (S), coated.
1P-2 75	1.6									Radiocarbon dated twig. **8265 (9235) C14 (Cal) yrs. BP.**
1P-3 4-6	1.6	5	10	5	5	0	0	1	0.5	lith-com, qtz to 3mm, fibrous white min.; insect-com. (exoskel & larvae cases); charc-com (sml. leaf & stem frags.); pln't mat'l-abn (aquatic & terr.), wood frags to 4mm, sml seed (looks dried); fish tooth.

Sample Code	depth (m)	Lithic Note 1	plant mat'l. Note 1	charcoal * Note 1	insect mat'l. Note 1	carbonates (presence) Note 2	Thecam. (presence) **	moisture estimate **	Sample volume estimate **	Observations
1P-3 14-16	1.7	1	10	10	10	0	0	3	0.5	lith-rre, qtz & non deaggr. clay; insect-abn. (exoskel & larvae cases-some daphnia); charc-com (leaf incl delicate leaf structures & lge stem (1 cm) frags.); pln't mat'l-abn (aquatic & terr.), wood frags to 1cm, v sml seeds (dessicated?); ostra (S), thin shelled. Dated twig: **8310 (9350) C14 (Cal) yrs. BP.**
1P-3 24-26	1.8	5	10	10	10	0	0	2	0.5	lith-com, qtz & mica, white fibrous min; insect-abn. (exoskel & rre. larvae cases); charc-abn (lge leaf & bark frags. - 5-6mm, sml. char. frags.); pln't mat'l-abn (aquatic & terr. plant frags.).
1P-3 34-36	1.9	5	10	10	10	0	0	3	1	lith-com, qtz & mica, clay balls; insect-abn. (exoskel & larvae cases); charc-abn, (leaf & twigs, datable, frags to 2mm, & 3-4 mm blk seed); pln't mat'l-abn (aquatic & terr. stems); ostra (S), very thin with holes through shell.
1P-3 54-56	2.1	5	10	5	5	0	0	2	0.5	lith-com, qtz <1mm, fibrous min; insect-com. (exoskel & larvae cases); charc-com, (lves & twigs/stems - datable), sml. charc frags; pln't mat'l-abn (aquatic with abn frags, & brn seed); 2 fish teeth.
1P-3 74-76	2.3	5	10	5	10	0	0	3	0.5	lith-com, qtz & mica <1mm; insect-abn. (exoskel incl. daphnia & larvae cases); charc-com, (lves, twigs, wood frags. - datable & amorph. frags.); pln't mat'l-abn (aquatic & terr. twigs, & seed case); frag. hair?

Sample Code	depth (m)	Lithic Note 1	plant mat'l. Note 1	charcoal * Note 1	insect mat'l. Note 1	carbonates (presence) Note 2	Thecam. (presence) **	moisture estimate **	Sample volume estimate **	Observations
1P-3 84-86	2.4	5	10	10	10	0	0	3	0.5	lith-com, qtz & mica <1mm; insect-abn. (exoskel incl. daphnia & larvae cases); charc-abn, (lves, twigs, wood frags. - datable & amorph. frags.); pln't mat'l-abn (aquatic & terr. twigs, & seed - 2mm). Dated two samples: 86-88 cm woody herb tissue **8760 (9773) C14 (Cal) yrs. BP;** and 86-88cm charred conifer needle **8800 (9827) C14 (Cal) yrs. BP.**
1P-3 94-96	2.5	5	5	10	5	0	0	3	0.5	lith-com, qtz & hornblende? to 4mm; insect-abn. (exoskel incl. daphnia & larvae cases); charc-abn, (leaf & wood frags to 4mm - datable, stems & amorph. frags.); pln't mat'l-com. (aquatic to 4mm, & terr. twigs).
1P-3 104-106	2.6	5	10	5	5	0	0	2	0.5	lith-com, qtz & micas; insect-abn. (exoskel & larvae cases); charc-com, (lves, twigs, amorph. frags, blk seed - datable); pln't mat'l-abn. (aquatic & terr. twigs); ostra (S); frag. bivalve. 1P3-106-108 sml potentilla seed; 104-106 Chenopodium seed (1).
1P-3 114-116	2.7	10	5	1	5	0	0	3	1	lith-abn, qtz to 2mm; insect-abn. (exoskel & rre larvae cases); charc-com, (leaf 4mm fragile, wood frags - datable); pln't mat'l-abn. (aquatic & terr. leaf frags & seed husk); ostra (ST).
1P-3 124-126	2.8	10	10	5	1	0	0	3	0.5	lith-abn, qtz to 2mm & non disaggr. clay; insect-rre. (exoskel & larvae cases); charc-com, (lves, stems, & amorph - datable); pln't mat'l-abn. (aquatic & terr. stem with leaflets).
1P-3 134-136	2.9	10	10	1	1	1	0	3	0.5	lith-abn, qtz to 3mm, & micas, carbonate lithics; insect-rre. (exoskel & larvae cases); charc-rre, (frags.incl leaf?); pln't mat'l-rre (aquatic, terr. leaf frags).

Sample Code	depth (m)	Lithic Note 1	plant mat'l. Note 1	charcoal * Note 1	insect mat'l. Note 1	carbonates (presence) Note 2	Thecam. (presence) **	moisture estimate **	Sample volume estimate **	Observations
1P-3 144-146	3.0	5	10	1	5	0	0	2	0.5	lith-com, qtz & micas < 1mm, white fibrous mineral; insect-com. (exoskel & larvae cases); charc-rre, (sml twigs); pln't mat'l-abn. (aquatic & terr. sml twigs).
1P-4 4-6	3.2	10	1	0	1	1	0	3	3	lith-abn, qtz, micas, granitic to 5mm, rre carbonates; insect-rre. (exoskel & larvae cases); charc-none; pln't mat'l-rre. (aquatic); rre brn vase - theca?.
1P-4 14-16	3.3	10	5	1	10	1	0	3	1	lith-abn, qtz, micas, dark min, opaque green/wht, to 2mm (carbonate); insect-abn. (exoskel & larvae cases); charc-rre, 1-2 mm twig frags; pln't mat'l-com (aquatic). Dated pollen at 17-18 cm **6060 (6930) C14 (Cal) yrs. BP**
1P-4 24-26	3.4	10	1	1	1	0	0	2	0.5	lith-abn, qtz, micas to 2mm, clay balls, 5mm; insect-rre. (exoskel & larvae cases); charc-rre, angular & fenestral; pln't mat'l-rre. (aquatic); 1mm brn vase.
1P-4 34-36	3.5	10	5	1	1	0	0	2	1	lith-abn, qtz & micas to 3mm; insect-rre. (exoskel & larvae cases); charc-rre; pln't mat'l-com (aquatic).
1P-4 44-46	3.6	10	5	5	1	0	0	3	1	lith-abn, qtz, micas, 5mm; insect-rre. (exoskel & larvae cases); charc-rre to com, twigs, fenestral, to 1mm, & amorphous; pln't mat'l-rre to com. (aquatic & 3mm seed, 4mm hollow plant stem); 4mm insect wing.
1P-4 54-56	3.7	10	1	1	1	0	0	2	1	lith-abn, qtz & biotite to 3mm, wht fibrous min; insect-rre. (exoskel & larvae cases); charc-rre; pln't mat'l-rre. (aquatic & terr., sml. twig (coated), blade of grass?).
1P-4 64-66	3.8	10	1	1	1	0	0	3	0.5	lith-abn, qtz & micas to 2mm, some non deaggr. clay; insect-rre. (exoskel incl daphnia & larvae cases); charc-rre, sml frags; pln't mat'l

										rre.(aquat)
Sample Code	**depth (m)**	**Lithic** Note 1	**plant mat'l.** Note 1	**charcoal *** Note 1	**insect mat'l.** Note 1	**carbonates (presence)** Note 2	**Thecam. (presence)** **	**moisture estimate ****	**Sample volume estimate ****	**Observations**
1P-4 74-76	3.9	10	1	0	1	1	0	3	2	lith-abn, qtz & chlorite? to 3mm, some carbonate lithics; insect-v rre. (larvae cases); charc-none; pln't mat'l-rre. (aquatic, 1.5 mm seed).
1P-4 76-78	3.9	10	1	1	1	1	0	2	1.5	lith-abn, qtz & micas to 3mm, abn non deaggr, clays balls, wht. opaque carbonate min; insect-none; charc-rre; pln't mat'l-com. (aquatic); ostra (ST,F,R) heavily coated.
1P-4 81-83	3.9	10	1	1	1	0	0	2	1	lith-abn, qtz & micas to 2mm, abn non deaggr, clays balls; insect-rre (larvae case); charc-rre, datable; pln't mat'l-rre. (aquatic); ostra (ST) some shells thin and broken, instars look robust, one articulated, represent 1-2 % of sample.
1P-4 84-86	4.0	10	1	1	1	1	0	3	2	Above pink clay: lith-abn, qtz to 3mm, wht dendritic min, carbonate frags; insect-rre (larvae case); charc-v rre (1 frag.); pln't mat'l-rre. (aquatic); ostra (ST) shells fragile, many broken, some coated, some instars have holes.
1P-4 96-98	4.1	10	5	1	0	0	0	3	1	Below pink clay: lith-abn, qtz, micas, chlorite? to 2mm; insect-none; charc-rre; pln't mat'l-com. (aquatic & sml wood frags.); ostra (ST) shells fragile, mostly broken, coated.
1P-4 104-106	4.2	10	1	1	0	0	0	2	2.5	lith-abn, qtz & micas, blk min. to 3mm, common fibrous wht min (not carbonate); insect-none; charc-rre; pln't mat'l-rre. (aquatic & sml. stems); Chenopodium seed (1), pelecypod hinge frag. 3mm.
1P-4 114-116	4.3	10	1	0	0	0	0	3	1	lith-abn, qtz & biotite to 2mm; insect-none; charc-none; pln't mat'l-v rre. (aquatic & sml wood frags.sml.).

1P-4 124-126	4.4	10	1	1	0	0	0	3	2	lith-abn, qtz & micas, to 1mm, fibrous wht min (not carbonate); insect-none; charc-rre; pln't mat'l-v rre. (aquatic - threadlike; sml leaf frag).
Sample Code	**depth (m)**	**Lithic** Note 1	**plant mat'l.** Note 1	**charcoal *** Note 1	**insect mat'l.** Note 1	**carbonates (presence)** Note 2	**Thecam. (presence)** **	**moisture estimate ****	**Sample volume estimate ****	**Observations**
1P-4 134-136	4.5	10	1	0	1	0	0	3	2	lith-abn, qtz & biotite, to 3mm, fibrous wht min; insect-rre (exoskel); charc-none; pln't mat'l-v rre. (aquatic - threadlike only, looks coated); ostra (ST), all broken.
1P-4 144-146	4.6	10	1	0	0	0	0	2	2	lith-abn, qtz to 3mm some micas & drk min.; opaque min; insect-v rre (exoskel); charc-none; pln't mat'l-rre. (aquatic); ostra (ST) note condition not observed due to sample unavailability.
Bottom of Core	4.64									

Note 1: For lithics, plant material, charcoal, and insect material: 1=rare; 5=common; 10=abundant.
Note 2: For carbonates and thecamoebians; 1=present, 0=not present (relative % were not estimated).

* note abundance of charcoal of 10, means its subsample volume was > 5%
** volume of material and moisture estimates based on scale 1=low (rare); 2=common; 3=high
ostra = ostracodes; ST=*C. subtriangulata*, F=*L. friabilis*; S=*C. sharpie*; R=*F. rawsoni.*

5.3 WOO06-7A-1P Scanned Core Images and Core Lithologic Descriptions

The following scanned core images WOO06-7A-1P1, 1P2, 1P3 and 1P4, provide a view of the sedimentology in the core. The coloured bars at the bottom of the scanned core are each 10 cm long. Core lithologic descriptions of these scanned images are provided on the following 4 pages.

1P1

1P2

1P3

1P4

6. SHO06-2A-1K

6.1 SHO06-2A-1K: Subsample Ostracode Data:

Table A-11: Ostracode Data – SL Site 2A (SHO06-2A-1K)					
sample code	Core Length (m)	*C. subtriangulata*	*L. friabilis*	*C. sharpei*	*F. rawsoni*
top core					
1K-1 3-4	0.0	0	0	0	0
1K-1 28-30	0.3	0	0	0	0
1K-1 52-54	0.5	0	0	0	0
1K-1 78-79	0.8	0	0	0	0
1K-1 102-104	1.0	0	0	0	0
1K-2 28-30	1.4	0	0	0	0
1K-2 52-54	1.6	0	0	0	0
1K-2 79-81	1.9	0	0	0	0
1K-3 22-24	2.1	0	0	0	0
1K-3 42-44	2.3	0	0	0	0
1K-4 23-25	2.6	0	0	0	0
1K-4 48-50	2.8	0	0	0	0
1K-4-69	3.0				
1K-4 74-76	3.1	0	0	0	0
1K-4 99-101	3.4	0	0	0	0
1K-4 114-116	3.5	**7**	0	**8**	**8**
1K-4 124-126	3.6	**2**	**1**	**6**	0
1K-4 147-149	3.9	**31**	0	**9**	**10**
1K-5 23-25	4.1	**13**	**7**	**20**	0
1K-5 49-50	4.6	0	**3**	**3**	**2**
1K-5 65-66	4.5				
1K-5 74-76	4.6	**4**	**6**	**6**	0
1K-5 99-101	4.9	**1**	**6**	**18**	**3**
1K-5 124-126	5.1	**3**	**5**	**36**	0
1K-5 147-149	5.3	**2**	**2**	**3**	**2**
1K-6 23-25	5.6	**3**	**1**	**11**	0
1K-6 32-33	5.6				
1K-6 38-40	5.7	**3**	**5**	**4**	0
1K-6 44-46	5.8	**1**	0	**3**	0
1K-6 48-50	5.8	**2**	**4**	**3**	0
1K-6 74-76	6.1	**2**	**12**	**5**	0
1K-6 99-101	6.3	**2**	0	**3**	0
1K-6 114-116	6.5	**2**	0	**2**	0
1K-6 123-125	6.6	0	0	**20**	0
1K-6 145-147	6.8	**3**	**1**	**3**	0
Bottom of Core					

6.2 SHO06-2A-1K: Subsample Lithic and Macrofossil Data, and Observations

Table A-12: SHO06-2A-1K Subsample Data

Sample Code	depth (m)	Lithic Note 1	plant mat'l. Note 1	charcoal * Note 1	insect mat'l. Note 1	carbonates (presence) Note 2	Thecam. (presence) **	moisture estimate **	Sample volume estimate **	Observations
top of core	0.0									no foam i.e. core depth = true depth.
1K-1 3-4	0.0	5	5	5	5	0	2	3	2	lith-abn clay balls, com qtz; insect-com.(exoskel & larvae cases), insect legs, daphnia; charc-com; pln't mat'l-com; theca-com; 2 fish bones.
1K-1 28-30	0.3	5	10	10	10	0	3	2	2	lith-com, qtz; com insect-com (rre exoskel & larvae cases); charc-abn (plant frags & amorphous); pln't mat'l-abn; theca-abn (2 types incl cannon-like).
1K-1 52-54	0.5	5	5	5	1	0	1	2	2	lith-com, qtz & clay balls; insect-rre (exoskel & larvae cases); charc-com; pln't mat'l.- com; theca-rre (2 types incl cannon-like).
1K-1 78-79	0.8	1	10	5	10	0	3	3	2	lith-rre, abn clay balls, rre qtz (opaque min); insect-abn (exoskel & larvae cases); charc-com (wood frags); pln't mat'l-abn (some leaf frags & a seed); theca-abn (5 species incl flat).
1K-1 102-104	1.0	1	5	5	3	0	2	2	2	lith-rre, abn clay balls, v rre qtz; insect-rre/com. (exoskel, Helodidae head & half el.; rre larvae cases) plnt-com (seeds 3-10 mm); charc-com (incl. seed pods); theca-com (2 types). Dated birch nutlets & Helodidae haed; **2525 (2636) C14 (Cal) yrs. BP**.
1K-2 28-30	1.4	1	1	5	5	0	2	2	2	lith-rre, abn clay balls, rre qtz (fibrous wht min.); insect-com (exoskel & larvae cases); charc-com (lrg wood & amorph.); pln't mat'l-rre; theca-com (2 types, vase and cannon shaped).
1K-2 52-54	1.6	1	1	10	10	1	2	3	2	lith-rre, abn clay balls, rre qtz, opaque min.(reacts HCl), insect-abn (exoskel & larvae cases); charc-abn (pln't & sml amorph.); pln't mat'l-rre aquatic, (seed); theca-com (3 types incl cannon-like); insect leg; fish tooth.

Sample Code	depth (m)	Lithic Note 1	plant mat'l. Note 1	charcoal * Note 1	insect mat'l. Note 1	carbonates (presence) Note 2	Thecam. (presence) **	moisture estimate **	Sample volume estimate **	Observations
1K-2 79-81	1.9	1	1	1	1	0	1	3	2	processed Champaign Ill: assumed moist and vol. same as nearby; lith-rre, abn non deaggr. clay balls, yellow matted min.) rre qtz; insect-rre.(exoskel & larvae cases); charc-rre; pln't mat'l-rre; theca-rre (2 types); fish tooth?
1K-3 22-24	2.1	5	5	5	5	0	2	2	1	lith-com, abn clay balls, com qtz; insect-rre. (exoskel & larvae cases); charc-com (up to 4mm wood frags.); pln't mat'l-com (incl leaf frag. & seed husk); theca-com (brn vase & vase, cannon-like). Single ostra (S) noted but no others, misidentified macrofossil? did not count.
1K-3 42-44	2.3	0	1	1	1	0	2	2	1	lith-none, abn non deaggr. clay balls, no qtz; insect-rre.(exoskel incl daphnia, & larvae cases); char-rre.(lrg frag 1-2 mm); plant mat'l-rre; theca-com (4 types).
1K4-23-25	2.6	1	1	10	1	1	1	3	1	lith-rre, com non disaggr. clay balls (mild react HCl), rre qtz, opaque min.; insect-rre. (exoskel & larvae cases); charc-abn (incl. 6 mm burnt twig) pln't mat'l-rre; theca rre (1 type) cannon-like.
1K-4 48-50	2.8	1	10	10	5	0	2	3	1	lith-rre, qtz; insect-com.(exoskel & larvae cases); charc-abn; pln't mat'l-abn (1 seed 2-3 mm, birch nutlet); theca-com cannon-like. Sample not avail. for carbonate test, at Paleotec.
1K-4-69	3.0									Dated wisps of organic. **7130 (7963) C14 (Cal) yrs. BP**
1K-4 74-76	3.1	1	5	1	1	1	0	2	1	lith-rre, com non deagrr clay balls (react HCl), rre qtz; insect-rre.(exoskel, rre larvae cases); charc-rre (sml frags & amorph); pln't mat'l-com (incl lge. aquatic leaf pieces); fish bone.
1K-4 99-101	3.4	1	5	1	1	1	0	1	1	lith-rre, abn non disaggr. clay balls (mildly react HCl), rre qtz; insect-rre.(exoskel & larvae cases); charc-com (sml amorph); pln't mat'l-com (incl leaflets); sml pelecypod frag.

Sample Code	depth (m)	Lithic Note 1	plant mat'l. Note 1	charcoal * Note 1	insect mat'l. Note 1	carbonates (presence) Note 2	Thecam. (presence) **	moisture estimate **	Sample volume estimate **	Observations
1K-4 114-116	3.5	1	10	5	1	0	0	2	1	lith-rre, qtz & micas, opaque min; insect-rre (exoskel & larvae cases); charc-com (sml wood frags & amorph); pln't mat'l-abn (aquatic leaves & terrestrial leaf frags; fish scale frags; ostra (S,R,ST); many broken except S.
1K-4 124-126	3.6	0	1	5	3	1	0	2	1	lith-none, com non deaggr. clay (react HCl); insect-rre-com.(com. exoskel & rre. larvae cases); charc-com (lge wood frags); pln't mat'l-rre (aquatic); ostra (F,S,ST) lge ST fragile, S&F intact.
1K-4 147-149	3.9	1	10	3	5	1	0	2	1.5	lith-abn non deaggr. clay balls (react HCl); qtz none; insect-com (exoskel & larvae cases); charc-rre-com (sml frags & amorph.); pln't mat'l-abn aquatic (incl leaflets); insect leg; ostra (S,R,ST) S intact, others mostly broken (adjusted count upwards by 25% to account for broken tests) .
1K-5 23-25	4.1	1	10	5	5	1	0	1	1.5	lith-abn non deaggr. clay balls (react to HCl); rre qtz; insect-com (exoskel & larvae cases); charc-com (sml frags & amorph.); pln't mat'l-abn aquatic (incl leaflets); ostra (S,R,F) S&F intact,1 S articulated, R many broken; fish vertebrae.
1K-5 49-50	4.6	1	10	10	5	1	0	1	1	lith-abn non deaggr.r clay balls; v rre qtz, carbonates; insect-com (exoskel & larvae cases); charc-abn (sml frags & amorph.); pln't mat'l-abn aquatic; ostra (S,R,F) all intact; unidentified ostra; fish scale.
1K-5 65-66	4.5									Dated. **6170 (7082) C14 (Cal) yrs. BP**
1K-5 74-76	4.6	0	5	5	5	1	0	1	1	lith-abn non disaggr clay balls (react HCl); qtz none; insect-com (exoskel & larvae cases); charc-com. (lge wood frag, sml amorph.); pln't mat'l-com aquatic (incl leaflets); ostra (S,F,ST) ST fragmented others intact; unidentified ostra; fish scale.
Sample Code	**depth (m)**	**Lithic** Note 1	**plant mat'l.** Note 1	**charcoal *** Note 1	**insect mat'l.** Note 1	**carbonates (presence)** Note 2	**Thecam. (presence)** **	**moisture estimate ****	**Sample volume estimate ****	**Observations**

1K-5 99-101	4.9	0	10	5	10	0	0	1	1	lith-abn non deaggr. clay balls; qtz none; insect-abn (exoskel & larvae cases); charc-com. (sml amorph.); pln't mat'l-com aquatic (incl leaflets); ostra (S,F,R,ST) mostly intact, some thin.
1K-5 124-126	5.1	10	10	5	5	0	0	1	1	lith-abn pellets gry/blk; rre qtz; insect-com (exoskel & larvae cases); charc-com. (sml amorph.); pln't mat'l-com aquatic (incl leaflets & sml twigs); ostra (S,F,ST) mostly intact.
1K-5 147-149	5.3	0	10	10	5	0	0	2	1	lith-abn non disaggr. clay balls, qtz-none; insect-com (exoskel & larvae cases); charc-com. (sml amorph. & wood frags); pln't mat'l-abn aquatic; ostra (S,F,ST,R) mostly intact, 2 articulated species(S,R), (each counted as 2 individuals), most intact, some thin & crusted.
1K-6 23-25	5.6	10	10	10	1	1	0	1	1	lith-com non disaggr. clay balls, qtz-none, opaque white min.(carbonate); insect-rre (exoskel & larvae cases); charc-abn. (lge leaf frags to 1cm); pln't mat'l-abn aquatic; ostra (S,F,ST) ST broken frag, 1 corroded S others intact.
1K-6 32-33	5.6									Dated. **6685 (7554) C14 (Cal) yrs. BP**
1K-6 38-40	5.7	1	5	5	10	1	0	2	1	lith-abn non deaaggr. clay balls, rre qtz, carbonate lithics; insect-abn (exoskel & larvae cases); charc-com. (rre sml twig); pln't mat'l-com aquatic (rre woody frags); ostra (S,F,ST) ST tests fragile & broken others intact; fish bone.
1K-6 44-46	5.8	1	10	1	1	0	0	1	1	lith-abn non deaggr. clay balls, rre qtz; insect-rre (exoskel (incl. daphnia) & larvae cases); charc-rre. (sml amorph.); pln't mat'l-abn aquatic; ostra (S,ST) good cond.
1K-6 48-50	5.8	1	10	1	5	0	0	1	1	lith-abn non deaaggr. clay balls, rre qtz; insect-com. (larvae cases only); charc-rre. (sml amorph.); pln't mat'l-abn aquatic; ostra (F,S,ST) ST lge pieces broken, others good cond; fish bone.

Sample Code	depth (m)	Lithic Note 1	plant mat'l. Note 1	charcoal * Note 1	insect mat'l. Note 1	carbonates (presence) Note 2	Thecam. (presence) **	moisture estimate **	Sample volume estimate **	Observations
1K-6 74-76	6.1	0	10	5	5	0	0	1	1	lith-rre non deaaggr. clay balls, qtz none; insect-rre. (larvae cases only); charc-com. (stems & sml amorph.); pln't mat'l-abn aquatic; ostra (F,S,ST) generally intact, 1 S articulated, some thin with holes; fish scale; gastropod shell frag.
1K-6 99-101	6.3	10	10	1	5	0	0	1	1	processed Champaign Ill.: assume moist and vol same as nearby; lith-abn, qtz; insect-com. (larvae cases only); charc-rre (sml amorph) pln't mat'l-abn (thin leaves to 1 cm); fish bone frag. Ostr (S,ST) thin shells ST broken.
1K-6 114-116	6.5	1	10	10	10	1	0	1	2	lith-rre, fsp, carbonate frags-com; insect-abn. (larvae cases only); charc-abn. (twigs, bark, sml-lge amorph., to 3mm, coated carbonate); pln't mat'l-abn aquatic; ostra (S,ST) intact.
1K-6 123-125	6.6	0	5	5	5	0	1	2	1	lith-v. rre, qtz (1 lith); insect-com. (exoskel & larvae cases); charc-com. (sml frags & amorph.); pln't mat'l-com aquatic; ostra (S) 1 articulated; fish vertebrae & other bones.
1K-6 145-147	6.8	5	10	5	1	1	1	2	1	lith-abn, unconsolidated clay balls, com qtz & clay pellets (carbonate); insect rre-com. (exoskel & larvae cases); charc-com. (incl lge 2mm bark? frag); pln't mat'l com-abn aquatic; ostra (S,ST,F) 1 articulated; theca-com 3 species 2 ornamented. Additional sample; 143-146 had no theca but had 3 S and 1 F ostra); abn plant mat'l including multiple seeds. Dated broad interval 135-147 cm tiny twig and moss stems. **5630 (6452) C14 (Cal) yrs. BP**
End of Core										

Note 1: For lithics, plant material, charcoal, and insect material: 1=rare; 5=common; 10=abundant.
Note 2: For carbonates and thecamoebians; 1=present, 0=not present (relative % were not estimated).

* note abundance of charcoal of 10, means its subsample volume was > 5%
** volume of material and moisture estimates based on scale 1=low (rare); 2=common; 3=high
ostra = ostracodes; ST=*C. subtriangulata*, F=*L. friabilis*; S=*C. sharpie*; R=*F. rawsoni.*

6.3 SHO06-2A-1K: Scanned Core Images and Core Lithologic Descriptions

The following scanned core images SHO06-2A-1K1 to 1K6, provide a view of the sedimentology in the core. The coloured bars at the bottom of the scanned core are each 10 cm long. Core lithologic descriptions of scanned images are provided on the next 6 pages.

1K1

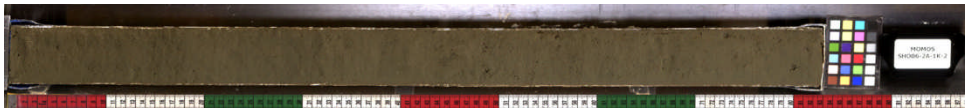

1K2

1K3

1K4

1K5

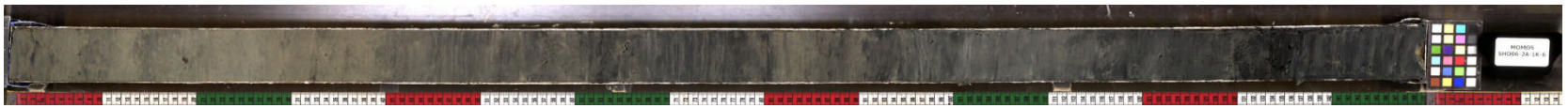

1K6

APPENDIX B: RADIOCARBON ANALYSIS REPORTS

1. LOTWs and SL Radiocarbon Samples

This appendix includes a radiocarbon sample summary table (Table B-1), copies of the Keck Carbon Cycle AMS Facility and the Lawrence Livermore National Laboratory Laboratories Radiocarbon radiocarbon analysis sheets, and selected photos from Paleotec Reports (Nov. 22, 2008 and May 02, 2009) which are associated with the KECK Laboratory reports.

Most ^{14}C dates were from organic fragments (i.e. macrofossils) picked by Alice Telka of Paleotec Services from subsamples processed at the University of Manitoba, or from subsamples processed at Paleotec Services, which were then dated at the Keck Carbon Cycle AMS Facility. Photos of some of these macrofossils are provided below in Appendix B, Section 4. Additional radiocarbon dates were obtained from pollen microfossil samples which were processed by staff at the LRC, and then dated at the Lawrence Livermore National Laboratory.

2. Radiocarbon Sample Summary Table

Table B-1: LOTWs and SL Radiocarbon Sample Summary

Sample #	Sample name	AMS Potential; Comments	Weight (mg)	$\delta^{13}C$ (‰)	±	fraction Modern	±	$D^{14}C$ (‰)	±	^{14}C age (BP)	±	Cal yrs (BP)	±
South Basin Site - WOO06-1A													
48250	1A-1K-2 19-21	freshwater clam periostracum	.028mgC	-	-	0.8339	0.005	-166	4.5	1460	4.5	1358	34
61723	1A-1K-2, 69-74	one conifer seed wing (no seed), beetle elytron, ant mandible.	.10 mgC	-	-	0.8118	0.0020	-188.2	2.0	1675	20	1572	15
141463	1A-1K-3, 62-63	pollen sample taken for LRC		-25		0.2175	0.002	-783	2.1	12260	80	14365	300
48217	1A-1K-3, 99-101	curlytop knotweeds achenes (5) partial bristles intact		-29.8	0.1	0.3992	0.0009	-600.8	0.9	7375	20	8228	45
54969	1A-1K-3, 141-144	Polygonum lapathifolium seeds (4)		-29.7	0.1	0.4112	0.0019	-588.8	1.9	7140	40	7973	26
NWA - Channel Site - WOO06-3A													
	3A-1K-2, 49-52	birch bract fragment-may be											
54970	3A-1K-6, 107-110	birch seed (small), Verbena seed (1), ant mandible, small weevil	.16 mgC	-	-	0.6959	0.0024	-304.1	2.4	2915	30	3070	61
NWA - Channel Site - WOO06-4A													
54971	4A-1K-1, 7-9	Scirpus seeds ~20 (two types, no attached bristles, some split		-25.0	0.1	0.7329	0.0022	-267.1	2.2	2495	25	2604	82
54972	4A-1K-2, 22-23	pre-select wood fragment: ~1 cm		-24.9	0.1	0.4525	0.0014	-547.5	1.4	6370	30	7319	42
54973	4A-1K-2, 42-43	pre-select wood fragment: ~4 wood fragments, largest is 1 cm		-26.3	0.1	0.4208	0.0013	-579.2	1.3	6955	30	7786	42
61725	4A-1K2 99-100	Scirpus achenes (3)		-25.1	0.1	0.3856	0.0011	-614.4	1.1	7655	25	8443	23
	4A-1K2 141-144	LRC pollen sample not analysed.											
NWA - Basin Site - WOO06-5A													
61726	5A-1K-2, 49-61	larch needle sml organic frgs, beetle heads.	.040 mgC	-	-	0.7718	0.007	-228	7.2	2080	80	2071	106
61729	5A-1K-3, 78-90	misc. insect parts & grass seed.	.029 mgC	-	-	0.6147	0.008	-385	8.1	3910	110	4343	158
34149	5A-1K-4, 39-41		.048mgC			0.3926	0.0031	-607.4	3.1	7510	70	8308	73
34149	5A-1K-4, 39-41		.048mgC	-	-	0.3926	0.0031	-607.4	3.1	7510	70	8308	73
34412	5A-1K-4 45-47		.090 mgC	-	-	0.3869	0.0012	-613.1	1.2	7630	25	8419	12
	5A-1K-4 55-57	Rumex half seed partial calyx fragment-insufficient wt	.080mgC										
34413	5A-1K-4 75-77		.41 mgC	-25.8	0.1	0.3665	0.0008	-633.5	0.8	8065	20	9008	7
34150	5A-1K-4 82-83		.2mgC	-	-	0.3513	0.0016	-648.7	1.6	8405	40	9437	41
34163	5A-1K-4 82-83		.36mgC	-	-	0.3566	0.0013	-643.4	1.3	8285	30	9317	65
	5A-1K-4 101-104	no organics											
141463	5A-1K-4 120-121	pollen sample taken for LRC		-25		0.1199	0.003	-880	3.2	17040	220	20386	442
	5A-1K-4 129-131	no organics											
34151	5A-1K-5 37.5		.027mgC	-	-	0.1430	0.0062	-857.0	6.2	15620	350	18802	452
	5A-1K5 79-81	no organics											
	5A-1K-5 132-134	no organics											
141466	5A-1K-5 140-142	pollen sample taken for LRC		-25		0.1123	0.001	-888	1.2	17560	90	20970	319

Sample #	Sample name	AMS Potential-Comments	Weight (mg)	$\delta^{13}C$ (‰)	±	fraction Modern	±	$D^{14}C$ (‰)	±	^{14}C age (BP)	±	Cal yrs (BP)	±
NWA - Basin Site - WOO06-6A													
34146	6A-1K-2 11-12	blackened organics				0.7688	0.0012	-231.2	1.2	2110	15	2091	28
61727	6A-1K-2 55-65	beetle parts	.063 mgC	-	-	0.6677	0.0040	-332.3	4.0	3245	50	3481	63
34159	6A-1K-2 97	shell debris				0.4312	0.0008	-568.8	0.8	6760	15	7616	17
	6A-1K-3 21-22	wispy organics 0.1 mg											
	6A-1K-3 141-143	no organics											
Kenora Site - WOO06-7A													
		12-14 cm: one third of a tiny											
61728	7A-1P-2 24-30	misc insect parts & misc org frags: one birch seed, very tiny	.13 mgC	-	-	0.4302	0.002	-570	1.6	6775	30	7630	26
48219	7A-1P-2 75	twig		-28.5	0.1	0.3573	0.0009	-642.7	0.9	8265	20	9235	45
48220	7A-1P-3 14-16	small wood frag.	.16 mgC	-	-	0.3554	0.0012	-644.6	1.2	8310	30	9350	49
61730	7A-1P-3 86-88	woody herb tissue frag (1)		-23	0.1	0.3360	0.0009	-664.0	0.9	8760	25	9773	68
61731	7A-1P-3 86-90	charred conif needle frags.		-27	0.1	0.3343	0.0010	-665.7	1.0	8800	25	9827	59
	7A-1P-3 101-103	101-103 cm: tiny (~1mm) leaf											
	7A-1P-3 104- 106	104-106 cm Chenopodium seed (1) & minute twig											
	7A-1P-3 106-108	106-108 cm: small Potentilla seed											
141465	7A-1P-4 17-18	pollen sample taken for LRC		-25		0.4702	0.001	-530	11	6060	190	6930	226
	7A-1P-4 40-41	no organics											
	7A-1P-4 67-70	barren of organics, no AMS											
	7A-1P-4 96-98	no organics											
	7A-1P-4 107-110	barren of organics, no AMS											
Shoal Lake Site - WOO06-2A													
48218	2A-1K-1 102-104	Birch nutlets (2), Helodidae head	.14mgC	-	-	0.7302	0.0014	-269.8	1.4	2525	20	2636	82
	2A-1K-4 48-50	no organics											
	2A-1K-4 59-61	wisps' of organics; insufficient in											
34148	2A-1K-4 69			-	-	0.4117	0.0010	-588.3	1.0	7130	20	7963	11
	2A-1K-4 114-118	wisps' of organics; insufficient in											
	2A-1K-4 124-125	no organics											
34414	2A-1K-5 65-66			-29.5	0.1	0.4639	0.0013	-536.1	1.3	6170	25	7082	53
34147	2A-1K-6 32-33			-	-	0.4351	0.0008	-564.9	0.8	6685	20	7554	26
	2A-1K-6 123-125	multiple fish vertebrae and bones not processed.											
61724	2A-1K-6 135-147	tiny twig, moss stems	.029mgC	-	-	0.4963	0.0080	-503.7	8.0	5630	130	6452	135

Note: Radiocarbon concentrations are given as fractions of the Modern standard, $D^{14}C$, and conventional radiocarbon age, following the conventions of Stuiver and Polach (Radiocarbon, v. 19, p.355, 1977).

3. Radiocarbon Analysis Reports

3.1 Keck Carbon Cycle AMS Facility Macrofossil Radiocarbon Reports

This section contains six radiocarbon dating reports from the Earth System Science Department of Keck Carbon Cycle AMS Facility at University of California, Irvine from the selected macrofossils provided by Paleotec Services.

The Keck Carbon Cycle AMS Facility reports are presented below and include the reports issued on the following dates:

- March 19, 2007
- March 28, 2007
- May 17, 2008
- May 18, 2008
- November 19, 2008
- May 02, 2009

KECK CARBON CYCLE AMS FACILITY

EARTH SYSTEM SCIENCE DEPT, UC IRVINE

^{14}C results | Teller | Mar 19 2007

UCIAMS #	Sample name	Other ID	δ^{13}C (‰)	±	fraction Modern	±	D^{14}C (‰)	±	^{14}C age (BP)	±
34146	LOW 6A-1K-2, 11-12				0.7688	0.0012	-231.2	1.2	2110	15
34147	SHO 2A-1K-6, 32-33				0.4351	0.0008	-564.9	0.8	6685	20
34148	SHO 2A-1K-4, 69				0.4117	0.0010	-588.3	1.0	7130	20
34149	LOW 5A-1K-4, 39-41 .048mgC				0.3926	0.0031	-607.4	3.1	7510	70
34150	LOW 5A-1K-4, 82-83 .2mgC				0.3513	0.0016	-648.7	1.6	8405	40
34151	LOW 5A-1K-5,37.5 .027mgC				0.1430	0.0062	-857.0	6.2	15620	350
34152	MPW1FG				0.8919	0.0014	-108.1	1.4	920	15
34159	LOW 6A-1K-2, 97 shell debris				0.4312	0.0008	-568.8	0.8	6760	15
34163	LOW 5A-1K-4, 82-83 (test, acid only) .36mgC				0.3566	0.0013	-643.4	1.3	8285	30

Radiocarbon concentrations are given as fractions of the Modern standard, D^{14}C, and conventional radiocarbon age, following the conventions of Stuiver and Polach (Radiocarbon, v. 19, p.355, 1977).

Sample preparation backgrounds have been subtracted, based on measurements of ^{14}C -free wood (organics) and calcite (carbonates).

All results have been corrected for isotopic fractionation according to the conventions of Stuiver and Polach (1977), with δ^{13}C values measured on prepared graphite using the AMS spectrometer. These can differ from d13C of the original material, if fractionation occurred during sample graphitization or the AMS measurement, and are not shown.

Comments: The shell debris sample LOW 6A-1K-2, 97 was chalky material that contained no hard carbonate. The sample was leached (50-75%) during pretreatment but there is still a possibility that exogenous carbonate was present in the material dated. The sample UCIAMS-34163 (silty clayey peat) was treated with acid only, whereas UCIAMS-34150 (and all of the other organic samples received the standard acid-base-acid treatment. The acid-only sample dates about 100 years younger than the aliquot that received the full ABA treatment.

Note: sample # 34152 is not from LOTWs and SL

KECK CARBON CYCLE AMS FACILITY

EARTH SYSTEM SCIENCE DEPT, UC IRVINE

^{14}C results | Paleotec/Teller | Mar 28 2007

UCIAMS #	Sample name	Other ID	δ^{13}C (‰)	±	fraction Modern	±	D^{14}C (‰)	±	^{14}C age (BP)	±
34412	LOW 5A-1K-4, 45-47cm	.090mgC	-	-	0.3869	0.0012	-613.1	1.2	7630	25
34413	LOW 5A-1K-4, 75-77cm	.41mgC	25.8	0.1	0.3665	0.0008	-633.5	0.8	8065	20
34414	SHO 2A-1K-5, 65-66cm		29.5	0.1	0.4639	0.0013	-536.1	1.3	6170	25

Radiocarbon concentrations are given as fractions of the Modern standard, D^{14}C, and conventional radiocarbon age, following the conventions of Stuiver and Polach (Radiocarbon, v. 19, p.355, 1977).

Size-dependent sample preparation backgrounds have been subtracted based on measurements of ^{14}C-free wood.

All results have been corrected for isotopic fractionation according to the conventions of Stuiver and Polach (1977), with δ^{13}C values measured on prepared graphite using the AMS spectrometer. These can differ from δ13C of the original material, if fractionation occurred during sample graphitization or the AMS measurement, and are not shown.

Comments: δ^{13}C values shown were measured to a precision of better than 0.1‰ on CO_2 aliquots, using a Finnigan Delta Plus IRMS with Gas Bench input.

One sample was too small to provide sufficient extra CO_2 for δ^{13}C measurements.

KECK CARBON CYCLE AMS FACILITY

EARTH SYSTEM SCIENCE DEPT, UC IRVINE

^{14}C results | Paleotec/Teller | May 17 2008

UCIAMS #	Sample name	Other ID	δ^{13}C (‰)	±	fraction Modern	±	D^{14}C (‰)	±	^{14}C age (BP)	±
48217	LOW 1A-1K-3, 99-101		-29.8	0.1	0.3992	0.0009	-600.8	0.9	7375	20
48218	SHO 2A-1K-1, 102-104 .14mgC				0.7302	0.0014	-269.8	1.4	2525	20
48219	LOW 7A-1P-2, 75		-28.5	0.1	0.3573	0.0009	-642.7	0.9	8265	20
48220	LOW 7A-1P-3, 14-16 .16mgC				0.3554	0.0012	-644.6	1.2	8310	30

Radiocarbon concentrations are given as fractions of the Modern standard, D^{14}C, and conventional radiocarbon age, following the conventions of Stuiver and Polach (Radiocarbon, v. 19, p.355, 1977).

Sample preparation backgrounds have been subtracted, based on measurements of ^{14}C-free wood.

All results have been corrected for isotopic fractionation according to the conventions of Stuiver and Polach (1977), with δ^{13}C values measured on prepared graphite using the AMS spectrometer. These can differ from δ^{13}C of the original material, if fractionation occurred during sample graphitization or the AMS measurement, and are not shown.

Comments:
δ^{13}C values shown above were measured to a precision of <0.1‰ relative to standards traceable to PDB, using a Thermo Finnigan Delta Plus stable isotope ratio mass spectrometer (IRMS) with Gas Bench input. Two of these samples were too small to provide the extra CO_2 aliquot for an IRMS δ13C measurement.

KECK CARBON CYCLE AMS FACILITY
EARTH SYSTEM SCIENCE DEPT, UC IRVINE

^{14}C results | Paleotec/Teller | May 18 2008

UCIAMS #	Sample name	Other ID	δ^{13}C (‰)	±	fraction Modern	±	D^{14}C (‰)	±	^{14}C age (BP)	±
48250	LOW 1A-1K-2 19-21 .028mgC				0.8339	0.0045	-166.1	4.5	1460	45

Radiocarbon concentrations are given as fractions of the Modern standard, D^{14}C, and conventional radiocarbon age, following the conventions of Stuiver and Polach (Radiocarbon, v. 19, p.355, 1977).

Sample preparation backgrounds have been subtracted, based on measurements of ^{14}C-free wood

All results have been corrected for isotopic fractionation according to the conventions of Stuiver and Polach (1977), with δ^{13}C values measured on prepared graphite using the AMS spectrometer. These can differ from δ^{13}C of the original material, if fractionation occurred during sample graphitization or the AMS measurement, and are not shown.

Comments:

This sample was too small to provide an extra CO_2 aliquot for an IRMS δ^{13}C measurement.

KECK CARBON CYCLE AMS FACILITY
EARTH SYSTEM SCIENCE DEPT, UC IRVINE

^{14}C results | Paleotec/Teller | Nov 19 2008

UCIAMS #	Sample name	Other ID	δ^{13}C (‰)	±	fraction Modern	±	D^{14}C (‰)	±	^{14}C age (BP)	±
54969	LOW 1A-1K-3, 141-144 cm		-29.7	0.1	0.4112	0.0019	-588.8	1.9	7140	40
54970	LOW 3A-1K-6, 107-110 cm	.16mgC	-	-	0.6959	0.0024	-304.1	2.4	2915	30
54971	LOW 4A-1K-1, 7-9 cm		-25.0	0.1	0.7329	0.0022	-267.1	2.2	2495	25
54972	LOW 4A-1K-2, 22-23 cm		-24.9	0.1	0.4525	0.0014	-547.5	1.4	6370	30
54973	LOW 4A-1K-2, 42-43 cm		-26.3	0.1	0.4208	0.0013	-579.2	1.3	6955	30

Radiocarbon concentrations are given as fractions of the Modern standard, D^{14}C, and conventional radiocarbon age, following the conventions of Stuiver and Polach (Radiocarbon, v. 19, p.355, 1977).

Sample preparation backgrounds have been subtracted, based on measurements of ^{14}C-free wood.

All results have been corrected for isotopic fractionation according to the conventions of Stuiver and Polach (1977), with δ^{13}C values measured on prepared graphite using the AMS spectrometer. These can differ from δ^{13}C of the original material, if fractionation occurred during sample graphitization or the AMS measurement, and are not shown.

Comments:
δ^{13}C values shown above were measured to a precision of <0.1‰ relative to standards traceable to PDB, using a Thermo Finnigan Delta Plus stable isotope ratio mass spectrometer (IRMS) with Gas Bench input.

Sample LOW 3A-1K-6, 107-110 cm did not contain enough material for stable isotope analysis.

^{14}C results — Teller/Paleotec — May 02 2009

UCIAMS #	Sample name	Other ID	δ^{13}C (‰)	±	fraction Modern	±	D^{14}C (‰)	±	^{14}C age (BP)	±
61723	LOW 1A-1K-2, 69-74 cm .10mgC				0.8118	0.0020	-188.2	2.0	1675	20
61724	SHO 2A-1K-6, 135-147 cm .029mgC				0.4963	0.0080	-503.7	8.0	5630	130
61725	LOW 4A-1K-2, 99-100 cm		25.1	0.1	0.3856	0.0011	-614.4	1.1	7655	25
61726	LOW 5A-1K-2, 49-61 cm .040mgC				0.7718	0.0072	-228.2	7.2	2080	80
61727	LOW 6A-1K-2, 55-65 cm .063mgC				0.6677	0.0040	-332.3	4.0	3245	50
61728	LOW 7A-1P-2, 24-30 cm .13mgC				0.4302	0.0016	-569.8	1.6	6775	30
61729	LOW 5A-1K-3, 78-90 cm .029mgC				0.6147	0.0081	-385.3	8.1	3910	110
61730	LOW 7A-1P-3, 86-88 cm		23.4	0.1	0.3360	0.0009	-664.0	0.9	8760	25
61731	LOW 7A-1P-3, 86-90 cm		26.5	0.1	0.3343	0.0010	-665.7	1.0	8800	25
61732	OFW-UPSTRM 2008 Basal Org-1		26.1	0.1	0.3699	0.0009	-630.1	0.9	7990	20
61733	OFW-FRIDAY 2006 Upper Org-1		24.7	0.1	0.4496	0.0011	-550.4	1.1	6420	20

Radiocarbon concentrations are given as fractions of the Modern standard, D^{14}C, and conventional radiocarbon age, following the conventions of Stuiver and Polach (Radiocarbon, v. 19, p.355, 1977).

Size-dependent sample preparation backgrounds have been subtracted based on measurements of ^{14}C-free wood.
All results have been corrected for isotopic fractionation according to the conventions of Stuiver and Polach (1977), with δ^{13}C values measured on prepared graphite using the AMS spectrometer. These can differ from δ^{13}C of the original material, if fractionation occurred during sample graphitization or the AMS measurement, and are not shown.

Comments:
δ^{13}C values shown above were measured to a precision of <0.1‰ relative to standards traceable to PDB, using a Thermo Finnigan Delta Plus stable isotope ratio mass spectrometer (IRMS) with Gas Bench input. The large uncertainties for some of these results are due to the very small sample sizes. Many of these samples were too small to provide sufficient extra CO2 for an IRMS δ^{13}C measurement.

Note: sample 61732 and 61733 are not samples from LOTWs and SL.

3.2 Lawrence Livermore National Laboratory Macrofossil Radiocarbon Reports

A report from the Center for Accelerator Mass Spectrometry at the Lawrence Livermore National Laboratory, in Livermore, California, was obtained providing the radiocarbon analysis from pollen subsamples selected by A. Mybro of the LRC.

CENTER FOR ACCELERATOR MASS SPECTROMETRY

Lawrence Livermore National Laboratory

^{14}C results

Submitter: Myrbo DATE: February 10, 2009

CAMS #	Sample Name	Other ID	$\delta^{13}C$	fraction Modern	±	$D^{14}C$	±	^{14}C age	±
141463	Momos06 1A-1K-3 62-63	N86490	-25	0.2175	0.0021	-782.5	2.1	12260	80
141464	Momos06 5A-1K-4 120-121	N86491	-25	0.1199	0.0032	-880.1	3.2	17040	220
141465	Momos06 7A-1P-4 (A) 17-18	N86492	-25	0.4702	0.0111	-529.8	11.1	6060	190
141466	Momos06 5A-1K-5 (A) 140-142	N86493	-25	0.1123	0.0012	-887.7	1.2	17560	90

1) $\delta^{13}C$ values are the assumed values according to Stuiver and Polach (Radiocarbon, v. 19, p.355, 1977) when given without decimal places. Values measured for the material itself are given with a single decimal place.

2) The quoted age is in radiocarbon years using the Libby half life of 5568 years and following the conventions of Stuiver and Polach (ibid.).

3) Radiocarbon concentration is given as fraction Modern, $D^{14}C$, and conventional radiocarbon age.

4) Sample preparation backgrounds have been subtracted, based on measurements of samples of ^{14}C-free coal. Backgrounds were scaled relative to sample size.

4. Photos of Selected Dated Macrofossils (Paleotec Services)

All macrofossil images provided by Alice Telka of Paleotec Services.

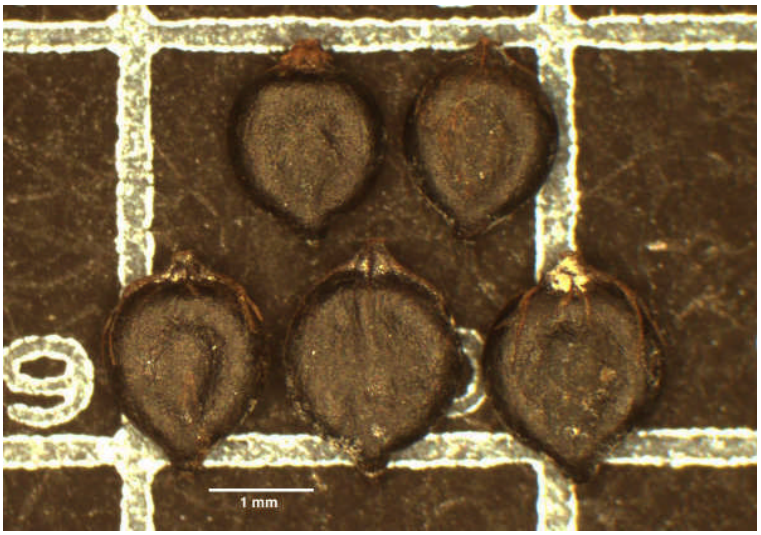

Figure B-1. LOW 1A-1K-3, 99-101 cm; five curlytop knotweed (*Polygonum lapathifolium*) achenes, weighing 2.86 mg have been AMS dated by the Keck Carbon Cycle AMS Facility, University of California, Irvine (May 17, 2008). An age of 7375 ± 20 yrs. BP (UCIAMS-48127) was obtained on the five achenes (expected age ~3.5 ka). Note that the achenes are well preserved with most having bristles attached.

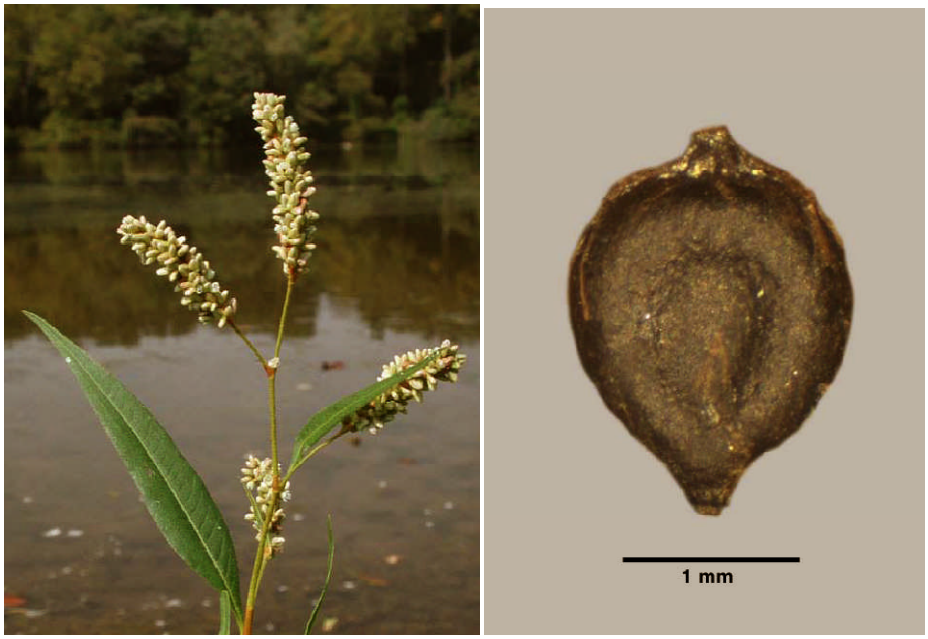

Figure B-2. Left: image of curlytop knotweed, *Polygonum lapathifolium*, an annual herb of moist meadows and wet shorelines (www.delawarewildflowers.org). Right: LOW 1A-1K-3, 99-101 cm macrofossil achene of *Polygonum lapathifolium*.

Figure B-3. LOW 1A-1K-3, 141-144 cm (inset); macrofossil achene of curlytop knotweed (*Polygonum lapathifolium*). Four achenes weighing 2.0 mg have been AMS radiocarbon dated by the Keck Carbon Cycle AMS Facility, University of California, Irvine (Nov. 19/08). An age of 7140 ± 40 yrs BP (UCIAMS-54969) was obtained on the four knotweed achenes (expected age ~ 9 ka). Background photo: Curlytop knotweed, an annual herb of moist meadows and wet shorelines (http://search.creativecommons.org/?q=Polygonum+lapathifolium+images&sourceid=Mozilla-search).

Figure B-4. LOW 4A-1K-1, 7-9 cm, (inset); macrofossil achene of bulrush (*Scirpus sp*.). Six achenes weighing ~20 mg have been AMS radiocarbon dated by the Keck Carbon Cycle AMS Facility, University of California, Irvine (Nov. 19/08). An age of 2495 ± 25 yrs BP (UCIAMS-54971) was obtained on the six bulrush achenes (expected age ~0.5 ka). Background: Photo of *Scirpus validus* growing in water up to 1 m deep along sheltered lakeshores, ponds and marshes (http://plants.ifas.ufl.edu/images/scival/sciva101.jpg).

Figure B-5. LOW 4A-1K-2, 22-23 cm; a wood fragment, weighing 28.2 mg has been AMS radiocarbon dated by the Keck Carbon Cycle AMS Facility, University of California, Irvine (Nov. 19/08). An age of 6370 ± 30 yrs BP (UCIAMS-54972) was obtained on the wood fragment (estimated age ~6.5 ka). For scale, background white grid lines are ~ 4 mm by 4 mm.

Figure B-6. LOW 4A-1K-2, 42-43 cm; a wood fragment, weighing 33.7 mg has been AMS radiocarbon dated by the Keck Carbon Cycle AMS Facility, University of California, Irvine (Nov. 19/08). An age of 6955 ± 30 yrs BP (UCIAMS-54973) was obtained on the wood fragment (estimated age ~7 ka). For scale, background white grid lines are ~ 4 mm by 4 mm. Top: one view of wood fragment. Bottom: opposite view of same wood fragment.

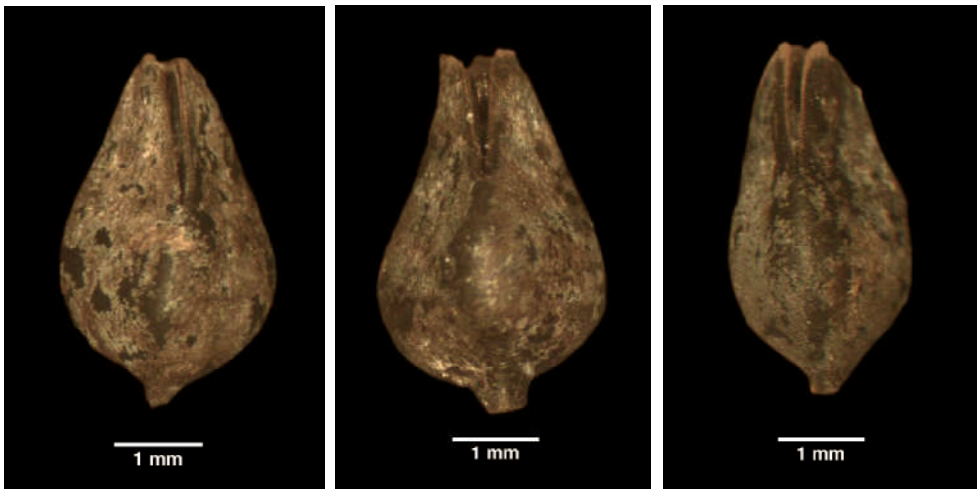

Figure B-7. LOW 4A-1K-2, 99-100 cm; three macrofossil bulrush (*Scirpus sp*.) achenes weighing 11.81 mg have been AMS radiocarbon dated by the Keck Carbon Cycle AMS Facility, University of California, Irvine. An age of 7655 ± 25 yrs BP (UCIAMS-61725) was obtained on the bulrush achenes (May 2, 2009).

Figure B-8. LOW 5A-1K-4, 45-47 cm; two golden dock (*Rumex maritimus*) macrofossil calyx and achene (achene is inside), (see Figure B-9 (left): photo of a *Rumex maritimus* achene). Seeds of both golden dock and goosefoot (Figure B-9 (right),*Chenopodium sp*.) weighing 1.04 mg were submitted to the Keck Carbon Cycle AMS facility, University of California, Irvine for AMS ^{14}C radiocarbon dating. An age of 7630 ± 25 yrs. BP (UCIAMS-34412) was obtained on the dated seeds (Mar. 28/07).

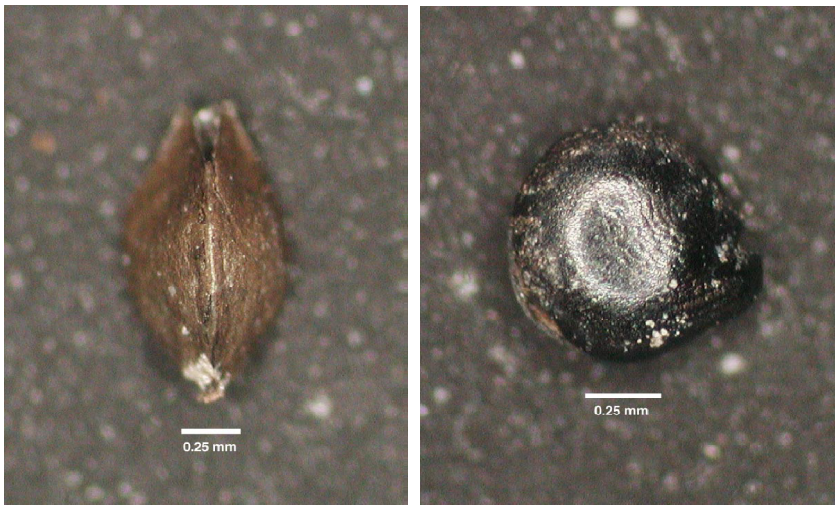

Figure B-9. LOW 5A-1K-4, 45-47 cm; left: golden dock (*Rumex maritimus*) macrofossil achene. right: goosefoot (*Chenopodium sp*.) macrofossil seed. Seeds of both golden dock and goosefoot weighing 1.04 mg were submitted to the Keck Carbon Cycle AMS facility, University of California, Irvine for AMS ^{14}C radiocarbon dating. An age of 7630 ± 25 yrs. BP (UCIAMS-34412) was obtained on the dated seeds (Mar. 28/07).

Figure B-10. LOW 5A-1K-4, 75-77 cm; two bulrush achenes *(Scirpus sp*.) weighing 2.23 mg were submitted to the Keck Carbon Cycle AMS facility, University of California, Irvine for AMS ^{14}C radiocarbon dating. The bulrush achenes yielded an age of 8065 ± 20 yrs. BP (UCIAMS-34413) (Mar. 28/07).

Figure B-11. LOW 7A-1P-2, 75 cm; one twig weighing 15.04 mg has been AMS dated by the Keck Carbon Cycle AMS Facility, University of California, Irvine (May 17, 2008). An age of 8265 ± 20 yrs. BP (UCIAMS-48219) was obtained on the twig (expected age ~4 ka). Top: one view of twig. Bottom: opposite view of twig.

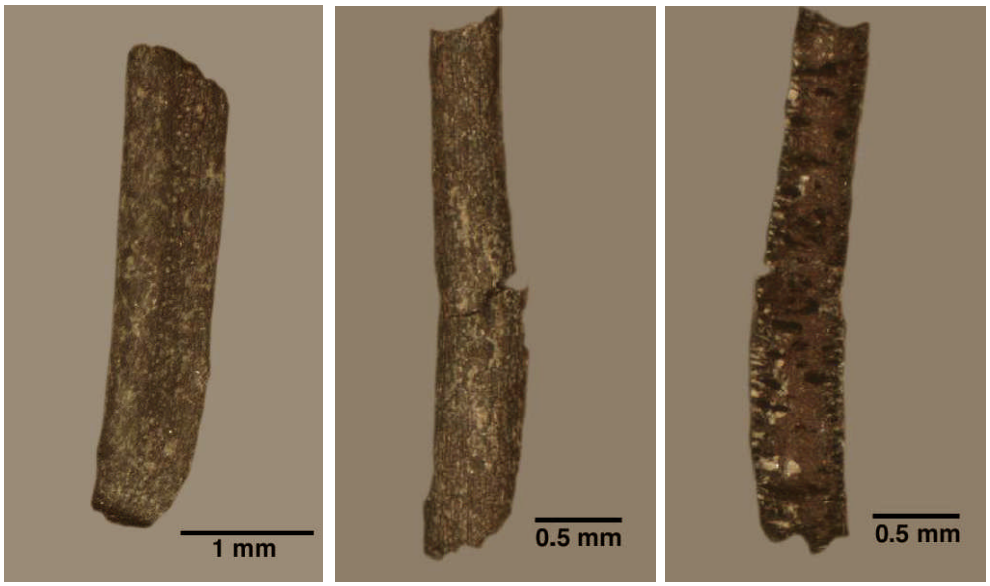

Figure B-12. LOW 7A-1P-3, 86-90 cm; charred conifer remains weighing 0.89 mg have been AMS radiocarbon dated by the Keck Carbon Cycle AMS Facility, University of California, Irvine. An age of 8800 ± 25 yrs BP (UCIAMS-61731) was obtained on the charred conifer remains (May 2, 2009).

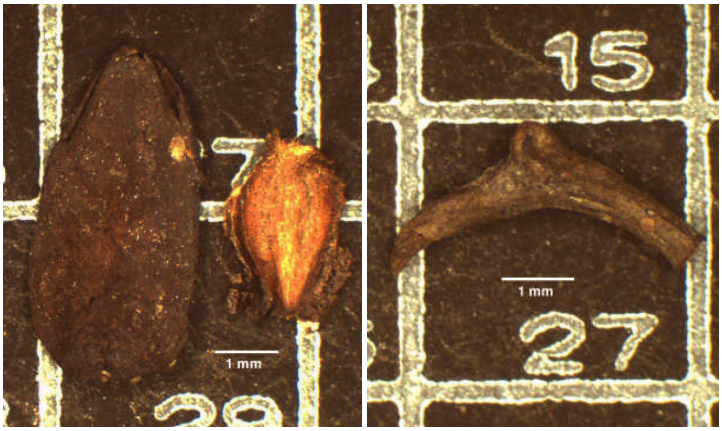

Figure B-13. SHO 2A-1K-1, 102-104 cm; lateral bud and two birch (*Betula*) nutlets weighing 0.86 mg have been AMS dated by the Keck Carbon Cycle AMS Facility, University of California, Irvine (May 17, 2008). An age of 2525 ± 20 yrs. BP (UCIAMS-48218) was obtained from the bud and birch nutlets (expected age ~2 ka). Right: LOW 7A-1P-3, 14 -16 cm. A small twig weighing 0.68 mg has also been AMS dated by the Keck Carbon Cycle AMS Facility, University of California, Irvine. An age of 8310 ± 30 yrs. BP (UCIAMS-48220) was obtained from the dated twig (expected age ~5 ka).

Figure B-14. SHO 2A-1K-5, 65-66 cm; *Drepanocladius sp*. moss fragments weighing 19.85 mg were submitted to the Keck Carbon cycle AMS facility, University of California, Irvine for AMS ^{14}C radiocarbon dating. An age of 6170 ± 25 yrs. BP (UCIAMS-34414) was obtained on the dated moss (Mar. 28/07).

APPENDIX C: XRD ANALYSIS

Five broadly spaced XRD Samples were taken in the Kenora core (WOO06-7A-1P). Jade generated diffractograms are provided for the following core sample intervals. A quartz peak is noted in all cores but additional peaks were not investigated further although they contain clay minerals. Only the samples at 2.8 m and 4.4 m both Lake Agassiz sequences show significant deviation.

Summary of sample locations:

WOO06-7A-1P-2-60-61 at ~ 1.5

WOO06-7A-1P-3-20-21 at ~ 1.8 m

WOO06-7A-1P-3-120-121 at ~ 2.8 m

WOO06-7A-1P-4-89-89.5 at ~ 4.0

WOO06-7A-1P-4-130-131 at ~ 4.4 m

WOO06-7A-1P-2-60-61:

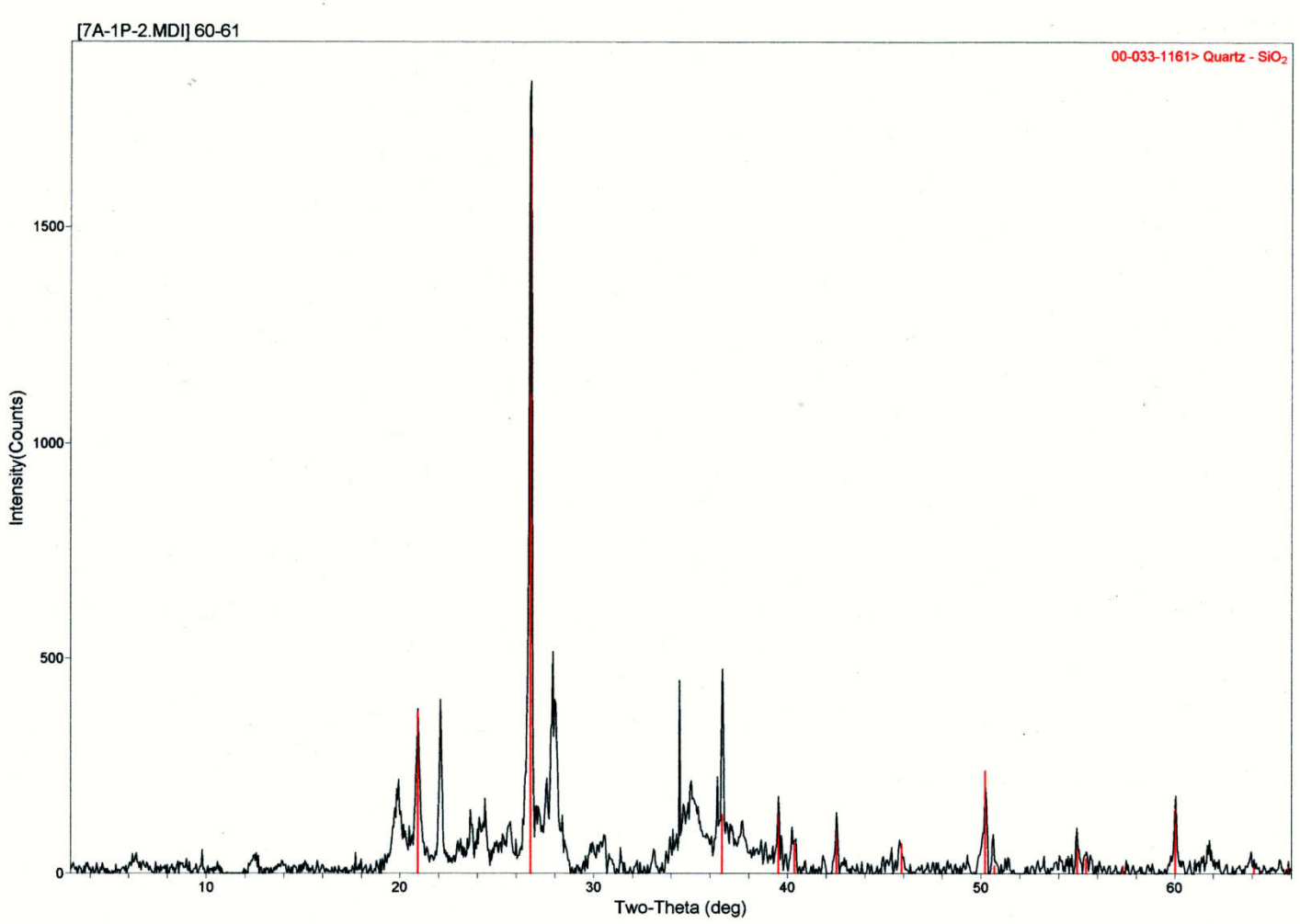

WOO06-7A-1P-3-20-21:

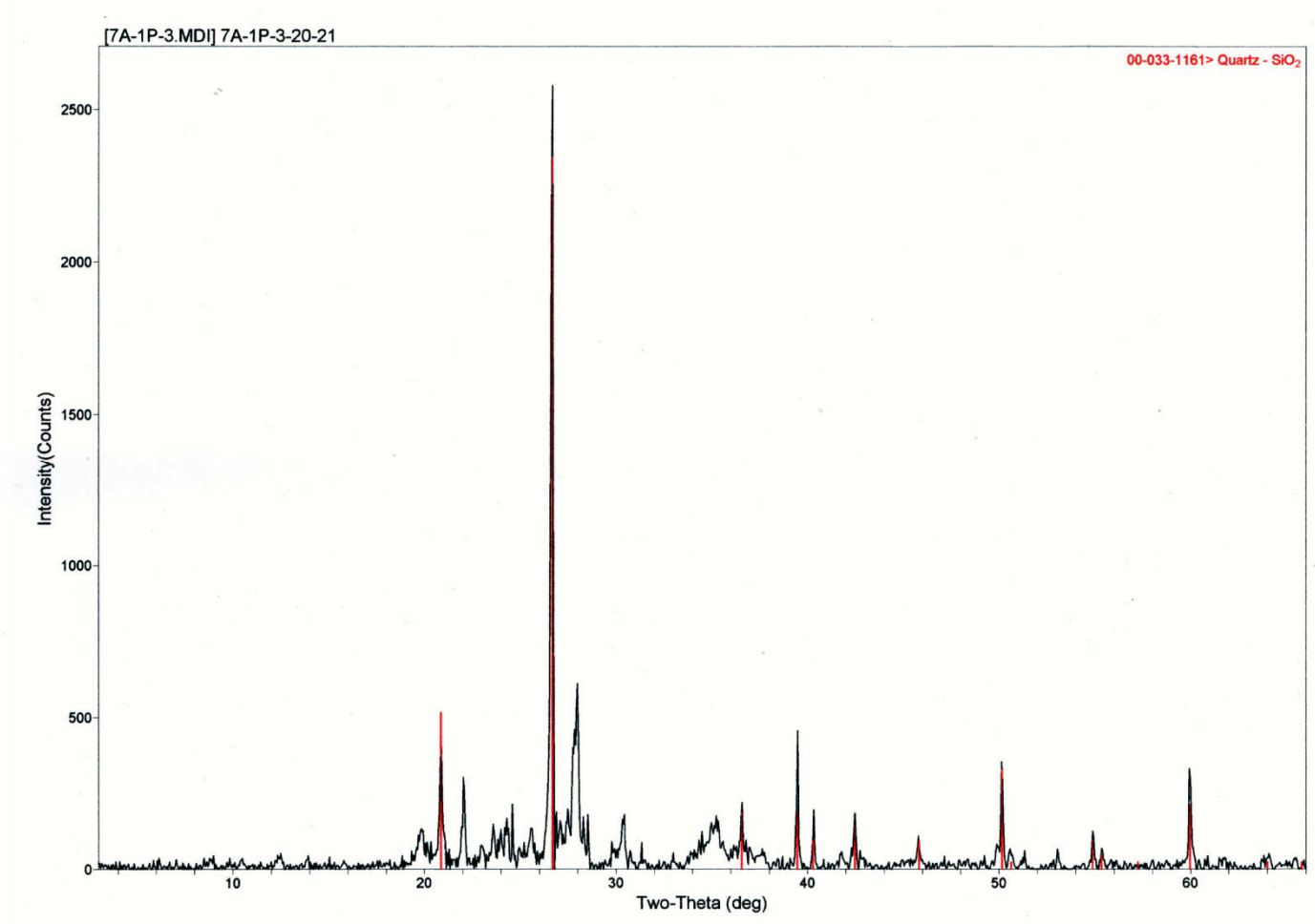

WOO06-7A-1P-3-120-121:

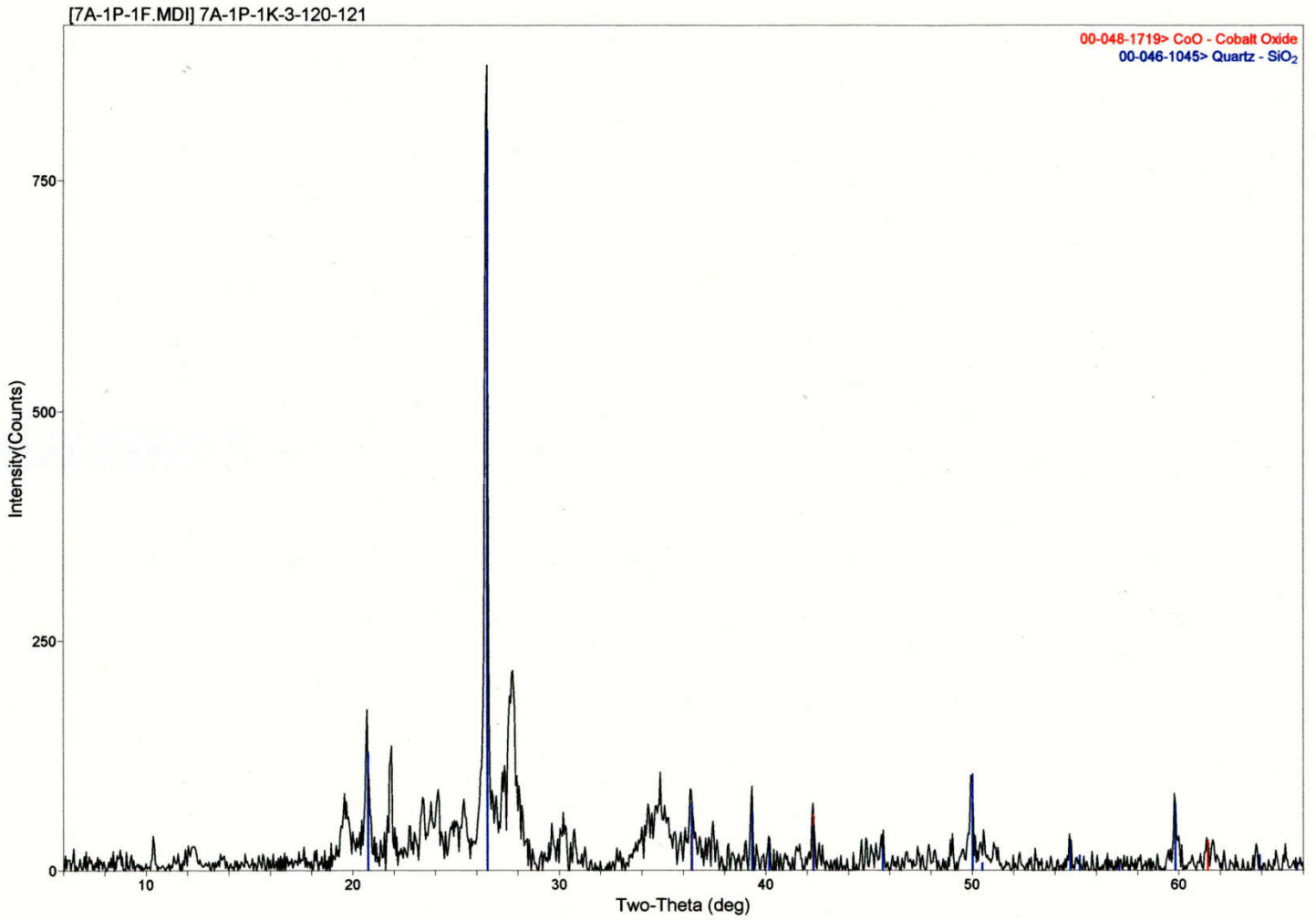

WOO06-7A-1P-4-89-89.5:

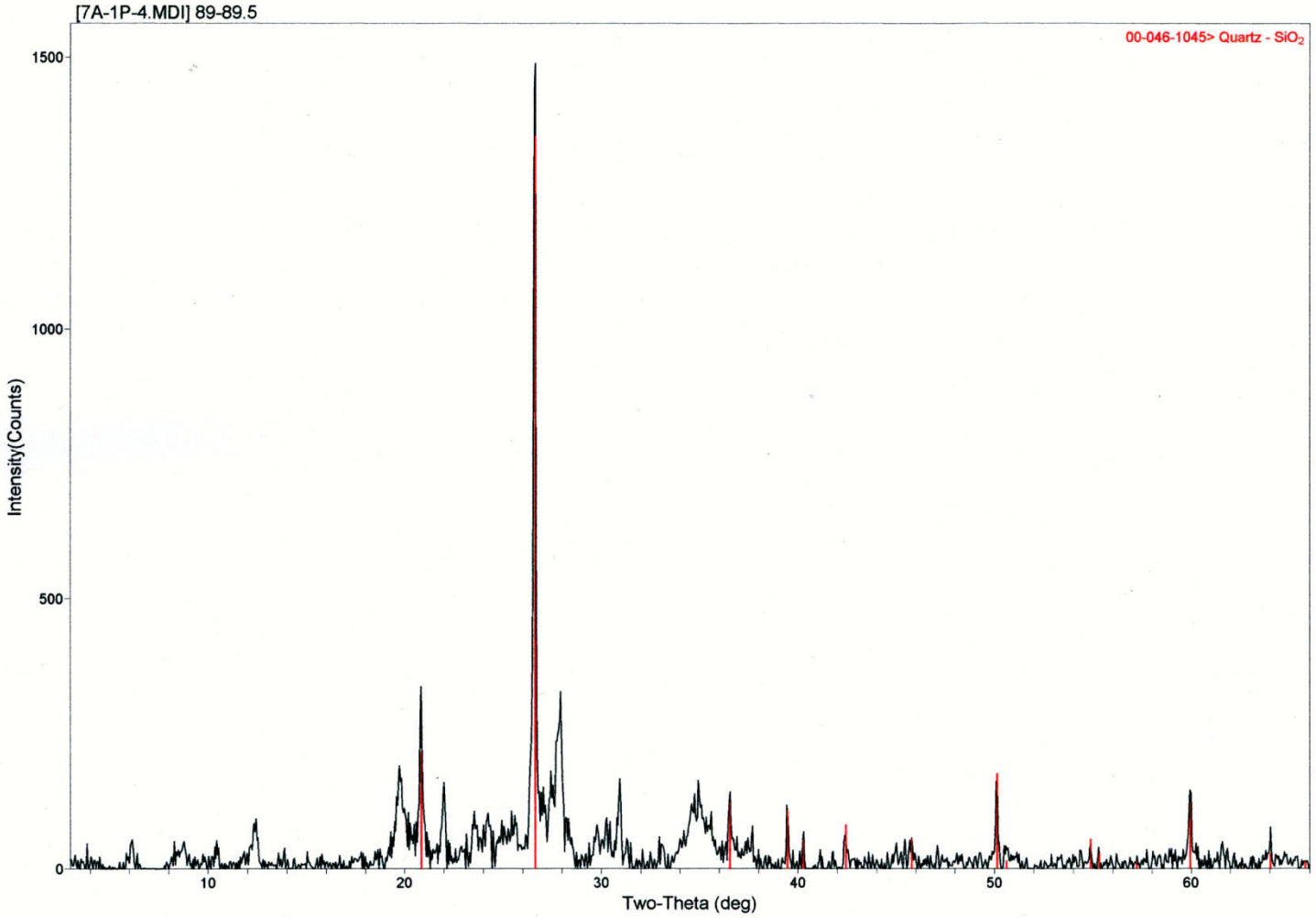

WOO06-7A-1P-4-130-131:

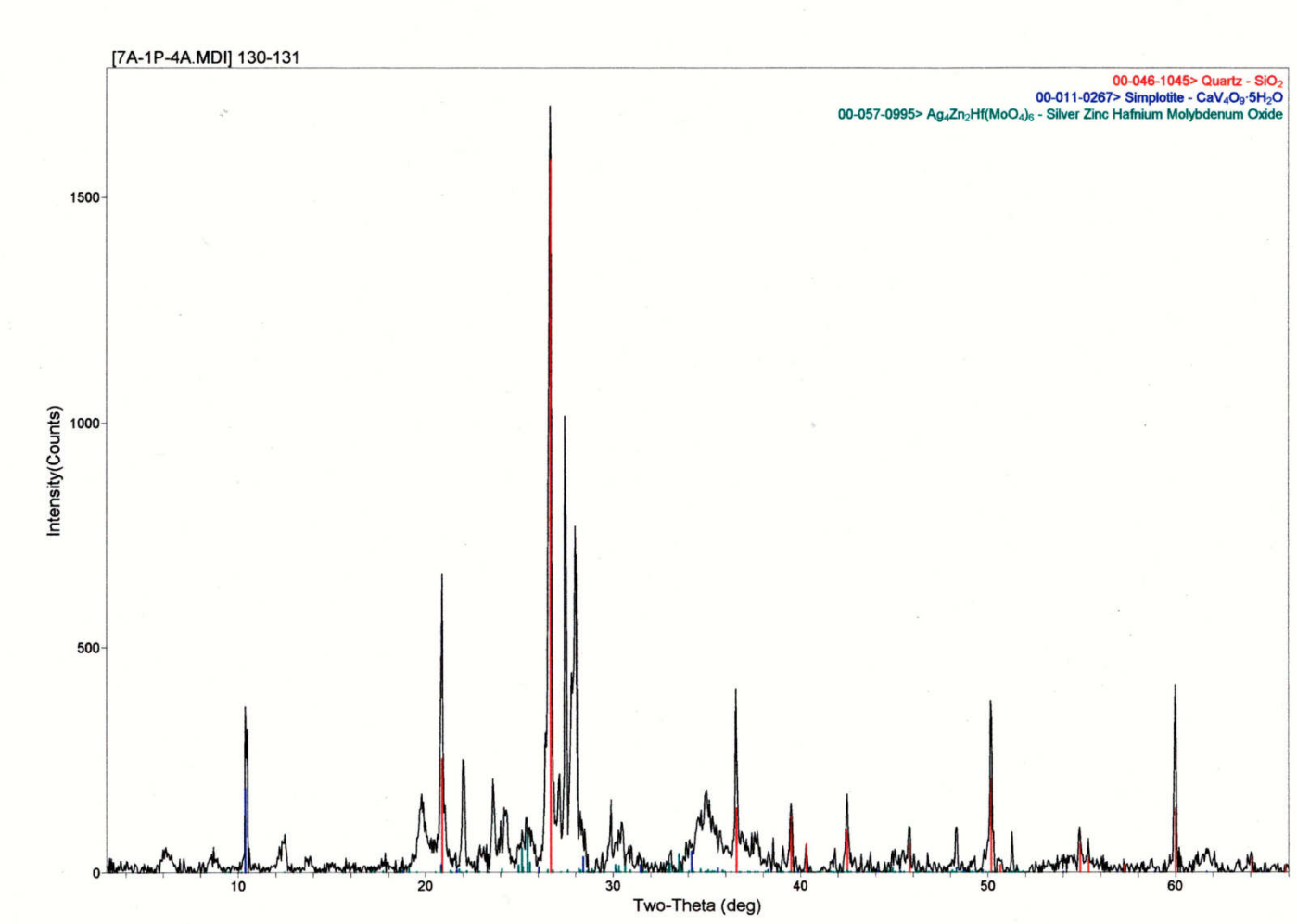

APPENDIX D: Moisture Analysis Data

Moisture samples were taken for the WOO06-1A, WOO06-3A, WOO06-5A, WOO06-7A, and SHO06-2A cores. The WOO06-3A core was not suitable for analysis and was not processed. The SHO06-2A core samples were very limited and were not processed although are provided below for information. The other data are provided below and were used to develop moisture profiles for the associated cores.

WOO06-1A

Core					Top Depth (cm)	Bottom Depth (cm)	Empty container	Wet Sample & container	Dry Sample & container	Weight loss	% loss
MOMOS	WOO05	1A	1K	1	4	5	6.9967	12.6048	7.5512	5.0536	90.1
MOMOS	WOO06	1A	1K	1	7	8	6.6307	14.1561	8.5512	5.6049	74.5
MOMOS	WOO06	1A	1K	1	14	15	6.6211	12.4366	7.9403	4.4963	77.3
MOMOS	WOO06	1A	1K	1	24	25	6.8092	13.5517	8.3274	5.2243	77.5
MOMOS	WOO06	1A	1K	1	34	35	6.8055	13.9292	8.4042	5.525	77.6
MOMOS	WOO06	1A	1K	1	44	45	6.6816	12.811	8.0856	4.7254	77.1
MOMOS	WOO06	1A	1K	1	54	55	6.6695	14.2116	8.5375	5.6741	75.2
MOMOS	WOO06	1A	1K	1	64	65	6.6336	13.579	8.3878	5.1912	74.7
MOMOS	WOO06	1A	1K	2	4	5					
MOMOS	WOO06	1A	1K	2	4	5	6.6022	17.3779	9.6607	7.7172	71.6
MOMOS	WOO06	1A	1K	2	14	15	6.4898	14.2838	8.9708	5.313	68.2
MOMOS	WOO06	1A	1K	2	24	25	6.4163	15.3681	9.5296	5.8385	65.2
MOMOS	WOO06	1A	1K	2	34	35	6.6776	13.445	8.9765	4.4685	66.0
MOMOS	WOO06	1A	1K	2	44	45	6.6306	14.9565	9.722	5.2345	62.9
MOMOS	WOO06	1A	1K	2	54	55	7.0021	15.8856	10.7168	5.1688	58.2
MOMOS	WOO06	1A	1K	2	64	65	6.6815	15.9847	10.394	5.5907	60.1
MOMOS	WOO06	1A	1K	2	74	75	6.6578	14.4504	10.338	4.1124	52.8
MOMOS	WOO06	1A	1K	2	84	85	6.663	15.3419	11.0035	4.3384	50.0
MOMOS	WOO06	1A	1K	2	94	95	6.6654	14.7533	10.4467	4.3066	53.2
MOMOS	WOO06	1A	1K	2	104	105	6.4148	12.2865	8.7897	3.4968	59.6
MOMOS	WOO06	1A	1K	2	114	115	6.6003	12.2959	9.335	2.9609	52.0
MOMOS	WOO06	1A	1K	3	4	5	6.6624	18.9402	12.9904	5.9498	48.5
MOMOS	WOO06	1A	1K	3	14	15	6.4079	19.0877	13.8375	5.2502	41.4
MOMOS	WOO06	1A	1K	3	24	25	6.6736	17.6616	12.8031	4.8585	44.2
MOMOS	WOO06	1A	1K	3	34	35	6.4186	17.4532	12.953	4.5002	40.8
MOMOS	WOO06	1A	1K	3	44	45	6.6762	18.9379	13.9754	4.9625	40.5
MOMOS	WOO06	1A	1K	3	54	55	6.6064	15.4345	11.9125	3.522	39.9
MOMOS	WOO06	1A	1K	3	64	65	6.6707	16.1232	12.7332	3.39	35.9
MOMOS	WOO06	1A	1K	3	74	75	6.9869	19.0273	15.1049	3.9224	32.6
MOMOS	WOO06	1A	1K	3	90	91	6.4965	17.1571	13.8433	3.3138	31.1
MOMOS	WOO06	1A	1K	3	94	95	6.662	17.3967	14.7358	2.6609	24.8
MOMOS	WOO06	1A	1K	3	105	106	6.6575	15.7796	13.6092	2.1704	23.8
MOMOS	WOO06	1A	1K	3	115	116	6.4351	14.888	12.8821	2.0059	23.7
MOMOS	WOO06	1A	1K	3	125	126	6.6334	14.8821	13.0042	1.8779	22.8
MOMOS	WOO06	1A	1K	3	135	136	6.6637	15.4037	13.3443	2.0594	23.6
MOMOS	WOO06	1A	1K	3	145	146	6.5271	15.4655	13.518	1.9475	21.8

WOO06-5A

Core					Top Depth (cm)	Bottom Depth (cm)	Empty container	Wet Sample & container	Dry Sample & container	Weight loss	% loss
MOMOS	WOO06	5A	1K	1	14	16	6.6	19.7249	11.24760	8.4773	64.6
MOMOS	WOO06	5A	1K	2	5	7	6.6	20.3708	11.08076	9.29004	67.5
MOMOS	WOO06	5A	1K	2	15	17	6.6	21.5935		missing	
MOMOS	WOO06	5A	1K	2	25	27	6.6	19.7412	11.09330	8.6479	65.8
MOMOS	WOO06	5A	1K	2	35	37	6.6	21.1728	11.73731	9.43549	64.7
MOMOS	WOO06	5A	1K	2	45	47	6.6	21.7162	11.98813	9.72807	64.4
MOMOS	WOO06	5A	1K	2	54	56	6.6	19.9837	11.63560	8.3481	62.4
MOMOS	WOO06	5A	1K	2	65	66	6.6	21.8278	12.65283	9.17497	60.3
MOMOS	WOO06	5A	1K	2	75	77	6.6	21.3501	12.35748	8.99262	61.0
MOMOS	WOO06	5A	1K	3	5	7	6.6	20.9325	12.59853	8.33397	58.1
MOMOS	WOO06	5A	1K	3	15	17	6.6	20.0944	11.26956	8.82484	65.4
MOMOS	WOO06	5A	1K	3	25	27	6.6	20.0803	11.70028	8.38002	62.2
MOMOS	WOO06	5A	1K	3	35	37	6.6	20.4073	11.86741	8.53989	61.9
MOMOS	WOO06	5A	1K	3	45	47	6.6	21.6447	12.30334	9.34136	62.1
MOMOS	WOO06	5A	1K	3	55	57	6.6	20.5025	11.71667	8.78583	63.2
MOMOS	WOO06	5A	1K	3	65	67	6.6	19.9775	11.78690	8.1906	61.2
MOMOS	WOO06	5A	1K	3	75	77	6.6	20.3953	12.27935	8.11595	58.8
MOMOS	WOO06	5A	1K	3	85	87	6.6	20.0464	12.30278	7.74362	57.6
MOMOS	WOO06	5A	1K	3	95	97	6.6	21.3317	12.62558	8.70612	59.1
MOMOS	WOO06	5A	1K	3	105	107	6.6	18.1743	11.25638	6.91792	59.8
MOMOS	WOO06	5A	1K	3	115	117	6.6	19.916	12.41534	7.50066	56.3
MOMOS	WOO06	5A	1K	3	125	127	6.6	21.6152	13.40092	8.21428	54.7
MOMOS	WOO06	5A	1K	3	135	137	6.6	19.7726	12.68991	7.08269	53.8
MOMOS	WOO06	5A	1K	3	143	145	6.6	19.8712	13.37605	6.49515	48.9
MOMOS	WOO06	5A	1K	3	145	146	6.6	17.5802	12.75813	4.82207	43.9
MOMOS	WOO06	5A	1K	3	148	149.5	6.6	21.3629	15.33285	6.03005	40.8
MOMOS	WOO06	5A	1K	4	2	4	6.6	19.5417	15.03707	4.50463	34.8
MOMOS	WOO06	5A	1K	4	5	7	6.6	21.6032	16.57198	5.03122	33.5
MOMOS	WOO06	5A	1K	4	8	9	6.6	17.9945	14.51282	3.48168	30.6
MOMOS	WOO06	5A	1K	4	13	15	6.6	24.0818	18.86778	5.21402	29.8
MOMOS	WOO06	5A	1K	4	18	20	6.6	21.5548	16.84242	4.71238	31.5
MOMOS	WOO06	5A	1K	4	25	27	6.6	25.3884	19.63695	5.75145	30.6
MOMOS	WOO06	5A	1K	4	35	37	6.6	23.3485	18.62601	4.72249	28.2
MOMOS	WOO06	5A	1K	4	49	51	6.6	21.1034	16.22381	4.87959	33.6
MOMOS	WOO06	5A	1K	4	55	57	6.6	21.4474	16.56080	4.8866	32.9
MOMOS	WOO06	5A	1K	4	65	67	6.6	22.4078	16.79619	5.61161	35.5
MOMOS	WOO06	5A	1K	4	81	82	6.6	16.1251	11.39121	4.73389	49.7
MOMOS	WOO06	5A	1K	4	82	83	6.6	10.6285	8.54157	2.08693	51.8
MOMOS	WOO06	5A	1K	4	83	85	6.6	17.4619	11.48892	5.97298	55.0
MOMOS	WOO06	5A	1K	4	87	89	6.6	17.6426	14.18718	3.45542	31.3
MOMOS	WOO06	5A	1K	4	95	97	6.6	20.3076	17.57615	2.73145	19.9
MOMOS	WOO06	5A	1K	4	105	107	6.6	19.4809	16.78522	2.69568	20.9
MOMOS	WOO06	5A	1K	4	115	117	6.6	20.3758	17.31013	3.06567	22.3
MOMOS	WOO06	5A	1K	4	125	127	6.6	20.4876	18.00463	2.48297	17.9
MOMOS	WOO06	5A	1K	4	135	137	6.6	19.7429	17.06453	2.67837	20.4
MOMOS	WOO06	5A	1K	4	145	147	6.6	21.5508	18.51329	3.03751	20.3
MOMOS	WOO06	5A	1K	5	5	7	6.6	23.2969	19.86609	3.43081	20.5
MOMOS	WOO06	5A	1K	5	15	17	6.6	24.1217	20.21665	3.90505	22.3
MOMOS	WOO06	5A	1K	5	25	27	6.6	22.3335	18.87914	3.45436	22.0
MOMOS	WOO06	5A	1K	5	35	37	6.6	25.2316	20.60171	4.62989	24.8
MOMOS	WOO06	5A	1K	5	45	47	6.6	22.1038	18.93827	3.16553	20.4
MOMOS	WOO06	5A	1K	5	55	57	6.6	24.5702	18.68617	5.88403	32.7
MOMOS	WOO06	5A	1K	5	85	87	6.6	28.6524	21.19523	7.45717	33.8
MOMOS	WOO06	5A	1K	5	95	97	6.6	27.3656	19.24561	8.11999	39.1
MOMOS	WOO06	5A	1K	5	105	107	6.6	26.3034	18.96231	7.34109	37.3
MOMOS	WOO06	5A	1K	5	115	117	6.6	26.0983	18.48994	7.60836	39.0
MOMOS	WOO06	5A	1K	5	125	127	6.6	28.4131	20.16898	8.24412	37.8
MOMOS	WOO06	5A	1K	5	135	137	6.6	28.5593	20.67443	7.88487	35.9
MOMOS	WOO06	5A	1K	5	145	147	6.6	28.7199	20.38837	8.33153	37.7

WOO06-7A

Core					Top Depth (cm)	Bottom Depth (cm)	Empty container	Wet Sample & container	Dry Sample & container	Weight loss	% loss
MOMOS	WOO06	7A	1P	1	10	11	6.6802	16.7185	9.0341	7.6844	76.6
MOMOS	WOO06	7A	1P	1	20	21	6.675	16.2898	8.8234	7.4664	77.7
MOMOS	WOO06	7A	1P	1	30	31	6.4178	17.1675	8.3142	8.8533	82.4
MOMOS	WOO06	7A	1P	1	40	41	6.5509	15.7427	8.1717	7.571	82.4
MOMOS	WOO06	7A	1P	1	50	51	6.4751	12.0779	7.556	4.5219	80.7
MOMOS	WOO06	7A	1P	1	60	61	6.6052	13.5111	8.0919	5.4192	78.5
MOMOS	WOO06	7A	1P	1	70	71	6.6532	14.3647	8.7403	5.6244	72.9
MOMOS	WOO06	7A	1P	1	80	81	6.994	14.9271	9.7382	5.1889	65.4
MOMOS	WOO06	7A	1P	2	1	2	6.812	13.1009	8.2741	4.8268	76.8
MOMOS	WOO06	7A	1P	2	10	11	6.811	14.3016	8.6956	5.606	74.8
MOMOS	WOO06	7A	1P	2	20	21	6.8087	14.4293	9.6522	4.7771	62.7
MOMOS	WOO06	7A	1P	2	30	31	6.4847	12.9689	9.0999	3.869	59.7
MOMOS	WOO06	7A	1P	2	40	41	6.4946	12.7098	8.7218	3.988	64.2
MOMOS	WOO06	7A	1P	2	50	51	6.642	13.0024	9.0042	3.9982	62.9
MOMOS	WOO06	7A	1P	2	60	61	6.406	12.3225	8.4411	3.8814	65.6
MOMOS	WOO06	7A	1P	2	70	71	6.4902	11.5777	8.2475	3.3302	65.5
MOMOS	WOO06	7A	1P	3	10	11	6.678	11.7925	8.4818	3.3107	64.7
MOMOS	WOO06	7A	1P	3	20	21	7.0053	12.2922	8.9432	3.349	63.3
MOMOS	WOO06	7A	1P	3	30	31	6.8088	11.7828	8.5486	3.2342	65.0
MOMOS	WOO06	7A	1P	3	40	41	6.4416	11.043	8.1461	2.8969	63.0
MOMOS	WOO06	7A	1P	3	50	51	6.6677	12.1642	8.6863	3.4779	63.3
MOMOS	WOO06	7A	1P	3	60	61	6.9848	13.3792	9.4968	3.8824	60.7
MOMOS	WOO06	7A	1P	3	70	71	6.6654	11.62	8.6417	2.9783	60.1
MOMOS	WOO06	7A	1P	3	80	81	6.8113	12.0844	8.981	3.1034	58.9
MOMOS	WOO06	7A	1P	3	90	91	6.4373	11.9535	8.7394	3.2141	58.3
MOMOS	WOO06	7A	1P	3	100	101	6.5434	11.6416	8.7412	2.9004	56.9
MOMOS	WOO06	7A	1P	3	110	111	6.8033	11.8425	8.9526	2.8899	57.3
MOMOS	WOO06	7A	1P	3	120	121	6.6346	12.1858	9.067	3.1188	56.2
MOMOS	WOO06	7A	1P	3	130	131	7.0033	12.2283	9.3648	2.8635	54.8
MOMOS	WOO06	7A	1P	3	140	141	6.673	12.5809	9.8234	2.7575	46.7
MOMOS	WOO06	7A	1P	3	150	151	6.4525	11.5048	9.1512	2.3536	46.6
MOMOS	WOO06	7A	1P	4	10	11	6.666	11.5914	9.4223	2.1691	44.0
MOMOS	WOO06	7A	1P	4	20	21	6.9972	13.2	9.9722	3.2278	52.0
MOMOS	WOO06	7A	1P	4	30	31	6.6673	12.5763	9.4924	3.0839	52.2
MOMOS	WOO06	7A	1P	4	40	41	6.6634	12.0559	9.5477	2.5082	46.5
MOMOS	WOO06	7A	1P	4	50	51	6.4849	11.2238	8.6758	2.548	53.8
MOMOS	WOO06	7A	1P	4	60	61	6.6696	11.6977	8.7212	2.9765	59.2
MOMOS	WOO06	7A	1P	4	70	71	6.6259	12.2237	8.973	3.2507	58.1
MOMOS	WOO06	7A	1P	4	80	81	6.403	14.3943	9.9343	4.46	55.8
MOMOS	WOO06	7A	1P	4	86	87	6.4093	12.8074	9.289	3.5184	55.0
MOMOS	WOO06	7A	1P	4	89	89.5	6.981	12.2346	9.2799	2.9547	56.2
MOMOS	WOO06	7A	1P	4	89.5	90	6.6658	10.9439	8.6377	2.3062	53.9
MOMOS	WOO06	7A	1P	4	95	96	6.4589	12.4578	9.3067	3.1511	52.5
MOMOS	WOO07	7A	1P	4	100	101	6.4906	12.1245	9.3067	2.8178	50.0
MOMOS	WOO06	7A	1P	4	110	111	6.6405	13.1893	10.1778	3.0115	46.0
MOMOS	WOO06	7A	1P	4	120	121	6.4933	12.6353	9.5208	3.1145	50.7
MOMOS	WOO06	7A	1P	4	130	131	6.6403	12.5541	9.6833	2.8708	48.5
MOMOS	WOO06	7A	1P	4	140	141	6.6715	14.1581	10.9862	3.1719	42.4
MOMOS	WOO06	7A	1P	4	150	151	6.8164	14.6625	11.9396	2.7229	34.7

SHO06-2A

Core					Top Depth (cm)	Bottom Depth (cm)	Empty container	Wet Sample & container	Dry Sample & container	Weight loss	% loss
MOMOS	SHO06	2A	1K	5	6	8		22.6565	14.15218	8.50432	37.5
MOMOS	SHO06	2A	1K	5	56	58		20.8151	13.28125	7.53385	36.2
MOMOS	SHO06	2A	1K	5	65	67		23.7436	18.01250	5.7311	24.1
MOMOS	SHO06	2A	1K	5	75	77		24.9602	18.00580	6.9544	27.9
MOMOS	SHO06	2A	1K	5	106	108		21.2856	13.32639	7.95921	37.4
MOMOS	SHO06	2A	1K	6	16	18		20.4148	12.87187	7.54293	36.9
MOMOS	SHO06	2A	1K	6	66	68		20.7058	13.44676	7.25904	35.1
MOMOS	SHO06	2A	1K	6	126	128		22.5928	14.08227	8.51053	37.7